



# Irrigation Practices, Water Consumption, & Return Flows in Colorado's Lower Arkansas River Valley



Field and Model Investigations

By Timothy K. Gates, Luis A. Garcia, Ryan A. Hemphill, Eric D. Morway, and Aymn Elhaddad

CWI Completion Report No. 221

CAES Report No. TR12-10



Additional copies of this report can be obtained from:

Colorado Water Institute  
E102 Engineering Building  
Colorado State University  
Fort Collins, CO 80523-1033  
Phone: 970-491-6308

Email: [cwi@colostate.edu](mailto:cwi@colostate.edu)

This report can also be downloaded as a PDF file from [www.cwi.colostate.edu](http://www.cwi.colostate.edu).

Colorado State University is an equal opportunity/affirmative action employer and complies with all federal and Colorado laws, regulations, and executive orders regarding affirmative action requirements in all programs. The Office of Equal Opportunity and Diversity is located in 101 Student Services. To assist Colorado State University in meeting its affirmative action responsibilities, ethnic minorities, women and other protected class members are encouraged to apply and to so identify themselves.

# Irrigation Practices, Water Consumption, & Return Flows in Colorado's Lower Arkansas River Valley

Field and Model Investigations

By  
Timothy K. Gates  
Luis A. Garcia  
Ryan A. Hemphill  
Eric D. Morway  
Aymn Elhaddad

Department of Civil and Environmental Engineering  
Colorado State University

Technical Completion Report No. 221  
Colorado Water Institute

Technical Report No. TR12-10  
Colorado Agricultural Experiment Station

June 2012



**Colorado State University**  
COLORADO AGRICULTURAL EXPERIMENT STATION

*Edits by Lindsey Middleton*

*Design by Lindsey Middleton  
and Jena J. Thompson*



# Contents

## **8 Acronyms and Variables**

## **9 Acknowledgements**

## **10 Summary**

## **12 Introduction**

12 *Irrigation in the Arkansas River Valley*

13 *Background and Scope of This Study*

14 *Study Objectives*

## **16 Study Sites and Conditions**

16 *Field Locations and Layouts*

19 *Hydrological Setting*

21 *Irrigation Characteristics*

22 *Crops*

22 *Soil Conditions*

## **28 Methodology**

28 *Field Water Balance*

50 *Irrigation Application Efficiency*

51 *Irrigation Water Quality Sampling*

51 *Shallow Groundwater Monitoring*

52 *Soil Water Salinity and Soil Water Content Surveys*

55 *Crop Yield Measurements*

56 *Sensitivity Analysis*

56 *Regional-Scale Modeling of Irrigation-Affected Flow and Salt Loading Processes*

## **60 Results**

60 *Irrigation Water Balance Components and Efficiency*

75 *Salt Concentration and Loading to and from Fields*

75 *Field Soil Water Salinity*

78 *Water Table Depth and Salinity*

93 *Crop Yield and ET in Relation to Soil Water Salinity and Irrigation*

98 *Sensitivity Analysis*

101 *Recharge to and Upflux from Groundwater*

106 *Return Flows and Salt Loads to Streams*

## **108 Summary, Conclusions, and Implications**

108 *General Findings*

110 *Answers to Specific Questions of Concern to Water Managers and Regulatory Agencies*

## **113 References**

# Figures

- 13 **Figure 1.** LARV in Colorado highlighting the upstream and downstream study regions
- 16 **Figure 2.** Monitored fields in Upstream Study Region.
- 17 **Figure 3.** Monitored fields in Downstream Study Region
- 17 **Figure 4 (left).** Layout of field US13
- 17 **Figure 5.** Layout of fields DS18A, DS18B, DS18C, DS18D, DS18E, DS18F, DS18G, and DS18H within the same farm unit
- 18 **Figure 6.** Layout of field US9, showing two separately irrigated cells within the field
- 19 **Figure 7.** Daily average flow rate in Arkansas River at (a) Catlin Dam Near Fowler, CO gauge and at (b) Below John Martin Reservoir gauge for study years compared to mean daily average flow rate for period 1975-2010
- 20 **Figure 8.** Cumulative precipitation recorded for each of the study years 2004-2008 and (a) averaged over the years 1992-2010 at the CoAgMet Rocky Ford (RFD01) weather station, and (b) averaged over the years 1998-2010 at the CoAgMet Lamar (LAM02/LAM04) weather station
- 21 **Figure 9.** Cumulative  $ET_r$  calculated for (a) each of the study years 2004-2008 and averaged over the years 1992-2010 at the CoAgMet Rocky Ford (RFD01) weather station, and (b) for study years 2006 and 2007 and averaged over the years 1999-2010 at the CoAgMet Lamar (LAM02/LAM04) weather station
- 24 **Figure 10.** Overlay of irrigated fields in the vicinity of the (a) Upstream and (b) Downstream Study Regions on the USDA NRCS soil textural classes, illustrating the variety of soil textures in the areas. For detailed information regarding soil textural class names and characteristics see <http://websoilsurvey.nrcs.usda.gov/app/HomePage.htm>
- 28 **Figure 11.** The field water balance showing the surface components and the root zone components
- 29 **Figure 12.** EZ Flow Ramp™ flume used to measure tailwater from field DS14 during 2005 and 2007
- 30 **Figure 13.** Permanent measurement structure for inflow to Field DS6, provided by Fort Lyon Canal Company during seasons 2005-2008
- 31 **Figure 14.** Weir structure for flow measurement onto fields DS4 and DS16 in 2008
- 32 **Figure 15.** Cutthroat flume for measurement of tailwater runoff from field US14C in 2008
- 32 **Figure 16.** Parshall flume for measurement of flow to field DS1 in 2008
- 33 **Figure 17.** Center pivot sprinkler system used to irrigated fields DS5, DS6, and DS17 in 2008
- 34 **Figure 18.** Applied and tailwater hydrographs for (a) field US8, 10-12 July 2008 irrigation event, and (b) field DS2, 17-19 August 2008 irrigation event
- 35 **Figure 19.** Stabilization pond for center pivot sprinkler on field DS19 in 2008
- 36 **Figure 20.** HOBO® rain gauge in Field US17E in 2008
- 37 **Figure 21.** Cumulative precipitation for field US20 during the 2005 irrigation season
- 38 **Figure 22.**  $ET_{gag}$  Model A atmometer in field DS2 during the 2006 season
- 40 **Figure 23.** Alfalfa  $ET_a$  adjusted for cutting compared to ReSET  $ET_a$
- 40 **Figure 24.** ReSET-calculated  $ET_a$  in the Upstream Study Region on 4 August 2008 with study fields circled
- 41 **Figure 25.** ReSET-calculated  $ET_a$  in vicinity of field US4 on 4 August 2008
- 41 **Figure 26.** ReSET-calculated  $ET_a$  in the Downstream Study Region on 28 July 2008 with study fields circled
- 42 **Figure 27.** ReSET-calculated  $ET_a$  in vicinity of fields DS8 and DS15 on 28 July 2008
- 43 **Figure 28.** Stihl® gas-powered earth auger used for soil sampling
- 48 **Figure 29.** Example plots of time of advance and time of recession of an irrigation stream along a field and the intake opportunity time
- 49 **Figure 30.** Illustration of linear infiltration distribution approximation used in this study
- 51 **Figure 31.** YSI® 30 handheld conductivity meter used for measuring EC and temperature
- 52 **Figure 32.** CSU field technician measuring depth to water table in well on Field DS12 using an open-spool tape, 2005
- 54 **Figure 33.** CSU technician conducting EM38 survey on a field in the LARV
- 55 **Figure 34.** Oakfield tube sampler
- 57 **Figure 35.** Distribution Sensitivity: Assumed, upper (red) and lower (green) bounds for the slope of the linear infiltration distribution, compared to the assumed baseline (black) distribution
- 58 **Figure 36.** Frequency histograms and fitted distributions of residuals (difference between simulated and observed values) of  $D_{wt}$  for (a) Upstream Study Region, and (b) Downstream Study Region
- 59 **Figure 37.** Simulated weekly groundwater return flow to the Arkansas River compared to total unaccounted-for return flow (with 95 percent confidence intervals) estimated using stream gauges for calibration and testing periods for river reaches along the (a) Upstream Study Region, and (b) Downstream Study Region
- 62 **Figure 38.** Total rainfall measured on monitored fields for (a) 25 May-30 Sep 2004, (b) 30 Jun-28 Sep 2005
- 63 **Figure 39.** Total rainfall measured on monitored fields for (a) 8 Apr-11 Oct 2006, and (b) 17 May-9 July 2007
- 63 **Figure 40.** Total rainfall measured on monitored fields for 12 Jun-29 Nov 2008

- 64 **Figure 41.** Histogram and fitted probability distribution of  $Q_A$  for (a) Upstream, (b) Downstream, and (c) total surface irrigation events over the entire study period
- 65 **Figure 42.** Histogram and fitted probability distribution of  $Q_A$  for (a) Upstream, (b) Downstream, and (c) total sprinkler irrigation events over the entire study period
- 66 **Figure 43.** Histogram and fitted probability distribution of TRF for (a) Upstream, (b) Downstream, and (c) total surface irrigation events over the entire study period
- 67 **Figure 44.** Histogram and fitted probability distribution of  $Q_I$  for (a) Upstream, (b) Downstream, and (c) total surface irrigation events over the entire study period
- 68 **Figure 45.** Histogram and fitted probability distribution of  $Q_I$  for (a) Upstream, (b) Downstream, and (c) total sprinkler irrigation events over the entire study period
- 70 **Figure 46.** Histogram and fitted probability distribution of DPF for (a) Upstream, (b) Downstream, and (c) total surface irrigation events over the entire study period
- 71 **Figure 47.** Histogram and fitted probability distribution of DPF for (a) Upstream, (b) Downstream, and (c) total sprinkler irrigation events over the entire study period
- 72 **Figure 48.**  $ET_r$  estimated from field atmometers,  $ET_p$  calculated with the ASCE Standardized Equation, and  $ET_a$  estimated with ReSET, for portions of the 2008 irrigation season for (a) field US4B (b) field US8, and (c) field US12
- 73 **Figure 49.**  $ET_r$  estimated from field atmometers,  $ET_p$  calculated with the ASCE Standardized Equation, and  $ET_a$  estimated with ReSET, for portions of the 2008 irrigation season for (a) field DS1, (b) field DS6B, and (c) field DS16
- 74 **Figure 50.** Histogram and fitted probability distribution of  $E_a$  (%) for (a) Upstream, (b) Downstream, and (c) total surface irrigation events over the entire study period
- 79 **Figure 51.** Box and whisker plots of  $EC_e$  estimated from midseason EM38 surveys on monitored fields in the Upstream Study Region in 2004 and 2005. Midline represents the median value; upper and lower edges of box represent 75 percentile and 25 percentile values, respectively; and upper and lower whiskers represented maximum and minimum values, respectively
- 79 **Figure 52.** Box and whisker plots of  $EC_e$  estimated from midseason EM38 surveys on monitored fields in the Upstream Study Region in 2006 and 2008. Midline represents the median value; upper and lower edges of box represent 75 percentile and 25 percentile values, respectively; and upper and lower whiskers represented maximum and minimum values, respectively. Plots for fields US4, US5A, US9, US12, US14A, US14B, and US14C for 2006 are for values surveyed in June (July or August surveys were not available). The plot for field US7 for 2006 is based upon values surveyed during November.
- 80 **Figure 53.** Box and whisker plots of  $EC_e$  estimated from midseason EM38 surveys on monitored fields in the Downstream Study Region in 2004 and 2005. Midline represents the median value; upper and lower edges of box represent 75 percentile and 25 percentile values, respectively; and upper and lower whiskers represented maximum and minimum values, respectively.
- 81 **Figure 54.** Box and whisker plots of  $EC_e$  estimated from midseason EM38 surveys on monitored fields in the Downstream Study Region in 2006 and 2007. Midline represents the median value; upper and lower edges of box represent 75 percentile and 25 percentile values, respectively; and upper and lower whiskers represented maximum and minimum values, respectively. The plot for field DS1 for 2006 are for values surveyed in June (July or August surveys were not available), for field DS13 for values surveyed during May, and for fields DS15 and DS16 for values surveyed during December.
- 81 **Figure 55.** Box and whisker plots of  $EC_e$  estimated from midseason EM38 surveys on monitored fields in the Downstream Study Region in 2008. Midline represents the median value; upper and lower edges of box represent 75 percentile and 25 percentile values, respectively; and upper and lower whiskers represented maximum and minimum values, respectively.
- 82 **Figure 56.** Color contour maps of  $EC_e$  estimated from (a) the July 8, 2008 EM38 survey for field US04, and (b) the June 3, 2008 EM38 survey for field DS11
- 83 **Figure 57.** Seasonal variation of  $D_{wt}$  in three wells within field DS11 during 2008 and into spring 2009
- 84 **Figure 58.** Box and whisker plots of  $D_{wt}$  values measured on fields in the Upstream Study Region for years 2004 and 2005. Midline represents the median value; upper and lower edges of box represent 75 percentile and 25 percentile values, respectively; and upper and lower whiskers represented maximum and minimum values, respectively.
- 85 **Figure 59.** Box and whisker plots of  $D_{wt}$  values measured on fields in the Upstream Study Region for years 2006 and 2008. Midline represents the median value; upper and lower edges of box represent 75 percentile and 25 percentile values, respectively; and upper and lower whiskers represented maximum and minimum values, respectively.
- 86 **Figure 60.** Box and whisker plots of  $D_{wt}$  values measured on fields in the Downstream Study Region for years 2005 and 2006. Midline represents the median value; upper and lower edges of box represent 75 percentile and 25 percentile values, respectively; and upper and lower whiskers represented maximum and minimum values, respectively.
- 87 **Figure 61.** Box and whisker plots of  $D_{wt}$  values measured on fields in the Downstream Study Region for years 2005, 2006, 2007, and 2008. Midline represents the median value; upper and lower edges of box represent 75 percentile and 25 percentile values, respectively; and upper and lower whiskers represented maximum and minimum values, respectively.
- 88 **Figure 62.** Seasonal variation of EC in three wells within field DS11 during 2008 and into spring 2009
- 89 **Figure 63.** Box and whisker plots of EC values measured on fields in the Upstream Study Region for years 2004 and 2005. Midline represents the median value; upper and lower edges of box represent 75 percentile and 25 percentile values, respectively; and upper and lower whiskers represented maximum and minimum values, respectively.
- 90 **Figure 64.** Box and whisker plots of EC values measured on fields in the Upstream Study Region for years 2006 and 2008. Midline represents the median value; upper and lower edges of box represent 75 percentile and 25 percentile values, respectively; and upper

and lower whiskers represented maximum and minimum values, respectively.

- 91 **Figure 65.** Box and whisker plots of EC values measured on fields in the Downstream Study Region for years 2005 and 2006. Midline represents the median value; upper and lower edges of box represent 75 percentile and 25 percentile values, respectively; and upper and lower whiskers represented maximum and minimum values, respectively.
- 92 **Figure 66.** Box and whisker plots of EC values measured on fields in the Downstream Study Region for years 2007 and 2008. Midline represents the median value; upper and lower edges of box represent 75 percentile and 25 percentile values, respectively; and upper and lower whiskers represented maximum and minimum values, respectively.
- 94 **Figure 67.** Normalized corn biomass versus  $EC_e$  measured at locations within surveyed fields in (a) Upstream Study Region, and (b) Downstream Study Region
- 95 **Figure 68.** Normalized alfalfa biomass versus  $EC_e$  measured at locations within surveyed fields in (a) Upstream Study Region, and (b) Downstream Study Region
- 97 **Figure 69.**  $ET_a$  estimated with ReSET from satellite imagery versus measured  $EC_e$  for (a) field US17, July 1999; (b) field US20, July 2001; (c) field US80, June 2001; (d) field DS106, July 2005; (e) field US80, July 2001; and (f) field US38, July 2006. Fitted regression curves with  $r^2$  values are shown on each plot
- 99 **Figure 70.** Range and baseline average values (horizontal bar) of DPF calculated over the considered range of values associated with errors in  $ET_a$ ,  $Q_p$ , initial  $S_{SW}$ , and TAW for (a) all surface irrigation events Upstream and Downstream, and (b) all sprinkler irrigation events Upstream and Downstream
- 100 **Figure 71.** Range and baseline average values (horizontal bar) of  $E_a$  calculated over the considered range of values associated with errors in  $ET_a$ ,  $Q_p$ , initial  $S_{SW}$ , and TAW for (a) all surface irrigation events Upstream and Downstream, and (b) all sprinkler irrigation events Upstream and Downstream
- 102 **Figure 72.** Average  $D_{wt}$  computed over irrigation seasons (a) 1999-2007 in the Upstream Study Region, and (b) 2002-2007 in the Downstream Study Region
- 103 **Figure 73.** Average recharge rate to the water table computed over irrigation seasons (a) 1999-2007 in the Upstream Study Region, and (b) 2002-2007 in the Downstream Study Region
- 104 **Figure 74.** Average ground water upflux rate to  $ET_a$  computed over irrigation seasons (a) 1999-2007 in the Upstream Study Region, and (b) 2002-2007 in the Downstream Study Region
- 105 **Figure 75.** Infiltrated water ( $Q_I + Q_p$ ) and recharge to the groundwater table, showing average values during the off seasons and during the irrigation seasons as plotted points and ratios of recharge to infiltrated water over the irrigation seasons as written percentages for (a) Upstream Study Region and (b) Downstream Study Region
- 106 **Figure 76.** Ratio of groundwater upflux to non-beneficial  $ET_a$  to crop  $ET_a$  computed by the regional models for the Upstream and Downstream Study Regions
- 106 **Figure 77.** Cumulative groundwater upflux to non-beneficial  $ET_a$  computed by the regional models for the Upstream and Downstream Study Regions and estimated for the entire LARV
- 107 **Figure 78.** Groundwater return flow to the Arkansas River within the Upstream and Downstream Study Regions estimated with the regional models (negative values indicate net loss of water from the river to the groundwater aquifer)
- 107 **Figure 79.** Salt load in groundwater return flow to the Arkansas River within the Upstream and Downstream Study Regions estimated with the regional models

## Tables

- 22 **Table 1.** Irrigation water source, type of irrigation system, and annual number of irrigation events monitored on fields in the Upstream Study Region
- 23 **Table 2.** Irrigation water source, type of irrigation system, and annual number of irrigation events monitored on fields in the Downstream Study Region
- 25 **Table 3.** Crops on fields in the Upstream Study Region
- 25 **Table 4.** Crops on fields in the Downstream Study Region
- 26 **Table 5.** Soil textural class and total available water (TAW) for monitored irrigated fields in the Upstream Study Region
- 27 **Table 6.** Soil textural class and total available water (TAW) for monitored irrigated fields in the Downstream Study Region
- 47 **Table 7.** Parameter values for use in estimating  $q_{II}$  for three different soil textures (Liu et al 2006)
- 61 **Table 8.** Summary statistics for  $Q_A$ ,  $Q_p$ , TRF, DPF, and  $E_a$  for all seasons over the study period
- 76 **Table 9.** TDS in applied irrigation water and tail water for investigated surface irrigation events Upstream and Downstream
- 76 **Table 10.** TDS in applied irrigation water and tail water for investigated sprinkler irrigation events Upstream and Downstream
- 77 **Table 11.** Salt load in applied irrigation water, tail water, and infiltrated water for investigated surface irrigation events Upstream and Downstream
- 78 **Table 12.** Salt load in applied irrigation water, tail water, and infiltrated water for investigated sprinkler irrigation events Upstream and Downstream

# Acronyms and Variables

- $\Lambda_i$ : Instantaneous evaporative fraction  
 $\Delta S_{SW}$ : The change in volume of water stored in soil root zone  
 $\rho_w$ : Density of water  
 $\theta$ : Actual soil water content  
 $\theta_{fc}$ : Soil-water content at  $-1/2$  bar matric potential (field capacity) expressed as a fraction of the bulk soil volume  
 $\theta_{wp}$ : Soil-water content at  $-15$  bar matric potential (permanent wilting point) expressed as a fraction of the bulk soil volume  
 $\tau$ : Difference between the time of recession and the time of advance for any given point along the length of the field, or intake opportunity time  
 $\hat{a}$ ,  $\hat{b}$ ,  $\hat{c}$ , and  $\hat{d}$ : Empirical coefficients for S-curve determined using a least-squares optimization  
 $a$ ,  $a_1$  and  $b_1$ ,  $a_2$  and  $b_2$ , *etc.*: empirical parameters that depend on soil texture  
**AOI**: Area of interest  
**ARIDAD**: Arkansas River Irrigation Data and Analysis Disc  
**CAES**: Colorado Agricultural Experiment Station  
**CD**: Concrete Ditch Water Delivery  
**CDPHE**: Colorado Department of Public Health and Environment  
**CDWR**: Colorado Division of Water Resources  
**CN**: Curve number  
**CoAgMet**: Colorado Agricultural Meteorological Network  
**CP**: Center Pivot  
**CSU**: Colorado State University  
**CV**: Coefficient of variation  
**CWCB**: Colorado Water Conservation Board  
**CWI**: Colorado Water Institute  
**DP**: Deep percolation  
**DPF**: Deep percolation fraction  
**DS/Downstream**: Downstream of the John Martin Reservoir  
 $D_{wt}$ : Water table depth  
 $D_{wt_c}$ : Critical water table depth  
 $D_{rz}$ : Depth of soil root zone below ground surface  
 $E_a$ : Irrigation application efficiency  
**EC**: Specific conductance (electrical conductivity at 25°C)  
 $EC_e$ : Saturated paste extract soil salinity  
**ED**: Earthen Ditch Water Delivery  
 $EM_H$ : Horizontal orientation measurement with EM83 tool  
 $EM_V$ : Vertical orientation measurement with EM83 tool  
**ET**: Evapotranspiration  
 $ET_a$ : Actual evapotranspiration  
 $ET_i$ : Instantaneous actual evapotranspiration  
 $ET_p$ : Potential crop ET at a particular time  
 $ET_r$ : Reference crop evapotranspiration  
 $f_0$ : Steady-state infiltration rate  
 $G_i$ : Heat conduction to the ground  
**GIS**: Geographic information system  
**GP**: Gated Pipe Water Delivery  
**GPS**: Global Positioning System  
**GUI**: Graphical User Interface  
 $H_i$ : Sensible heat flux  
**IDS**: Integrated Decision Support  
**IDSCU**: Integrated Decision Support Consumptive Use Model  
 $k$ : Empirical coefficient for infiltration  
 $k_c$ : Crop coefficient  
**LARV**: Lower Arkansas River Valley  
**LAVWCD**: Lower Arkansas Valley Water Conservancy District  
 $L_v$ : Latent heat of vaporization  
**NASS**: National Agricultural Statistics Service  
**NRCS**: Natural Resources Conservation Service  
**NVDI**: Normalized difference vegetation index  
**PVC**: Polyvinyl chloride  
 $Q_A$ : Net volume of water applied to the field by irrigation over  $\Delta t$   
 $Q_{DP}$ : Volume of water leaving the root zone by deep percolation over  $\Delta t$   
 $Q_{ET}$ : Volume of water leaving the root zone by evapotranspiration over  $\Delta t$   
 $Q_f$ : Volume of water infiltrated into the soil root zone from irrigation over  $\Delta t$   
 $Q_p$ : Volume of water infiltrated into the soil from effective rainfall over  $\Delta t$   
 $Q_{PT}$ : Total volume of rainfall over  $\Delta t$   
 $Q_R$ : Volume of precipitation runoff over  $\Delta t$   
 $Q_{TW}$ : Tailwater runoff volume over  $\Delta t$   
 $Q_U$ : Volume of water entering the root zone by upflux from the groundwater table over  $\Delta t$   
 $q_u$ : Rate of water entering root zone by upflux from the groundwater table  
 $q_{u_{max}}(D_{wt}, ET_p)$ : Maximum potential groundwater upflux rate (mm/day) as a function of  $D_{wt}$  and  $ET_p$   
 $R_{n,i}$ : Net radiation  
**SECWCD**: Southeastern Colorado Water Conservancy District  
 $S_R$ : Maximum soil retention volume per unit area  
 $S_{SW}$ : Volume of water stored in the root zone  
 $S_{SW_c}(D_{wt})$ : Critical soil water content at which upflux is initiated and, a function of  $D_{wt}$   
 $S_{SW_{FC}}$ : Water content in the root zone at field capacity  
 $S_{SW_s}(D_{wt})$ : Steady soil water content (mm), a function of  $D_{wt}$   
 $S_{SW_{WP}}$ : Water content in the root zone at wilting point  
**TAW**: Total available water  
**TDS**: Total dissolved solids  
**TRF**: Tailwater runoff fraction  
**USDA**: U.S. Department of Agriculture  
**US/Upstream**: Upstream of the John Martin Reservoir  
 $W_{bag}$ : Weight of plastic bag (used in  $WC_{AD}$  analysis)  
**WBC**: Water balance component  
 $WC_{AD}$ : Air-dried gravimetric water content  
 $W_{can}$ : weight of metal can (used in  $WC_{OD}$  analysis)  
 $WC_{OD}$ : Oven-dried gravimetric water content  
 $W_{ds}$ : Weight of dry soil sample (including bag) (used in  $WC_{AD}$  and  $WC_{OD}$  analysis)  
 $W_{ws}$ : Weight of wet soil sample (including bag) (used in  $WC_{AD}$  and  $WC_{OD}$  analysis)  
 $z$ : Infiltration depth

# Acknowledgements

This study was funded primarily by grants from the Colorado Water Conservation Board, the Colorado Division of Water Resources, the Colorado Department of Public Health and Environment, the Southeastern Colorado Water Conservancy District, the Lower Arkansas Valley Water Conservancy District, and the Colorado Agricultural Experiment Station. Financial support also was provided by the Colorado Water Institute, the United States Department of Agriculture (USDA), the United States Bureau of Reclamation, and the United States Geological Survey. Valuable in-kind support was provided by the La-Junta Area Office of the USDA Natural Resources Conservation Service, and the attentive and able assistance of Lorenz Sutherland in that office especially is appreciated. The study could not have been conducted without the interested cooperation of more than 120 landowners in the LARV, including about 40 who allowed intensive monitoring of their irrigation practices. Numerous students, technicians, and professionals lent their care and capabilities to the monitoring and analysis of irrigated fields and to project management. The authors particularly are indebted to the able assistance of Nathan Baker who helped with literature review, data analysis, modeling runs, and documentation. They also thank Roberto Arranz, J.J. Autry, Mike Bartolo, Adam Berrada, Chad Bohac, Mallory Cline, Morgan Cline, Tyler Curley, Ginger Davidson, Jeff Davidson, Ahmed Eldeiry, Patrick Greenbank, Jack Goble, Lenay Goble, Andres Jaramillo, Matthew Klein, Paula Miller, Dave Patterson, Ryan Pelton, Bret Schafer, Grant Seeley, Samantha Stuart, Matthew Vandiver, Ben Weber, Mike Weber, and Corda Williams. The authors are very grateful for all of this support and cooperation.



## Photo Credits:

**Cover:** From top left, irrigation, Fort Lyon Canal, a field, and sprinkler in the Lower Arkansas River Valley. Photos by Bill Cotton, CSU Photography

**Title page & 80:** Catlin Canal. Photo by Bill Cotton, CSU Photography

**Table of Contents & 116:** Aerial view of the Fort Lyon Canal in the Lower Arkansas River Basin. Photo by Bill Cotton, CSU Photography

**This page:** Irrigation in the Arkansas River valley. Photo by Bill Cotton, CSU Photography

**Page 11, Page 96:** Lower Arkansas River Valley. Photo by Bill Cotton, CSU Photography

**Page 15:** Aerial view of the Fort Lyon Canal in the Lower Arkansas River Basin. Photo by Bill Cotton, CSU Photography

**Page 18-19:** John Martin Reservoir in the Lower Arkansas River Basin. Photo by Bill Cotton, CSU Photography

**Page 22-23 & 45:** Field in Lower Arkansas River Valley. Photo by Bill Cotton, CSU Photography

**Page 26-27 & 75:** Bents Old Fort National Historic Site. Photo by J. Stephen Conn

**Page 40:** Water ripples. Photo by Jeremy Reid

**Page 43:** Aerial view of the Lower Arkansas River Basin. Photo by Bill Cotton, CSU Photography

**Page 47:** Field irrigation. Photo by Kay Ledbetter

**Page 60:** Canal in the Lower Arkansas River Valley. Photo by Bill Cotton, CSU Photography

**Page 68, Page 76-77:** Irrigation on Roger Maddox Farm near Swink, Colorado. Photo by Bill Cotton, CSU Photography

**Page 83, Page 93, Page 98, Page 110:** Fields in the Lower Arkansas River Valley. Photo by Bill Cotton, CSU Photography  
**Page 88:** Farm in Lower Arkansas River Valley. Photo by Bill Cotton, CSU Photography

**Page 103:** Aerial view of the Arkansas River between La Junta and Las Animas, Colorado. Photo by Bill Cotton, CSU Photography

**Back Cover:** Aerial view of the Fort Lyon Canal in the lower Arkansas River basin. Photo by Bill Cotton, CSU Photography

# Summary

The Lower Arkansas River Valley (LARV) in Colorado has a long history of rich agricultural production, but is facing the challenges of soil salinity and waterlogging from saline shallow groundwater tables, high concentrations of salts and minerals in the river and its tributaries, water lost to non-beneficial consumption, and competition from municipal water demands. Significant improvements to the irrigated stream-aquifer system are possible, but they are constrained by the need to comply with the Arkansas River Compact. Making the best decisions about system improvements and ensuring compact compliance require thorough baseline data on irrigation practices in the LARV. This report summarizes the methods, analysis, results, and implications of an extensive irrigation monitoring study conducted by Colorado State University (CSU) during the 2004-2008 irrigation seasons in representative study regions upstream and downstream of John Martin Reservoir (referenced herein as Upstream and Downstream). A total of 61 fields (33 surface-irrigated, 28 sprinkler-irrigated) were investigated. Results from 523 monitored irrigation events on these fields are presented. Data and modeling results from more extensive studies conducted by CSU between 1999 and 2008 also are provided.

Data on applied irrigation, field surface water runoff, precipitation, crop evapotranspiration (ET), irrigation water salinity, soil water salinity, depth and salinity of groundwater tables, upflux from shallow groundwater, crop yield, return flows to streams, and salt loads to streams are presented. Deep percolation and application efficiency for irrigation events on each field are estimated using a water balance method implemented within the CSU Integrated Decision Support Consumptive Use (IDSCU) Model. Tailwater runoff (surface water runoff at the end of a field) fraction ranges from zero to 69 percent on surface irrigated fields, averaging about eight percent, while deep percolation fraction ranges from zero to 90 percent, averaging about 24 percent. Application efficiency ranges from two to 100 percent on surface irrigated fields, with an average of about 68 percent. No significant runoff is observed on sprinkler-irrigated fields, and estimated deep percolation typically is negligible. On sprinkler-irrigated fields average application efficiency is about 82 percent, but in many cases these fields are under-irrigated. Upflux from shallow groundwater tables below irrigated fields

is estimated to average about six percent of crop ET, ranging between zero percent and 40 percent. Average measured total dissolved solids concentration of applied surface irrigation water is 532 mg/L Upstream and 1,154 mg/L Downstream. Average estimated salt load applied per surface irrigation event is 997 lb/acre Upstream and 2,480 lb/acre Downstream. Average estimated salt load applied per sprinkler irrigation event is 1,217 lb/acre Upstream and 446 lb/acre Downstream. Soil saturated paste electrical conductivity averaged over all Upstream fields ranges from 3.7-4.7 deciSeimens per meter (dS/m) over the monitored seasons and from 4.5-6.4 dS/m over Downstream fields. Water table depth averaged over Upstream fields varies from 7.8-12.1 feet over the monitored seasons and average specific conductance (EC) of groundwater varies from 1.8-2.3 dS/m. Water table depth averaged over Downstream fields varies from 12.6-15.0 feet with average EC from 2.3-3.0 dS/m. Analysis reveals trends of decreasing crop ET with increasing soil salinity on several investigated fields. Trends of decreasing relative crop yield with increasing soil salinity on corn and alfalfa fields also are detected.

Calibrated regional groundwater models indicate an average recharge rate to shallow groundwater of 0.10 in/day and 0.06 in/day over modeled irrigation seasons 1999-2007 Upstream and 2002-2007 Downstream, respectively. Upflux to non-beneficial ET in the regions is estimated to be about 26,000 ac-ft/year Upstream and 35,000 ac-ft/year Downstream, with an approximation for the entire LARV being 82,000 ac-ft/year. Average groundwater return flow rate to the Arkansas River within the Upstream and Downstream regions is estimated as 30.9 ac-ft/day per mile and 12 ac-ft/day per mile along the river, respectively. Salt load in return flow to the river over the modeled years is estimated at about 93 tons/week per mile Upstream and about 62 tons/week per mile Downstream.

The significance and implications of these findings are discussed. Also, a number of specific questions of concern to water managers and regulatory agencies are addressed.



# Introduction

## Irrigation in the Arkansas River Valley

The LARV in Colorado has long been known for its valuable agricultural production. The introduction of extensive irrigation to the fertile alluvial soils in the valley in the late 19th century has created a widespread agriculturally based economy with important benefits not only on a regional scale, but also to the state of Colorado (Sherow 1990). Over the years, however, groundwater tables in the basin have risen in elevation and in salt concentration due to excessive irrigation, seepage from earthen canals, and inefficient drainage systems, creating a number of challenging problems. These high-saline water tables have in turn salinized and waterlogged much of the rich soil of the river valley, causing reductions in crop yield. High water tables also produce high hydraulic gradients that drive subsurface flows back to tributaries, open drains, and to the river.

In some locations along the LARV, these return flows can dissolve salts and minerals (like selenium and uranium) that naturally occur in the Arkansas Valley's marine shale outcrops and bedrock and from shale-derived soils as the water moves through the underlying aquifer, further increasing constituent loads as they make their way back to streams (Gates et al. 2009). In other locations along the LARV, particularly east of La Junta, precipitation of calcium sulfate (gypsum), calcium carbonate (lime), and other salts may serve to mitigate these salt loading problems. Lastly, high groundwater tables extend out under uncultivated and fallow land where substantial amounts of water are non-beneficially consumed and groundwater solute concentrations rise due to evaporative upflux from the shallow water table (Niemann et al. 2011).

There are a total of about 270,000 irrigated acres in the LARV, with irrigation practiced on about 14,000 fields. Water supply is provided by 25 canals that divert water from the river in accordance with Colorado water law and from about 2,400 wells that pump from the alluvial groundwater. The vast majority of fields are irrigated using surface-irrigation methods with less than about five percent irrigated with sprinklers (typically, center-pivot sprinklers) or drip lines.

The LARV irrigation system's operation is severely constrained by the Arkansas River Compact (with Kansas), which prohibits changes to the system that would increase the irrigated acreage of the return flow

patterns (amount, spatial pattern, and timing) so as to cause the flow in the Arkansas River to be "materially depleted in usable quantity or availability for use to the water users in Colorado and Kansas." Hence, reductions in excess surface or subsurface flows that result from increases in irrigation efficiency, with the aim of mitigating the problems described above, are prohibited unless otherwise augmented. Improvements in irrigation application efficiency (by reducing surface runoff and/or deep percolation, DP) and/or in conveyance efficiency (by reducing canal seepage) that diminish return flows to the river must be offset by appropriate changes in river operation, such as with amended releases from reservoir storage. If improved irrigation efficiency can indeed be achieved in conjunction with such offsetting measures, then crop yields can be increased, river water quality can be improved, and water can be conserved (Triana et al. 2010a, 2010b).

An evaluation of on-going water use practices and the potential impacts of improvements to any water resources system requires the establishment of an accurate description of the current state, or the baseline, of the system. In the irrigated alluvial lands of the LARV, such a baseline needs to be determined for irrigation practices and efficiency, with consideration to interventions that could address current irrigation problems while complying with the Arkansas River Compact. A baseline evaluation involves estimating the various features and water balance components of field irrigation systems, including the following:

- Irrigation timing, total water applied, water consumed for crop evapotranspiration (ET), tailwater runoff, DP below the root zone, and upflux returned from the shallow water table
- Salinity of irrigation and drainage water
- The movement and accumulation of dissolved salts on irrigated fields
- General soil characteristics
- Groundwater table characteristics
- Crop yields that result from irrigation practices

Such data may provide insight into the effect of soil water salinity, as affected in part by irrigation water salinity, and irrigation practices on crop yield and ET. Analysis of such data would show the fraction of

irrigation diversions from the river that are consumed beneficially by crops, as compared to the fractions that return to the river system via surface and groundwater flows as well as those that are non-beneficially consumed.

## Background and Scope of This Study

During the irrigation seasons over the period 2004-2008, CSU conducted an extensive field investigation of current irrigation practices in the LARV, primarily under funding from the Colorado Water Conservation Board (CWCB), the Colorado Division of Water Resources (CDWR), the Colorado Department of Public Health and Environment (CDPHE), the Southeastern Colorado Water Conservancy District (SECWCD), the Lower Arkansas Valley Water Conservancy District (LAVWCD), and the Colorado Agricultural Experiment Station (CAES). Additional support was provided from other agencies listed in the “Acknowledgments” section at the end of this report.

Data were gathered from numerous fields, spread across two study regions under both conventional surface irrigation methods and sprinkler irrigation technologies

(such as sprinkler and drip irrigation). The first study region was located upstream of John Martin Reservoir (Upstream), extending between Fowler and Las Animas, and the second region was downstream of the reservoir (Downstream), extending between McClave and the Colorado-Kansas state line (Figure 1). These two areas generally coincide with the study regions where CSU has been conducting intensive field-scale and regional-scale studies of the irrigated stream-aquifer system of the LARV since 1999 (Burkhalter and Gates 2005, Gates et al. 2006).

During the 2004, 2005, and 2006 irrigation seasons, CSU collected data from a total of 33 fields, 14 in the Upstream Study Region and 19 in the Downstream Study Region. Three of the Upstream fields were served by a sprinkler, three were supplied with surface water, and one was supplied with groundwater. Sprinklers supplied with surface water served five of the fields in the downstream area—four from the Fort Lyon Canal, and one from the Amity Canal.

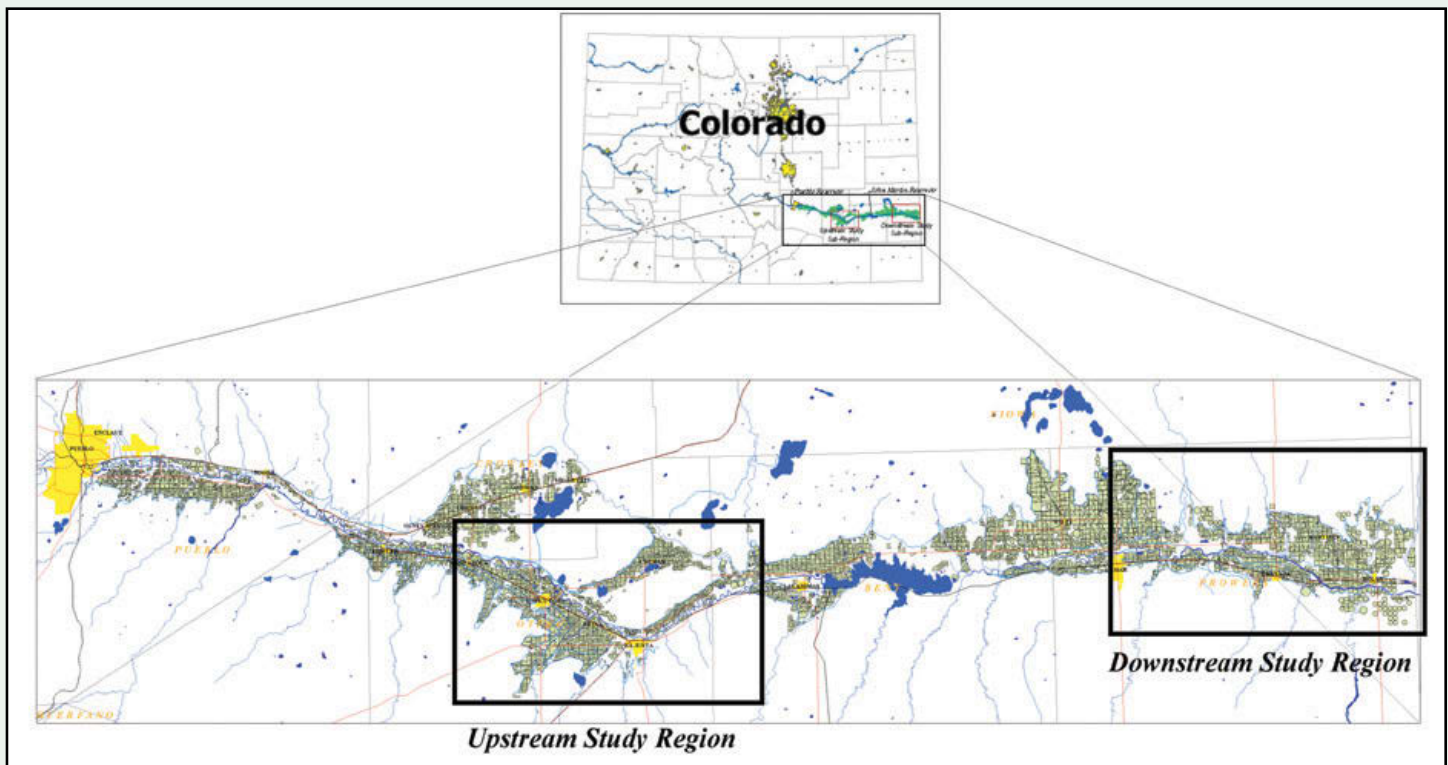


**Figure 1.** LARV in Colorado highlighting the upstream and downstream study regions

This work was performed primarily under a contract with the CWCB entered in May 2004, to address questions raised in the *Kansas v. Colorado* litigation before the U.S. Supreme Court regarding whether and how salinity and/or irrigation timing and amount affect crop yield and ET in the LARV. Major support also was provided for these efforts from the CDPHE, the SECWCD, the LAVWCD, and the CAES. As part of this effort, CSU conducted measurements on participating farmers' fields regarding their irrigation practices and salinity conditions.

In 2007, with funding primarily from the CDPHE, the SECWCD, the LAVWCD, and the CAES, measurements were made only in the Downstream region, where eight surface-irrigated fields and five sprinkler-irrigated fields were monitored. In 2008, data from a larger sample size were desired to improve confidence in the conclusions that could be drawn from the 2004-2007 data, and to examine more carefully the differences between sprinkler irrigation and surface irrigation. CSU conducted this research largely under a contract funded by CDWR for "Early-Season Monitoring of Irrigation Practices under Conventional and Improved Technologies in Colorado's Lower Arkansas River Valley" and a purchase order funded by CWCB for "Late Season Monitoring" of the same type, with assistance from the LAVWCD and the CAES. Under these two agreements, irrigation events were measured on a total of 10 surface-irrigated fields (including a number of corners on sprinkler-irrigated fields) and 19 sprinkler-irrigated fields. All of the sprinkler-irrigated fields drew water from canals, and one was supplemented with well water.

Over the entire study period from 2004-2008, 229 surface irrigation events on 33 separate fields and 291 sprinkler irrigation events on 28 separate fields were measured and evaluated. Three subsurface drip systems in the Upstream Study Region also were monitored in 2005, but the results are not reported herein. The data gathered in this study, in conjunction with other available data gathered by CSU under related projects, allow a description of existing conventional and sprinkler technologies and the possible effects of soil salinity and irrigation management practices on ET, crop yield, and return flows to the stream system. This description was extended from the field scale to the regional scale using calibrated and tested groundwater models.

This document describes the study objectives, setting, methodology, and results. Broad conclusions and implications are drawn regarding baseline irrigation practices in the LARV. Questions that still remain, and recommendations for addressing them, are presented.

## Study Objectives

The objectives of the study described in this report are summarized as follows:

1. Measure, estimate, or calculate each major irrigation water balance component (WBC) and associated properties for a few irrigation events on each of several representative irrigated fields over the study period. Fields irrigated by both conventional and improved technology (sprinkler) systems are considered. Considered WBCs include:
  - Irrigation flow onto the field
  - Irrigation surface flow off the field (tailwater runoff)
  - Precipitation
  - Infiltration
  - Evapotranspiration
  - Soil water storage
  - Upflux from shallow groundwater
  - Deep percolation
  - Sprinkler evaporation and drift
2. Calculate irrigation application efficiency,  $E_a$ , for measured irrigation events under conventional and improved technology systems
3. Conduct measurements to describe irrigation water quality:
  - Specific conductance of irrigation water applied and in tailwater runoff water
  - Salt ions in irrigation water applied and tailwater runoff water
4. Measure and/or estimate characteristics of shallow groundwater under irrigated fields:
  - Water table depth
  - Specific conductance of groundwater
  - Salt ions in groundwater

5. Conduct measurements to estimate soil water salinity distributed over irrigated fields
  6. Conduct measurements to estimate crop yields over irrigated fields
  7. Address issues associated with uncertainty in the data
  8. Use calibrated regional-scale models to perform a preliminary extension of the results of field-scale studies to regional-scale conditions for the LARV in regard to crop ET, upflux from water tables to ET, return flows and salt loads to streams, and other processes that vary over LARV regions that are representative of conditions Upstream and Downstream
  9. Use data derived from measurements, estimation, and calculation to address some questions of concern to water managers and regulatory agencies, including the following:
    - How do the characteristic irrigation WBC and  $E_a$  values for sampled conventional surface irrigation systems compared to those for improved technology (especially sprinkler) systems?
    - Do the characteristic WBC and  $E_a$  values for irrigation events seem to vary significantly from canal to canal; which is to say, do the values appear to be affected by total water supply available from one canal to another, within a single year?
    - Do the characteristic WBC and  $E_a$  values vary significantly from year to year within the same canal system; i.e., are they affected by total water supply available within a canal?
    - Do the characteristic WBC and  $E_a$  values differ between surface-water supplied sprinklers and groundwater-supplied systems?
    - Is there any indication of intentional bias introduced into the study by irrigators hoping to demonstrate that the achievable WBC and  $E_a$  values using surface-supplied sprinklers is no different than that associated with flood and furrow methods?
    - Do the data indicate any effect of soil salinity on crop yield? If so, what conclusions can be reached with these data, and what additional information is necessary to adequately quantify the impact of soil salinity on crop yield in the LARV?
- Do the data indicate any effect of irrigation timing or amount on crop yield? If so, what conclusions can be reached with these data, and what additional information is necessary to adequately quantify the impact of irrigation management practices on crop yield in the LARV?
  - What are the known or assumed possibilities and limitations for correlating crop yield and soil salinity to ET for the fields included in this study?
  - Does crop type appear to affect WBC and  $E_a$  under sprinkler systems?
  - Do sprinkler irrigators typically apply sufficient volumes of water necessary to meet the ET requirement of crops?
  - Do sprinkler irrigators apply sufficient water to meet the salt leaching requirement for the soil root zone?
  - What is the difference in the WBC and  $E_a$  values for sprinkler systems that practice leaching and those that do not?
  - Are there significant differences in deep percolation and leaching fraction for various types of sprinkler systems?
  - How do alfalfa crop yields from sprinkler irrigated fields compare with those irrigated by flood and furrow irrigation methods?
  - How do water table depth and salinity, soil salinity, and crop yields relate to WBC and  $E_a$ ?

# Study Sites and Conditions

## Field Locations and Layouts

A total of 22 separate field units in the Upstream Study Region and 39 in the Downstream Study Region were included in the 2004-2008 study. Monitored fields were selected based upon the following criteria: (1) a distribution over the spatial extent of the monitored regions, including a variety of types of irrigation systems and water sources; (2) cooperation of land owners/operators with study objectives and methods; and (3) accessibility and layout that facilitated feasible and accurate measurement of desired components. Figures 2 and 3 show the locations of the monitored fields within the Upstream and Downstream regions, respectively.

Monitored fields are identified based upon which study region they are part of (US for Upstream and DS for Downstream) and by a number, usually assigned in

the order in which the field was included in the study (Figures 2 and 3). For fields that are part of the same farm unit and share the same water right, a letter is added following the identification number (e.g., DS6A, DS6B). Separate fields were defined on the same farm unit when they contained different crops, were irrigated by different methods, and/or were separated by physical boundaries. Field US13 (Figure 4) is an example of a singular field parcel selected for monitoring within a farm. An example of a case where several fields make up portions of the same farm unit is shown in Figure 5. Fields DS18A, DS18B, DS18C, and DS18D were defined as separate fields within the same center pivot sprinkler circle because they contained different crops. Fields DS18E, DS18F, DS18G, and DS18H form the corners of the quarter section block containing the center pivot sprinkler. These corner fields were each independently surface irrigated. Maps showing layouts of all of the study fields are available on an accompanying Arkansas River Irrigation Data and Analysis Disc (ARIDAD) upon request from the Colorado Water Institute at CSU ([CWI@ColoState.edu](mailto:CWI@ColoState.edu)).

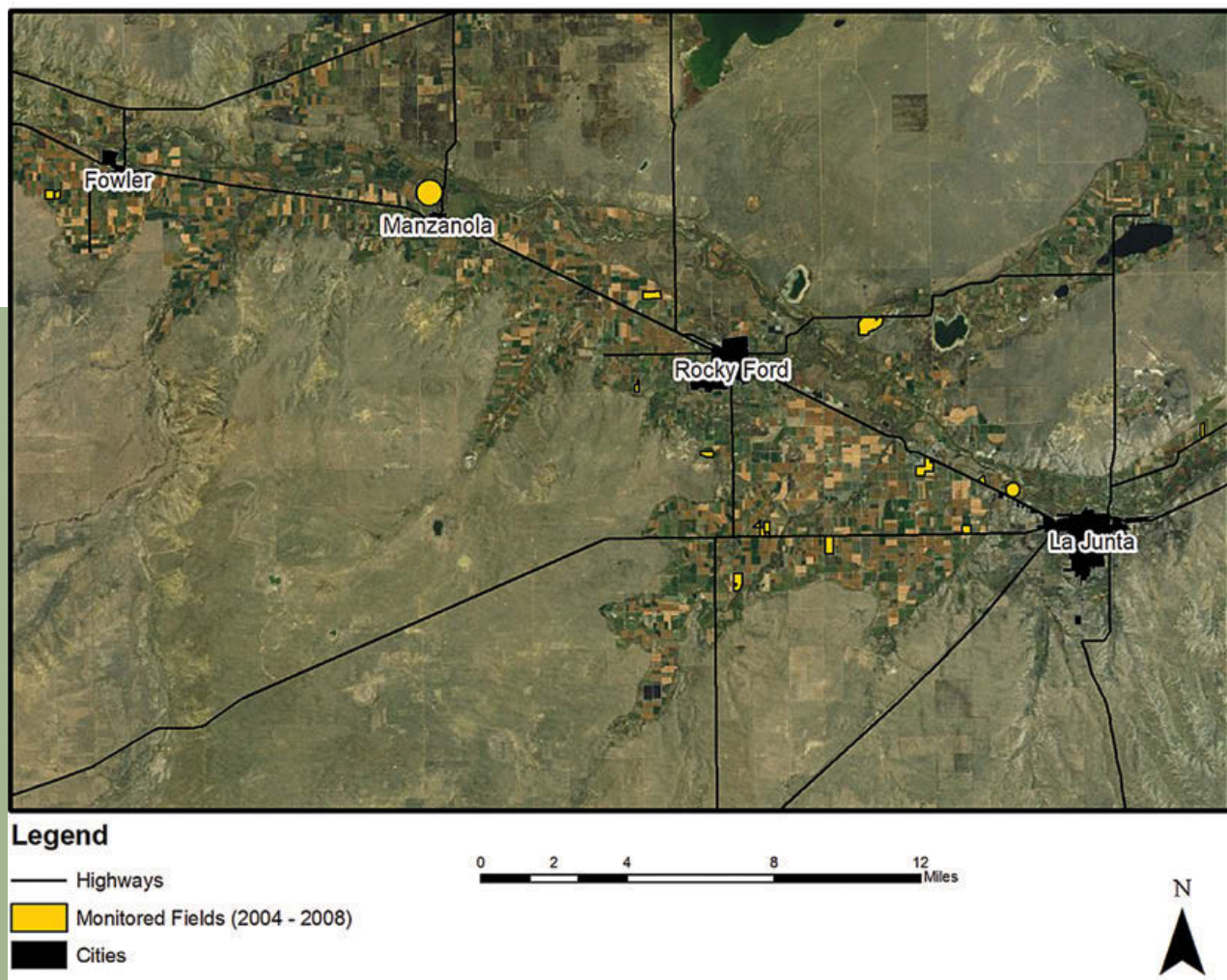
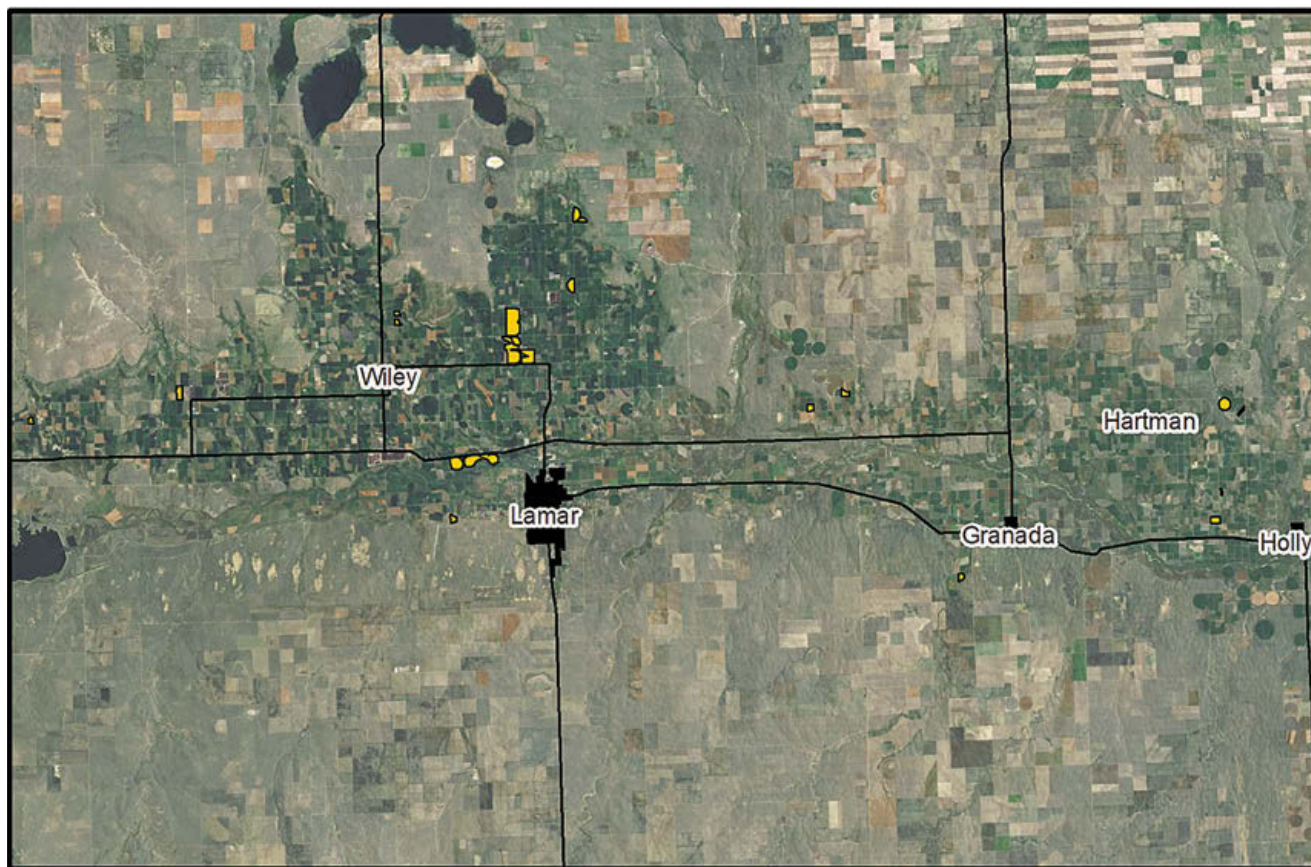


**Figure 2.** Monitored fields in Upstream Study Region



**Legend**

- Highways
- Monitored Fields (2004 - 2008)
- Cities



**Figure 3.** Monitored fields in Downstream Study Region

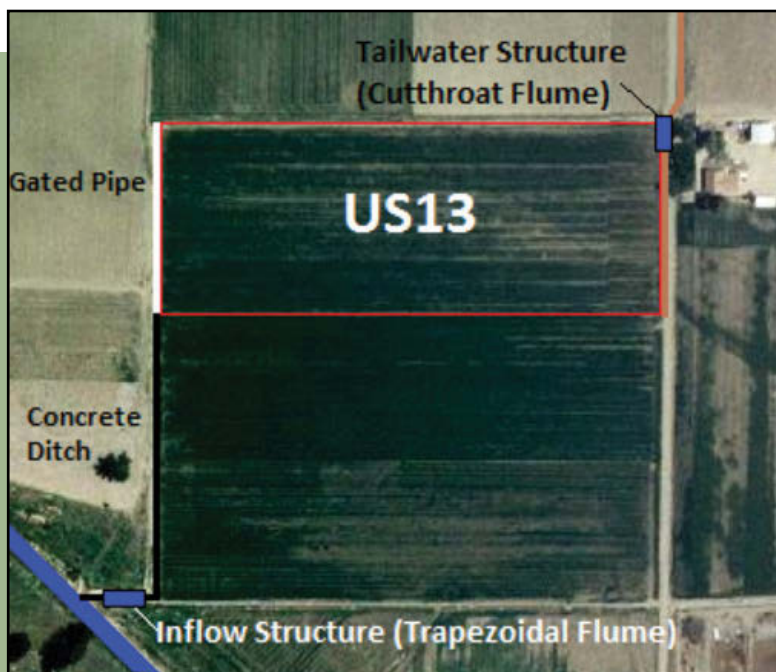


**Figure 4 (left).** Layout of field US13

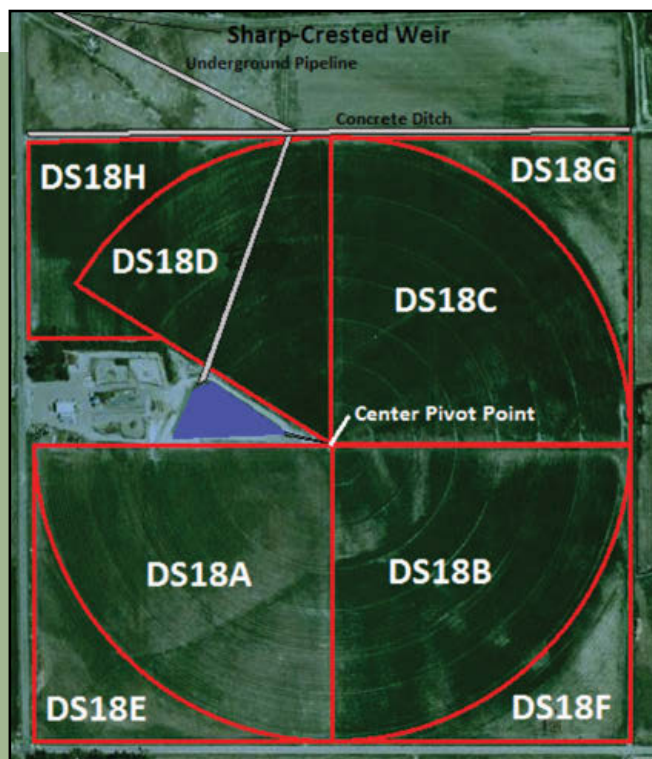


**Figure 5.** Layout of fields DS18A, DS18B, DS18C, DS18D, DS18E, DS18F, DS18G, and DS18H within the same farm unit

In many fields, particularly those utilizing surface water from canal systems with rotational water allotment operations, the duration of an irrigation event was too short to irrigate the entire field area. During dry periods, these fields often went several weeks between irrigation events, so that irrigation of the entire field spanned a period of several weeks or longer. Similarly, for fields under canal systems with more junior water rights, or during drought conditions, irrigation water often was directed away from the monitored field to another field containing a higher-valued crop in need of water application. The most typical case was to direct water from alfalfa crops to corn or sorghum crops. These practices created differences in infiltrated water, soil-water content, and actual ET rates across the field area over

time. Hence, fields monitored in this study often were subdivided into cells, or subfields, for the purpose of measuring and modeling irrigation events. In many irrigation events, available irrigation water was applied to only one cell. In other events, multiple cells within a field were irrigated simultaneously. For example, field US9 was divided into two cells, as seen in Figure 6.

For center-pivot sprinkler irrigated fields utilizing surface water, especially for rotational allotment canal systems, the difference in starting and ending locations of the rotating sprinkler line during an irrigation event often created “wedges” within a field that received different applied irrigation amounts than did other parts of the field over time. In many cases, the frequency of irrigation events dampened the effect of differences in

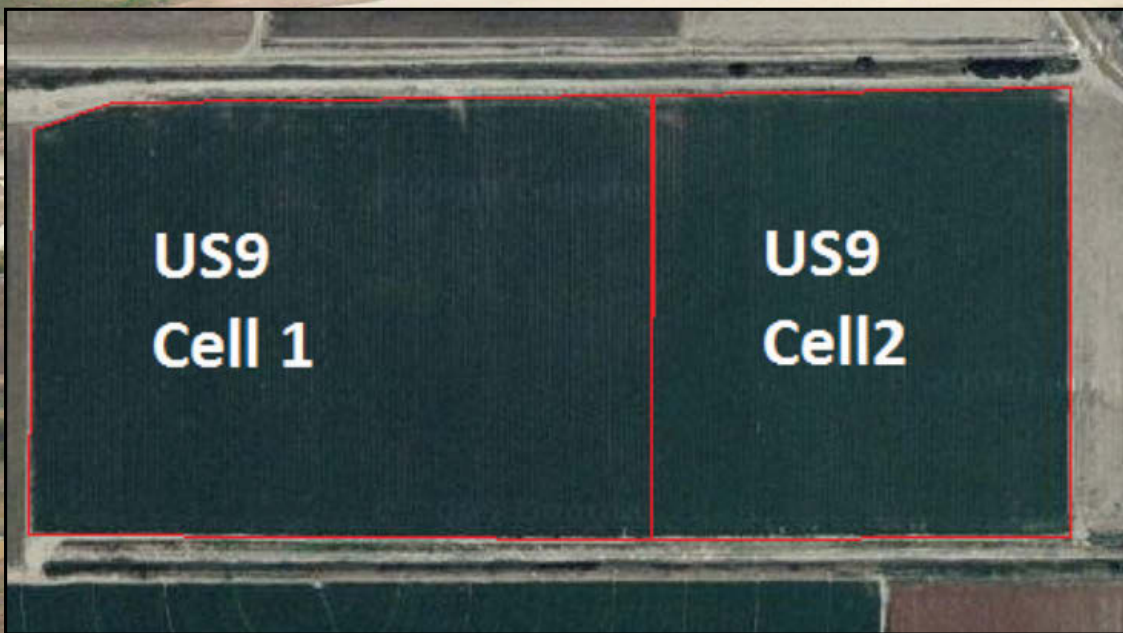


**Figure 6.** Layout of field US9, showing two separately irrigated cells within the field

**John Martin Reservoir in the Lower Arkansas River Basin**

irrigation timing on actual ET across the field area, but in some cases it did not.

Several fields were dropped from the study along the way for various reasons (such as physical changes to an irrigation system making it infeasible to monitor). A number of fields received no application of irrigation water during some seasons, due to water availability situations or the timing of the study, and data collection on these fields was limited to soil textural analysis, precipitation, ET, and soil salinity surveys.

## Hydrological Setting

The hydrological conditions in the LARV during the period of this study (2004-2008) in relation to long-term

hydrological conditions can be inferred from the plots in Figures 7 through 9. Figure 7 shows plots of the daily average flow rate in the Arkansas River at the Catlin Dam Near Fowler, Colorado (Station ID 07119700) gauging station, located near the upstream end of the Upstream Study Region, and at the gauging station Below John Martin Reservoir (Station ID 07130500), located near the upstream end of the Downstream region. A plot is shown for average conditions over the period 1975 (first year of Pueblo Reservoir)-2010 along with corresponding plots for each year within the period of this study. Cumulative daily precipitation recorded at the Colorado Agricultural Meteorological Network (CoAgMet) Stations at Rocky Ford (RFD01) in the Upstream Study Region averaged over 1992-2010

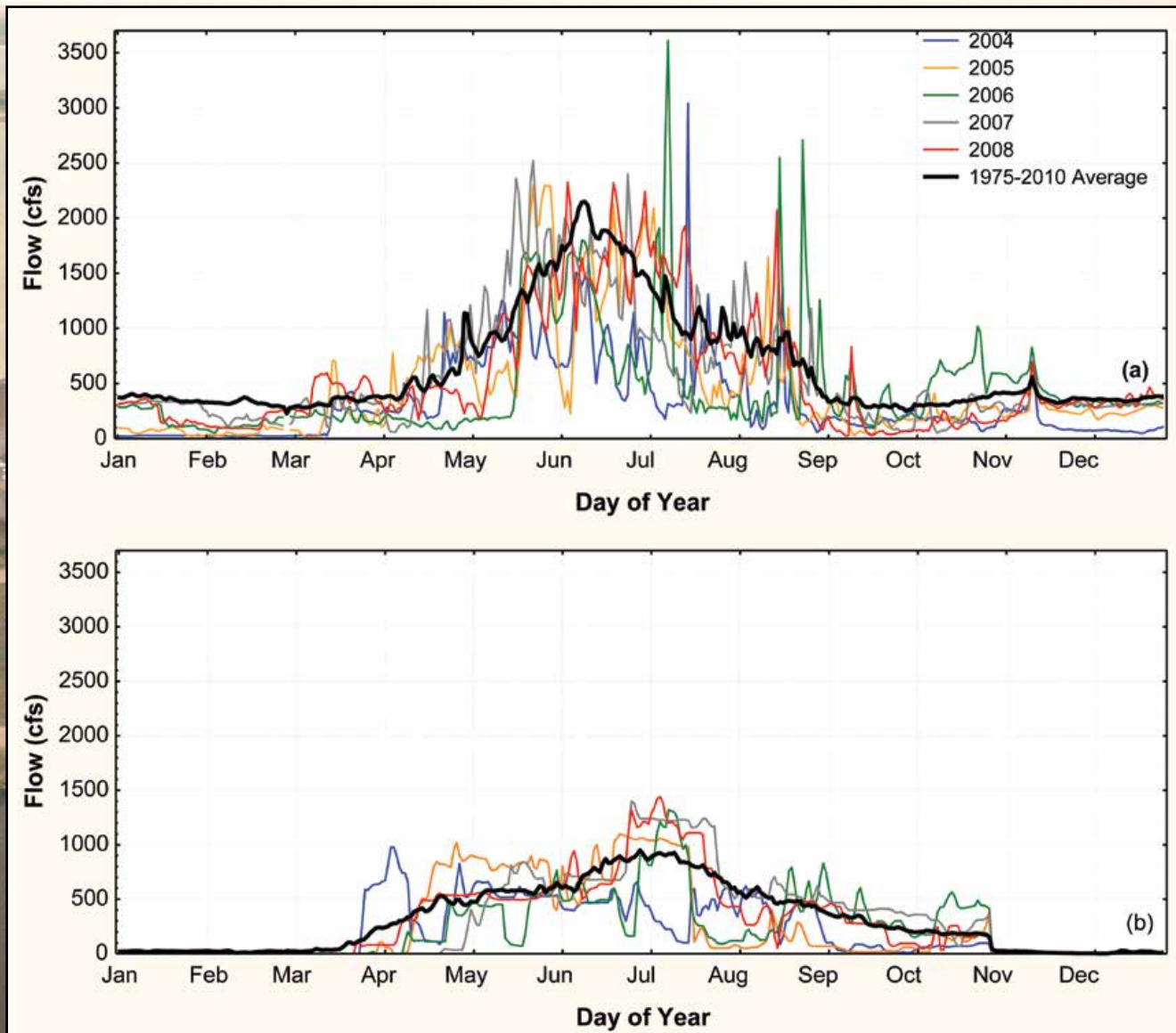


**Figure 7.** Daily average flow rate in Arkansas River at (a) Catlin Dam Near Fowler, CO gauge and at (b) Below John Martin Reservoir gauge for study years compared to mean daily average flow rate for period 1975-2010

and at Lamar (LAM02/LAM04) in the Downstream Study Region, averaged over 1998-2010, are plotted in Figure 8 with comparison precipitation plots for each of the years of this study. Cumulative daily reference crop evapotranspiration ( $ET_r$ ) calculated using the Penman-Monteith method (Allen 2005) for each of the study years, compared with the 1992-2010 average, are plotted for the Rocky Ford (RFD01) CoAgMet station in Figure 9a. Similar plots for the Lamar (LAM02/LAM04) station for the years 2006 and 2007 (data were incomplete for the other study years) are compared with the 1999-2010 average in Figure 9b.

Comparison of the regulated river flow at the Catlin Dam Near Fowler, Colorado and Below John Martin Reservoir gauges during the study period to mean regulated flow rates over 1975-2010 reveal that the study period generally represents a relatively dry period of

record in terms of streamflow, although there are times within each year when conditions were wetter than average. The 2004-2006 seasons were particularly dry, with 2007 and 2008 being closer to normal. Total annual flow volumes at the Catlin Dam Near Fowler, Colorado gauge on the Arkansas River for 2004, 2005, 2006, 2007, and 2008 were 50 percent, 73 percent, 71 percent, 90 percent, and 86 percent, respectively, of the mean annual flow volume over 1975-2010. Total annual flow volumes at the Below John Martin Reservoir gauge for 2004, 2005, 2006, 2007, and 2008 were 69 percent, 81 percent, 75 percent, 103 percent, and 96 percent, respectively, of the mean annual flow volume over 1975-2010.

Though the study period was relatively dry in relation to river flows available for diversion, the data in Figures 8 indicate that rainfall in the study regions over this period was close to normal or above normal with the

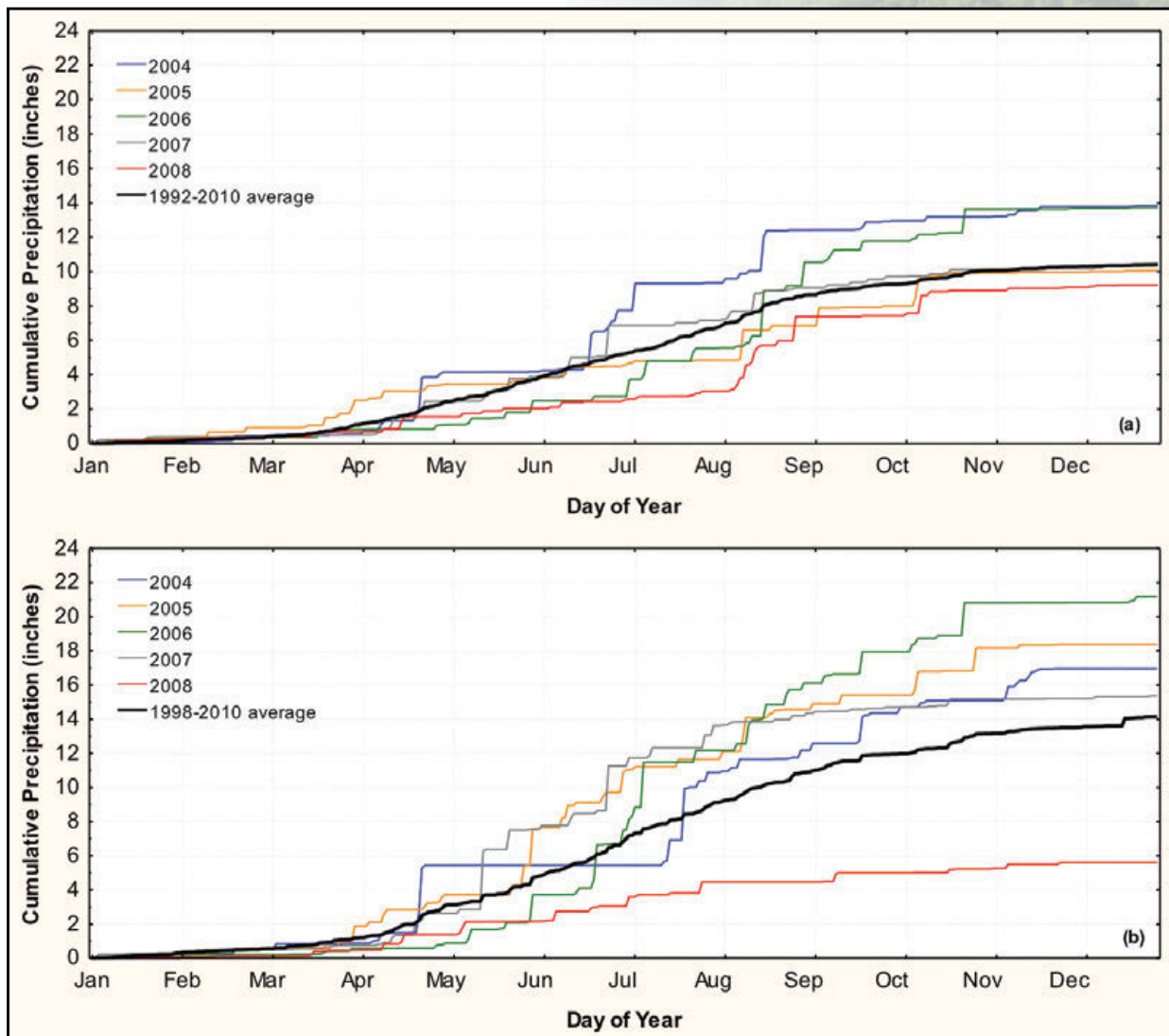


**Figure 8.** Cumulative precipitation recorded for each of the study years 2004-2008 and (a) averaged over the years 1992-2010 at the CoAgMet Rocky Ford (RFD01) weather station, and (b) averaged over the years 1998-2010 at the CoAgMet Lamar (LAM02/LAM04) weather station

exception of 2008. Precipitation at the Rocky Ford (RFD01) weather station in years 2004, 2005, 2006, and 2007 was 133 percent, 96 percent, 132 percent, and 100 percent, respectively, of the 1992-2010 average, while 2008 precipitation was 89 percent of the 1992-2010 average. At the Lamar (LAM02/LAM04) weather station, precipitation in years 2004, 2005, 2006, and 2007 was 120 percent, 130 percent, 150 percent, and 109 percent, respectively, of the 1998-2010 average, while 2008 precipitation was only 40 percent of the 1998-2010 average.

Also, from Figure 9,  $ET_r$  over the study period appears to be generally below the average over recent years.  $ET_r$  estimated from data at the Rocky Ford (RFD01) weather station in years 2004, 2005, 2006, 2007, and 2008 was 91 percent, 97 percent, 100 percent, 87 percent, and 98 percent, respectively, of the 1992-2010 average. At the

Lamar (LAM02/LAM04) weather station, estimated  $ET_r$  for 2006 and 2007 was 96 percent and 89 percent, respectively, of the 1999-2010 average.

### Irrigation Characteristics

For each field (or farm collection of fields), the irrigation water source, the type of irrigation system, and the number of irrigations measured during each season are summarized in Tables 1 and 2 for the Upstream and Downstream Study Regions, respectively. Most of the fields were supplied water from one of seven different canals. Groundwater wells provided water to 10 of the fields studied. A total of 33 conventional surface irrigated fields were studied. The 28 sprinkler-irrigated fields (eight Upstream, 20 Downstream) analyzed for this report were irrigated by 14 different center-pivot sprinkler systems (four Upstream, 10 Downstream).

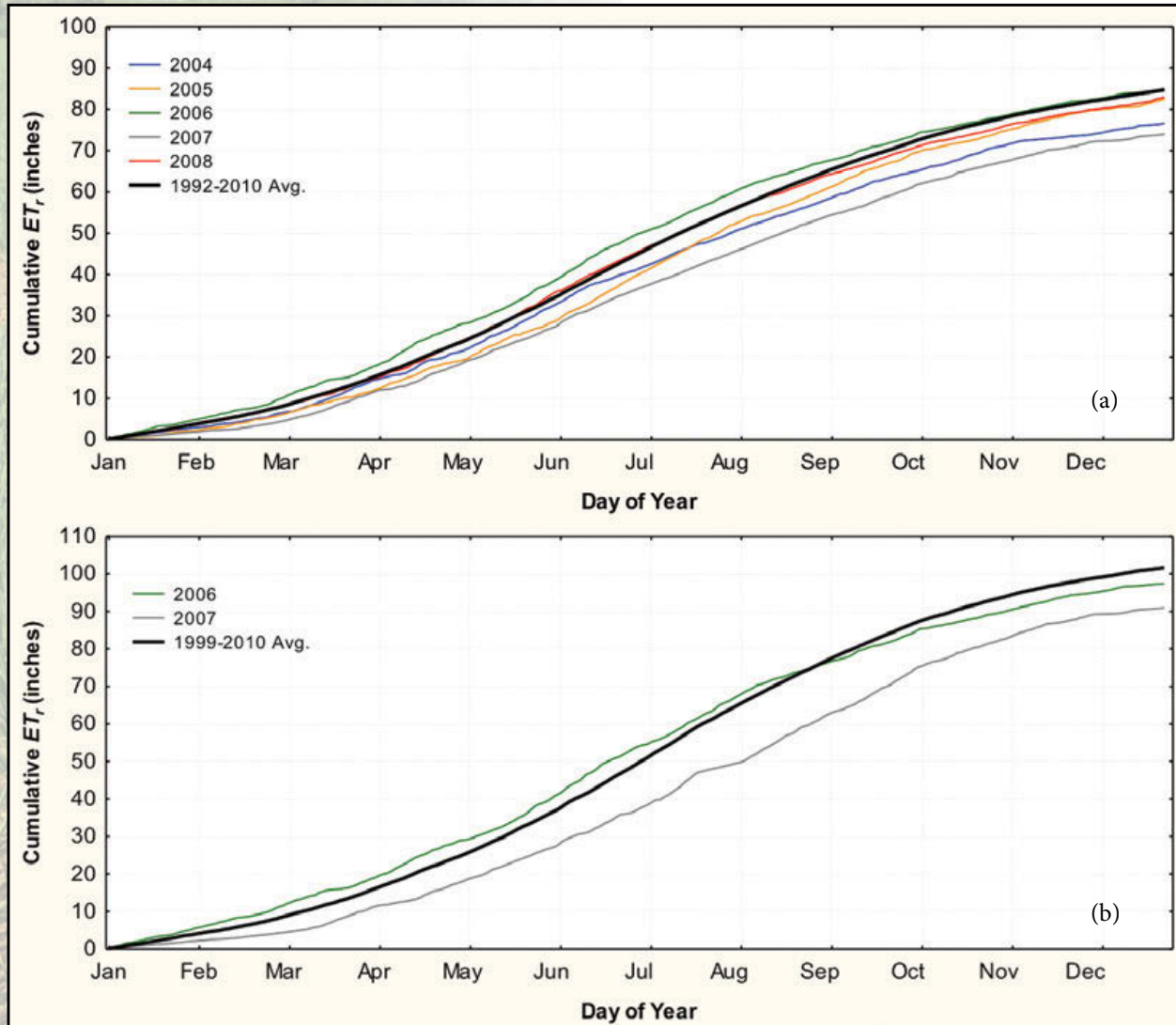


**Figure 9.** Cumulative  $ET_r$ , calculated for (a) each of the study years 2004-2008 and averaged over the years 1992-2010 at the CoAgMet Rocky Ford (RFD01) weather station, and (b) for study years 2006 and 2007 and averaged over the years 1999-2010 at the CoAgMet Lamar (LAM02/LAM04) weather station

The larger number of sprinkler-irrigated fields in the Downstream region was the result of a larger population of center-pivot irrigation systems available to study in that area. Canals may divert water rights for irrigation from the Arkansas River over the period March 15 to November 15. The average earliest date of monitored irrigation events across all fields in this study was May 17, and the average latest date was September 6.

## Crops

Major crops in the LARV in order of cropped area are alfalfa, corn, grass hay, wheat, sorghum, dry beans, cantaloupe, watermelon, and onions (USDA NASS Colorado Field Office 2009). The crop type on each monitored field in this study for each irrigation season is summarized in Tables 3 and 4 for the Upstream and Downstream Study Regions, respectively.

## Soil Conditions

Soils within the LARV generally consist of a variety of clay loam, loam, silty clay loam, silty loam, and sandy loam textural classes. Tables 5 and 6 present soil texture data and estimated total available water (TAW) for the surveyed fields derived from soil samples collected in the field and from the U.S. Department of Agriculture (USDA) Natural Resources Conservation Service (NRCS) soil surveys (USDA 2010) in the Upstream and Downstream Study Regions, respectively. Figure 10 illustrates overlays of the irrigated fields in the vicinity of the Upstream and Downstream Study Regions onto the variety of general textural classes from USDA NRCS soil surveys.

**Table 1.** Irrigation water source, type of irrigation system, and annual number of irrigation events monitored on fields in the Upstream Study Region

Field	Water Source	Type of Irrigation System (*)	Annual Number Monitored Irrigation Events				
			2004	2005	2006	2007	2008
US4	Well	Sprinkler (CP)	0	2	6	0	0
US4A	Well	Sprinkler (CP)	0	0	0	0	7
US4B	Well	Sprinkler (CP)	0	0	0	0	0
US5A	Catlin Canal	Sprinkler (CP)	0	9	9	0	12
US6	Catlin Canal	Surface (CD)	0	3	5	0	0
US7	Catlin Canal	Surface (CD)	0	3	7	0	0
US8	Fort Lyon Canal	Surface (CD)	1	2	2	0	2
US9	Catlin Canal	Surface (GP)	0	5	5	0	0
US10	Rocky Ford Highline Canal	Surface (GP)	0	5	4	0	0
US12	Rocky Ford Highline Canal	Surface (CD)	3	8	3	0	3
US13	Rocky Ford Highline Canal	Surface (GP)	0	7	4	0	5
US14A	Rocky Ford Highline Canal	Surface (GP)	0	3	1	0	2
US14B	Rocky Ford Highline Canal	Surface (GP)	0	3	1	0	4
US14C	Rocky Ford Highline Canal	Surface (GP)	0	3	1	0	3
US15	Catlin Canal	Surface (ED)	0	0	0	0	2
US17A	Catlin Canal	Surface (CD)	0	0	0	0	3
US17E	Well	Sprinkler (CP)	0	0	0	0	5
US17F	Well	Sprinkler (CP)	0	0	0	0	2
US18A	Well	Sprinkler (CP)	0	0	0	0	7
US18B	Well	Sprinkler (CP)	2	11	0	0	3
US20	Rocky Ford Highline Canal	Surface (GP)	2	0	0	0	0
US22	Catlin Canal	Surface (CD)	0	0	0	0	0
<b>Total</b>			<b>8</b>	<b>64</b>	<b>48</b>	<b>0</b>	<b>60</b>

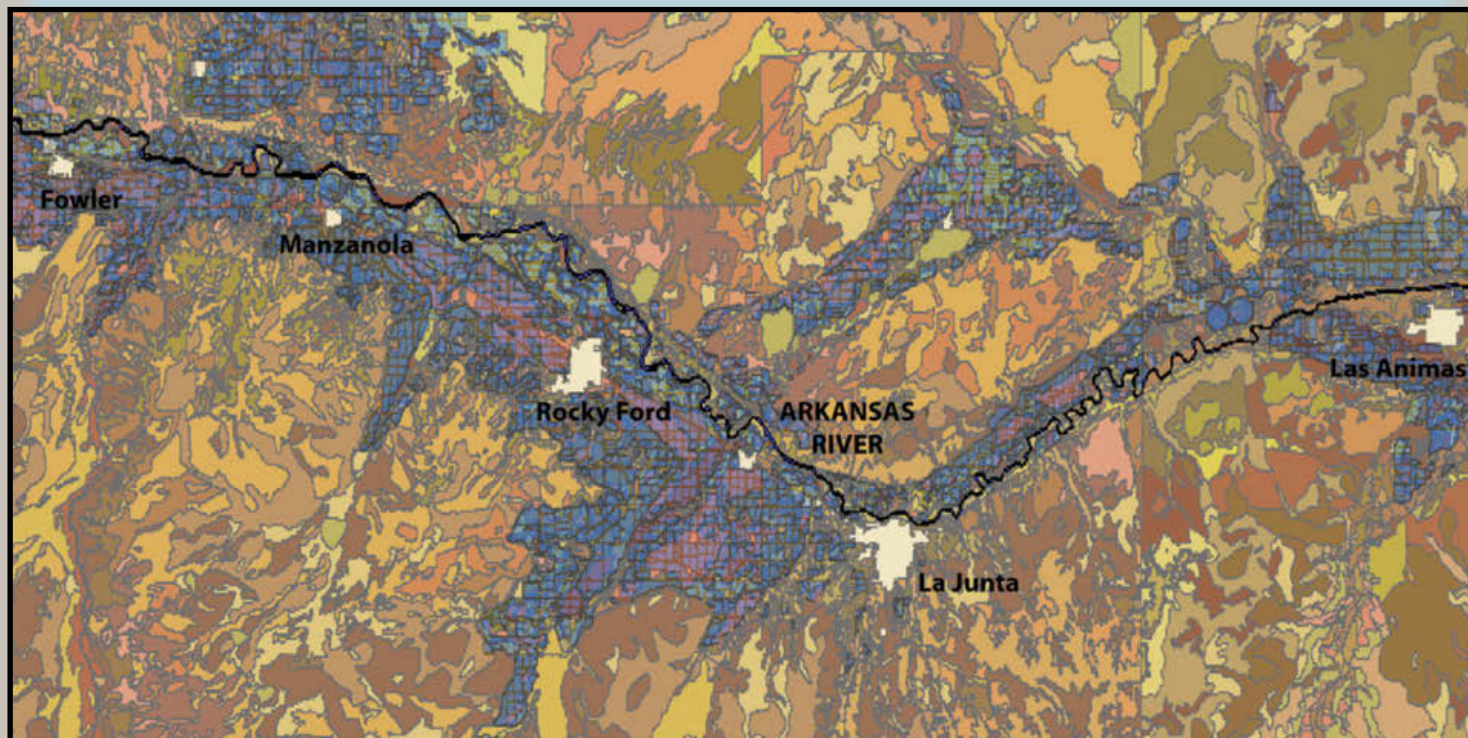
\*CD-Concrete Ditch Water Delivery, CP-Center Pivot, ED-Earthen Ditch Water Delivery, GP-Gated Pipe Water Delivery

**Table 2.** Irrigation water source, type of irrigation system, and annual number of irrigation events monitored on fields in the Downstream Study Region

Field	Water Source	Type of Irrigation System	Annual Number Monitored Irrigation Events				
			2004	2005	2006	2007	2008
DS1	Fort Lyon Canal	Surface (ED, GP)	2	5	6	8	6
DS2	Fort Lyon Canal	Surface (ED,CD)	0	3	6	9	6
DS3	Fort Lyon Canal	Surface (ED)	0	4	3	3	0
DS4A	Fort Lyon Canal	Surface (CD)	1	0	0	0	0
DS4A1	Fort Lyon Canal	Sprinkler (CP)	0	0	9	9	8
DS4A2	Fort Lyon Canal	Sprinkler (CP)	0	8	0	0	0
DS4B	Fort Lyon Canal	Surface (CD)	2	0	0	0	6
DS4C	Fort Lyon Canal	Surface (CD)	0	0	0	0	1
DS5A	Fort Lyon Canal	Sprinkler (CP)	0	9	7	12	5
DS5B	Fort Lyon Canal	Surface (ED)	0	0	0	0	3
DS6A	Fort Lyon Canal	Surface (ED)	0	0	0	0	4
DS6B	Fort Lyon Canal	Surface (GP)	0	1	2	4	0
DS6Ba	Fort Lyon Canal	Surface (GP)	0	0	0	0	3
DS7	Amity Canal/Well	Surface (ED)	0	3	0	1	0
DS7s	Amity Canal	Sprinkler (CP)	0	0	0	0	4
DS8	Well	Surface (ED)	0	2	0	0	0
DS9	Amity Canal	Sprinkler (CP)	0	2	0	3	3
DS10	Amity Canal	Surface (ED)	0	1	0	1	0
DS11	Buffalo Canal	Surface (ED)	0	1	0	0	2
DS12	Fort Bent Canal	Surface (CD)	0	1	3	0	0
DS13	Lamar Canal	Surface (ED)	0	4	0	0	0
DS14	Fort Lyon Canal	Surface (GP)	0	2	0	4	0
DS15	Well	Surface (ED,CD)	0	0	5	2	3
DS16	Fort Lyon Canal	Sprinkler (CP)	0	0	9	8	7
DS17A	Fort Lyon Canal	Sprinkler (CP)	0	0	0	12	8
DS18A	Fort Lyon Canal	Sprinkler (CP)	0	0	0	0	7
DS18B	Fort Lyon Canal	Sprinkler (CP)	0	0	0	0	9
DS18C	Fort Lyon Canal	Sprinkler (CP)	0	0	0	0	5
DS18D	Fort Lyon Canal	Sprinkler (CP)	0	0	0	0	7
DS19A	Fort Lyon Canal	Sprinkler (CP)	0	0	0	0	12
DS19B	Fort Lyon Canal	Sprinkler (CP)	0	0	0	0	8
DS19C	Fort Lyon Canal	Sprinkler (CP)	0	0	0	0	2
DS19D	Fort Lyon Canal	Sprinkler (CP)	0	0	0	0	13
DS19M	Fort Lyon Canal	Sprinkler (CP)	0	0	0	0	11
DS20A	Fort Lyon Canal	Sprinkler (CP)	0	0	0	0	5
DS20B	Fort Lyon Canal	Sprinkler (CP)	0	0	0	0	7
DS20G	Fort Lyon Canal	Sprinkler (CP)	0	0	0	0	2
DS21	Amity Canal	Surface (CD)	0	0	0	0	1
DS22	Amity Canal	Sprinkler (CP)	0	0	0	0	5
Total			5	46	50	76	163

\*CD-Concrete Ditch Water Delivery, CP-Center Pivot, ED-Earthen Ditch Water Delivery, GP-Gated Pipe Water Delivery

a.



b.

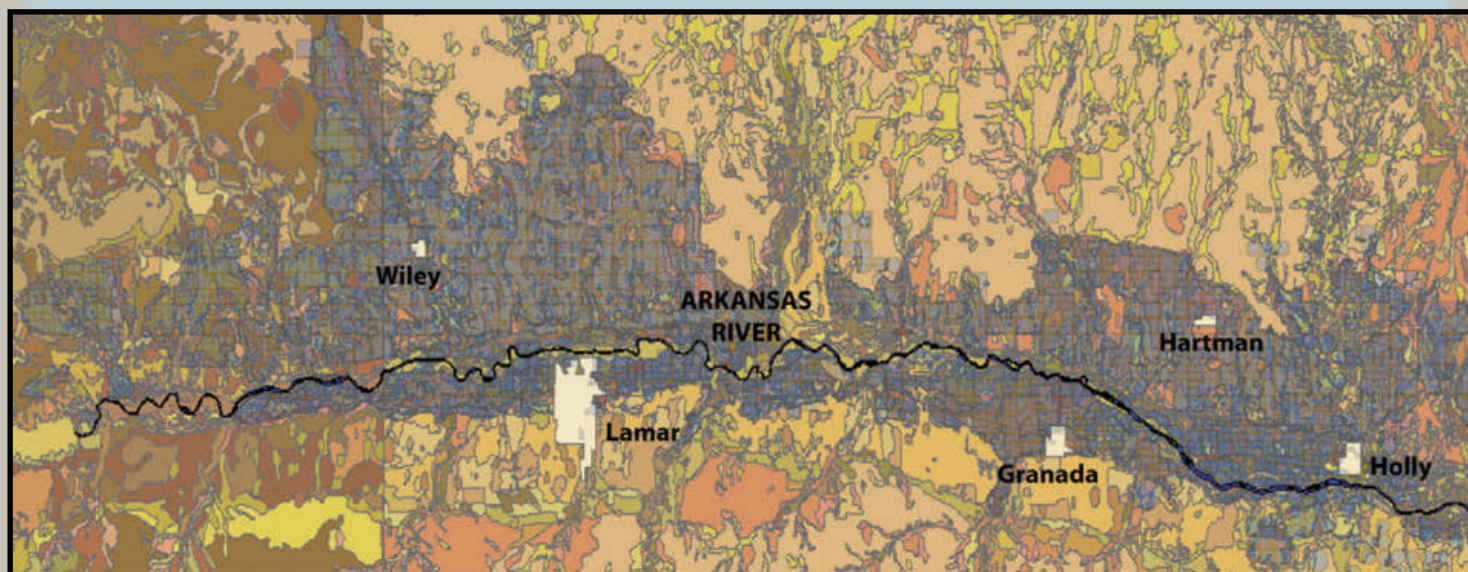


**Figure 10.** Overlay of irrigated fields in the vicinity of the (a) Upstream and (b) Downstream Study Regions on the USDA NRCS soil textural classes, illustrating the variety of soil textures in the areas. For detailed information regarding soil textural class names and characteristics see <http://websoilsurvey.nrcs.usda.gov/app/HomePage.htm>

**Table 3.** Crops on fields in the Upstream Study Region

Field	Crop by Year				
	2004	2005	2006	2007	2008
US4		A	A		
US4A					WS,CG
US4B					A
US5A		ON	ON		ON
US6		A	A		
US7		A	A		
US8	SS	G	G		G
US9		A	A		
US10		A	A		
US12	A	A	A		A
US13		CG	CG		CG
US14A		G	G		G
US14B		G/A	G/A		G/A
US14C		G	G		G
US15					G
US17A					A
US17E					CG
US17F					FS
US18A					S, W
US18B					W,C
US20	A	A			
US22	A				

Abbreviations: A – alfalfa, C – canola, CT – cantaloupe, CG – corn grain, CS – corn silage, FS – forage sorghum, G – grass, G/A – grass/alfalfa mix, O – oats, ON – onions, S – sunflowers, SG – sorghum grain, SS – sorghum silage, W – wheat, WG – wheat grain, WS – wheat silage.

**Table 4.** Crops on fields in the Downstream Study Region

Field	Crop by Year				
	2004	2005	2006	2007	2008
DS1	CG	A	A	A	A
DS2		A	A	A	A
DS3		CS	SS	SS	
DS4A	A				
DS4A1			A	A	A
DS4A2		A			
DS4B	SG				A
DS4C					A
DS5A		CG	FS	CG	A
DS5B					A
DS6A					CG
DS6B		A	A	A	
DS6Ba					A
DS7		CS		WS	
DS7s					CS
DS8		CG			
DS9		CG		CG	CG
DS10		CG		CG	
DS11		A			A
DS12		A	A		
DS13		CS		O	
DS14		FS		CG	
DS15			CS	CG	CG
DS16			FS	A	A
DS17A				A	A
DS18A					WG,CS
DS18B					A
DS18C					WG
DS18D					A
DS19A					A
DS19B					WG
DS19C					WG
DS19D					A
DS19M					A, CS
DS20A					A
DS20B					CG
DS20G					WG
DS21					A
DS22					CS,WG

Abbreviations: A – alfalfa, C – canola, CT – cantaloupe, CG – corn grain, CS – corn silage, FS – forage sorghum, G – grass, G/A – grass/alfalfa mix, O – oats, ON – onions, S – sunflowers, SG – sorghum grain, SS – sorghum silage, W – wheat, WG – wheat grain, WS – wheat silage.

**Table 5.** Soil textural class and total available water (TAW) for monitored irrigated fields in the Upstream Study Region

Field	Field Survey					NRCS				
	Soil Type	Avg % Clay	Avg % Sand	Avg % Silt	Avg TAW (in/ft)	Soil Type	Avg % Clay	Avg % Sand	Avg % Silt	Avg TAW (in/ft)
US1	No Field Samples Collected					SCL	26.54%	11.16%	62.30%	2.01
US2	No Field Samples Collected					SaL, L	18.77%	43.87%	37.33%	1.73
US3	No Field Samples Collected					SCL	47.17%	6.60%	46.23%	2.04
US4	L	11.51%	54.43%	34.06%	1.45	L	18.06%	43.56%	36.33%	1.52
US4A	SaL	10.57%	58.10%	31.34%	1.36	L	17.04%	47.04%	28.38%	1.47
US4B	L	12.45%	50.77%	36.78%	1.53	L	19.28%	39.31%	36.57%	1.58
US5A	L	22.85%	31.34%	45.81%	1.87	SCL	27.20%	8.40%	64.40%	2.04
US6	No Field Samples Collected					L	22.07%	29.75%	48.18%	1.84
US7	No Field Samples Collected					L	25.83%	14.08%	60.08%	1.99
US8	L	17.83%	34.29%	47.88%	1.89	SCL	27.20%	8.40%	64.40%	2.04
US9	No Field Samples Collected					L	15.71%	59.02%	25.27%	1.59
US10	No Field Samples Collected					L	26.73%	16.20%	57.08%	1.99
US12	SL, L	18.26%	38.16%	43.58%	1.79	SCL	25.60%	8.80%	65.70%	2.04
US13	SaL	14.37%	50.29%	35.34%	1.53	SCL	25.60%	8.80%	65.70%	2.04
US14A	L	15.28%	40.14%	44.58%	1.78	SCL	27.20%	8.40%	64.40%	2.04
US14B	L	17.58%	46.15%	36.27%	1.63	SCL	27.39%	21.97%	50.67%	2.04
US14C	SaL, L	17.41%	44.99%	37.60%	1.63	CL	27.63%	38.39%	34.06%	2.04
US15	L	20.25%	41.68%	38.07%	1.66	SCL	27.20%	8.40%	64.40%	2.04
US17A	No Field Samples Collected					SCL	49.19%	20.32%	30.47%	1.94
US17E	SL, L	19.27%	29.81%	50.92%	1.98	SCL	36.55%	8.54%	54.91%	2.04
US17F	SL, L	19.27%	29.81%	50.92%	1.98	C, SCL	37.59%	8.39%	54.02%	2.04
US18A	No Field Samples Collected					L, SCL	25.59%	15.11%	59.30%	1.98
US18B	No Field Samples Collected					L, SCL	21.15%	33.59%	45.26%	1.80
US20	No Field Samples Collected					SCL	26.86%	9.83%	63.31%	2.03
US22	No Field Samples Collected					SCL	25.80%	13.30%	60.90%	1.96

Key: CL = clay loam, L = loam, SCL = silty clay loam, SaL = sandy loam, SL = silty loam

**Table 6.** Soil textural class and total available water (TAW) for monitored irrigated fields in the Downstream Study Region

Field	Field Survey					NRCS				
	Soil Type	Avg % Clay	Avg % Sand	Avg % Silt	Avg TAW (in/ft)	Soil Type	Avg % Clay	Avg % Sand	Avg % Silt	Avg TAW (in/ft)
DS1	SL, L	16.62%	34.14%	49.23%	1.92	CL	25.60%	11.10%	63.30%	2.16
DS2	SL, L	17.22%	34.65%	48.13%	1.89	CL	26%	11%	63%	2.16
DS3	No Field Samples Collected					CL	25.68%	16.00%	58.32%	2.06
DS4A	SL, L	16.70%	33.97%	49.32%	1.92	CL	25.30%	14.80%	59.90%	2.04
DS4A1	SL, L	16.70%	33.97%	49.32%	1.92	CL	25.30%	14.80%	59.90%	2.04
DS4A2	SL, L	16.70%	33.97%	49.32%	1.92	CL	25.30%	14.80%	59.90%	2.04
DS4B	SL	13.96%	35.63%	50.40%	1.93	CL	25.30%	14.80%	59.90%	2.04
DS4C	L	21.26%	33.32%	45.42%	1.83	CL	25.30%	14.80%	59.90%	2.04
DS5A	SL, L	19.76%	29.08%	51.16%	1.98	CL	25.82%	14.28%	59.90%	2.04
DS5B	No Field Samples Collected					CL	29.00%	8.10%	63.20%	2.28
DS6A	SL	10.10%	37.59%	52.30%	1.95	CL	25.30%	14.80%	59.90%	2.04
DS6B	SL	13.36%	36.11%	50.52%	1.98	CL	23.86%	22.86%	53.30%	2.06
DS6Ba	SL	13.36%	36.11%	50.52%	1.98	CL	21.74%	34.74%	43.56%	2.09
DS7	L	21.28%	31.68%	47.04%	1.89	CL	29.21%	45.43%	27.79%	1.75
DS7s	L	21.28%	31.68%	47.04%	1.89	CL	29.96%	39.57%	30.48%	1.61
DS8	No Field Samples Collected					CL	25.30%	14.80%	59.90%	2.04
DS9	L	13.27%	42.79%	43.94%	1.75	CL	24.67%	14.67%	61.85%	2.06
DS10	L	11.77%	39.62%	48.61%	1.87	CL	25.61%	36.37%	38.01%	1.94
DS11	No Field Samples Collected					CL	22.52%	44.45%	33.07%	1.98
DS12	No Field Samples Collected					CL	23.48%	20.96%	56.10%	1.97
DS13	L	14.08%	42.29%	43.63%	1.728	CL	23.95%	12.24%	66.30%	2.04
DS14	No Field Samples Collected					CL	26.07%	17.20%	56.73%	2.08
DS15	SL	16.30%	26.80%	56.90%	2.12	CL	25.30%	14.80%	59.90%	2.04
DS16	SL	13.56%	36.13%	13.56%	1.92	CL	25.30%	14.80%	59.90%	2.04
DS17A	SL	19.35%	29.17%	51.49%	2.00	CL	26.11%	13.99%	59.90%	2.04
DS18A	L, SL, CL	20.44%	31.03%	48.54%	1.92	CL	25.23%	14.17%	60.59%	1.99
DS18B	SL	14.45%	30.93%	54.61%	2.06	CL	25.26%	14.43%	60.31%	2.01
DS18C	SL, L	14.58%	36.46%	48.95%	1.90	CL	25.29%	16.04%	58.69%	2.04
DS18D	SL, L	16.39%	34.97%	48.64%	1.90	CL	25.30%	15.56%	59.16%	2.04
DS19A	L	17.22%	36.64%	46.14%	1.84	CL	26.12%	16.05%	57.83%	2.09
DS19B	SL, L	16.61%	30.63%	52.76%	2.01	CL	25.31%	14.82%	59.87%	2.04
DS19C	SL, L	15.89%	33.47%	50.64%	1.96	CL	25.30%	14.80%	59.90%	2.04
DS19D	SL	12.73%	30.43%	56.84%	2.10	CL	25.39%	14.93%	59.68%	2.05
DS19M	L, CL	26.72%	30.71%	42.57%	1.80	CL	26.06%	15.95%	57.99%	2.09
DS20A	L	18.35%	33.63%	48.02%	1.90	CL	25.40%	15.89%	58.72%	2.05
DS20B	SL	15.80%	32.47%	51.73%	1.99	CL	25.57%	15.06%	59.37%	2.03
DS20G	L	18.12%	32.14%	49.74%	1.94	CL	25.30%	14.80%	59.90%	2.04
DS21	SL	16.90%	32.49%	50.61%	1.96	CL	25.30%	14.80%	59.90%	2.04
DS22	L	17.21%	45.00%	37.79%	1.62	CL	17.63%	61.88%	20.56%	1.92

Key: CL = clay loam, L = loam, SCL = silty clay loam, SaL = sandy loam, SL = silty loam

# Methodology

## Field Water Balance

Assuming constant fluid density, the water balance within the soil root zone of an irrigated field over a time period  $\Delta t$  can be represented by the following equation (Figure 11):

$$Q_I + Q_P + Q_U - Q_{ET} - Q_{DP} = \Delta S_{SW} \quad (1)$$

wherein  $Q_I$  = the volume of water infiltrated into the soil root zone from irrigation over  $\Delta t$ ,  $Q_P$  = the volume of water infiltrated into the soil from effective precipitation over  $\Delta t$ ,  $Q_U$  = the volume of water entering the root zone by upflux from the groundwater table over  $\Delta t$ ,  $Q_{ET}$  = the volume of water leaving the root zone by evapotranspiration over  $\Delta t$ ,  $Q_{DP}$  = the volume of water leaving the root zone by deep percolation over  $\Delta t$ , and  $\Delta S_{SW}$  = the change in volume of water stored in the root zone over  $\Delta t$ . The value of  $Q_I$  is calculated as:

$$Q_I = Q_A - Q_{TW} \quad (2)$$

wherein  $Q_A$  = the net volume of water applied to the field by irrigation over  $\Delta t$ , and  $Q_{TW}$  = the tailwater

runoff volume over  $\Delta t$ . The terms in Equations (1) and (2) can be expressed in units of volume or depth (volume per unit field area).

## Flow Onto and Off of Fields

The irrigation water volume diverted to each surface-irrigated field were measured using Parshall, trapezoidal, EZ Flow Ramp™, and cutthroat flumes, as well as weir structures, all equipped with stilling wells and automatic water-level loggers. Flumes in these types of applications are estimated to have measurement accuracy of about  $\pm 15$  percent. This diverted volume, less any transit losses in small delivery ditches, provided an estimate of the applied volume,  $Q_A$ , flowing onto a field. Such structures also were used to measure tailwater volume,  $Q_{TW}$ , flowing off of surface-irrigated fields. In most cases, portable flume structures were installed and used (e.g., Figure 12). Whenever possible, however, permanent flow measurement structures owned by a cooperator or the canal company were used (e.g., Figure 13). In-line McPropeller® flow meters (by McCrometer®) equipped with an instantaneous flow rate indicator and totalized flow volume odometer were used to measure water

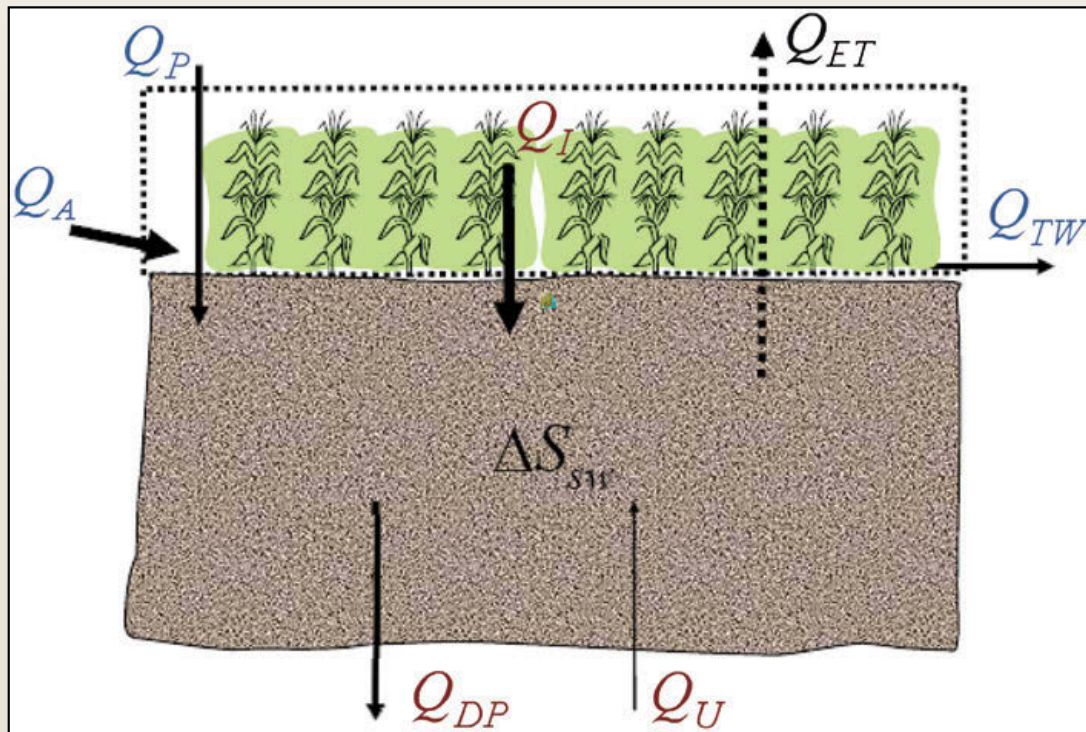


**Figure 11.** The field water balance showing the surface components and the root zone components

applied to sprinkler-irrigated fields. These meters have a rated accuracy of  $\pm 2$  percent of reading and a repeatability of  $\pm 0.25$  percent, and were installed by certified professionals. Significant tailwater runoff was never observed on monitored sprinkler-irrigated fields during this study. The different flow measurement structures used on the monitored fields are described in files available on the ARIDAD.

The following guidelines were used in the selection and installation of portable flumes:

1. Location was chosen so that (a) free (modular) flow conditions (Bos 1989) were present through the structure at all times (for this reason, installation in headland ditches was not attempted, since water level regulation during the irrigation process usually creates submerged (drowned) flow conditions for a period of time), and (b) the length of earthen transit channel between the structure and the irrigated field was minimized
2. Structure was sized suitable to the expected range of flow rates
3. Structure floor was raised six to 12 inches (depending on upstream channel bank elevation) from channel floor using packed soil to discourage submerged flow conditions



**Figure 12.** EZ Flow Ramp™ flume used to measure tailwater from field DS14 during 2005 and 2007



**Figure 13.** *Permanent measurement structure for inflow to Field DS6, provided by Fort Lyon Canal Company during seasons 2005-2008*

4. Structure was installed such that the horizontal portion of the floor was level in directions parallel and perpendicular to flow
5. Area between the channel and the structure sidewalls was packed with soil to discourage movement or shifting of the structure
6. Canvas material was placed under downstream end of structure extending into downstream channel to prevent erosion of soil and shifting of structure
7. Area between sidewalls of upstream face of the structure and the channel was packed with soil (to the same height as the top of the structure) and overlain with canvas material to prevent leakage and erosion of soil (except in the case of trapezoidal flumes)
8. Structure was equipped with a staff gage, polyvinyl chloride (PVC) stilling well (no less than four inch diameter, except for trapezoidal flumes which were 2.5 inch diameter), vented cap, and vinyl delivery tube (three-fourths inch diameter). Stilling wells were used to house automatic water level recorders while delivery tubes were used to connect the

stilling well to the inside of the flume structure (at the staff gage) in order to maintain an equivalent net water depth between the two. Stilling well floor typically was lowered at least 4 inches below the flume floor to maintain water level recording accuracy in the event of low flow conditions. Stilling wells were not lowered beneath the flume floor in the case of trapezoidal flumes.

Permanent flow measurement structures were used if the following conditions were met:

1. Structure was sound (no leaks, level in directions parallel and perpendicular to flow, no deformities)
2. Structure was appropriate for measuring expected flow rates (proper size, dimensions, and type)
3. Structure was suitable for the construction of a stilling well (and in some cases a delivery tube) for water level measurement
4. Free flow conditions were present through structure
5. Flow approach to the structure was appropriate (to discourage improper flow velocities or turbulence through the structure)

6. Structure was located a short distance (less than one-fourth mile) from field boundaries in situations where an earthen transit channel was used (in order to minimize error in transit water losses)
7. Water was not divided between multiple fields downstream of the flow measurement structure

For this study, HOB0® U20-001-01 water-level recorders (pressure transducers) manufactured by Onset™ were used to continuously record pertinent water levels in each flow measurement structure during irrigation events on surface-irrigated fields. HOB0™ U20-001-01 water-level recorders have an operating range of zero to 30 ft of water (at sea level) and a typical error of  $\pm 0.015$  ft of water. They were programmed to record absolute pressure readings every five minutes over the duration of an irrigation event. Flow rate values and total applied/tailwater volumes later were derived from these pressure readings using appropriate rating equations for each flow measurement device. Early in the study in 2004, Level TROLL® 300 water level recorders by In-Situ, Inc. were used to measure water levels associated with water measurement structures on several fields. Another type of pressure transducer also was used in 2004, but problems were discovered with these devices and data were deemed to be unreliable. Localized barometric pressure was recorded at a five minute interval throughout the duration of the irrigation season using a HOB0® U20-001-01 water level recorder installed in a free-draining, ventilated PVC tube buried at the ground surface in a regionally centralized location (in both the Upstream and the Downstream regions).

Transit loss is defined as the amount of irrigation water that seeps or evaporates from an earthen transit channel between the flow measurement structure (inflow or tailwater) and the point of inflow to or outflow from a monitored irrigated field. Transit losses were considered negligible in concrete ditch and pipeline systems. Transit loss amounts were not considered in earthen headland or tailwater ditches directly adjacent to a field area; instead, this flow was assumed to be part of the irrigation amount applied to the field. Transit loss amounts were estimated based upon prior CSU studies on canal seepage rates in the LARV (Susfalk et al. 2008), using estimated wetted perimeter values for the transit channel, length of the transit channel between flow-measurement structure and the irrigated field, and the duration of flow in the transit channel. Since the location of each flow measurement structure location was carefully considered when selecting fields, transit loss calculations were required for a total of only five fields during the study.

To account for changes in the water destination or switching of water to neighboring fields, CSU personnel associated with this project maintained communication with cooperating farmers in addition to visually inspecting fields on a daily basis during irrigation events. Care was taken to insure that flow-measurement structures remained unsubmerged during operation. Figures 14-16 show some of the different flow-measurement devices employed over the period of the study. The center pivot irrigation system shown in Figure 17 was metered and used to irrigate fields DS5, DS6, and DS17.

**Figure 14.** Weir structure for flow measurement onto fields DS4 and DS16 in 2008





**Figure 15.** *Cutthroat flume for measurement of tailwater runoff from field US14C in 2008*



**Figure 16.** *Parshall flume for measurement of flow to field DS1 in 2008*



**Figure 17.** Center pivot sprinkler system used to irrigated fields DS5, DS6, and DS17 in 2008

The procedure followed in the measurement and calculation of applied irrigation and tailwater depths on surface irrigated fields is summarized as follows:

1. Manual readings of water depth at the gauging location for each flow measurement structure were taken throughout the duration of each irrigation event (daily if possible). These were used as a means of calibration and comparison of the water level recorder data. In addition, flow measurement structures were checked daily to insure that equipment was functioning properly and that all inflows and outflows were being accounted for.
2. Flow measurement structures were inspected daily during irrigation events to insure that:
  - Structure was sealed (no leakage around sides or underneath)
  - Structure was level in directions parallel and perpendicular to the flow
  - Structure, approach channel, and immediate downstream channel were free of debris
  - Stilling well and delivery tube were free of sediment (stilling wells were pumped during and after each irrigation)
  - Stilling well, delivery tubes, and fittings were secured in proper location and not leaking
  - Stilling well cap was secure and properly ventilated
  - Staff gage was secured in proper location
  - Canvas material was in proper location and not hindering flow through structure
  - Bottom of water-level sensor was resting on floor of stilling well
  - String was connected to water-level sensor cap and tied to stilling well

- Flow meters were recording instantaneous flow rate and totaled volume where applicable
3. The net water pressure (at the gauging location) was calculated by subtracting the recorded regional barometric pressure value and an elevation pressure correction from the absolute pressure value was obtained from the water level recorder in the structure for each five minute interval during the irrigation event. The net water level (at the staff gauge) was determined by converting the pressure values into water depth values and then subtracting
    4. The net water level values were converted into flow rate values using the appropriate rating equations for each measurement structure for each five-minute interval. The volume of water passing through the measurement structure during each five-minute interval was determined by averaging the flow rate values at the start and end of the interval and multiplying them by the interval length. The total volume passing through

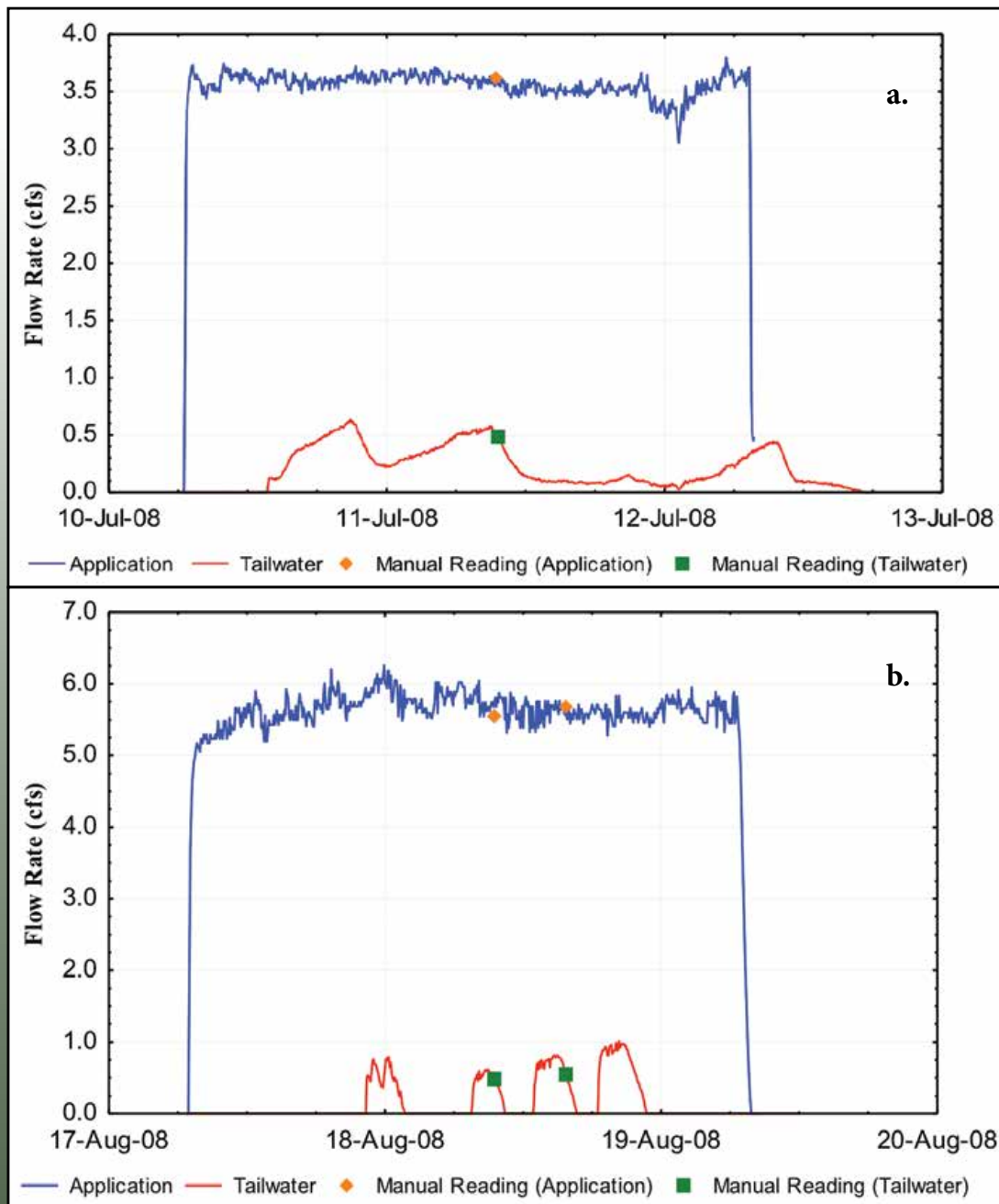


**Figure 18.** Applied and tailwater hydrographs for (a) field US8, 10-12 July 2008 irrigation event, and (b) field DS2, 17-19 August 2008 irrigation event

the structure during the irrigation event was determined by summing all of the five-minute volumes.

5. After the conclusion of an irrigation event, Garmin eTrex™ GPS units in conjunction with software from GPS Trackmaker® and ArcView® (from ESRI) were used to manually record irrigation boundaries and subsequently to calculate irrigated area values for each irrigation event. Garmin eTrex™ global positioning system (GPS) units have horizontal accuracy specifications of  $\pm 9.8$  ft (3m).
6. A hydrograph depicting applied irrigation flow rates and tailwater flow rates was generated for each irrigation event on each field. Figure 18 shows examples for fields US8 and DS2 for the 2008 season, including plots of manual readings.
7. Infiltrated irrigation depth was calculated as  $Q_I = (Q_A - Q_{TW}) / \text{Irrigated Area}$ .
8. Tailwater fraction (TRF) =  $Q_{TW} / Q_A$ , was computed for each irrigation event and reported in units of percent.

The dates of the irrigation events measured on each of the fields reported herein are summarized in files on the ARIDAD.

Totalizing flow meters on center pivot sprinkler irrigation systems were read regularly during each irrigation event (daily if possible). Since significant tailwater runoff was not observed from any of the sprinkler-irrigated fields, no tailwater measurement structures were required. As with surface irrigation events, irrigated areas were calculated using GPS points taken around the irrigated boundaries following each irrigation event.

An additional component unique to the analysis of sprinkler-irrigated fields using water from canals was the need to estimate stabilization pond seepage losses using measured flow rate on inflow ditches, flow meter readings from pivots, local precipitation data, pond area measurements, and regional free water surface evaporation data. Two of these ponds are shown in Figure 19.



**Figure 19.** Stabilization pond for center pivot sprinkler on field DS19 in 2008

## Precipitation

Rain gauges were installed at or near all monitored fields during the irrigation season. The rain gauges were equipped with a tipping bucket (HOBO™ RG2) and data logger (HOBO™ Event Data Logger) (Figure 20). Because of localized variability in precipitation during the summer months, one rain gauge was installed on or directly adjacent to each monitored field except in cases where several monitored fields were conglomerated in close proximity (less than one mile) to one another. In these cases, the rain gauge was installed at a central location between the fields. The rain gauges were calibrated prior to installation in the fields and were mounted on four inch diameter PVC pipe posts per manufacturer's recommendations. Special care was taken to ensure that rain gauges were not installed near vertical obstructions (e.g., trees, power poles, buildings) or near areas irrigated by sprinkler systems. They were maintained on a weekly basis by CSU personnel. Maintenance included inspection of electrical wiring from the rain gauge to the data logger, verification of



**Figure 20.** HOBO® rain gauge in Field US17E in 2008

battery life, and removal of dirt/debris from collection cone and tipping bucket. Batteries were replaced in data loggers once during the summer (typically in late July). In cases where rain gauge/data logger malfunction occurred, precipitation data were taken from another CSU rain gauge or CoAgMet station depending on which was in closer proximity. Rain gauges were removed from the field at the end of each monitored irrigation season.

Data loggers on the rain gauges generally were downloaded mid-season (late July) and at the end of the season (mid-November) using HOBO® BoxCar 3.7 software on a laptop computer. Downloaded files were converted to Microsoft® Excel files with output containing precipitation depth over time (month, day, year, hour and minute). Analyses for daily and cumulative precipitation were carried out. Figure 21 displays a typical graph showing cumulative rainfall for a selected field US20 in 2005. For water balance analysis, total rainfall depth was computed over the selected period  $\Delta t$  and reduced using the SCS model described below to account for surface runoff to estimate  $Q_p$ .

To reduce total rainfall to effective infiltrated rainfall,  $Q_p$ , the SCS runoff model empirical method was used (USDA 1986). In this method, total rainfall is adjusted to account for three factors: soil water content, rainfall intensity, and rainfall amount. Soil water content is used to find a curve number (CN) that is in turn used to calculate the effective rainfall. The “average” CN used for the fields in this study area is 82; as found in tables of soil data provided in USDA (1986). The CN is adjusted based on the volume of water per unit area (depth),  $W_5$ , that has entered the system in the five days before a rainfall event by the following:

$$CN = \begin{cases} 66 & \text{for } W_5 < 1.42 \text{ in} \\ 82 & \text{for } 1.42 \text{ in} < W_5 < 2.09 \text{ in} \\ 95 & \text{for } W_5 > 2.09 \text{ in} \end{cases}$$

Once a CN as been determined, the maximum soil retention volume per unit area (depth),  $S_R$ , can be calculated as follows:

$$S_R = 1000/CN - 10 \quad (3)$$

$S_R$  represents the volume that the soil profile can receive before surface runoff occurs.

To calculate the volume of precipitation runoff per unit area (depth),  $Q_R$ , caused by a rainfall event the following equation is used:

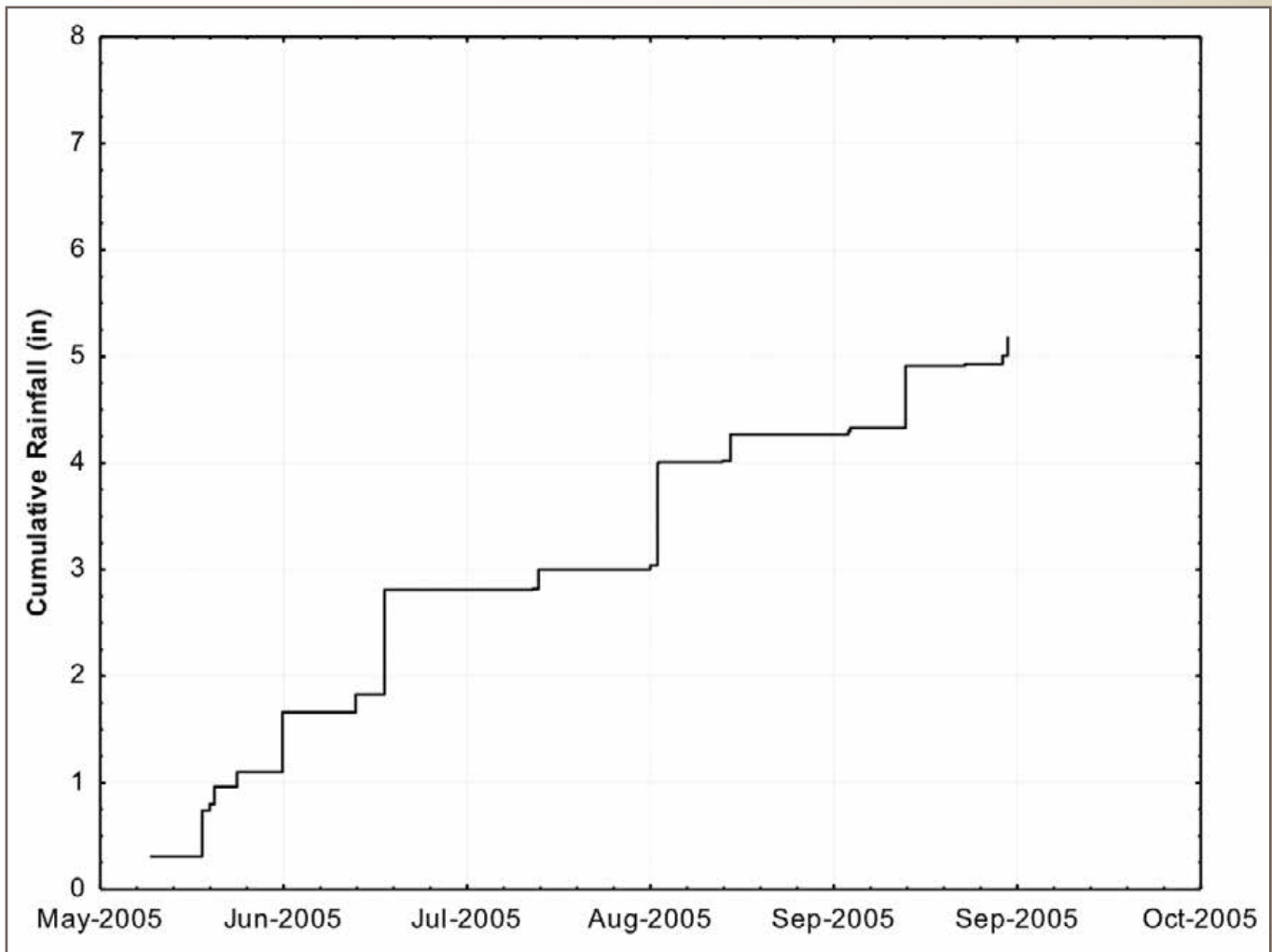


**Figure 21.** Cumulative precipitation for field US20 during the 2005 irrigation season

$$Q_R = \begin{cases} \frac{(Q_{PT} - 0.2S_R)^2}{(Q_{PT} + 0.8S_R)} & \text{for } Q_{PT} > 0.2S_R \\ 0 & \text{for } Q_{PT} \leq 0.2S_R \end{cases} \quad (4)$$

wherein  $Q_{PT}$  is the total depth (in inches) of the rainfall event. Once  $Q_R$  has been calculated the effective rainfall ( $Q_p$ ) can be calculated as follows:

$$Q_p = Q_{PT} - Q_R \quad (5)$$

### Evapotranspiration

#### Reference Evapotranspiration Calculated from ASCE Standardized Equation

The ASCE Standardized Reference Evapotranspiration Equation is based on a combination equation which combines an energy component and an advection component. The methodology depends upon net solar radiation, soil heat flux density, mean daily air temperature, mean daily

wind speed, saturation vapor pressure, mean actual vapor pressure as well as other physical parameters, and is described in detail in Allen et al (2005). The ET calculated by the ASCE equation for each crop is based on the ET of a long reference crop, referred to as  $ET_r$ . In this study alfalfa was used as the long reference crop. The ET of a particular crop at a particular time is then calculated as a fraction of the  $ET_r$  at that time. If the crop is healthy, well-watered, and not adversely affected by salinity or other hazards, this fraction of the  $ET_r$  may be assumed to be a function of the growth stage of the crop and is called the crop coefficient,  $k_c$ . Since the growth stage of a crop changes throughout the growing season the  $k_c$  value changes as well. This variation of  $k_c$  with time usually can be represented by a linear equation or a third-order polynomial depending on the growth stage. The potential crop ET at a particular time is calculated as  $ET_p = k_c ET_r$ .

### *Reference Evapotranspiration Estimated from Evaporimeters*

Manual atmometers (ETgage® Model A), manufactured by the *ETgage Company*™ of Loveland, Colorado, were used as another means of estimating  $ET_r$  in the monitored fields. Alfalfa reference ET diffusion covers (#54) were used on each of the atmometers. Rigid vertical wires were also utilized on the top of each ET simulator to discourage bird fouling. An example of an atmometer setup is shown in Figure 22 for field DS2 for the 2006 season.



Each field was monitored individually unless other monitored fields were within a distance of one mile, in which case the neighboring fields were served by only one atmometer. Each atmometer was mounted on a two by four inch wooden post via steel bracket and installed with the evaporative surface at a height of 39 inches above the ground surface. Per manufacturer's recommendations, atmometers that were not installed within a particular field's boundaries were installed immediately outside the field in an area with suitable vegetative covering. This generally was the case with tall crops such as corn and forage sorghum.

Atmometers were installed in early May and were removed from the field in early October each season in order to prevent freeze damage to equipment. They were thoroughly cleaned and inspected for damage prior to each season. New "wafers" and alfalfa reference ET diffusion covers (#54) were added to each atmometer prior to each season as well.

Atmometers were maintained by CSU personnel on a weekly basis from May through August and a bi-weekly basis for the remainder of the season. Weekly maintenance included inspection of equipment for damaged parts, inspection of diffusion covers for fouling (with dirty covers being replaced by new ones), recording of water level in apparatus sight glass, and addition of distilled water to the atmometer reservoir when more than 2/3 empty. Damage to atmometers was rare but occasionally sight tubes were damaged by large hail or ceramic cups were cracked from freezing temperatures. In cases where atmometer equipment damage occurred,  $ET_r$  data were taken from the closest CSU atmometer.

Recorded atmometer data included water level in the sight glass as well as time (month, day, year, hour and minute). Values of total  $ET_r$  between readings were estimated as the difference between the recorded water levels.

### *Actual Evapotranspiration Estimated from Remote Sensing*

Daily average values of actual ET ( $ET_a$ ) over the study regions were estimated using the ReSET land surface energy balance model (Elhaddad and Garcia 2008) to process available satellite images of the study regions.

**Figure 22.** *ETgage*® Model A atmometer in field DS2 during the 2006 season

Summing up values of  $ET_a$  over a study period  $\Delta t$ , and multiplying by the area of an irrigated field provided an estimate of  $Q_{ET}$  for use in the field water balance. The ReSET model is built on the same theoretical basis of its two predecessors, METRIC (Allen et al. 2007 a,b) and SEBAL (Bastiaanssen et al 1998 a,b) with the additional ability to handle data from multiple weather stations. This enhances regional  $ET_a$  estimates by taking into consideration the spatial variability of weather conditions through data acquired from different weather stations (across the area covered by the remote sensing system/imager). ReSET can be used in both the calibrated and the un-calibrated modes. The calibrated mode is similar to METRIC in which  $ET_r$  calculated from weather station data is used to set the maximum  $ET_a$  value in the processed area, while in the un-calibrated mode the model follows a procedure similar to SEBAL where no maximum  $ET_a$  value is imposed.

Satellite images from the Landsat 5 or Landsat 7 satellites were used in this study. Multispectral images including the visible (bands 1-3), infrared (bands 4, 5, and 7), and thermal (band 6) ranges of spectrum are captured by these satellites. All bands have a linear spatial resolution of 30 m except for the thermal band. The thermal band has a 120 m resolution for Landsat 5 and a 60 m for Landsat 7. Images of the two study regions are captured every 16 days by these satellites. The cycles of the two satellites are offset by eight days for an image over a given region, and are offset by nine days between the two regions. When clouds occur over the monitored field sites or extensively throughout the regions, satellite images cannot be used to estimate  $ET_a$ . Images processed by the ReSET method yielded estimated patterns of  $ET_a$  at a 30 m  $\times$  30 m resolution. It has been estimated that ReSET and similar methods produce daily average values on the satellite date with errors on the order of 5-15 percent (Bastiaanssen et al. 1998a, Elhaddad and Garcia 2008).

For a given instant of time, the land surface energy balance equation can be written as:

$$R_{n,i} = L_v \rho_w ET_i + H_i + G_i \quad (6)$$

wherein  $R_{n,i}$  is the net radiation,  $L_v$  is the latent heat of vaporization,  $\rho_w$  is the density of water,  $ET_i$  is the instantaneous actual ET,  $H_i$  is the sensible heat flux, and  $G_i$  is the heat conduction to the ground (the subscript  $i$  denotes instantaneous values). The value of  $R_{n,i}$  is computed from the surface albedo, surface temperature, digital elevation models, normalized difference

vegetation index (NDVI), and surface roughness using the method developed by Bastiaanssen (2000). The visible bands (1, 2, and 3) and infrared bands (4, 5, and 7) are used to compute the surface albedo, and surface temperature is calculated from band 6. NDVI is calculated from bands 3 and 4, and  $G_i$  is computed using NDVI, albedo, surface temperature, and the sensible heat flux.  $H_i$  is calculated by selecting and processing "wet" and "dry" pixels within the satellite image. A "wet" pixel is one where  $ET_i$  occurs at the atmospheric requirement, implying that  $H_i = 0$ . A "dry" pixel occurs where  $ET_i$  is assumed to be zero, so that  $H_i = R_{n,i} - G_i$ . Once the wet and dry  $H_i$  values are known, the values for  $H_i$  at other pixels within the satellite image can be calculated.

After values of  $R_{n,i}$ ,  $G_i$ , and  $H_i$  have been estimated, Eq. (6) is used to calculate the latent heat flux ( $L_v \rho_w ET_i$ ) (Bastiaanssen et al. 1998). The following equation is then used to compute the instantaneous evaporative fraction ( $\Lambda_i$ ):

$$\Lambda_i = \frac{L_v \rho_w ET_i}{L_v \rho_w ET_i + H_i} = \frac{L_v \rho_w ET_i}{R_{n,i} - G_i} \quad (7)$$

The daily average value of  $\Lambda_i$  is computed through the following equation, assuming that  $ET_a$  remains constant throughout the entire day:

$$ET_a = \frac{86,400 \Lambda_i R_n}{L_v \rho_w} \quad (8)$$

The value of  $R_n$  in this equation is the 24-hour net radiation, which can be estimated using the approach of Duffie and Beckman (1991), and 86,400 is the time conversion from one second to 24 hours. It is assumed in Eq. (8) that the net soil heat flux over the 24-hr period is zero.

An additional adjustment to the seasonal  $ET_a$  calculated with ReSET for alfalfa fields was implemented for this study to account for alfalfa cutting. The ReSET model generates a seasonal  $ET_a$  value by interpolating between Landsat image dates using a ratio based on  $ET_r$  and the ReSET  $ET_a$  at the date of the two Landsat images that bound a period and the  $ET_r$  values for each day between the Landsat image dates. As part of the current project, alfalfa cutting dates were collected. In order to improve the seasonal ReSET  $ET_a$  estimates an additional adjustment was implemented to account for the alfalfa cuttings. To model the effect of cutting on  $ET_a$  the following equation was used:

$$ET_a = k_c ET_r$$

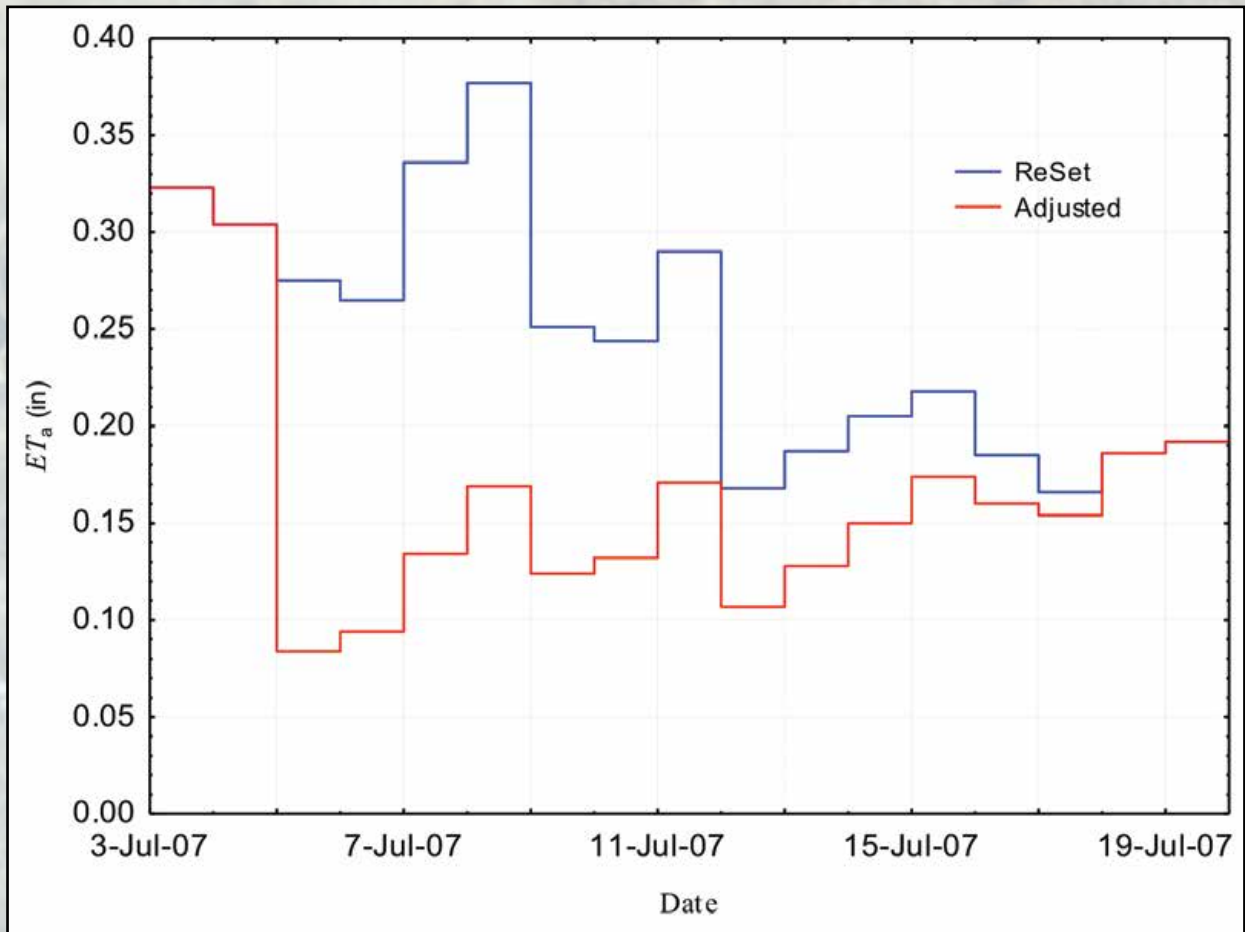


Figure 23. Alfalfa  $ET_a$  adjusted for cutting compared to ReSET  $ET_a$

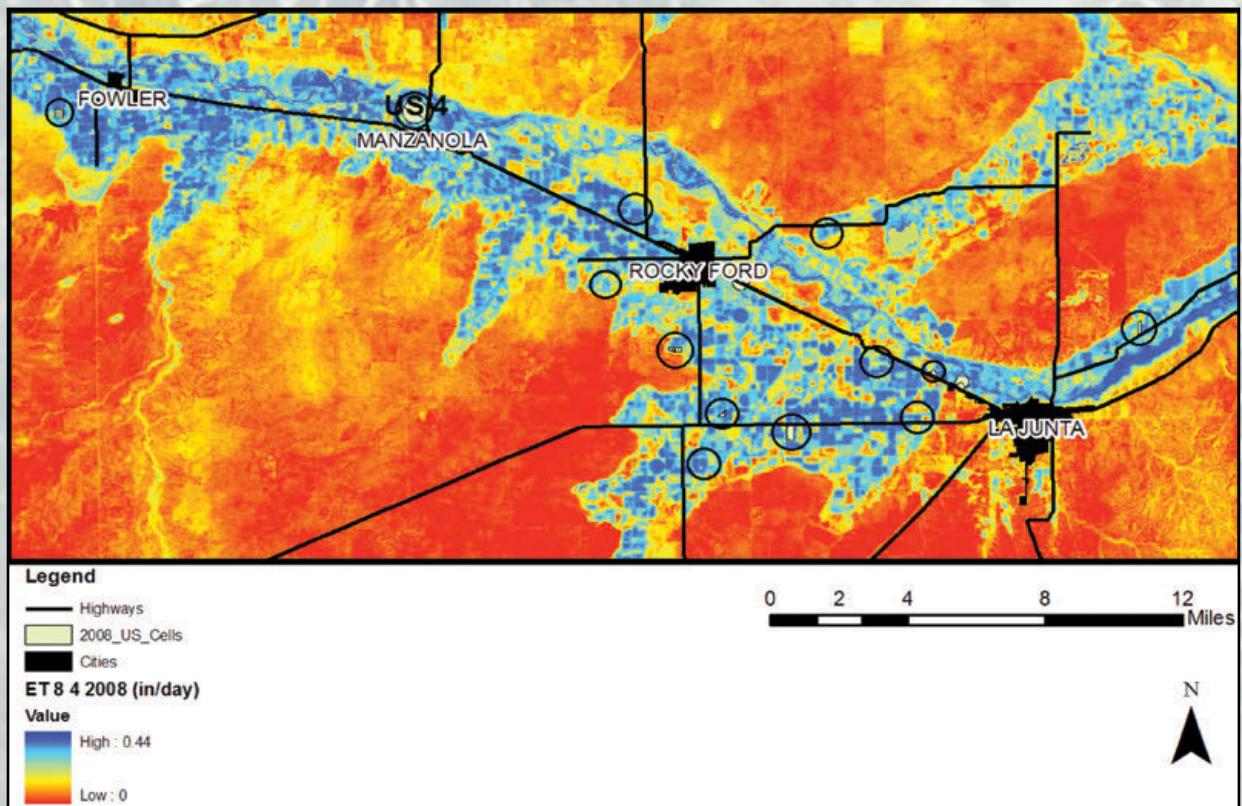
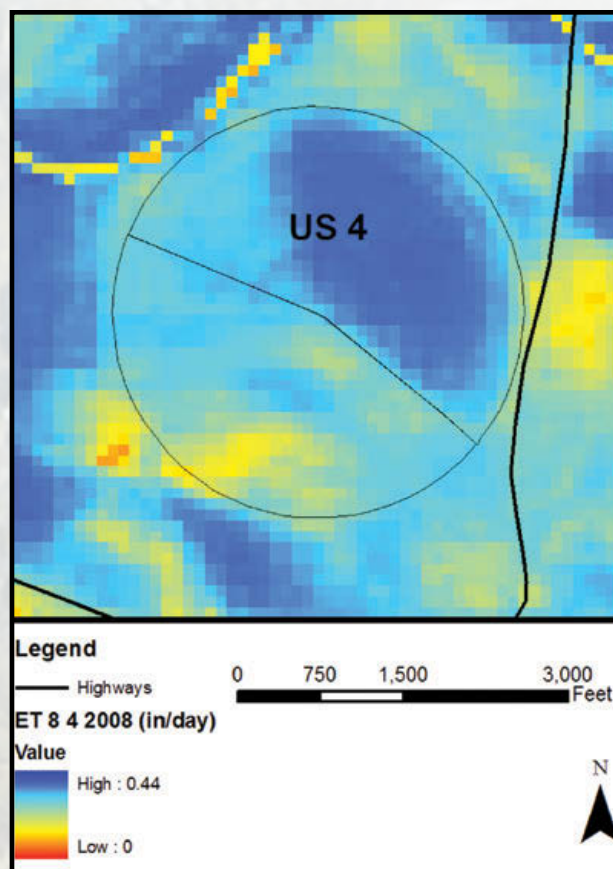


Figure 24. ReSET-calculated  $ET_a$  in the Upstream Study Region on 4 August 2008 with study fields circled

Where  $k_c$  is the crop coefficient.  $k_c$  for alfalfa just after cutting was assumed as 0.3 and was increased linearly until the next Landsat image date to simulate crop growth. Additional investigation is being conducted to determine the best procedure to account for alfalfa cutting dates in the seasonal ReSET  $ET_a$  estimate.

An example raster image of ReSET-calculated values of  $ET_a$  at 30 m  $\times$  30 m resolution is shown in Figure 24 for the Upstream Study Region for 19 July 2008. Figure 25 illustrates a close-up of field US4 within this image, illustrating the variability of  $ET_a$  within the field. A similar image for 28 July 2008 is shown in Figure 26 for the Downstream Study Region. A close-up view of fields DS8 and DS15 within this image is presented in Figure 27. Values of  $ET_a$  were averaged over the pixels within each monitored field cell to obtain estimates for use within the field water balance calculations.



**Figure 25.** ReSET-calculated  $ET_a$  in vicinity of field US4 on 4 August 2008

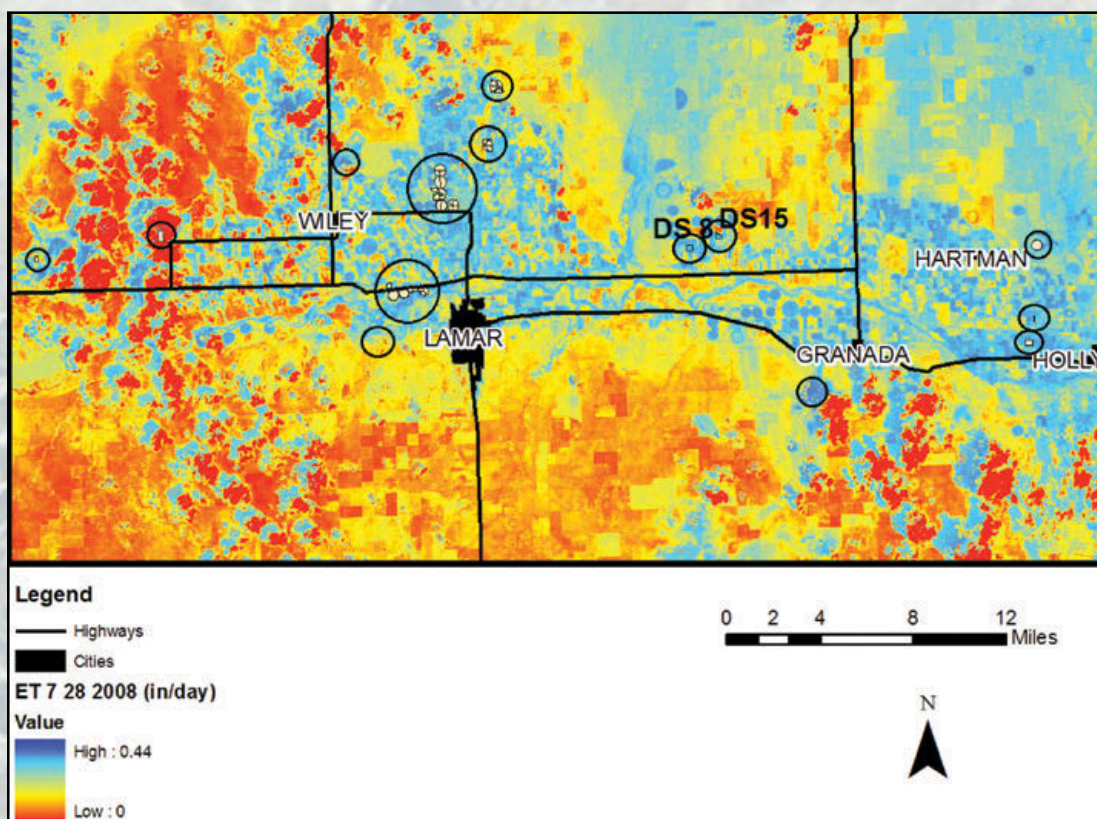


**Figure 26.** ReSET-calculated  $ET_a$  in the Downstream Study Region on 28 July 2008 with study fields circled

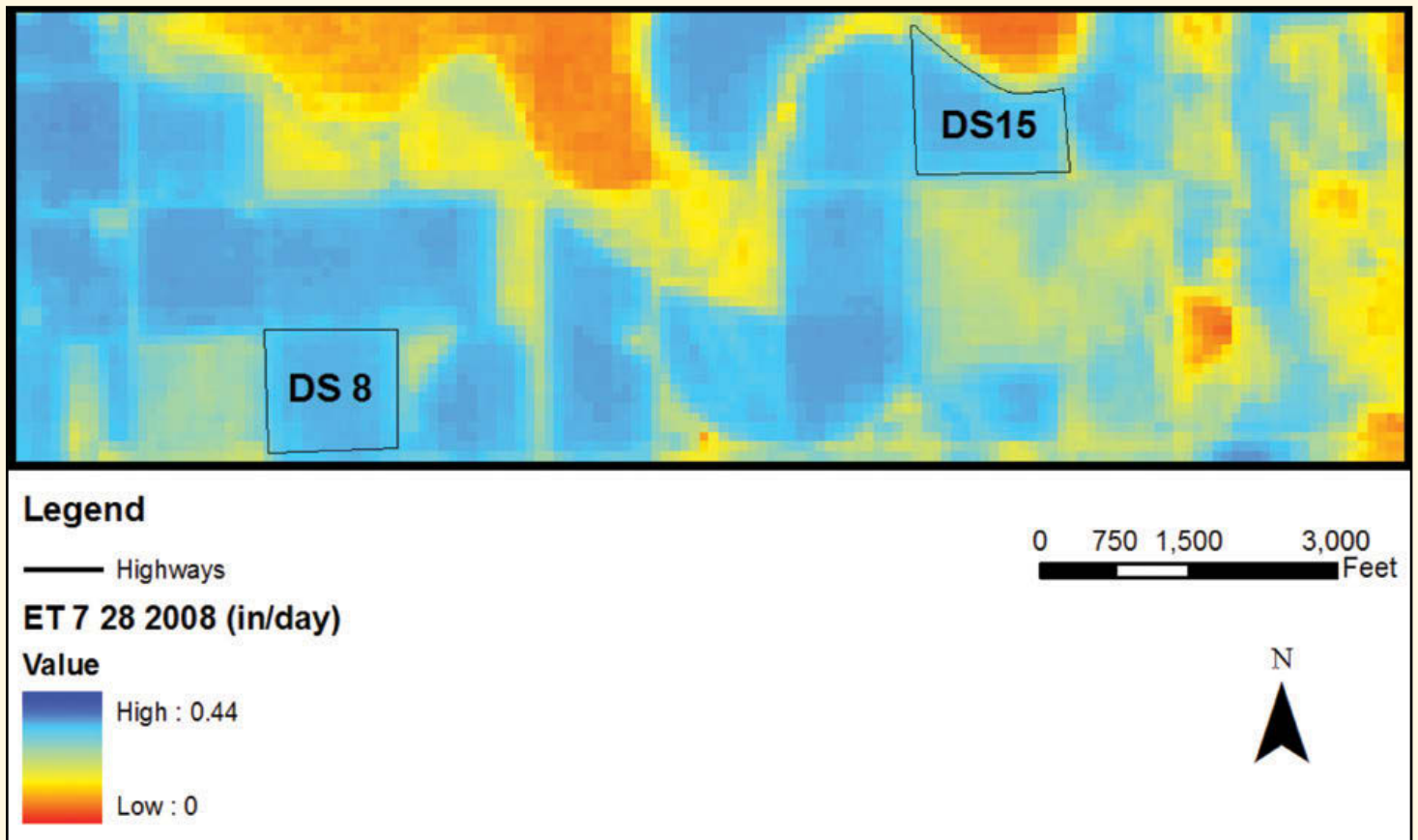


Figure 27. ReSET-calculated  $ET_a$  in vicinity of fields DS8 and DS15 on 28 July 2008

### Soil Water Storage

One of the most important properties in evaluating irrigation water balance components and application efficiency is the water storage capacity of the soil root zone. When infiltrated irrigation water exceeds the soil water storage capacity at a given location in a field, excess water will percolate downward below the root zone as  $Q_{DP}$  and move toward the groundwater table. Between irrigation events the root zone soil water content will vary in response to ET,  $Q_p$ , and  $Q_U$  but is assumed to be limited by the storage capacity. If the soil water content drops too low, the crop will be unable to transpire sufficient water, crop growth and yield may decline and, under extended dry conditions, the crop will perish.

In the current study, the soil water storage capacity was defined using the total available water (TAW) in inches:

$$TAW = D_{rz} (\theta_{fc} - \theta_{wp}) \quad (9)$$

wherein  $D_{rz}$  = depth of soil root zone below ground surface,  $\theta_{fc}$  = soil-water content at  $-1/3$  bar matric potential (field capacity) expressed as a fraction of the bulk soil volume, and  $\theta_{wp}$  = soil-water content at  $-15$  bar matric potential (permanent wilting point) expressed as a fraction of the bulk soil volume. The actual stored volume of soil water ( $S_{SW}$ ) at any given time, expressed in inches (volume per unit field area), was defined as  $S_{SW} = D_{rz} \theta$  wherein  $\theta$  = the actual soil water content, expressed as a fraction of the bulk soil volume. In calculating a water balance for a field over a time period  $\Delta t$ , the term  $\Delta S_{SW}$  in Eq. (1) is defined as the change in  $S_{SW}$  over  $\Delta t$ .

In large regional-scale irrigation survey projects, it is common to estimate  $\theta_{fc}$  and  $\theta_{wp}$  using soil texture data. The method described by Saxton and Rawls (2006), based upon a very large USDA soils database, was used to do so in the current study. Soil textures were estimated for the monitored fields by taking soil samples and/or by using data from the USDA NRCS Soil Survey.

### *Estimation of Soil Texture from Field Samples*

Samples for soil texture were gathered from six locations within each of about 44 of the monitored fields in 2008.

The following procedure was used to determine the sample locations within a given field:

1. The USDA-NRCS Soil Survey Geographic (SSURGO) Database was used to create an “Area of Interest” (AOI) for each monitored field (USDA 2010). The subsequent soil map was used to determine the locations of soil samples collected on each field.
2. For fields with one primary soil type, samples were collected at locations near the midpoints of six sections of similar size within the field.
3. For fields with multiple soil types, soil sampling locations were distributed based generally upon a spatially weighted average of primary soil types within the field. For example, if a particular field contained two primary soil types (e.g., RoB, RoC) with soil type RoB comprising two-thirds of the field area and RoC comprising one-third of the field area, four soil samples were collected from within the RoB area and two soil samples were collected from within the RoC area.
4. For fields consisting of more than six primary soil types, soil samples were collected from the six soil type areas comprising the largest proportion of the total field area.
5. Soil types comprising less than 10 percent of the total field area generally were not sampled.

At each sampling location within a field the following procedure was used to collect soil samples for textural analysis:

1. The soil surface at each location was cleared of crop residue by hand or with a spade.
2. A Stihl® gas-powered earth auger (Figure 28) with an 18 inch by 1.5 inch diameter auger and two 18 inch extensions were utilized to bore to a depth of approximately 48 inches at each location. The auger generally was pulled from the hole five times per location to either remove soil from the auger flighting or to add extensions to the auger.
3. All soil augered to the ground surface (approximately 500 grams per location) was collected by hand or using a small spade and placed in a plastic double-lock freezer bag.



**Figure 28.** *Stihl® gas-powered earth auger used for soil sampling*

The hydrometer method of mechanical analysis was used in the soils laboratory at CSU to determine the fraction of clay, silt, and sand for each soil sample (Klute 1986). Soil texture classification then was determined based upon these relative fractions.

#### *Estimation of Soil Texture from NRCS Soil Survey*

Data from the USDA-NRCS Soil Survey Geographic (SSURGO) Database, using the Soil Data Mart web-based application, were extracted for each monitored field. These data include estimated soil texture,  $\theta_{fc}$ ,  $\theta_{wp}$ , available water holding capacity (in inches of water per ft of soil), and bulk density.

Through the Soil Data Mart web-based application, satellite imagery of each field was overlain with a field boundary map to create an area of interest (AOI). For this AOI, weighted representative averages for each of the aforementioned soil properties and each soil type were calculated to a depth of 48 inches. Output from the Soil Data Mart included the following for each AOI (field):

- Summary of the soil type(s) present within the AOI (field) and the fractional contribution of each soil type to the total AOI
- USDA soil texture rating for each soil type
- Available water holding capacity (inch/inch) for each soil type, which is equivalent to  $TAW/D_{rz}$
- Water content at -15 bar (permanent wilting point) expressed as percent of total volume at saturation for each soil type
- Water content at  $-\frac{1}{3}$  bar (or field capacity) expressed as percent of total volume at saturation for each soil type
- Bulk density at  $-\frac{1}{3}$  bar for each soil type
- Clay content ( percent by weight of the soil material that is less than  $7.87 \times 10^{-5}$  inches in diameter) for each soil type
- Silt ( percent by weight of the soil material that is greater than  $7.87 \times 10^{-5}$  inches and less than  $1.97 \times 10^{-3}$  inches in diameter) for each soil type
- Sand content ( percent by weight of the soil material that is greater than  $1.97 \times 10^{-3}$  inches and less than 0.08 inches in diameter) for each soil type





### *Estimation of Average TAW*

For fields in which soil samples were gathered, the models developed by Saxton and Rawls (2006) were used to estimate  $\theta_{fc}$ ,  $\theta_{wp}$ , and other soil properties for each sample based upon texture. An average value of TAW was estimated for each monitored field using the values computed for all soil samples collected in each field.

Average soil water properties also were calculated for each monitored field using the data extracted from the USDA-NRCS Soil Survey Geographic (SSURGO) Database through the Soil Data Mart application. Average values for each soil property for each field then were calculated as weighted averages based upon the fractional contribution of each soil type to the total AOI.

### *Estimation of Soil Water Content*

Estimation of average  $S_{SW}$  over areas encompassing several acres, where textural and structural characteristics often vary substantially, is a very difficult and expensive task. A large number of samples, across the areal extent of the field and with depth, usually are required for an accurate estimate at any given time. Such an effort was beyond the scope of this project; however, limited sampling of the monitored irrigated fields was conducted periodically over the course of the study. Typically, soil samples were collected in conjunction with soil salinity surveys that were conducted on each monitored field two to three times during each irrigation season. The methodology is described in a sequel section entitled “Soil Water Salinity and Soil Water Content Surveys”.

### *Upflux from Shallow Groundwater*

Shallow groundwater tables can provide substantial upflux of water to the root zone of crops (Ayars et al 2006, Grismer and Gates 1988). The rate of upflux depends upon the ET rate, soil characteristics, soil water content, crop root characteristics, and depth to the water table. Following Liu et al (2006), the rate of upflux,  $q_u$  (mm/day), from a shallow water table to the root zone of an irrigated field was estimated as:

$$q_u = \begin{cases} q_{u_{max}}(D_{wt}, ET_p) & \text{if } S_{SW} < S_{SW_S}(D_{wt}) \\ q_{u_{max}}(D_{wt}, ET_p) \left( \frac{S_{SW_c}(D_{wt}) - S_{SW}}{S_{SW_c}(D_{wt}) - S_{SW_S}(D_{wt})} \right) & \text{if } S_{SW_S}(D_{wt}) \leq S_{SW} \leq S_{SW_c}(D_{wt}) \\ 0 & \text{if } S_{SW} > S_{SW_c}(D_{wt}) \end{cases} \quad (10)$$

wherein  $q_{u_{max}}(D_{wp}ET_p)$  is the maximum potential groundwater upflux rate (mm/day) and is a function of  $D_{wt}$  and  $ET_p$ ,  $D_{wt}$  is the average water table depth (m) for the current time step,  $ET_p$  is the daily average potential crop evapotranspiration (ET) rate (mm/day) for the given crop and the current time step,  $S_{SW}$  is the average soil water content (mm) for the preceding time step,  $S_{SW_s}(D_{wt})$  is the steady soil water content (mm) and is a function of  $D_{wp}$  and  $S_{SW_c}(D_{wt})$  is the critical soil water content at which upflux is initiated and is a function of  $D_{wt}$ . Note that variable names used herein are different than those used in Liu et al (2006). Values of  $q_u$  can be integrated over a selected time period  $\Delta t$  to obtain  $Q_U$  for water balance analysis.

In the current study, the value of  $q_{u_{max}}$  in Eq. (10) was modeled as a function of  $D_{wt}$  and  $ET_a$  computed by ReSET:

$$q_{u_{max}}(D_{wt}, ET_p) = \begin{cases} ET_a & \text{if } D_{wt} < D_{wt_c} \\ a_1 D_{wt}^{b_1} & \text{if } D_{wt} > D_{wt_c} \end{cases} \quad (11)$$

wherein  $a_1$  and  $b_1$  are empirical parameters that depend upon soil texture, as presented in Table 7.

The critical water table depth,  $D_{wt_c}$ , may be estimated as the following linear function of  $ET_p$ :

$$D_{wt_c} = \begin{cases} a_2 ET_p + b_2 & \text{if } ET_p \leq 4 \text{ mm/day [0.157 in/day]} \\ 1.4 & \text{if } ET_p > 4 \text{ mm/day [0.157 in/day]} \end{cases} \quad (12)$$

The value of  $S_{SW_s}$  depends upon  $D_{wt}$  and the water content in the root zone at wilting point,  $S_{SW_{WP}}$  (mm), and may be estimated from:

$$S_{SW_s}(D_{wt}) = \begin{cases} a_3 D_{wt}^{b_3} & \text{if } D_{wt} \leq 3m [9.84 ft] \\ S_{SW_{WP}} & \text{if } D_{wt} > 3m [9.84 ft] \end{cases} \quad (13)$$

Liu et al (2006) indicate that the parameter  $a_3$  may be estimated as equal to  $1.1(S_{SW_{FC}} + S_{SW_{WP}})/2$  where  $S_{SW_{FC}}$  (mm) is the water content in the root zone at field capacity and  $S_{SW_{WP}}$  (mm) is the water content at wilting point. The value of the parameter  $b_3$  depends upon soil texture, as presented in Table 7.

Similarly,  $S_{SW_c}$  depends upon  $D_{wt}$  and may be estimated from:

$$S_{SW_c}(D_{wt}) = a_4 D_{wt}^{b_4} \quad (14)$$

Liu et al (2006) indicate that the parameter  $a_4$  may be estimated as the value of  $S_{SW_{FC}}$  for the given root zone depth. The value of the parameter  $b_4$  depends upon soil texture, as presented in Table 7.

## Infiltration Uniformity

During a typical surface irrigation event, water is introduced at the head end of the field where it begins its advance over the length of the field toward the tail end. At the tail end of the field, water ponds if the field is diked, or exits the field as tailwater runoff if the field is not diked. The surface flow finally recedes after the inflow at the head is cut off. The depth of infiltrated irrigation water at any point along the length of the field is directly related to the length of time that irrigation water is in contact with the soil surface and the soil infiltration properties at that location. This duration of time commonly is referred to as the intake opportunity time ( $\tau$ ) (Figure 29). Mathematically,  $\tau$  is defined as the difference between the time of recession and the time of advance for any given point along the length of the field. At a given location, infiltration generally decreases from a maximum rate at the beginning of the infiltration process to a constant rate as the intake opportunity time increases. This constant rate of infiltration is called the steady-state (or basic) infiltration rate. In some cases, the duration of an irrigation event may not be long enough for the basic infiltration rate to be reached. A model commonly used to predict infiltration is the modified Kostiakov-Lewis equation:

$$z = k\tau^a + f_0\tau \quad (15)$$

wherein  $z$  = infiltration depth (inches),  $\tau$  = intake opportunity time (minutes),  $f_0$  = steady-state infiltration rate (inches/minute), and  $k, a$  = empirical coefficients (Elliott and Walker 1982).

Steady-state infiltration rate can be determined by 1) conducting infiltration tests in the field immediately prior to the irrigation, 2) subtracting the tailwater runoff flow rate from the inflow (applied irrigation) rate just prior to shutoff of inflow (assuming that the tailwater runoff flow rate has reached a relatively constant value), or 3) referencing published infiltration data based upon the soil type of the field. Using the inflow and tailwater hydrographs from the irrigation itself generally is considered the most accurate method of determining  $f_0$  but only if the duration of the irrigation is long enough for the tailwater flow rate to reach a constant value. The coefficients  $k$  and  $a$  can be determined by 1) referencing published data based upon general soil characteristics in the field, 2) solving irrigation mass balance equations simultaneously for two points along the field length using field data for advance time, application rate, and  $f_0$ , as well as assumed values for subsurface flow shape

**Table 7.** Parameter values for use in estimating  $q_u$  for three different soil textures (Liu et al., 2006)

Parameter	Value for Silt Loam Soil	Value for Sandy Loam Soil	Value for Clay Loam Soil
$a_1$	4.6	7.55	1.11
$b_1$	-0.65	-2.03	-0.98
$a_2$	-1.3	-0.15	-1.4
$b_2$	6.6	2.1	6.8
$b_3$	-0.27	-0.54	-0.16
$b_4$	-0.17	-0.16	-0.32

and Manning's roughness coefficient, or 3) using an optimization algorithm that calibrates  $k$  and  $a$  values by minimizing the difference between measured parameters (such as advance time, tailwater hydrograph points, and recession times) and simulated parameters (found through solving equations of mass conservation and momentum conservation) (this method also can be used to solve for  $f_0$ ) (Walker 2005). After measuring advance and recession times along the length of the field and determining  $k$ ,  $a$ , and  $f_0$ , the infiltrated depth then can be calculated for any point along the length of the field.

The time, personnel, equipment, and financial requirements associated with collecting and analyzing field data for determining the parameters  $k$ ,  $a$ , and  $f_0$  for use in the Modified Kostikov equation were infeasible for a large-scale study of this type. Instead, a more simplified approach was followed in which infiltration depth was considered to approximate a linear function of intake opportunity time.

The validity of the linear infiltration assumption was tested by comparing results from the SIRMOD® model of



surface irrigation which uses an optimization algorithm (Walker 2003) for seven closely monitored corn furrows in 2004. After comparison it was concluded that the most accurate application of the linear approximation was for irrigation events where set cutoff times, advance times, and recession times trended toward lower values. As these times increased, the accuracy in infiltrated depths near the head end of the field and near the tail end of the field decreased when modeled using a linear approximation. Based upon the scope of the current study and the infeasibility of calibrating empirical coefficients based upon measured data, the linear infiltration approximation was deemed suitable to meet the study objectives. However some sensitivity analysis was done and is presented in a section below.

The procedure for calculating infiltrated depths across surface-irrigated subfields is described below:

1. The following data for each irrigation event were entered into an Excel® spreadsheet:
  - Irrigation event start time (month, day, year, hour, minute)

- Irrigation event end time (month, day, year, hour, minute)
- Net applied volume (total diverted volume minus transit losses and pond losses where applicable)
- Net tailwater runoff (total tailwater runoff volume minus transit losses where applicable)
- Number of irrigation sets completed during the irrigation event [This value was (i) based upon examination of the tailwater runoff hydrograph when tailwater loss occurred, or (ii) calculated by dividing the total irrigated area width by generalized set widths when no tailwater loss occurred]
- General advance time to tail end of field for each set [This value was (i) based upon examination of the tailwater hydrograph when tailwater loss occurred, or (ii) calculated as the sum of the average set cutoff time, which was calculated by dividing the irrigation duration by the number of completed sets, and the average

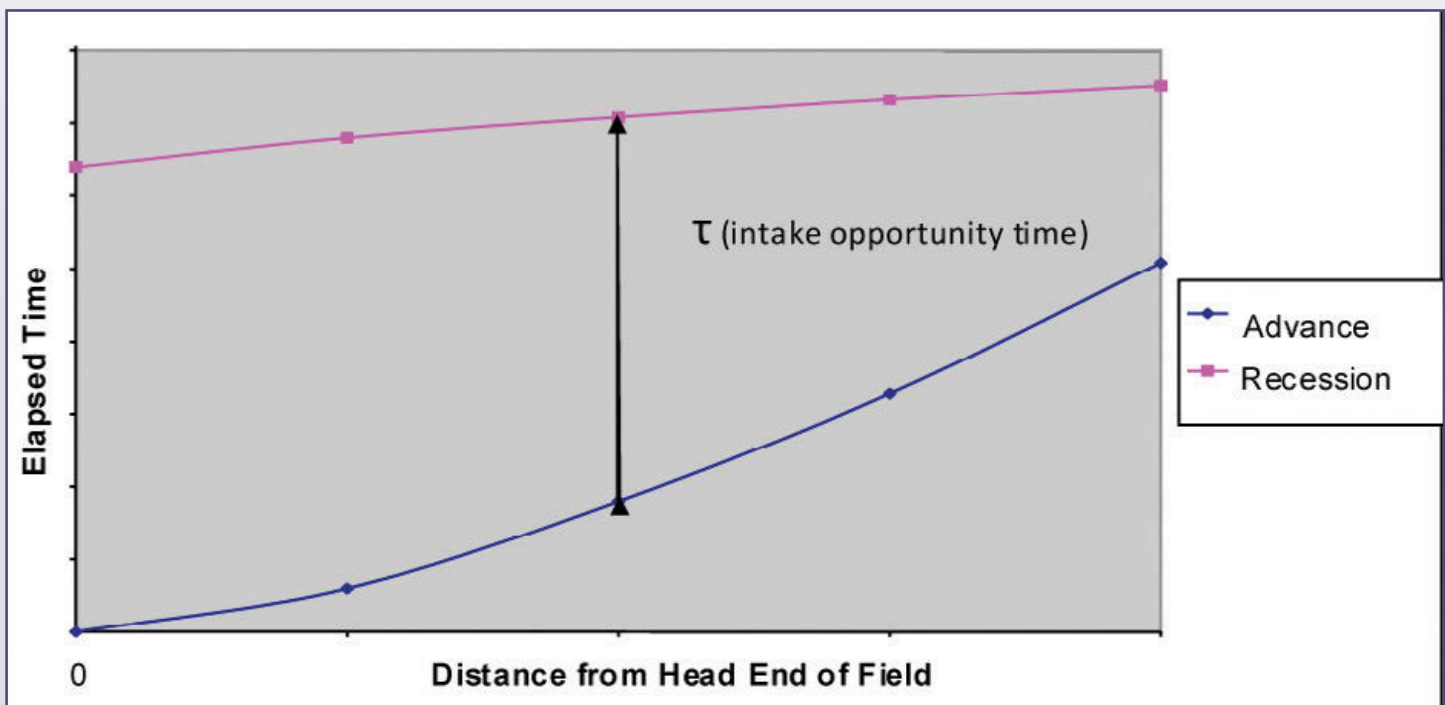


**Figure 29.** Example plots of time of advance and time of recession of an irrigation stream along a field and the intake opportunity time

recession time when no tailwater loss occurred. This calculation assumes that the advancing water front just reaches the tail end of the field, without creating tailwater runoff, before receding because of cutoff].

- Area irrigated during irrigation event
  - Cells (subfields) irrigated during irrigation event
  - General set width estimation
  - Average recession time to bottom end of field (This value was based upon field length. The range of average recession times across all monitored fields was 20 minutes to 60 minutes based upon observations from CSU personnel).
2. The following parameters were calculated for the irrigation event assuming a linear infiltration depth function from the head end to the tail end of the field, lateral uniformity across the irrigated area,

and linear advance and recession from the head to the tail end of the field (Figure 30):

- Average intake opportunity time at head end of field ( $\tau_0$ )
- Average intake opportunity time at  $1/3$  of field length ( $\tau_{L/3}$ )
- Average intake opportunity time at  $2/3$  of field length ( $\tau_{2L/3}$ )
- Average intake opportunity time at tail end of field ( $\tau_L$ )
- Infiltrated depth at field head end ( $z_0$ )
- Infiltrated depth at  $1/3$  of field length ( $z_{L/3}$ )
- Infiltrated depth at  $2/3$  of field length ( $z_{2L/3}$ )
- Infiltrated depth at tail end of field ( $z_L$ )

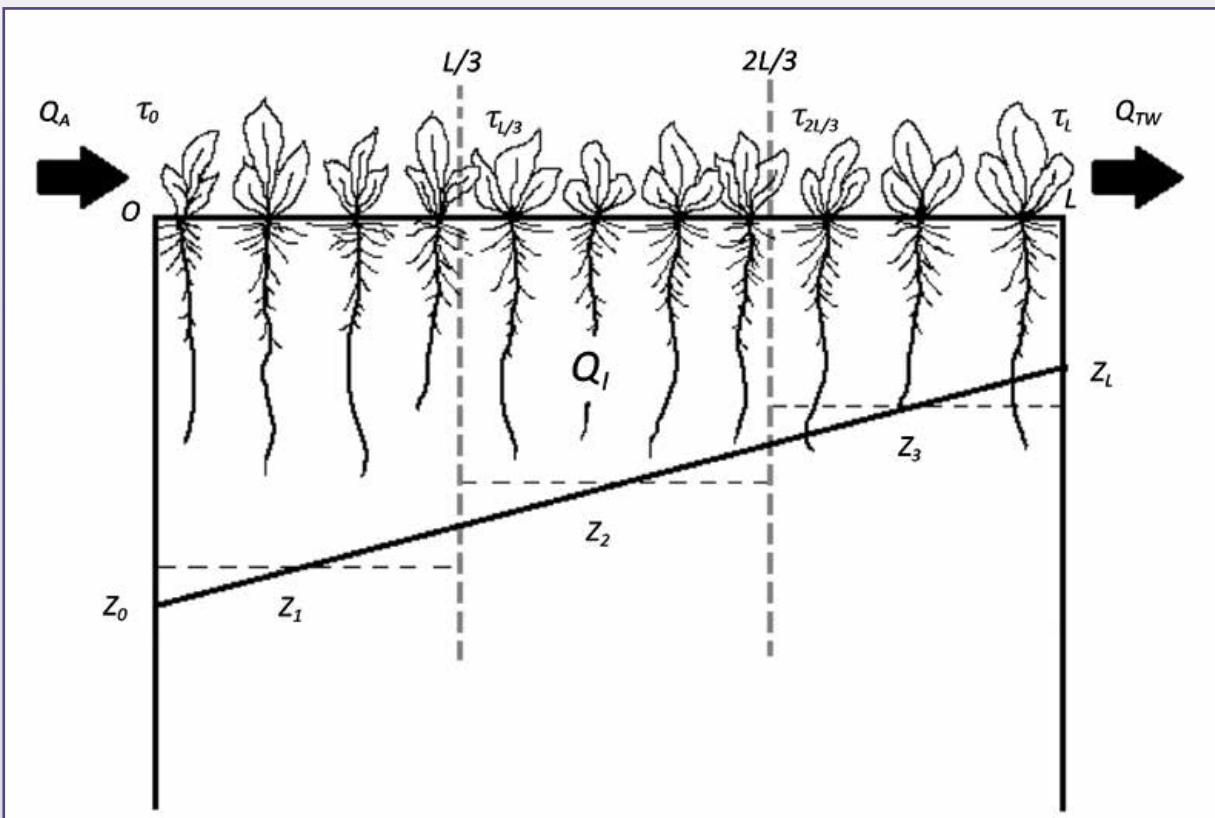


Figure 30. Illustration of linear infiltration distribution approximation used in this study

The calculation process consisted of solving for  $z_0$  by changing values of  $z_L$  subject to the following constraints:  $(z_L/z_0) = (\tau_L/\tau_0)$ , and calculated total infiltrated volume equaled infiltrated volume estimated as the difference between field measurements of total applied irrigation volume,  $Q_A$ , and total tailwater runoff volume,  $Q_{TW}$ . This insured that mass balance was preserved throughout the calculation steps. Finally, average infiltrated depth ( $z_1, z_2, z_3$ ) values were calculated for each  $\frac{1}{3}$  segment of the field based upon the geometric relationships between the infiltrated depths previously calculated.

The results that were transferred into the IDSCU irrigation mass balance model, described in the following section, included (1) average infiltrated depth values for each  $\frac{1}{3}$  segment of the field, (2) cells irrigated during an event, and (3) date of irrigation. For irrigation events spanning more than one day (for surface-irrigated fields) the first day of the irrigation was used for input into the IDSCU model. For sprinkler irrigated fields (for which irrigation events sometimes spanned several weeks or more) total infiltrated depth was divided by irrigation duration so that infiltrated depth values used in the IDSCU model were offered on a daily basis.

### Deep Percolation

The IDSCU model (Garcia and Patterson 2009) was used to estimate various WBC values. The IDSCU Model was developed by the Integrated Decision Support (IDS) Group at Colorado State University. It contains a FORTRAN program for estimating  $ET_r$  and  $ET_p$  for specified crops, for solving Eqs. (1) and (2) for daily values of  $S_{SW}$  over the entire period of study within the irrigation season, and for daily values of  $Q_{DP}$  over time periods encompassing each irrigation event within the season. IDSCU also contains a Graphical User Interface (GUI) for processing and displaying input and output data.

Estimation of  $Q_{DP}$  for an irrigation event using IDSCU requires an estimate of  $S_{SW}$  prior to the first measured irrigation event, and daily input data on  $Q_A$ ,  $Q_P$ ,  $Q_{TW}$ , and  $Q_{ET}$ . Daily values of  $Q_U$  are computed within IDSCU as  $Q_U = q_U \Delta t$  using Eqs. (7)-(11) with coefficients from Table 7 for the given soil type. Data on soil characteristics and crop root zone depth for determining TAW also are required. In IDSCU, if the total amount of  $Q_I$  during the period  $\Delta t$  of an irrigation event is enough to create a value of  $\Delta S_{SW}$  that causes  $S_{SW}$  to exceed the

value at field capacity  $D_{rz}\theta_{fc}$ , then  $Q_{DP}$  is assumed to occur as a result of the irrigation event and is calculated as  $Q_{DP} = S_{SW} - D_{rz}\theta_{fc}$ . In other words, it is assumed that gravity drainage will occur as deep percolation below the crop root zone to bring  $S_{SW}$  back to  $D_{rz}\theta_{fc}$ . To account for nonuniform infiltration, which typically occurs on surface irrigated fields, this water balance calculation is subdivided to different portions of the field as described in the preceding section.

To calibrate the IDSCU model, values for initial soil water content and TAW were adjusted to obtain a reasonable match between predicted and measured values of average  $S_{SW}$  on days when measured data from soil water surveys were available. Typically, data for one or two days of soil water surveys were available. On the average, the percent difference of predicted values of average  $S_{SW}$  from measured values was -15 percent over all fields and all irrigation seasons.

### Sprinkler Evaporation and Drift

In the analysis described here,  $Q_I$  for sprinkler-irrigated fields was assumed to be equivalent to  $Q_A$  (exiting the sprinkler nozzles) less an assumed five percent loss to evaporation and wind drift (Howell 2006, Kansas State Univ. 1997).

### Irrigation Application Efficiency

The term "irrigation efficiency" is widely used in relation to several aspects of irrigated agriculture and can be interpreted in several ways (Bos and Nugteren 1990). In this study we are concerned with irrigation application efficiency,  $E_a$ , as a measure of the performance of an individual irrigation event at the field scale. It is expressed here as a percentage and is defined as "The ratio of the amount of water stored in the actual or potential crop root zone to the total amount of water applied to the crop during a particular irrigation event." In simple terms, it can be thought of as the percentage of the total applied water that the crop can potentially consume in producing marketable yield. In equation form, irrigation application efficiency can be expressed for a time period  $\Delta t$  encompassing an irrigation event as (Hoffman et al 2007):

$$E_a = \Delta S_{SW} / Q_A \quad (16)$$

There is no irrigation system that can apply water without water losses at the field scale. These losses may occur due to evaporation and wind drift during

application, tailwater surface runoff, and DP.  $E_a$  is an indicator of efficiency on a field-scale level only; it does not consider conveyance losses from the water source to the irrigated fields. It may or may not consider the transit losses from small ditches within a field.

### Irrigation Water Quality Sampling

Periodically, measurements were made of the EC (as specific conductance at 25°C) and temperature of the irrigation water stream applied to a field and/or the tail water stream running off a field. A YSI® 30 Handheld Conductivity Meter (Figure 31), calibrated daily using a standard saline solution of known concentration, was used to make the measurements and the probe was rinsed with distilled water between measurements. Usually, only one measurement of irrigation water and tail water were made during a single irrigation event, but occasionally two measurements were made and averaged.

Total dissolved solids (TDS) were estimated from EC readings using equations developed from a companion CSU project in the LARV. This project collected water samples from numerous groundwater wells in the Upstream Study Region over the period 2006-2009 and in the Downstream Study Region over the period 2003 - 2009. About 142 surface water samples from Upstream and 427 surface water samples from Downstream were analyzed in the laboratory for specific salt ions and TDS, and regression equations were developed relating lab-determined TDS to field-measured EC in dS/m. The resulting power equations (statistically significant at a significance level  $\alpha = 0.05$ ) used, for the Upstream and Downstream regions respectively, were:

$$\text{TDS} = 868\text{EC} - 124.1, r^2 = 0.94 \quad (17)$$



**Figure 31.** YSI® 30 handheld conductivity meter used for measuring EC and temperature

$$\text{TDS} = 797\text{EC} - 111.0, r^2 = 0.77 \quad (18)$$

Whenever possible, if EC measurements were not taken in the irrigation water stream during an irrigation event, the EC of the irrigation stream was assumed to be equal to the EC measured with a YSI® 30 meter by the companion CSU project in the supply canal at a sampling location nearest to the irrigated field and on a date closest to the irrigation event. For fields supplied from pumping wells, the EC measured in a groundwater monitoring well located in or near the field and closest to the supply well was used to estimate the EC of the irrigation water.

### Shallow Groundwater Monitoring

The alluvial groundwater table generally is quite shallow in the LARV. Observation wells were drilled on or near each monitored field to measure the  $D_{wp}$  EC (specific conductance at 25°C), and temperature of the water table. These data provide information about the response of the groundwater to deep percolation from irrigation and about upflux of saline groundwater into the crop root zone.

A minimum of one observation well was installed within or adjacent to each monitored field except in cases where several monitored fields were immediately adjacent to one another. In such cases one well could serve to represent multiple fields. Over 50 percent of fields contained two or more observation wells. Observation well locations were chosen based upon the following criteria: (1) sites where vehicle/farm equipment traffic was minimal, (2) sites where surface water intrusion from irrigation channels, drainages, or pot holes was minimal, and (3) sites where wells could be located within a cropping area without searching for long periods of time (especially important in the case where observation wells were located within the cultivated field area and where well casings were level with the ground surface).

Observation wells were drilled to a maximum depth of 30 ft and with an average depth of approximately 20 ft. Well casing consisted of 2½" slotted (0.016 inch slot width with 3.1 in<sup>2</sup> slot area per lineal foot) schedule 40 PVC pipe with a removable female cap fitting placed at the top. Wells located outside of the field area were allowed casing heights that extended above the ground surface by several inches to several feet. Wells located within the field area typically were allowed casing heights level with the ground surface to deter damage

to and from farm equipment. Soil surrounding each well casing was packed with a tamping bar and covered with bentonite clay on an annual basis to impede surface water intrusion.

### Measurement of Water Table Depth

Observation wells generally were monitored on a bi-weekly basis from May through September and a monthly basis for the rest of the year. The value of  $D_{wt}$  was measured from the top of the well casing using a 100 ft open-spool tape with a small weight and calibrated Styrofoam float attached to the end (Figure 32). The casing height above the ground surface also was measured each time. Where applicable,  $D_{wt}$  data from other concurrent CSU groundwater studies were used to complement data collected in this project.



**Figure 32.** CSU field technician measuring depth to water table in well on Field DS12 using an open-spool tape, 2005

### Measurement of Specific Conductance in Groundwater

Groundwater temperature and EC measurements were made using a YSI® 30 Handheld Conductivity Meter which was calibrated daily using a standardized saline solution. The probe was rinsed with distilled water between observation well readings. Typically, three sets of EC measurements were taken: near the water table, near the bottom of the well, and midway between the water table and the bottom of the well. The average of these three measurements was used to estimate EC of the groundwater in the well.

Total dissolved solids (TDS), or total salt ions in solution, were estimated from EC readings using equations developed from the companion CSU project in the LARV. About 363 groundwater samples from Upstream and 898 groundwater samples from Downstream were analyzed in the laboratory for specific salt ions and TDS, and regression equations were developed relating lab-determined TDS in mg/L to field-measured EC in dS/m. The resulting power equations (statistically significant at a significance level  $\alpha = 0.05$ ) used, for Upstream and Downstream regions respectively, were:

$$\text{TDS} = 847.6\text{EC}^{1.06}, \quad r^2 = 0.93 \quad (19)$$

$$\text{TDS} = 1066.7\text{EC}^{0.93}, \quad r^2 = 0.83 \quad (20)$$

### Soil Water Salinity and Soil Water Content Surveys

#### Field Measurement with Electromagnetic Induction Meters

Surveys to estimate soil water salinity were conducted on monitored fields throughout the duration of the project with two surveys completed on each field during 2004, 2005, and 2008 (typically in June and November) and three surveys completed on each field during 2006 and 2007 (typically in May, July, and November). Surveys for soil water salinity were conducted using EM38 electromagnetic induction meters developed by Geonics™, Ltd. (Mississauga, ON, Canada) and Garmin eTrex Legend® GPS units (Figure 33). When placed on the ground the EM38 induces an electromagnetic field that allows for measurement of bulk soil electrical conductivity (dS/m) at the site. At each site, measurements are made with the EM38 oriented both horizontally and vertically. The horizontal orientation

measurement,  $EM_H$ , renders a bulk conductivity measurement to an effective depth of about 0.75 m and the vertical orientation measurement,  $EM_V$ , to an effective depth of about 1.5 m. The readings have an accuracy of about plus five percent at 30 mS/m.

EM38 meters were calibrated according to manufacturer's specifications prior to the start of surveying on each field. Battery levels were checked periodically throughout the surveying process and generally changed after about 15 hours of continuous use. During the surveying process, special care was taken by CSU personnel to wear attire that would not alter ground conductivity readings. This included the use of footwear not containing metal and the removal of metallic objects from their attire.

For fields rectangular or square in shape, geo-referenced soil water salinity surveys were initiated near one corner of the field with EM38 readings and GPS coordinates were obtained, using a Garmin eTrex Legend handheld GPS unit, at each point on a 150-ft square grid pattern throughout the field area. For fields with a total area less than 10 acres, EM38 readings and GPS coordinates were obtained at each point on a 100-ft square grid pattern throughout the field area. Surveys typically were started near one corner and followed a path adjacent to one field boundary to the opposite end of the field. A new path was started either 150 ft or 100 ft adjacent to the initial path and continued to the opposite end of the field. This process was continued from the starting field boundary to the opposite field boundary. For fields circular in shape (center pivots), geo-referenced soil water salinity surveys were initiated at a point between the two outside sprinkler towers with EM38 readings and GPS coordinates obtained each 150 ft on a circular-shaped path around the field area. Following the completion of the initial path, a new path was initiated at a point about 150 ft inwards from the first path. This process was continued from the outside boundary to the center point of the field.

### Soil Water Content Measurements

Soil samples were collected for gravimetric soil water content analysis immediately following the completion of each soil salinity survey. The procedure below was followed:

1. Soil sampling locations were determined by visually dividing the field into four quadrants and identi-

fying a location near the approximate midpoint of each quadrant as a sampling location.

2. The soil surface at each location was cleared of crop residue by hand or spade.
3. During the 2004-2007 seasons, Oakfield tube samplers (Figure 34) were used to extract soil samples from a depth of approximately 24 inches at each location. During the 2008 season, a Stihl® gas-powered earth auger with an 18 inch by 1.5 inch diameter auger and two 18 inch extensions was used to bore to a depth of approximately 48 inches at each location. The auger was generally pulled from the hole five times per location either to remove soil from auger flighting or to add extensions to the auger. For each sampling location, all extracted soil was collected from the sampler by hand or using a small spade, placed in a plastic double-lock freezer bag, and labeled.
4. In most cases, each sample was weighed within one hour following collection using a portable, electronic scale (ACCULAB® PP401).
5. Soil temperature at a six inch depth from the ground surface was measured at each sampling location using a digital thermometer (ACURITE® 00645W2).
6. Soil samples were allowed to air dry in a low humidity greenhouse environment at the CSU-Arkansas Valley Research Center near Rocky Ford, Colorado for approximately three weeks. Soil samples were not transferred from plastic bags for the drying process; the bags were simply opened and exposed to air.
7. Following the drying period, soil samples were weighed again, as were empty plastic sampling bags.
8. Air-dried gravimetric water content ( $WC_{AD}$ ) was estimated for each sample using the following equation:
 
$$WC_{AD} = (W_{ws} - W_{ds}) / (W_{ds} - W_{bag}) \quad (21a)$$
 wherein  $W_{ws}$  = weight of wet soil sample (including bag),  
 $W_{ds}$  = weight of dry soil sample (including bag), and  
 $W_{bag}$  = weight of plastic bag.

9. Oven-dried gravimetric water content ( $WC_{OD}$ ) was estimated from  $WC_{AD}$  for each sample using the following method.

- Values of  $WC_{AD}$  were determined for a portion of 297 soil samples in 2008. Another portion of each of the same samples was placed in a can and dried in an oven to determine oven-dried water content as

$$WC_{OD} = (W_{ws} - W_{ds}) / (W_{ds} - W_{can}) \quad (21b)$$

wherein  $W_{ws}$  = weight of wet soil sample (including can),

$W_{ds}$  = weight of dry soil sample (including can), and

$W_{can}$  = weight of metal can

- Statistical analysis revealed that on average,  $WC_{OD}$  exceeded  $WC_{AD}$  by 0.013 (about 8.8 percent). Thus, the following was used to estimate  $WC_{OD}$  from measured values of  $WC_{AD}$ :

$$WC_{OD} = WC_{AD} + 0.013 \quad (22)$$

### Estimation of $EC_e$ from EM38 Measurements

EM38 readings are affected by soil water content and soil temperature and must be adjusted. Values of  $EM_V$  measured in dS/m with the EM38 were converted to

adjusted values,  $EM_V'$ , using a temperature correction factor,  $f_{tc}$  (Richards 1954):

$$EM_V' = (f_{tc})EM_V \quad (23)$$

with  $f_{tc} =$

$$1.8509 - 0.0516951(T) + 0.000858442(T^2) - 0.00000613535(T^3) \quad (24)$$

where  $T$  is the soil temperature ( $^{\circ}C$ ) measured in the field in  $^{\circ}C$ . Finally, saturated paste extract soil salinity,  $EC_e$  was estimated using calibration equations developed by Wittler et al. (2006) for the Upstream and Downstream Study Regions. For fields in the Upstream region,  $EC_e$  in dS/m was estimated from:  $EC_e =$

$$2.33 + 7.16(EM_V'/100)^{1.44} + 9.41WC - 23.18(EM_V'/100)(WC) \quad (25)$$

For fields in the Downstream region,  $EC_e$  in dS/m was estimated from:  $EC_e =$

$$0.45 + 7.23(EM_V'/100)^{1.78} + 19.54WC - 34.06(EM_V'/100)(WC) \quad (26)$$

**Figure 33.** CSU technician conducting EM38 survey on a field in the LARV



## Preparing Soil Salinity Maps

The ArcGIS 9.3 geographic information systems software was used to generate maps of  $EC_e$  for each field survey using kriging interpolation techniques. Kriging methods depend on mathematical and statistical models that rely on the notion of correlation between  $EC_e$  values at locations within a field based upon the distance between the locations. The procedure is described in Eldeiry and Garcia (2008).

## Crop Yield Measurements

To estimate crop yield, crop biomass samples were collected on each of the monitored fields one to three times per season for the duration of the project. The procedure for collecting crop biomass samples is outlined below:

1. Crop biomass sampling locations were determined for each field in two ways:
  - If previous soil water salinity survey data were available for the field, six separate locations were chosen based upon the three areas of highest soil water salinity concentration and the three areas of lowest soil water salinity concentration.
  - If soil water salinity survey data were not available, the field was divided into six equal-sized areas with the approximate midpoint of each area considered the crop biomass sampling location.
2. For each sampling location, three different types of data were collected: crop biomass, EM38 measurements, and samples for soil water content. Methods used in taking EM38 measurements and gathering soil samples for estimating gravimetric soil water content are described in the section “Soil Water Salinity and Soil Water Content Surveys”. Biomass sampling was conducted as follows:
  - For alfalfa and alfalfa/grass mix crops, biomass samples were collected at each sampling location by either of the two following methods:
    - i. If the crop had not been cut, a 3.3-ft (1 meter) square frame constructed of  $\frac{1}{2}$  inch thick steel rod was placed on the ground and all vegetation was hand-cut with scissors and hedge trimmers to a height of about one inch above ground level. All cut vegetation was then placed in a mesh onion sack (bushel size) for greenhouse drying. Biomass samples for wheat crops also were collected in this manner.
    - ii. If the crop had been cut into windrows by the grower, a length of windrow (ranging from one ft to five ft) was measured, collected by hand, and placed in a mesh onion sack for greenhouse drying. In addition, the distance from the centerline of the windrow to the centerline of an adjacent windrow was measured and recorded for the purpose of calculating biomass/area values. For each sample within a given field, the length of windrow collected for drying was the same. Sampled areas varied between fields only and never between samples within a given field.
  - For row crops including corn (for grain or ensilage) and sorghum (for grain, ensilage, or forage), crop biomass samples were collected as follows:
    - i. For each sampling location a number of plants were hand-cut (using a hacksaw) at a height of about one inch above the ground surface and placed into a mesh onion sack for greenhouse drying. For each sample within a given field, the number of plants collected for drying was the same. Sample sizes varied between fields only and never between samples within a given field.



Figure 34. Oakfield tube sampler.

- ii. For each sampling location, a plant population count was conducted by measuring a 10-ft length of row and then counting the number of plants growing in that span.
3. Following the completion of sampling, crop biomass samples were allowed to air dry for a minimum of three weeks in a low humidity greenhouse environment at the CSU Arkansas Valley Research Center near Rocky Ford, Colorado. Following drying, crop samples were weighed.

The crop biomass data were normalized in order to make comparisons between fields. For alfalfa, the data were normalized by dividing measured yields by an estimated maximum yield per cutting of tons per acre. Colorado Agricultural Experiment Station (2008) provides data on the crop yields for a number of alfalfa variety trials from 2004-2006. On the average, the total yields from entire fields for three cuttings were found to be about 2.3 tons/acre per cutting. Therefore a maximum of three tons/acre was selected since in order to obtain an average of 2.3 tons/acre over an entire field the maximum for any one small plot in the field could be higher. Colorado Agricultural Experiment Station (2008) also reports the average biomass yields for corn silage planted on small plots to be about 32.8 tons/acre. Thus, a maximum of 33 tons/acre was used to normalize the corn biomass data obtained in this report

## Sensitivity Analysis

Sensitivity of values of the deep percolation fraction,  $DPF = Q_{DP}/Q_A$  (percent), and  $E_a$  estimated by the IDSCU model to approximate errors in selected input parameters was investigated. The aim was to provide an estimate of the likely range of values that DPF and  $E_a$  could take on in light of the uncertainty in measuring and estimating some of the parameters deemed to play a key role in estimating losses of water due to downward percolation and associated efficiency of water application.

### *Sensitivity to Evapotranspiration, Infiltrated Irrigation Volume, and Soil Water Storage*

The IDSCU model was run using values of  $ET_a$ ,  $Q_p$ , initial  $S_{SW}$ , and TAW that constitute upper and lower ends of an estimate error bound. The error range between the upper and lower bound values for each parameter was defined as plus or minus a percentage of

defined baseline parameter values, considered the best estimates, for each monitored field and each season. The error bound used for each of the considered input parameters was +/- 20% for  $ET_a$ , +/- 20% for  $Q_p$ , +/- 20% for initial  $S_{SW}$ , and +/- 20% for TAW. Adjustments to considered input parameters were conducted independently, with all other parameters maintained at their baseline values. Average values of DPF and  $E_a$  over all surface irrigation events and all sprinkler irrigated events were computed for both the upper and lower bound values of each considered input parameter. These values could be compared to those previously computed by IDSCU using baseline values for all parameters.

### *Sensitivity to Infiltration Distribution Pattern*

Sensitivity to the infiltration distribution pattern on surface-irrigated fields also was investigated. To estimate sensitivity to the assumed linear distribution pattern, reasonable upper and lower bounds of the slope of the infiltration depth function were calculated. The upper bound was found by increasing the infiltrated irrigation depth for the baseline condition, computed as described in the section "Infiltration Uniformity", on the first third of the irrigated cell by 30 percent while simultaneously decreasing the infiltrated depth on the last third of the irrigated cell by 30 percent. The lower bound was defined in a similar fashion but with the increase and decrease occurring on opposite ends of the irrigated cell. Average values of  $E_a$  were calculated for each bound for all the surface irrigated events. Figure 35 depicts the assumed linear distribution associated with the upper and lower bounds, compared to that for the baseline condition.

## Regional-Scale Modeling of Irrigation-Affected Flow and Salt Loading Processes

Though the number of irrigated fields monitored in this study was relatively large for an effort of this type, it was quite small compared to the total number of irrigated fields in the LARV. To examine the behavior of the irrigated stream-aquifer system over regional scales, a revised version of a computational groundwater model described by Burkhalter and Gates (2005, 2006) was applied to the Upstream and Downstream study regions. The modeled area in the Upstream Study Region encompassed about 125,000 ac, of which about 65,300

ac are irrigated. Downstream the modeled area covered about 136,300 ac, of which about 81,600 ac are irrigated. The flow component of the revised model, used in this study, uses an amended version of the MODFLOW saturated zone groundwater flow model (Harbaugh 2005) coupled with the UZF unsaturated zone model (Niswonger et al 2006). The governing flow equations are solved using finite-difference approximations applied to a computational grid size of 250 m by 250 m with two vertical layers and time steps of one week. The model has been calibrated and tested against a large data set gathered over the period 1999-2007 in the Upstream region and 2002-2007 in the Downstream region. The calibration targets include depth to the groundwater table at 88 sites Upstream and at 99 sites Downstream, groundwater return flows to tributaries and streams estimated by water balance calculations using stream flows measured at numerous gaging sites, measured seepage from irrigation canals, estimates of  $ET_a$  using ReSET and satellite data, and measured upflux from shallow groundwater tables under naturally-vegetated fields. Baseline estimates of  $Q_{DP}$  from the IDSCU model

were used to estimate targets for recharge to the shallow water table aquifer computed by the regional models. Also, estimates of tailwater runoff fraction,  $TRF = Q_{TW}/Q_A$  (percent), from the field study were used to guide the estimation of values of  $Q_I$  for the regional model. The calibration period was April 1999 to March 2004 and the test period was April 2004 to October 2007 for the Upstream Study Region. For the Downstream region, the calibration period was April 2002 to March 2006 and the test period was April 2006 to October 2007. Distributed values of the following model parameters were adjusted by optimization using the UCODE automated parameter estimation software and/or by manual adjustment: horizontal saturated hydraulic conductivity, effective vertical saturated hydraulic conductivity in the unsaturated zone, soil saturated water content, specific yield, canal conductance, and tributary and stream conductance. Manual methods were used to adjust values of the following parameters: aquifer thickness, ET extinction depth ( $D_{wt}$  value at which groundwater upflux to ET ceases),  $ET_p$  adjustment factor, etc. Histograms of the residual differences between simulated and observed

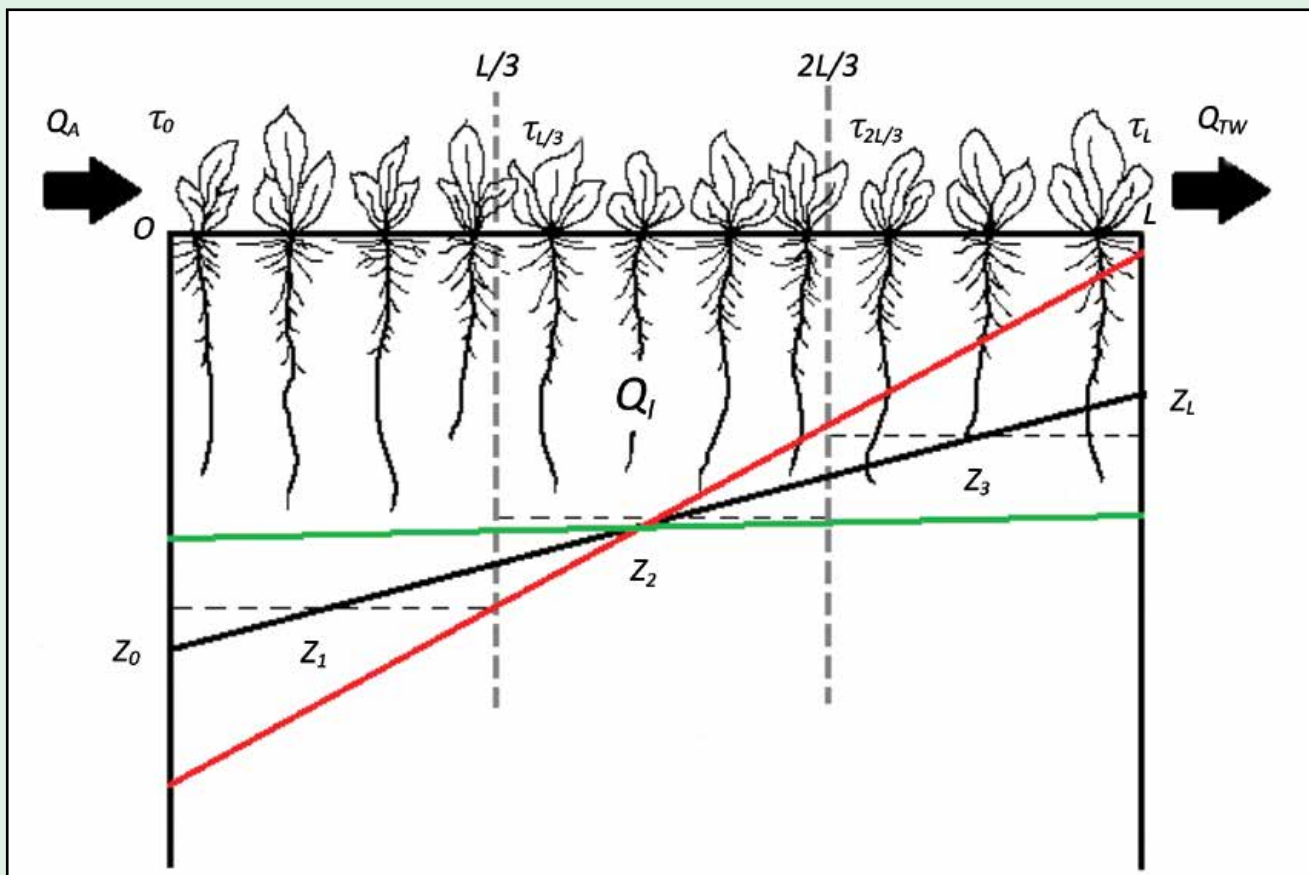


**Figure 35.** Distribution Sensitivity: Assumed, upper (red) and lower (green) bounds for the slope of the linear infiltration distribution, compared to the assumed baseline (black) distribution

values of  $D_{wt}$  for both calibration and test periods for the Upstream and Downstream region are shown in Figure 36. Figure 37 shows plots of simulated values of groundwater return flow along reaches of the Arkansas River, compared to estimates of total unaccounted-for return flow (which includes both groundwater and unaccounted-for surface water return flows) for both calibration and test periods for the Upstream and Downstream region. These figures reveal that the model

is reasonably accurate in predicting groundwater head and groundwater return flow for the period of study. Work is currently underway to refine estimates of groundwater return flow. Detailed descriptions of the model will be available in an article under preparation by Morway et al. (2012).

For the current study, focus was given to regional model predictions of spatial and temporal distributions of recharge to the shallow aquifer as affected

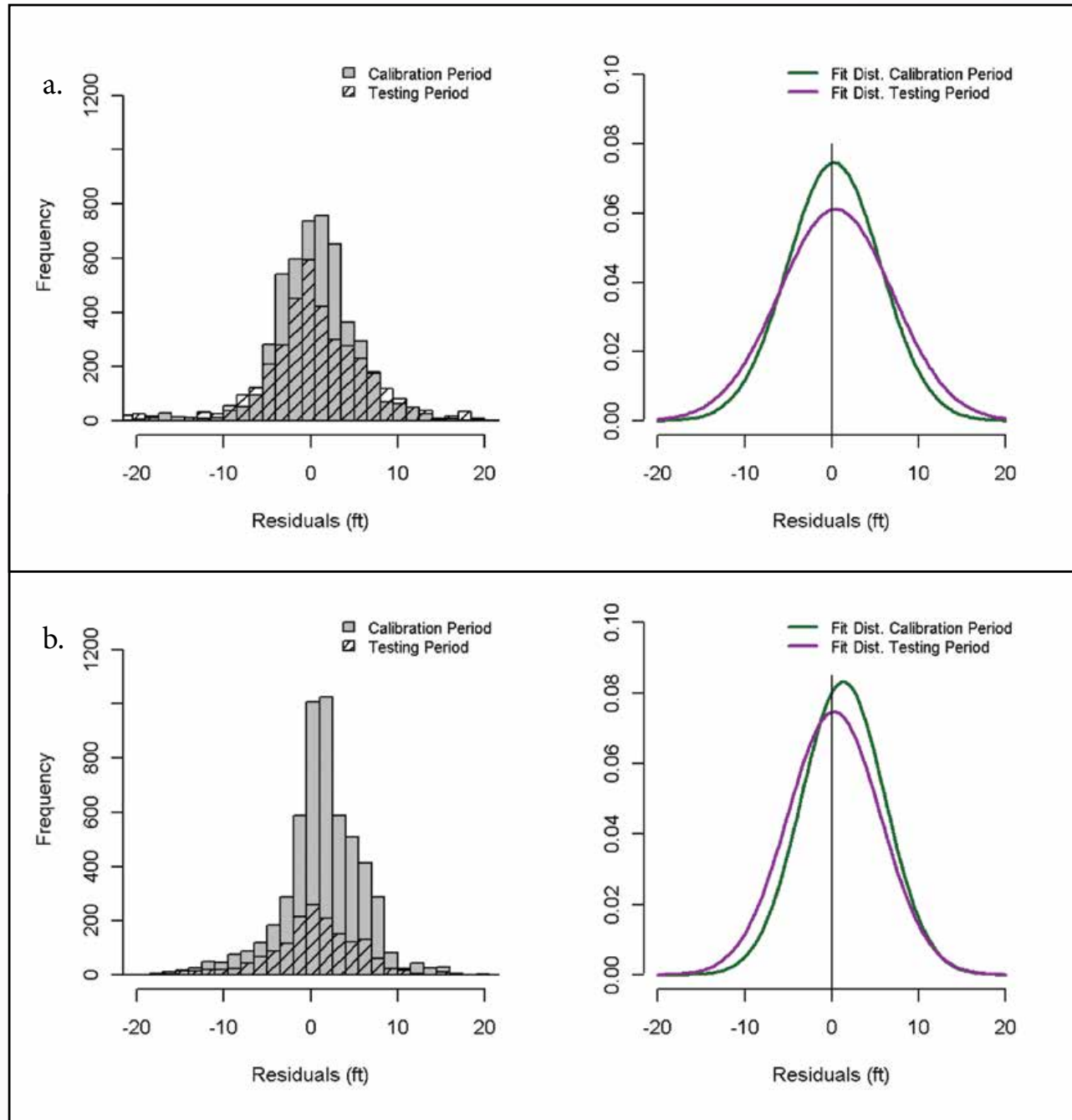


**Figure 36.** Frequency histograms and fitted distributions of residuals (difference between simulated and observed values) of  $D_{wt}$  for (a) Upstream Study Region, and (b) Downstream Study Region

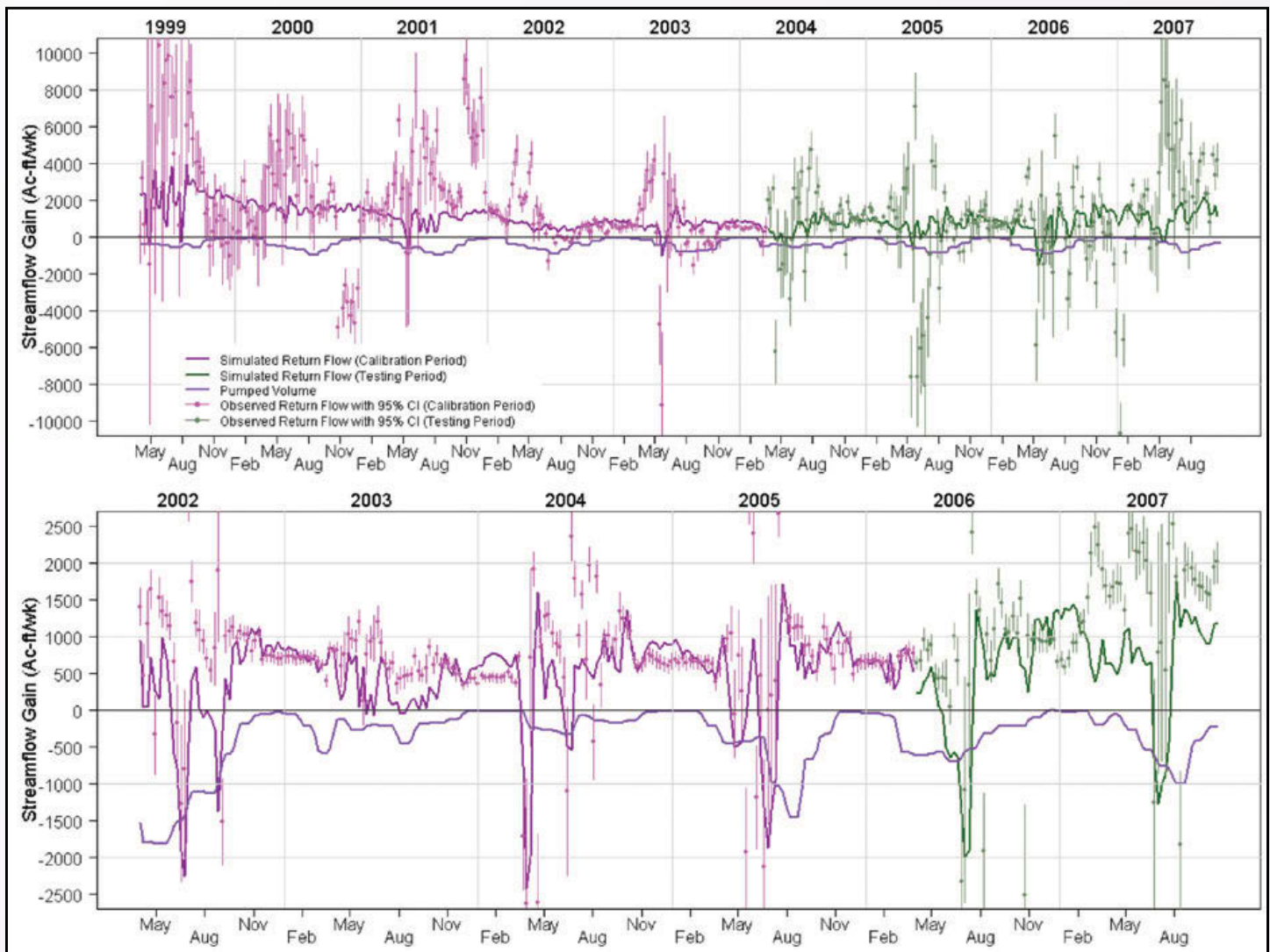


**Figure 37.** Simulated weekly groundwater return flow to the Arkansas River compared to total unaccounted-for return flow (with 95 percent confidence intervals) estimated using stream gauges for calibration and testing periods for river reaches along the (a) Upstream Study Region, and (b) Downstream Study Region

by deep percolation, non-beneficial water consumption due to upflux from the shallow aquifer under naturally-vegetated and fallow fields, and return flows and salt loads from groundwater to the main stem of the Arkansas River within the two study regions. These are key variables to understanding the effect of irrigation practices on the stream-aquifer system and on compliance with the Arkansas River Compact.

Salt loads in groundwater return flow to the Arkansas River were estimated for this study by multiplying predicted groundwater return flow rates by groundwater salt concentrations interpolated for each respective computational link along the river. Groundwater salt concentrations were extrapolated from measurements

made by a companion CSU study in multiple observation wells distributed over the study regions. Current work is underway to improve salt load estimates through the use of calibrated and tested MT3D solute transport models in conjunction with the MODFLOW-UZF models of the study regions.

# Results

## Irrigation Water Balance Components and Efficiency

The WBC and  $E_a$  values computed for each field and each irrigation event within each irrigation season over the entire study period are summarized for the Upstream and Downstream surface-irrigated fields and sprinkler-irrigated fields in files on the IDAD. Summary statistics of measured or estimated  $Q_A$ ,  $Q_P$ , TRF, DPF, and  $E_a$  values are presented in Table 8 for Upstream, Downstream, and total monitored fields for each of the seasons within the study period.

### Precipitation

Histograms of  $Q_{PT}$  for each field, both Upstream and Downstream, over the entire study period are shown in Figures 38, 39 and 40. Figure 38 shows the total measured rainfall for selected periods within each of the 2004 and 2005 irrigation seasons for both Upstream and Downstream fields. Similar plots for selected periods within the 2006, 2007 and 2008 seasons are shown in Figures 39 and 40. The mean value of total seasonal  $Q_P$  for the selected periods over the entire study was 6.60 inches mean value, 1.98 inches minimum, and 14.87 inches maximum. The CV for  $Q_P$  was about 40 percent.

### Irrigation Water Applied

Frequency histograms and fitted probability distribution functions of  $Q_A$  for surface-irrigation events over the entire study period are shown in Figure 41 for Upstream fields, Downstream fields, and the total of all fields. The mean values of  $Q_A$  for surface irrigation events on Upstream, Downstream, and total fields monitored were 7.4 inches, 9.1 inches, and 8.2 inches, respectively. For about 90 percent of the total surface irrigation events monitored,  $Q_A$ , ranged between 4.0 inches and 13.41 inches. The CV of  $Q_A$  for the total surface irrigation events was about 51 percent.

Histograms and fitted probability distribution functions of  $Q_A$  for sprinkler-irrigation events over the entire study period are shown in Figure 42 for Upstream fields, Downstream fields, and the total of all fields. For sprinkler irrigation events the mean values of  $Q_A$  on Upstream, Downstream, and total fields monitored were 2.0 inches, 2.3 inches, and 2.2 inches, respectively. Values of  $Q_A$  for about 90 percent of the total sprinkler irrigation events monitored ranged between 1.1 inches

and 3.0 inches. The CV of  $Q_A$  for the total sprinkler irrigation events was about 72 percent.

### Tailwater Runoff Fraction

TRF (%) values for all surface irrigation events are plotted as frequency histograms and fitted distribution functions in Figure 43 for Upstream fields, Downstream fields, and the total of all fields. The mean value for the Upstream, Downstream, and total surface irrigation events was 8.4 percent, 7.4 percent, and 8.0 percent, respectively. About 90 percent of the total TRF values ranged between about zero percent and 18.5 percent, and the CV for the total events was about 109 percent. No tailwater runoff was observed for sprinkler irrigation events during this study.

### Infiltrated Water

For surface-irrigation events over the entire study period, frequency histograms and fitted probability distribution functions of  $Q_I$  are shown in Figure 44 for Upstream fields, Downstream fields, and the total of all fields. Mean values of  $Q_I$  for surface irrigation events on Upstream, Downstream, and total fields monitored were 6.7, 8.3, and 7.5 inches, respectively. Values of  $Q_I$  ranged between about 3.7 and 12.3 inches for about 90 percent of the total surface irrigation events monitored. The CV of  $Q_I$  for the total surface irrigation events was about 52 percent. Since there was no observed tailwater runoff for any of the sprinkler irrigation events,  $Q_I$  for sprinkler events were estimated as 95 percent of corresponding  $Q_A$  values accounting for air evaporation and wind drift losses.

Histograms and fitted probability distribution functions of  $Q_I$  for sprinkler-irrigation events over the entire study period are shown in Figure 45 for Upstream fields, Downstream fields, and the total of all fields. The mean values of  $Q_I$  for sprinkler irrigation events monitored on Upstream, Downstream, and total fields were 1.8 inches, 2.1 inches, and 2.1 inches, respectively. For about 90 percent of the total sprinkler irrigation events monitored values of  $Q_I$  ranged between 1.1 inches and 2.9 inches. The CV of  $Q_I$  for the total sprinkler irrigation events was about 72 percent.

**Table 8.** Summary statistics for  $Q_A$ ,  $Q_P$ , TRF, DPF, and  $E_a$  for all seasons over the study period

		2004				2005				2006				2007				2008			
		Mean	Min	Max	CV (%)	Mean	Min	Max	CV (%)	Mean	Min	Max	CV (%)	Mean	Min	Max	CV (%)	Mean	Min	Max	CV (%)
<b>Upstream</b>																					
<i>Surface Irrigation Events</i>																					
No. of events	8				53				33				0				24				
$Q_A$ (in)	7.4	3.7	13.8	49.5	6.9	2.2	16.4	46.6	7.9	2.0	14.9	50.0	-	-	-	-	7.9	0.9	18.7	49.6	
$Q_I$ (in)	6.8	3.6	13.6	52.7	6.2	2.2	14.3	43.2	7.1	1.8	14.5	51.3	-	-	-	-	7.2	0.9	17.2	45.9	
TRF (%)	8.8	0.4	32.4	121.7	8.0	0.0	28.7	100.1	10.1	0.0	33.2	84.1	-	-	-	-	6.7	0.0	27.0	103.6	
DPF (%)	35.9	0.0	73.6	75.7	15.8	0.0	81.6	115.8	18.0	0.0	58.2	105.0	-	-	-	-	24.4	0.0	64.9	86.3	
$E_a$ (%)	55.3	24.3	99.6	53.3	76.2	16.4	100.0	26.7	71.9	39.5	100	26.7	-	-	-	-	69.0	34.8	100.0	31.6	
<i>Sprinkler Irrigation Events</i>																					
No. of events	0				11				15				0				36				
$Q_A$ (in)	-	-	-	-	1.7	1.0	2.6	24.8	1.7	0.9	2.3	26.8	-	-	-	-	2.1	0.5	10.7	95.0	
$Q_I$ (in)	-	-	-	-	1.6	1.0	2.5	24.8	1.7	0.9	2.2	26.8	-	-	-	-	2.0	0.5	9.7	92.5	
TRF (%)	-	-	-	-	0.0	0.0	0.0	-	0.0	0.0	0.0	-	-	-	-	-	0.0	0.0	0.0	-	
DPF (%)	-	-	-	-	7.9	0.0	50.0	207.1	11.5	0.0	55.4	208.8	-	-	-	-	24.1	0.0	95.2	132.6	
$E_a$ (%)	-	-	-	-	87.1	45.0	95.0	18.8	83.5	29.6	95.0	28.6	-	-	-	-	71.0	4.8	95.0	44.7	
<b>Downstream</b>																					
<i>Surface Irrigation Events</i>																					
No. of events	5				27				25				32				35				
$Q_A$ (in)	3.2	2.7	4.5	24.0	9.5	2.2	23.3	43.8	7.8	1.6	21.7	57.7	10.3	4.5	26.3	52.4	9.2	2.7	16.2	36.4	
$Q_I$ (in)	3.1	2.7	4.2	21.0	8.2	2.0	19.4	45.9	7.3	1.5	21.7	60.8	9.5	4.4	26.0	55.9	8.6	1.4	16.2	41.7	
TRF (%)	1.2	0.0	6.1	223.6	13.1	0.0	68.7	104.8	6.4	0.0	21.9	89.9	8.0	0.0	21.4	85.3	4.6	0.0	27.0	162.9	
DPF (%)	0.0	0.0	0.0	-	26.9	0.0	67.7	85.2	34.2	0.0	89.1	85.4	26.8	0.0	86.3	87.6	31.1	0.0	86.1	82.0	
$E_a$ (%)	98.8	93.9	100.0	2.7	60.0	18.3	100.0	39.3	59.4	6.4	100.0	47.5	65.2	2.8	100.0	35.3	64.2	13.9	100.0	37.9	
<i>Sprinkler Irrigation Events</i>																					
No. of events	0				19				25				44				128				
$Q_A$ (in)	-	-	-	-	2.5	0.7	12.7	104.2	2.2	1.1	3.3	28.2	2.2	0.6	13.2	88.6	2.3	0.8	11.4	61.3	
$Q_I$ (in)	-	-	-	-	2.4	0.6	12.2	105.3	2.1	1.1	3.1	28.1	2.1	0.5	12.3	87.8	2.2	0.8	11.2	61.9	
TRF (%)	-	-	-	-	0.0	0.0	0.0	-	0.0	0.0	0.0	-	0.0	0.0	0.0	-	0.0	0.0	0.0	-	
DPF (%)	-	-	-	-	7.8	0.0	49.0	181.8	17.2	0.0	92.2	158.4	3.0	0.0	69.9	391.6	14.0	0.0	66.2	158.1	
$E_a$ (%)	-	-	-	-	87.2	46.0	95.0	16.3	78.2	2.8	95.0	34.6	92.0	25.4	95.0	12.7	81.0	16.9	95.0	27.2	
<b>Total</b>																					
<i>Surface Irrigation Events</i>																					
No. of events	13				80				58				32				59				
$Q_A$ (in)	5.8	2.7	13.8	61.3	7.8	2.2	23.3	48.2	7.9	1.6	21.7	52.9	10.3	4.5	26.3	52.4	8.7	0.9	18.7	41.7	
$Q_I$ (in)	5.4	2.7	13.6	61.6	6.9	2.0	19.4	46.7	7.2	1.5	21.7	55.3	9.6	4.4	26.0	55.9	8.1	0.9	17.2	41.8	
TRF (%)	5.8	0.0	32.6	158.2	9.7	0.0	68.8	108.0	8.5	0.0	33.3	90.1	8.0	0.0	21.4	85.4	5.6	0.0	27.2	129.9	
DPF (%)	22.1	0.0	73.6	124.9	19.5	0.0	81.6	105.0	25.0	0.0	89.0	100.4	26.8	0.0	86.3	87.6	28.4	0.0	86.1	84.0	
$E_a$ (%)	72.1	24.5	100.0	42.7	70.8	16.5	100.0	32.1	66.5	6.5	100.0	36.2	65.1	2.8	100.0	35.3	66.0	13.9	100.0	35.1	
<i>Sprinkler Irrigation Events</i>																					
No. of events	0				30				40				44				164				
$Q_A$ (in)	-	-	-	-	2.2	0.7	12.7	95.1	2.0	0.9	3.3	29.5	2.2	0.6	13.2	88.6	2.3	0.5	11.4	68.8	
$Q_I$ (in)	-	-	-	-	2.1	0.6	12.2	96.2	1.9	0.9	3.1	29.4	2.1	0.5	12.3	87.8	2.2	0.5	11.2	68.5	
TRF (%)	-	-	-	-	0.0	0.0	0.0	-	0.0	0.0	0.0	-	0.0	0.0	0.0	-	0.0	0.0	0.0	-	
DPF (%)	-	-	-	-	7.8	0.0	50.0	188.0	15.1	0.0	92.2	172.1	3.0	0.0	69.6	391.6	16.2	0.0	95.2	153.4	
$E_a$ (%)	-	-	-	-	87.2	45.0	95.0	16.9	80.2	2.8	95.0	32.1	92.0	25.4	95.0	12.7	78.8	4.8	95.0	31.4	

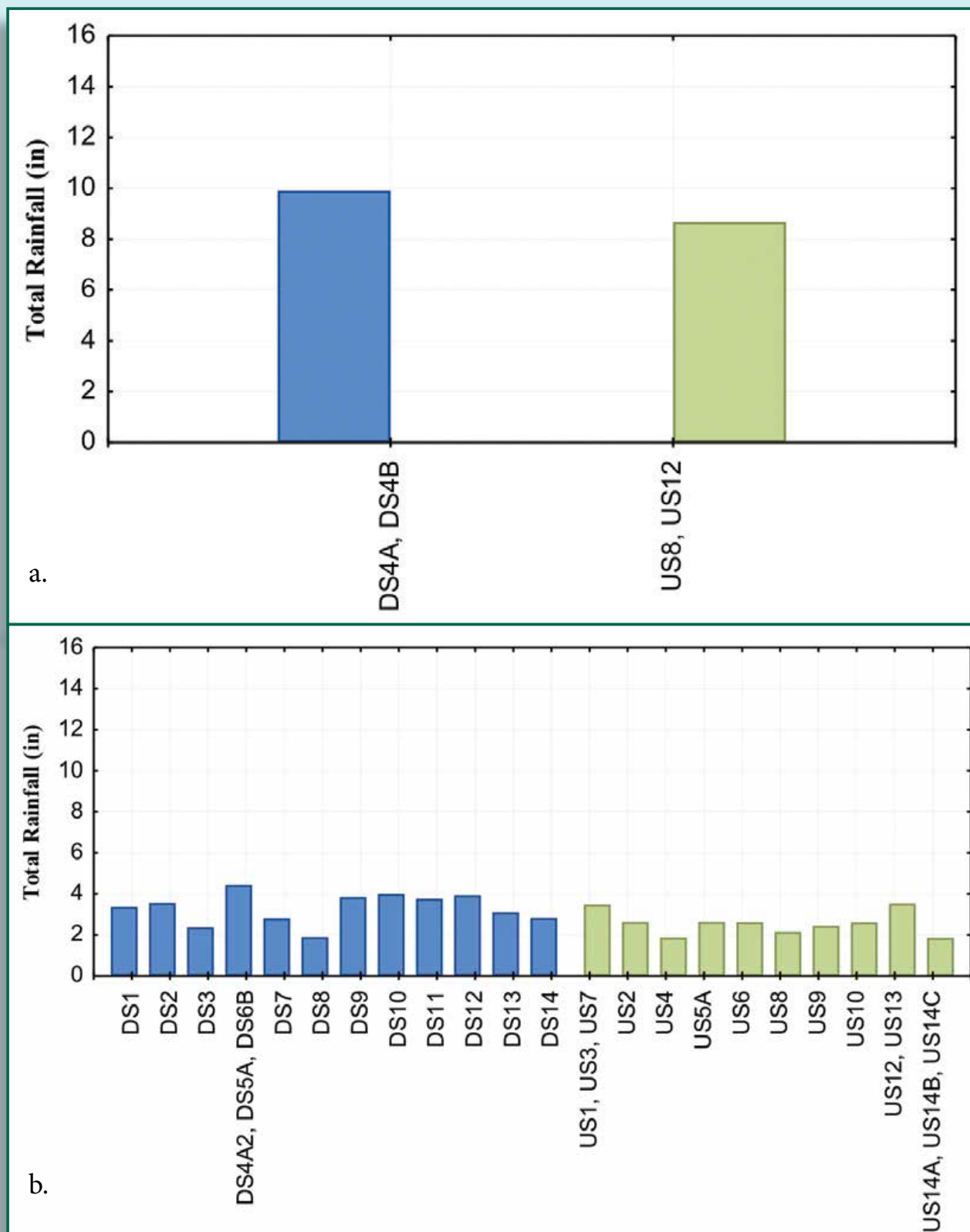


**Figure 38.** Total rainfall measured on monitored fields for (a) 25 May-30 Sep 2004, (b) 30 Jun-28 Sep 2005

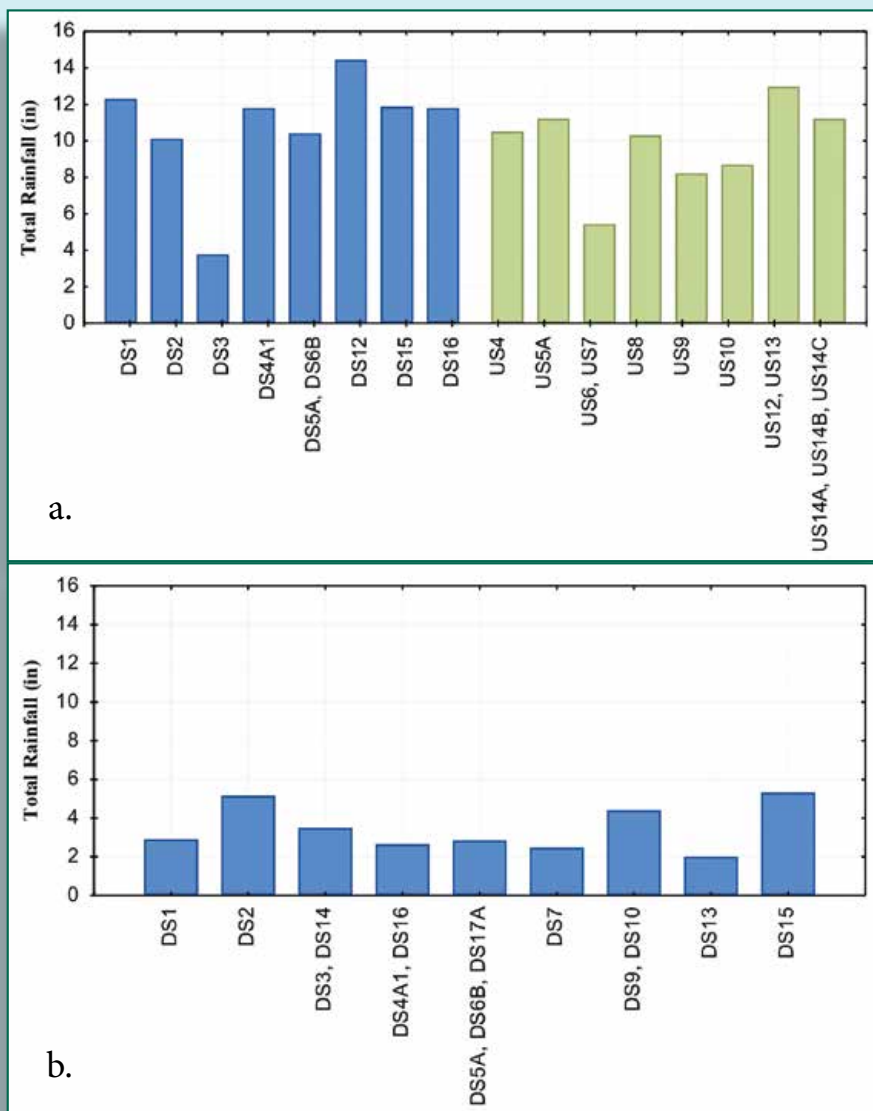


**Figure 39.** Total rainfall measured on monitored fields for (a) 8 Apr-11 Oct 2006, and (b) 17 May-9 July 2007

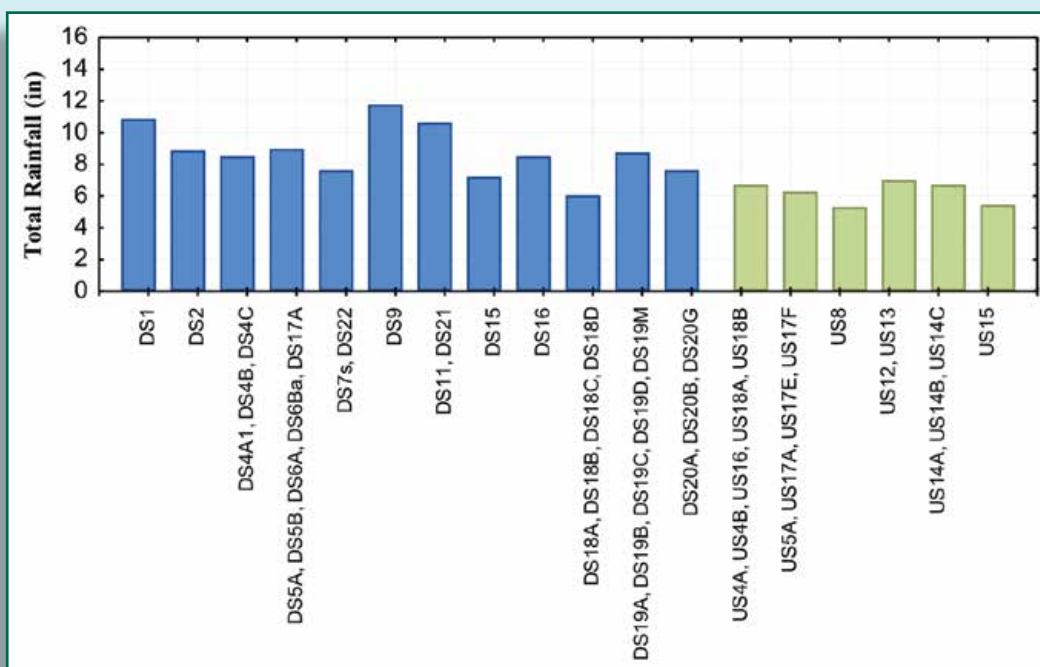


**Figure 40.** Total rainfall measured on monitored fields for 12 Jun-29 Nov 2008

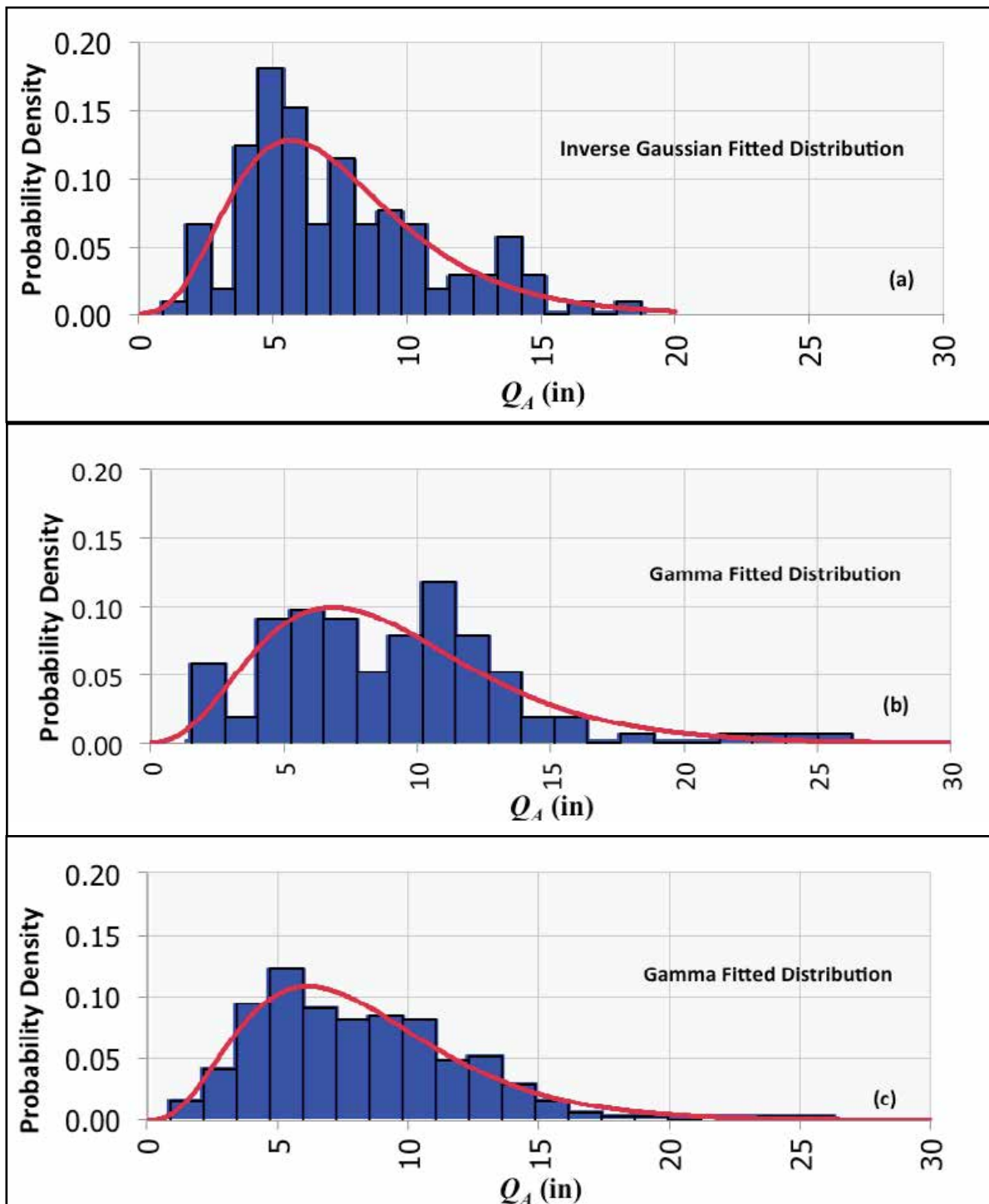


**Figure 41.** Histogram and fitted probability distribution of  $Q_A$  for (a) Upstream, (b) Downstream, and (c) total surface irrigation events over the entire study period

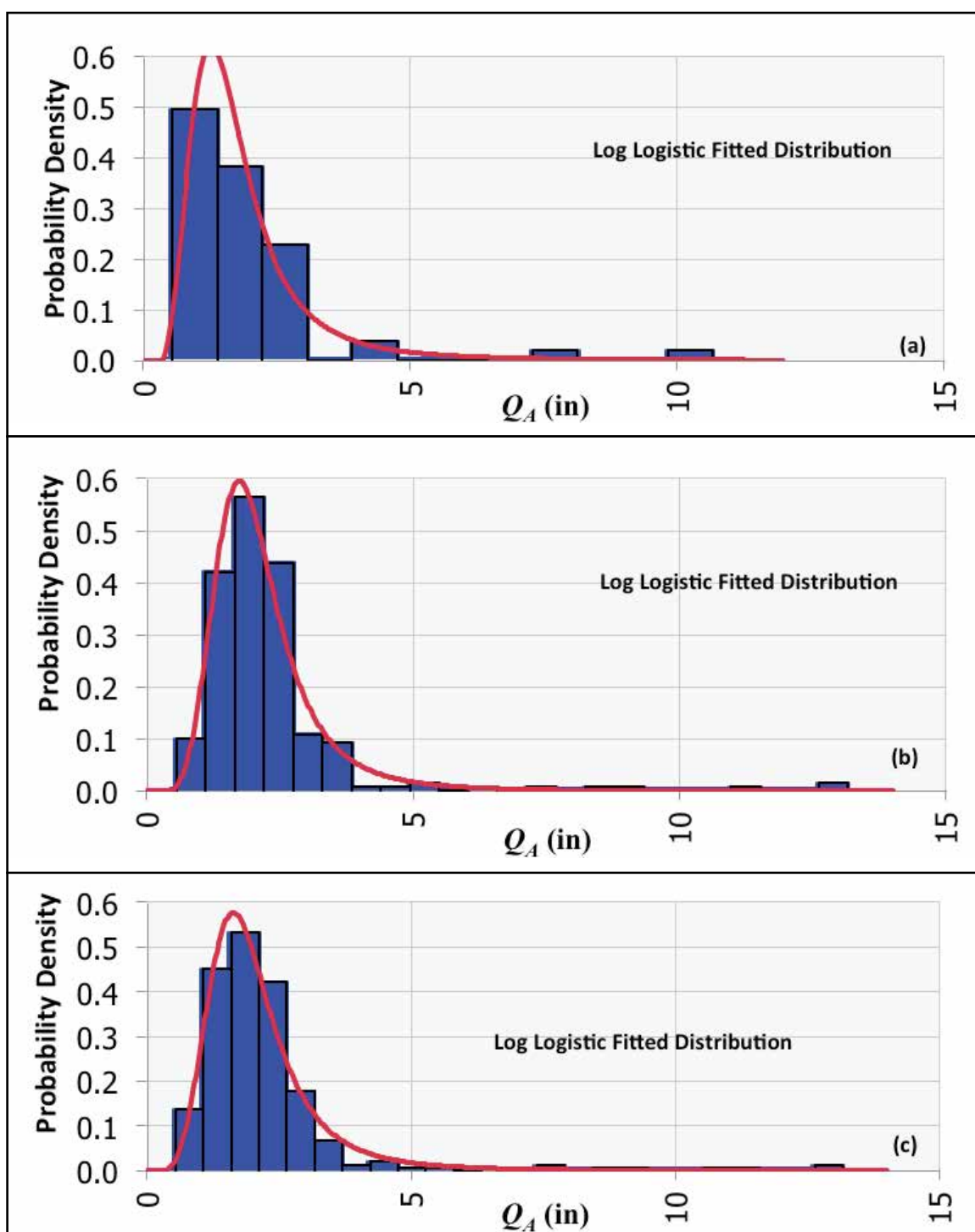


**Figure 42.** Histogram and fitted probability distribution of  $Q_A$  for (a) Upstream, (b) Downstream, and (c) total sprinkler irrigation events over the entire study period

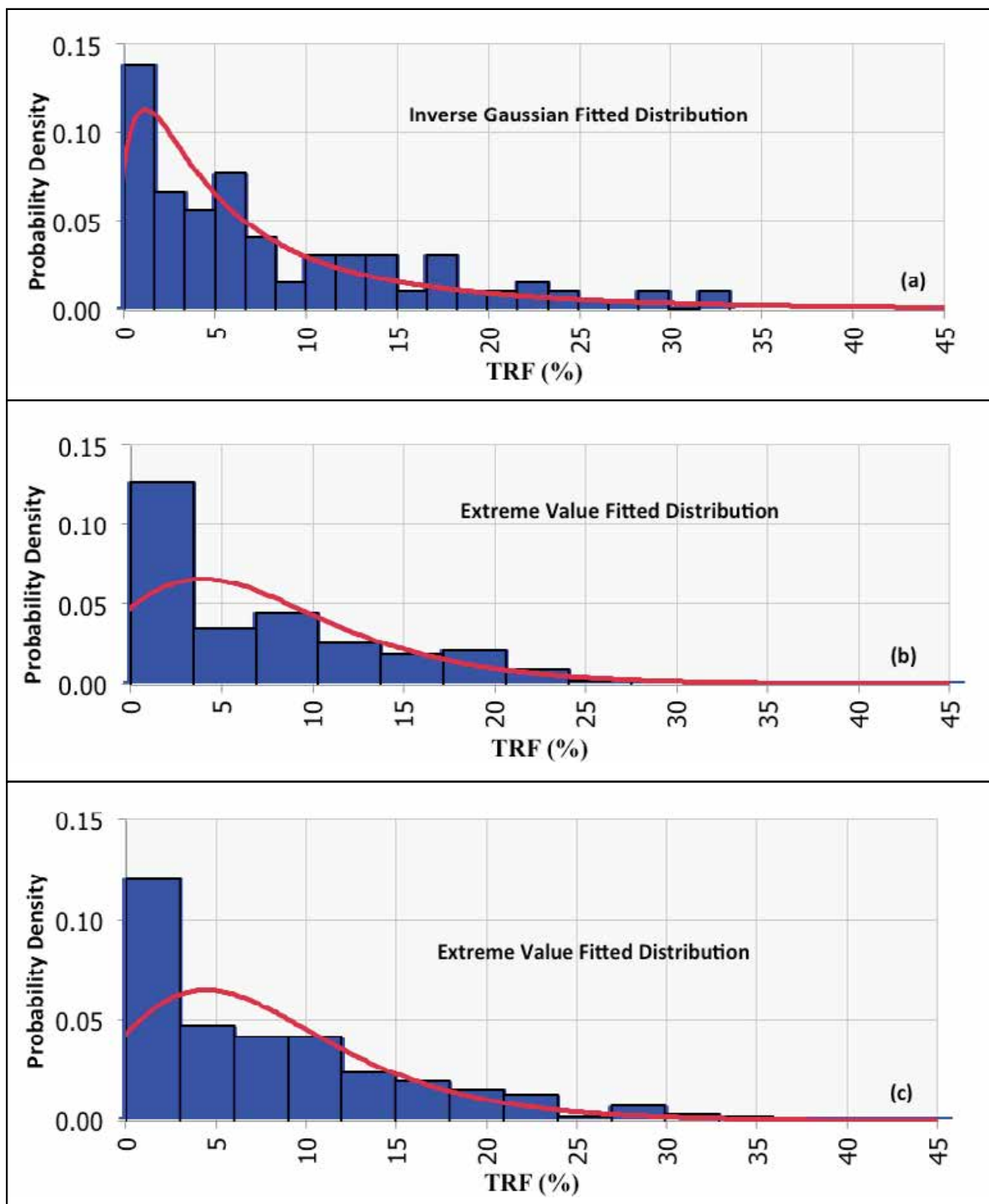


**Figure 43.** Histogram and fitted probability distribution of TRF for (a) Upstream, (b) Downstream, and (c) total surface irrigation events over the entire study period

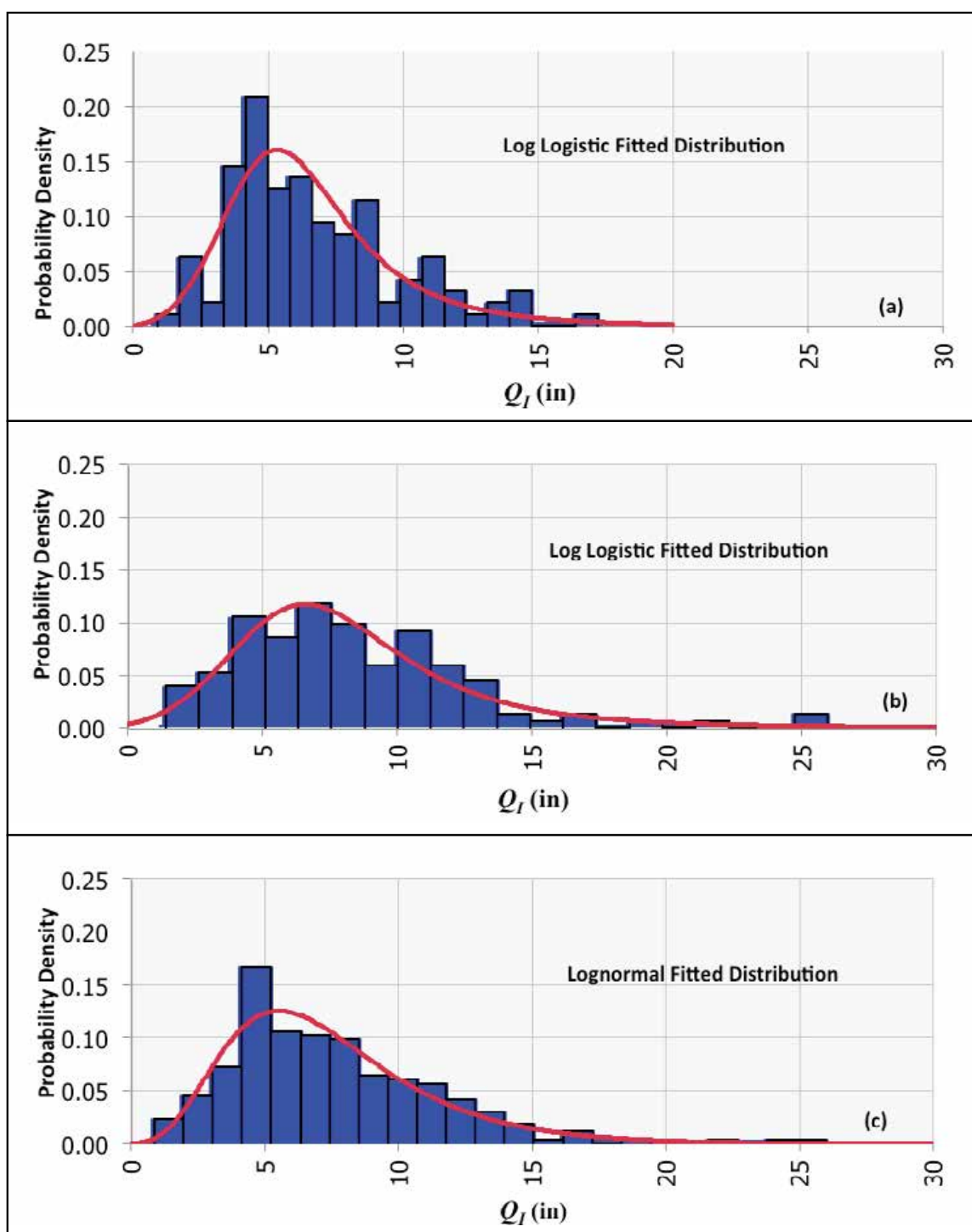


**Figure 44.** Histogram and fitted probability distribution of  $Q_I$  for (a) Upstream, (b) Downstream, and (c) total surface irrigation events over the entire study period

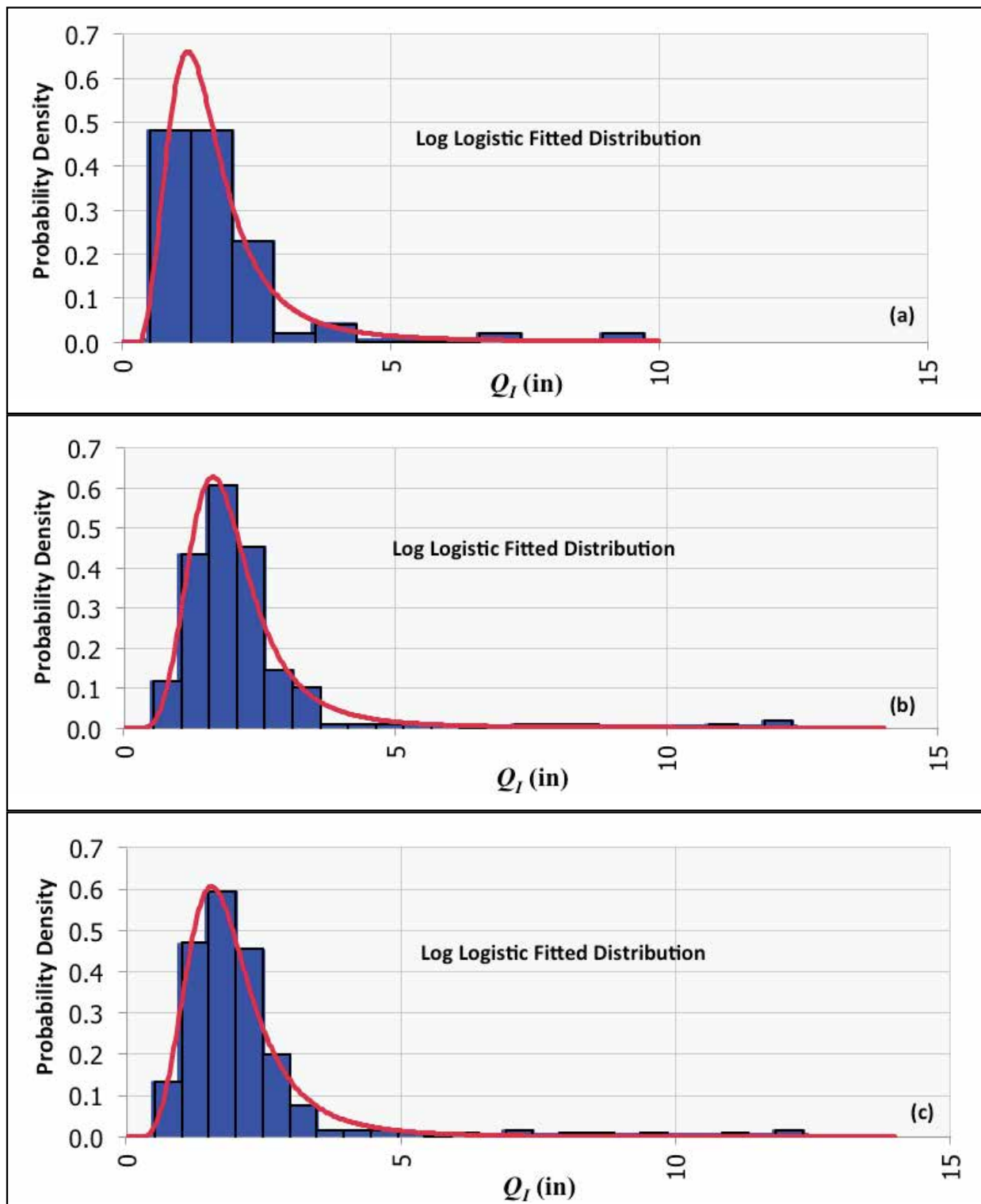


**Figure 45.** Histogram and fitted probability distribution of  $Q_I$  for (a) Upstream, (b) Downstream, and (c) total sprinkler irrigation events over the entire study period

### Deep Percolation Fraction

Values of DPF (percent) for all surface irrigation events are plotted as frequency histograms and fitted distribution functions in Figure 46 for Upstream fields, Downstream fields, and for all fields. The mean value for the Upstream, Downstream, and total surface irrigation events was 19.5 percent, 27.7 percent, and 24.1 percent, respectively. About 90 percent of total DPF values ranged between about 0.0 percent and 60.0 percent, and the CV for the total events was about 97 percent.

For sprinkler-irrigation events, histograms and fitted probability distribution functions of DPF over the entire study period are shown in Figure 47 for Upstream fields, Downstream fields, and the total of all fields. The mean values of DPF for sprinkler irrigation events monitored on Upstream, Downstream, and total fields were 18.2 percent, 11.6 percent, and 13.0 percent, respectively. For about 90 percent of the total sprinkler irrigation events monitored values of DPF ranged between 0.0 percent and 55.1 percent. The CV of DPF for the total sprinkler irrigation events was about 176 percent.

### Crop Evapotranspiration

Daily values of  $ET_r$ ,  $ET_p$ , and  $ET_a$  estimated for the overall periods modeled by IDSCU for each irrigated field are summarized in files the available ARIDAD. Example plots of cumulative seasonal  $ET_r$  estimated with field atmometers,  $ET_p$  calculated using the ASCE Standardized Equation, and  $ET_a$  estimated from ReSET, are shown for portions of the 2008 season for fields US4B, US8, and US12 in Figure 48. Figure 49 presents similar plots for fields DS1, DS6B, and DS16. The plots reveal that typically seasonal values of  $ET_p$  for particular crops are less than seasonal values of  $ET_r$ , reflecting the effects of varying crop types and stages of growth. Also, values of  $ET_a$  are less than values of  $ET_p$ , possibly indicating the effects of salinity, available soil water, and cultural practices on limiting crop ET.

### Upflux from Shallow Groundwater Table

Mean values of  $Q_U$  for Upstream, Downstream, and total fields are 8.8 percent, 3.3 percent and 5.5 percent of  $ET_a$ , respectively. In about 97 percent of Upstream fields  $Q_U$  was estimated to contribute to  $ET_a$ . In the Downstream region 84 percent of the monitored fields had  $Q_U$  that contributed to  $ET_a$ .

### Irrigation Application Efficiency

About 90 percent of monitored surface irrigation events had computed values of  $E_a$  between 35.2 percent and 97.8 percent. For surface-irrigation events over the entire study period, frequency histograms and fitted probability distribution functions of  $E_a$  are shown in Figure 50 for Upstream fields, Downstream fields, and the total of all fields. The mean values for the Upstream, Downstream, and total surface irrigation events were 72.1 percent, 64.9 percent, and 67.9 percent, respectively. There were a number of deficit surface irrigations that were observed during the study, which yielded very little deep percolation and high values of  $E_a$ . Values of  $E_a$  for sprinkler irrigation events were routinely very high, averaging about 76.9 percent Upstream and 83.5 percent Downstream with an overall average of 82.0 percent, since there were no observed tailwater runoff losses and estimated DP losses typically were very low. Values of  $E_a$  for surface and sprinkler irrigation in the LARV are comparable to typical average values of 65 percent for surface graded furrow irrigation and 85 percent for center pivot sprinklers (with spray heads without end guns) reported by Howell (2003). Howell (2003) reports “attainable” efficiencies of 75 percent and 95 percent for these respective irrigation methods.

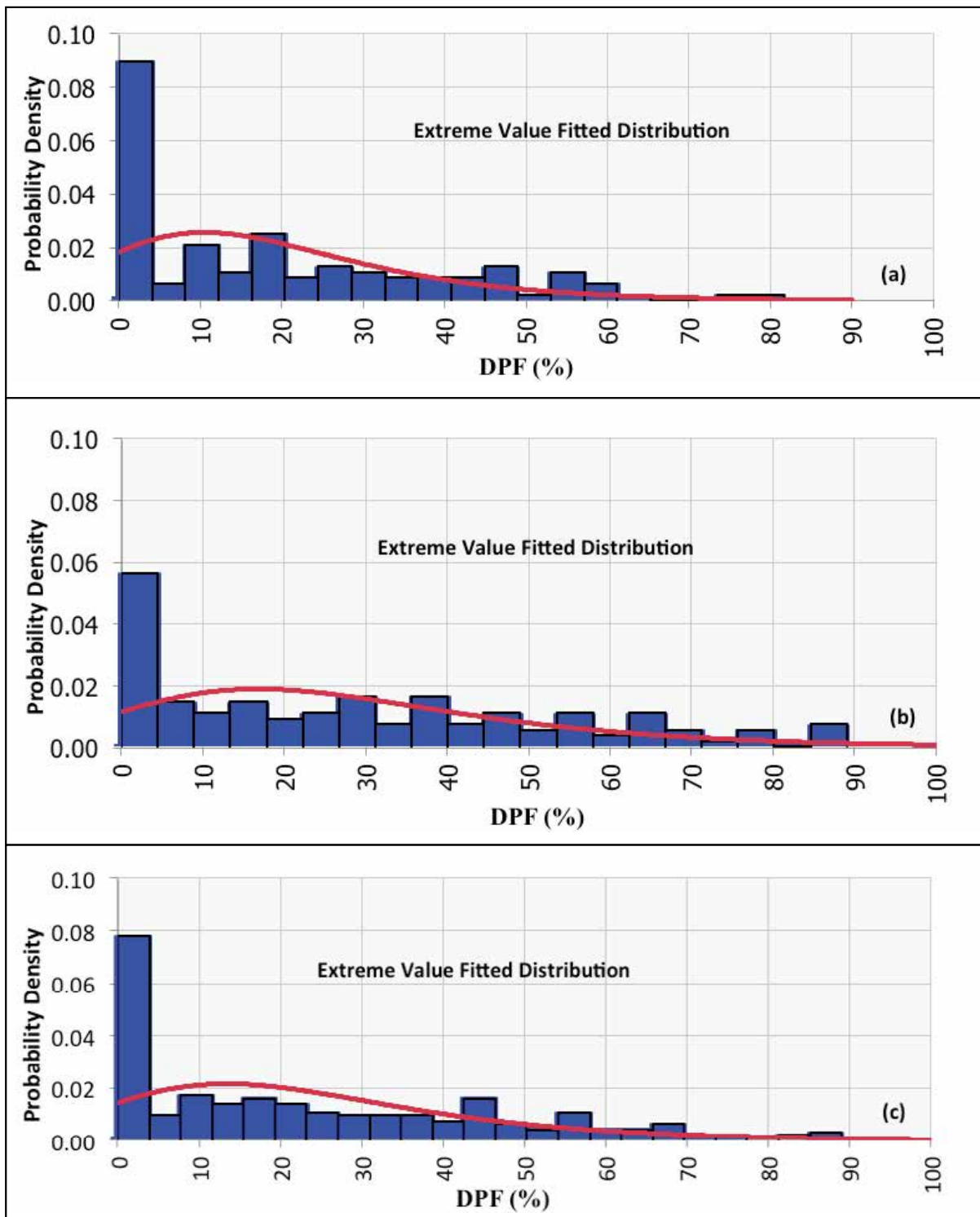


**Figure 46.** Histogram and fitted probability distribution of DPF for (a) Upstream, (b) Downstream, and (c) total surface irrigation events over the entire study period

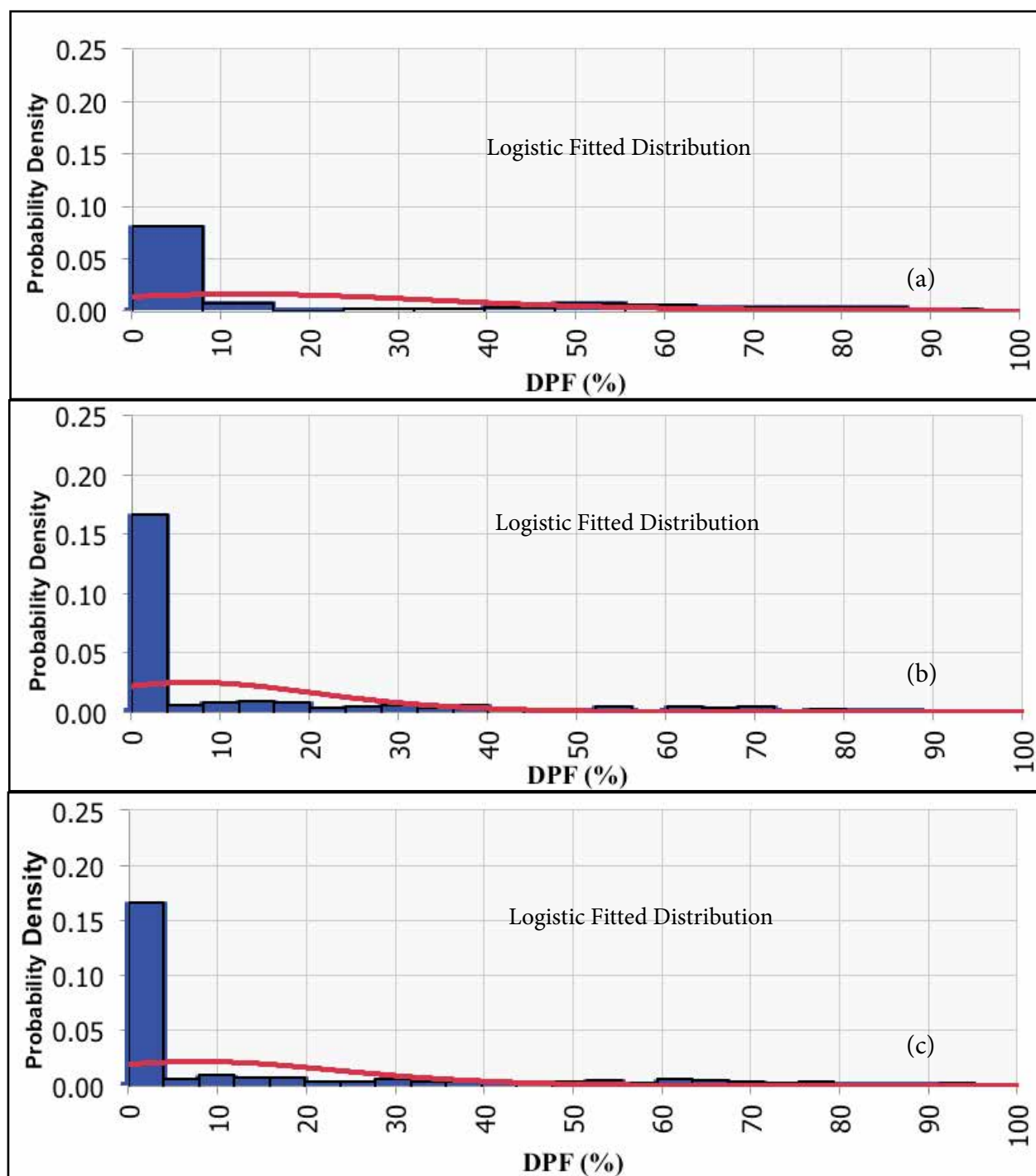


**Figure 47.** Histogram and fitted probability distribution of DPF for (a) Upstream, (b) Downstream, and (c) total sprinkler irrigation events over the entire study period

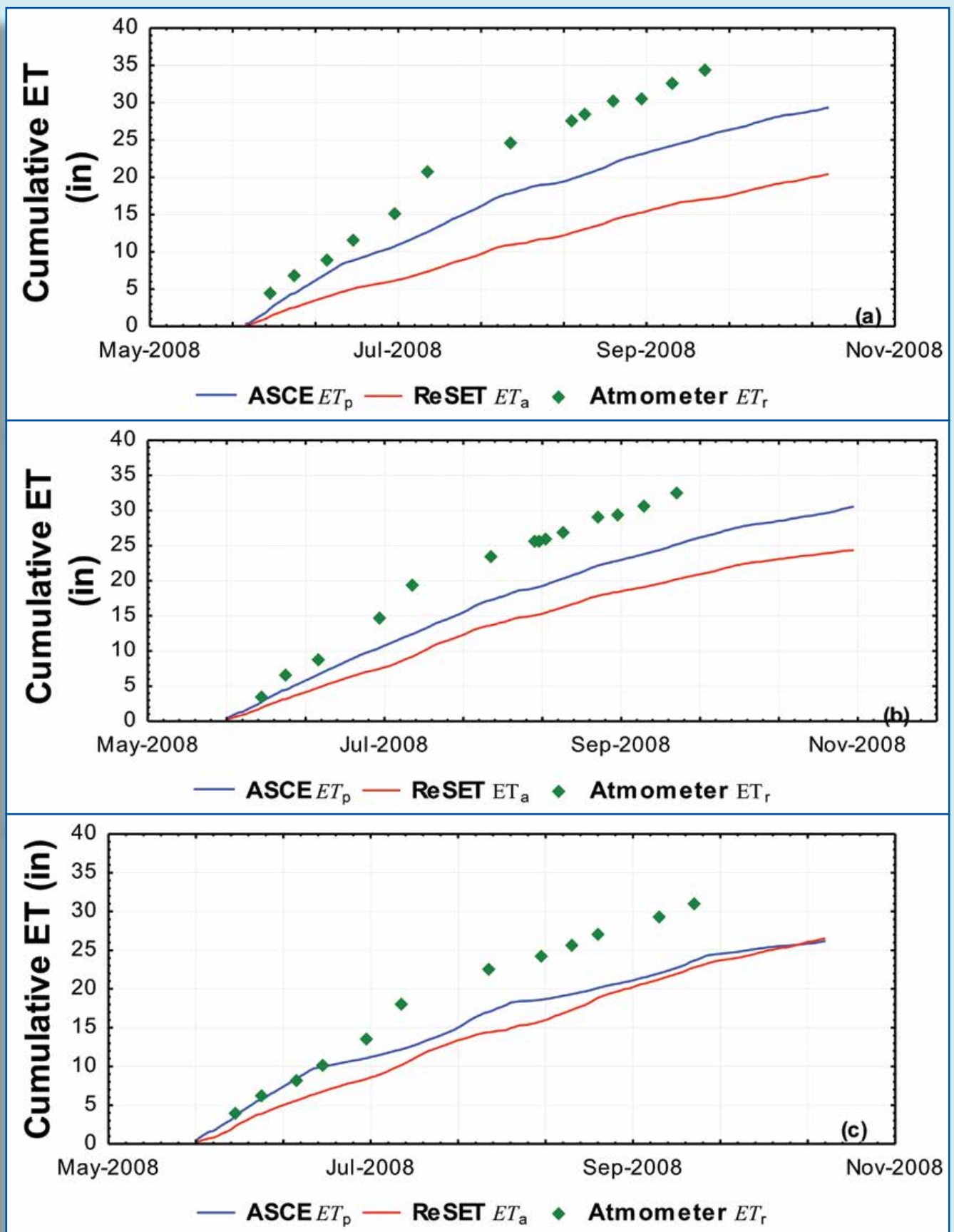


**Figure 48.**  $ET_r$  estimated from field atmometers,  $ET_p$  calculated with the ASCE Standardized Equation, and  $ET_a$  estimated with ReSET, for portions of the 2008 irrigation season for (a) field US4B (b) field US8, and (c) field US12

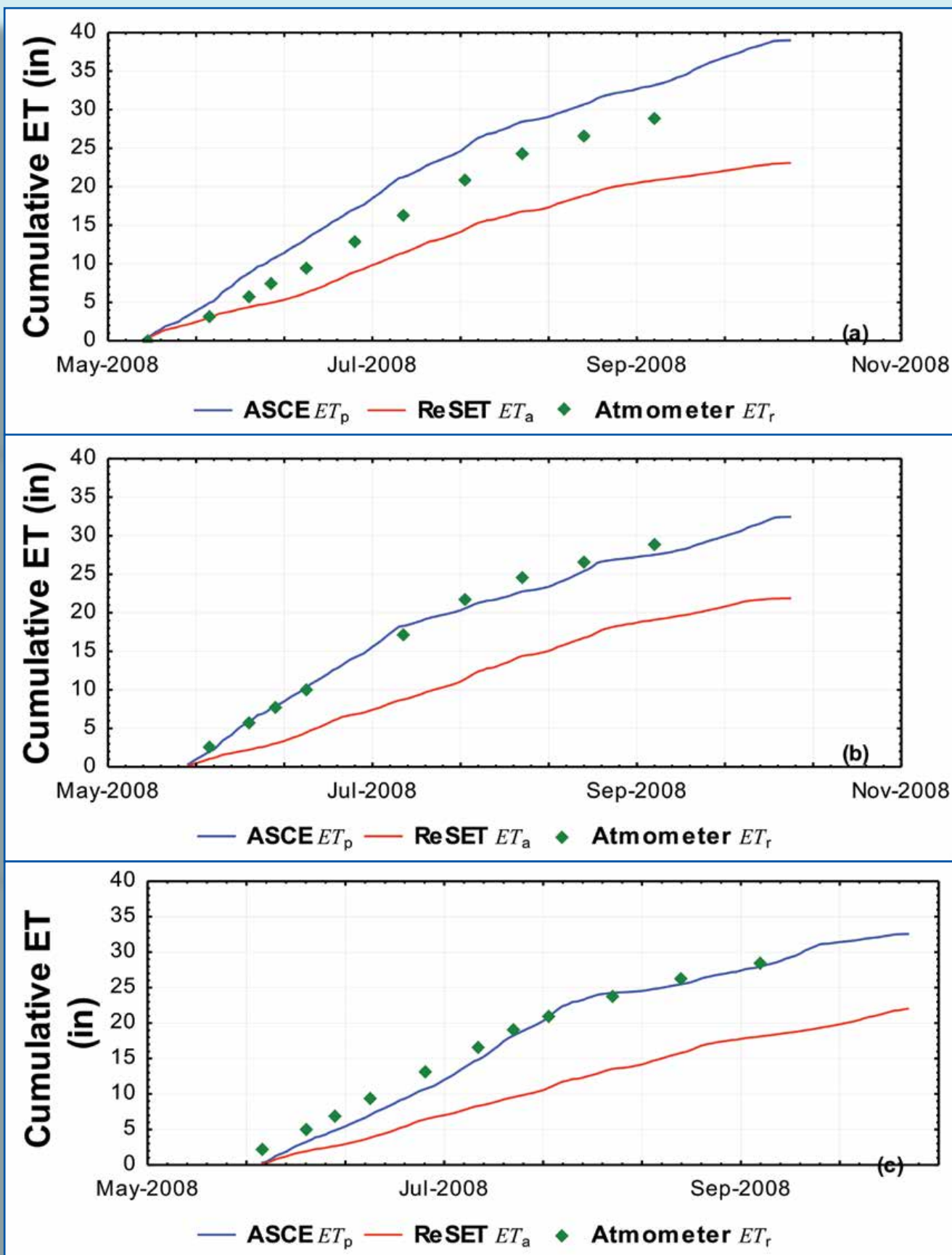


**Figure 49.**  $ET_r$  estimated from field atmometers,  $ET_p$  calculated with the ASCE Standardized Equation, and  $ET_a$  estimated with ReSET, for portions of the 2008 irrigation season for (a) field DS1, (b) field DS6B, and (c) field DS16

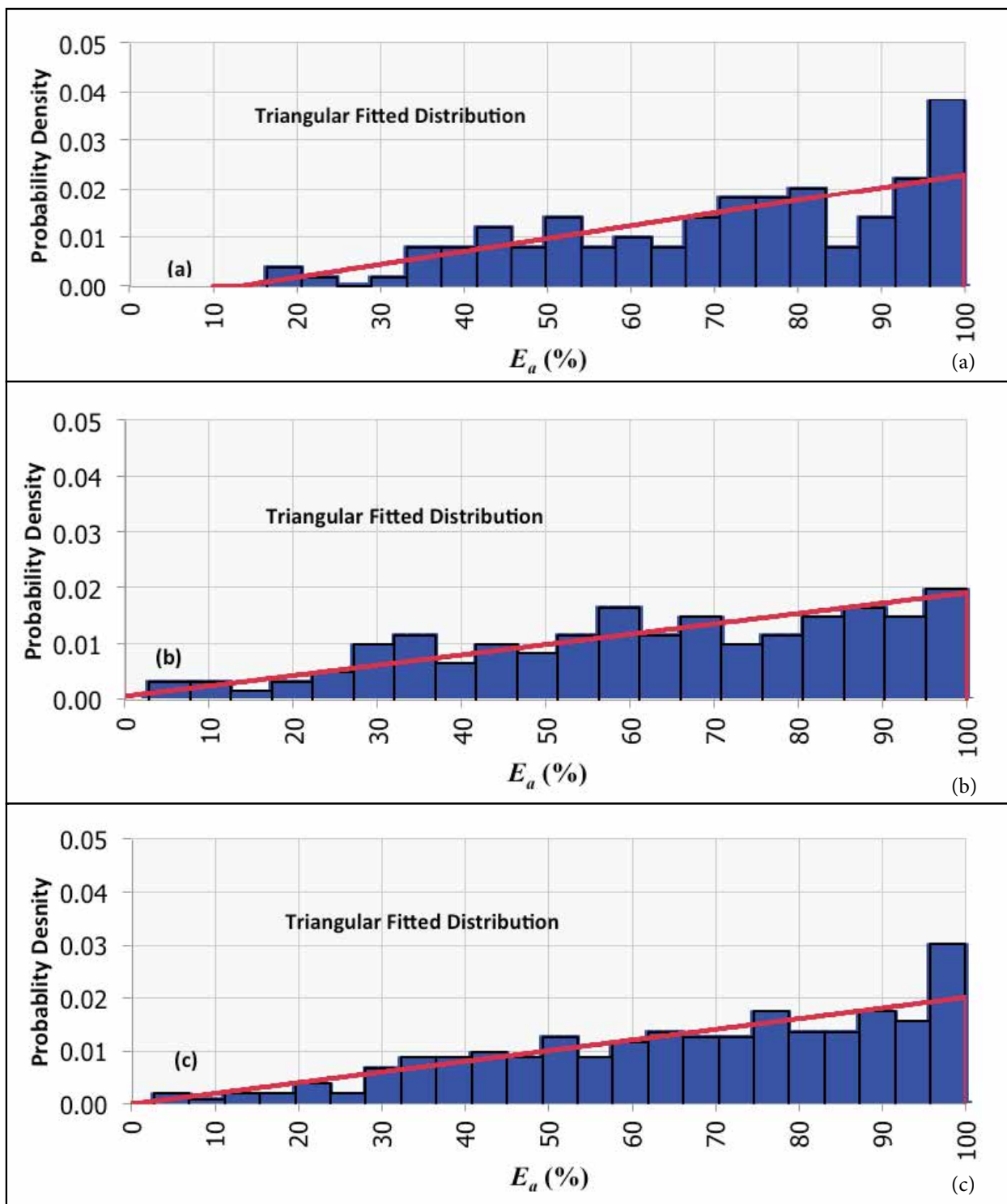


**Figure 50.** Histogram and fitted probability distribution of  $E_a$  (%) for (a) Upstream, (b) Downstream, and (c) total surface irrigation events over the entire study period

## Salt Concentration and Loading to and from Fields

Summary statistics of estimated TDS concentrations in applied irrigation water and in tail water are presented in Table 9 for a number of surface irrigation events Upstream and Downstream. Similar statistics for sprinkler irrigation events are given in Table 10. TDS levels in sprinkler irrigation water in the Upstream region are markedly higher than those in surface water since the source for all but one of the eight sprinklers is groundwater pumping wells. On the other hand, the sprinklers in the Downstream region are supplied by canal water.

The higher the DPF value for a given irrigation event, the greater is the potential for leaching of salts out of the root zone soil profile. In fact, DPF often is referred to as the “leaching fraction” (Hoffman and Shalhevet 2007). Assuming the overall average DPF value of about 24 percent for surface irrigation, TDS levels in applied surface irrigation in the study regions typically would be acceptable for moderately sensitive crops under well-drained conditions (Pratt and Suarez 1990). However, many of the fields are underlain by shallow saline water tables which contribute upflux of dissolved salt back into the soil root zone. For sprinkler irrigated fields, with average DPF of only 13.0 percent and with higher TDS levels in applied irrigation water, the hazard to crop productivity is even greater, especially for fields irrigated from groundwater pumping wells.

Table 11 presents statistics of estimated salt loads in applied irrigation water, tail water runoff, and infiltrated water for surface irrigation events Upstream and

Downstream. Average applied salt load per irrigation event was about 997 lb/ac over all investigated surface irrigated fields Upstream and about 2,480 lb/ac Downstream. Similar statistics are presented in Table 12 for sprinkler irrigation events. Over all investigated sprinkler irrigated fields, average applied salt load per irrigation event was about 1,217 lb/ac Upstream and about 446 lb/ac Downstream.

## Field Soil Water Salinity

Box and whisker summary plots of the statistics of  $EC_e$  values estimated from EM38 surveys conducted midseason (typically July or August) on Upstream fields are presented in Figures 51 and 52. Figures 53 - 55 present the  $EC_e$  estimated from midseason EM38 surveys conducted on Downstream fields. Figure 56 presents example contour maps of  $EC_e$  for two surveyed fields. Similar maps of soil water salinity for surveys on the other fields are provided in files on the available ARIDAD.

The average  $EC_e$  in monitored fields within the Upstream Study Region ranged from 1.8 dS/m to 9.3 dS/m over all surveys conducted during the study period. Averages in Downstream fields were considerably higher, ranging from 2.7 dS/m to 12 dS/m. Figures 51 - 55 indicate that many of the fields contained areas where soil salinity exceeded the threshold of three to five dS/m above which crop yields typically are reduced for corn and alfalfa. Preliminary data on crop yields in relation to  $EC_e$  are presented in a following section.



**Table 9.** TDS in applied irrigation water and tail water for investigated surface irrigation events Upstream and Downstream

Year	Number of Irrigation Events	TDS (mg/L)		
		Minimum	Maximum	Average
<b>Upstream Study Region</b>				
Applied Irrigation Water				
2004	8	521.7	975.7	633.9
2005	57	300.4	710.1	424.6
2006	41	172.8	5421.9	795.1
2008	24	115.5	1059.5	304.5
All Years	130	115.5	5421.9	532.2
Tail Water				
2004	-	-	-	-
2005	-	-	-	-
2006	-	-	-	-
2008	20	160.6	1040.8	409.7
All Years	20	160.6	1040.8	409.7
<b>Downstream Study Region</b>				
Applied Irrigation Water				
2004	5	842.5	1078.4	975.1
2005	29	692.7	3107.3	1308.0
2006	33	628.2	2657.3	1340.2
2007	37	158.9	3140.4	1090.2
2008	44	525.8	3175.3	987.7
All years	148	158.9	3175.3	1154.3
Tail Water				
2004	-	-	-	-
2005	-	-	-	-
2006	-	-	-	-
2007	9	756.5	1419.1	1037.3
2008	11	471.2	1354.9	969.2
All years	20	471.2	1419.1	999.9

**Table 10.** TDS in applied irrigation water and tail water for investigated sprinkler irrigation events Upstream and Downstream

Year	Number of Irrigation Events	TDS (mg/L)		
		Minimum	Maximum	Average
<b>Upstream Study Region</b>				
Applied Irrigation Water				
2004	-	-	-	-
2005	15	511.3	4157.2	1264.9
2006	15	336.8	3509.5	1239.6
2008	38	298.6	2888.6	1692.2
All Years	68	298.6	4157.2	1498.1
Tail Water				
2004	-	-	-	-
2005	-	-	-	-
2006	-	-	-	-
2008	-	-	-	-
All Years	-	-	-	-
<b>Downstream Study Region</b>				
Applied Irrigation Water				
2004	N/A	N/A	N/A	N/A
2005	12	691.9	899.1	783.7
2006	27	628.2	1559.8	1031.7
2007	54	67.5	1592.4	864.5
2008	150	483.1	2884.2	816.0
All years	243	67.5	2884.2	849.1
Tail Water				
2004	-	-	-	-
2005	-	-	-	-
2006	-	-	-	-
2007	-	-	-	-
2008	-	-	-	-
All years	-	-	-	-

**Table 11.** Salt load in applied irrigation water, tail water, and infiltrated water for investigated surface irrigation events Upstream and Downstream

Year	Salt Load (lb/ac)			Year	Salt Load (lb/ac)		
	Minimum	Maximum	Average		Minimum	Maximum	Average
<b>Upstream Study Region</b>				<b>Downstream Study Region</b>			
<b>Applied Irrigation Water</b>				<b>Applied Irrigation Water</b>			
2004	507.5	1672.5	1015.0	2004	657.0	850.3	744.6
2005	187.8	1909.4	676.3	2005	353.4	8226.9	3056.7
2006	72.6	11813.6	1617.5	2006	220.1	9945.9	2587.2
2007	-	-	-	2007	4.0	10522.7	2609.0
2008	92.5	4491.8	691.1	2008	308.9	7349.7	2108.3
All Years	72.6	11813.6	996.7	All years	4.0	10522.7	2480.0
<b>Tail Water</b>				<b>Tail Water</b>			
2004	-	-	-	2004	-	-	-
2005	-	-	-	2005	-	-	-
2006	-	-	-	2006	-	-	-
2007	-	-	-	2007	95.4	505.4	253.3
2008	0.0	357.9	83.9	2008	17.6	503.4	259.3
All Years	0.0	357.9	83.9	All years	17.6	505.4	256.6
<b>Infiltrated Water</b>				<b>Infiltrated Water</b>			
2004	-	-	-	2004	-	-	-
2005	-	-	-	2005	-	-	-
2006	-	-	-	2006	-	-	-
2007	-	-	-	2007	1126.8	505.4	2562.4
2008	92.1	4133.9	642.6	2008	625.1	503.4	1747.6
All Years	92.1	4133.9	642.6	All years	625.1	505.4	2114.3



**Table 12.** Salt load in applied irrigation water, tail water, and infiltrated water for investigated sprinkler irrigation events Upstream and Downstream

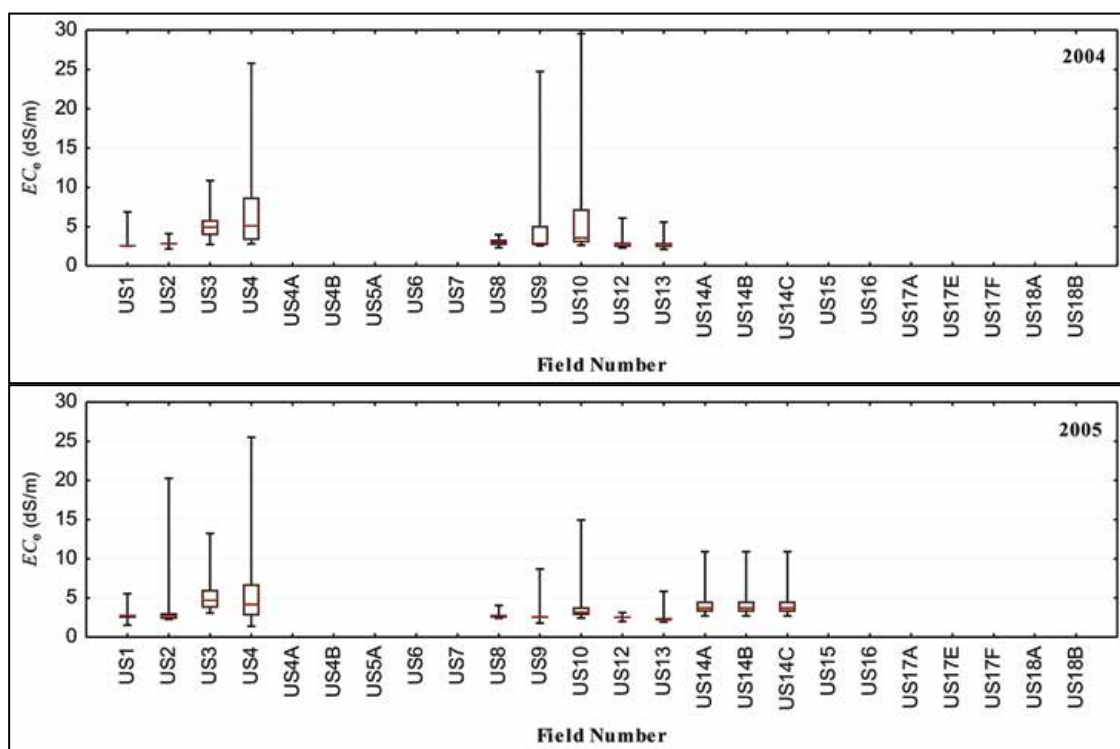
Year	Salt Load (lb/ac)			Year	Salt Load (lb/ac)		
	Minimum	Maximum	Average		Minimum	Maximum	Average
<b>Upstream Study Region</b>				<b>Downstream Study Region</b>			
<b>Applied Irrigation Water</b>				<b>Applied Irrigation Water</b>			
2004	N/A	N/A	N/A	2004	-	-	-
2005	145.8	18429.9	2657.3	2005	126.9	848.8	337.0
2006	103.3	1844.2	475.9	2006	154.8	1172.8	525.6
2007	-	-	-	2007	0.3	4118.7	439.7
2008	56.9	6983.4	940.2	2008	0.0	2666.0	442.5
All Years	56.9	18429.9	1216.6	All years	0.0	4118.7	445.9
<b>Tail Water</b>				<b>Tail Water</b>			
2004	-	-	-	2004	-	-	-
2005	-	-	-	2005	-	-	-
2006	-	-	-	2006	-	-	-
2007	-	-	-	2007	-	-	-
2008	-	-	-	2008	-	-	-
All Years	-	-	-	All years	-	-	-
<b>Infiltrated Water</b>				<b>Infiltrated Water</b>			
2004	-	-	-	2004	-	-	-
2005	-	-	-	2005	-	-	-
2006	-	-	-	2006	-	-	-
2007	-	-	-	2007	-	-	-
2008	-	-	-	2008	-	-	-
All Years	-	-	-	All years	-	-	-

## Water Table Depth and Salinity

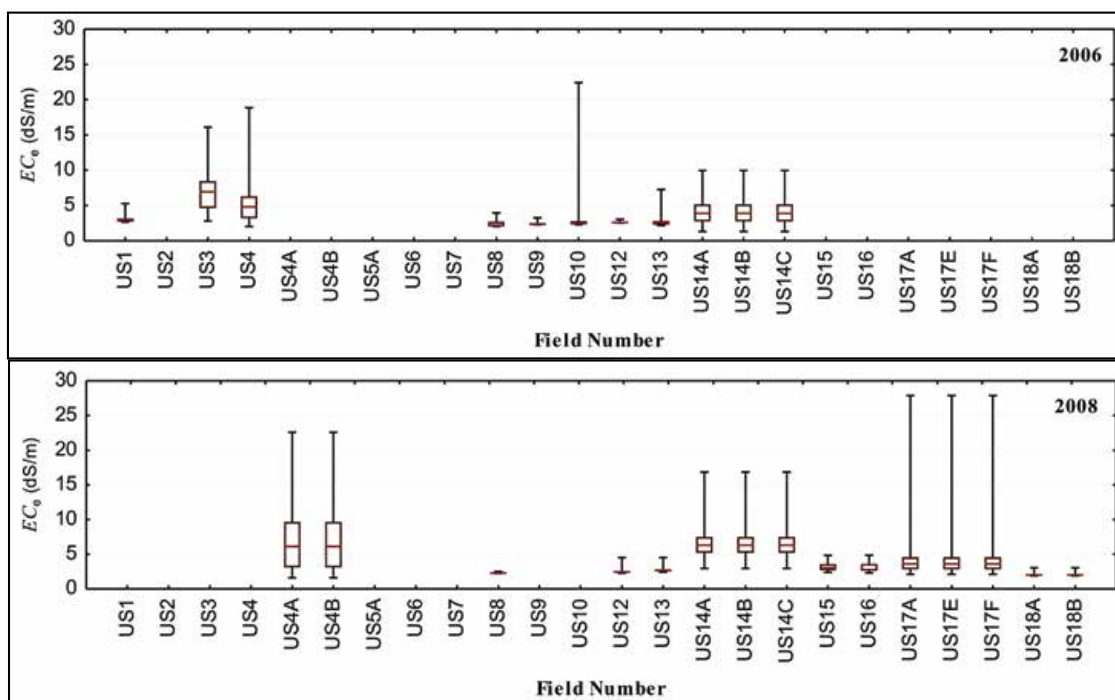
Values of  $D_{wt}$  and EC measured in wells within the monitored fields reveal significant variability over the seasons, within each season, and from field to field. Figure 57 illustrates  $D_{wt}$  readings for wells in field DS11 during 2008, illustrating the degree of spatial and temporal variability within the fields. Figures 58 through 61 present “box and whisker” plots of averaged  $D_{wt}$  measured in Upstream and Downstream fields over the study period. These values represent averages over all wells within a given field and indicate the degree of temporal variability within the respective irrigation seasons. Dry well observations were not considered in this analysis. Fields not displayed on Figures 58 through

61 had wells that were dry for the entire observation period.

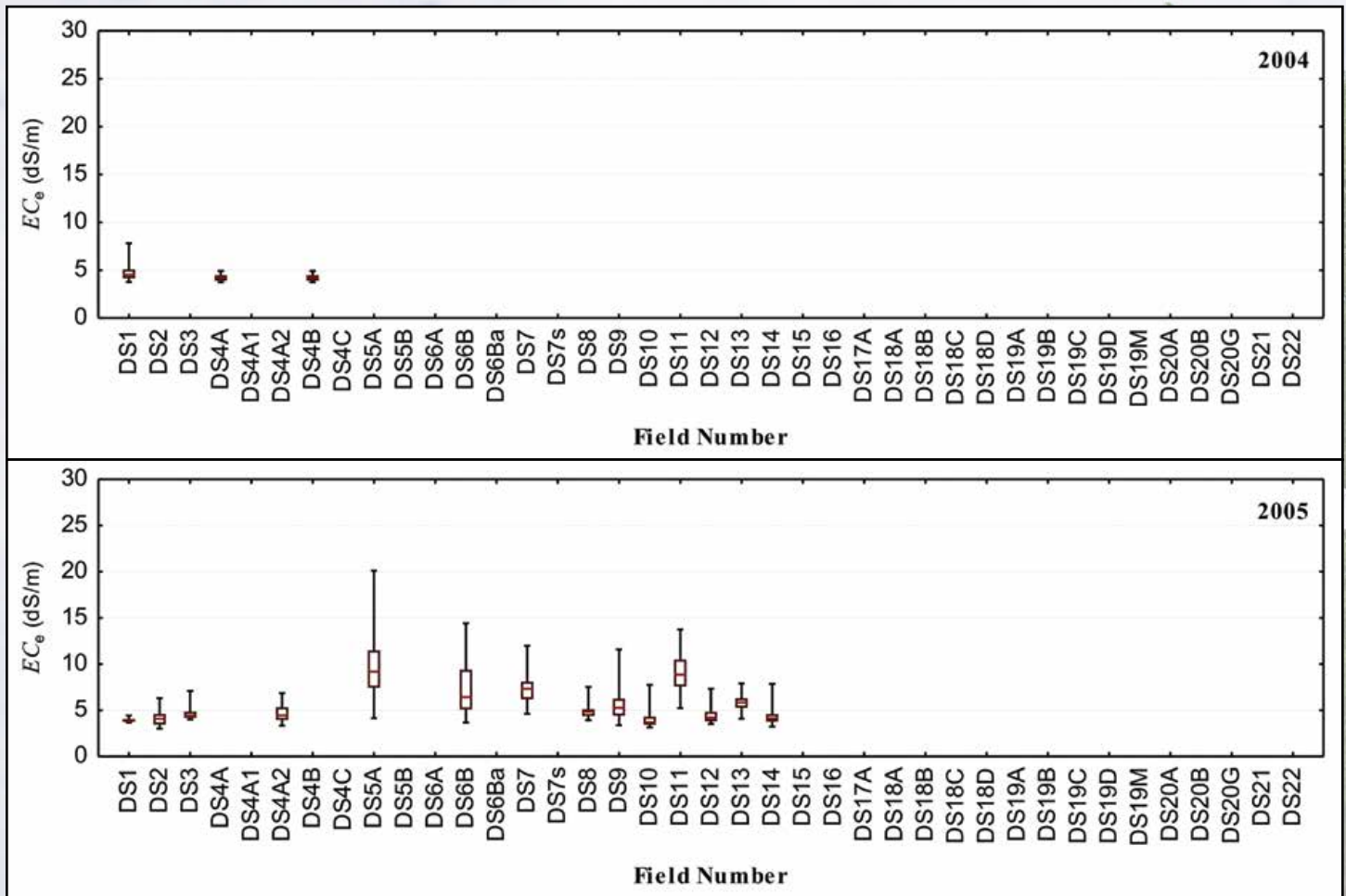
Figure 62 depicts an example of seasonal variation of EC among wells for field DS11 during 2008. Box and whisker plots of average EC measured on Upstream and Downstream fields over the study period are given in Figures 63 through 66, respectively. These EC values are averaged among all wells in a particular field. Fields not displayed on Figures 63 through 66 had wells that were dry for the entire observation period.



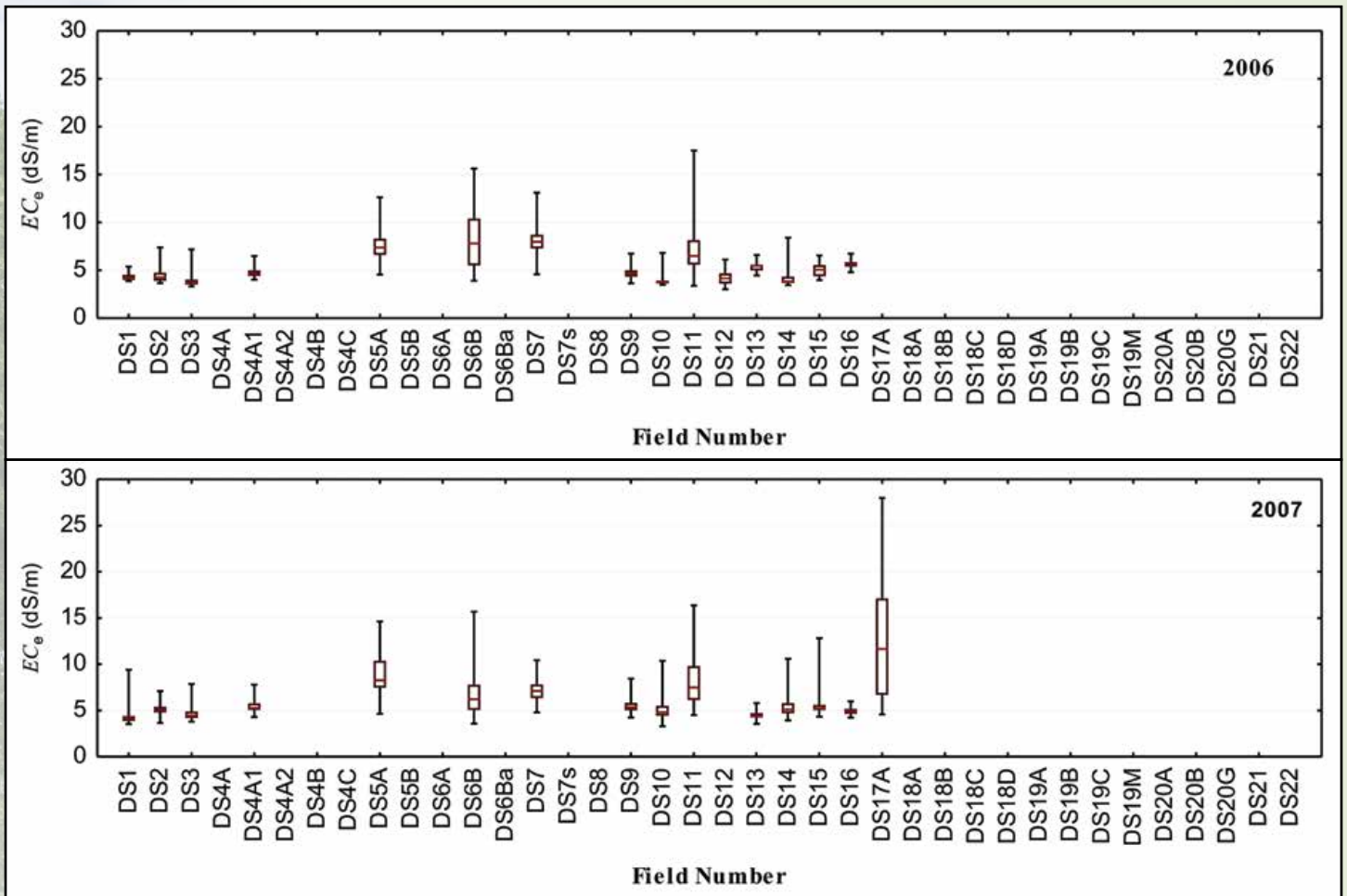
**Figure 51.** Box and whisker plots of  $EC_e$  estimated from midseason EM38 surveys on monitored fields in the Upstream Study Region in 2004 and 2005. Midline represents the median value; upper and lower edges of box represent 75 percentile and 25 percentile values, respectively; and upper and lower whiskers represented maximum and minimum values, respectively.



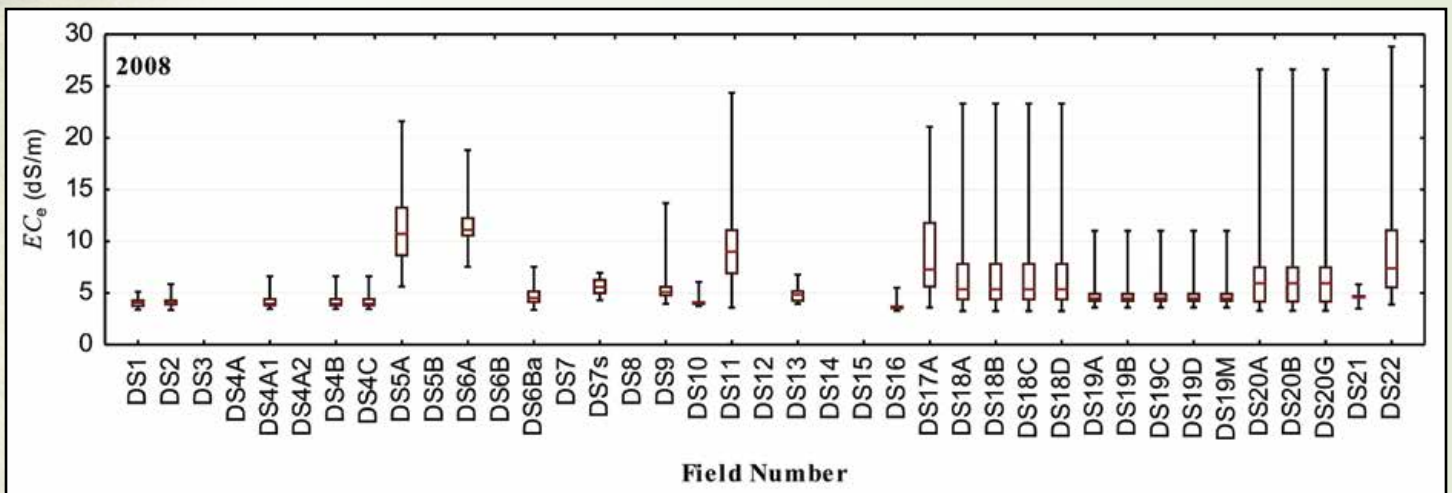
**Figure 52.** Box and whisker plots of  $EC_e$  estimated from midseason EM38 surveys on monitored fields in the Upstream Study Region in 2006 and 2008. Midline represents the median value; upper and lower edges of box represent 75 percentile and 25 percentile values, respectively; and upper and lower whiskers represented maximum and minimum values, respectively. Plots for fields US4, US5A, US9, US12, US14A, US14B, and US14C for 2006 are for values surveyed in June (July or August surveys were not available). The plot for field US7 for 2006 is based upon values surveyed during November.



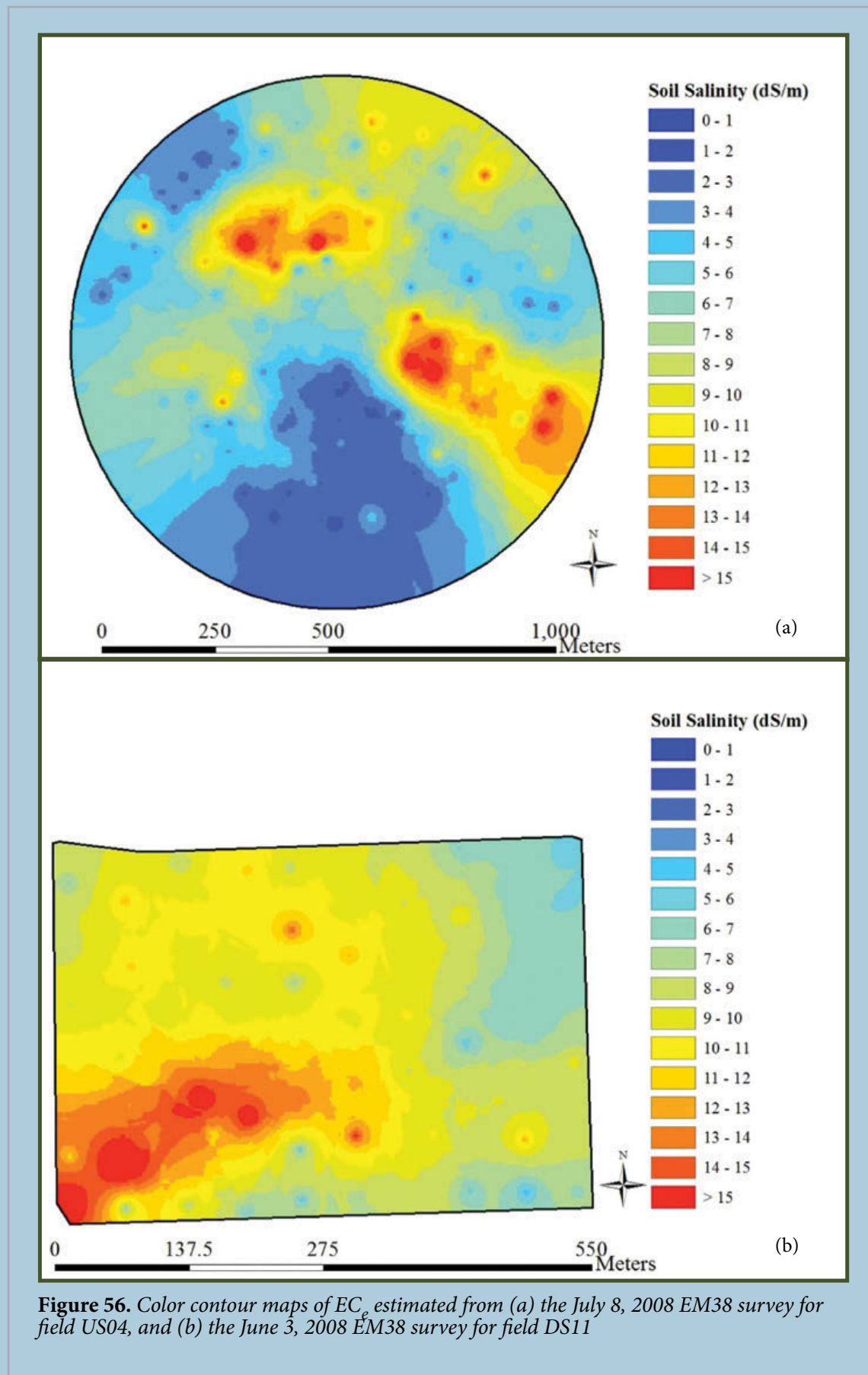
**Figure 53.** Box and whisker plots of  $EC_e$  estimated from midseason EM38 surveys on monitored fields in the Downstream Study Region in 2004 and 2005. Midline represents the median value; upper and lower edges of box represent 75 percentile and 25 percentile values, respectively; and upper and lowerwhiskers represented maximum and minimum values, respectively.



**Figure 54.** Box and whisker plots of  $EC_e$  estimated from midseason EM38 surveys on monitored fields in the Downstream Study Region in 2006 and 2007. Midline represents the median value; upper and lower edges of box represent 75 percentile and 25 percentile values, respectively; and upper and lower whiskers represented maximum and minimum values, respectively. The plot for field DS1 for 2006 are for values surveyed in June (July or August surveys were not available), for field DS13 for values surveyed during May, and for fields DS15 and DS16 for values surveyed during December.



**Figure 55.** Box and whisker plots of  $EC_e$  estimated from midseason EM38 surveys on monitored fields in the Downstream Study Region in 2008. Midline represents the median value; upper and lower edges of box represent 75 percentile and 25 percentile values, respectively; and upper and lower whiskers represented maximum and minimum values, respectively.



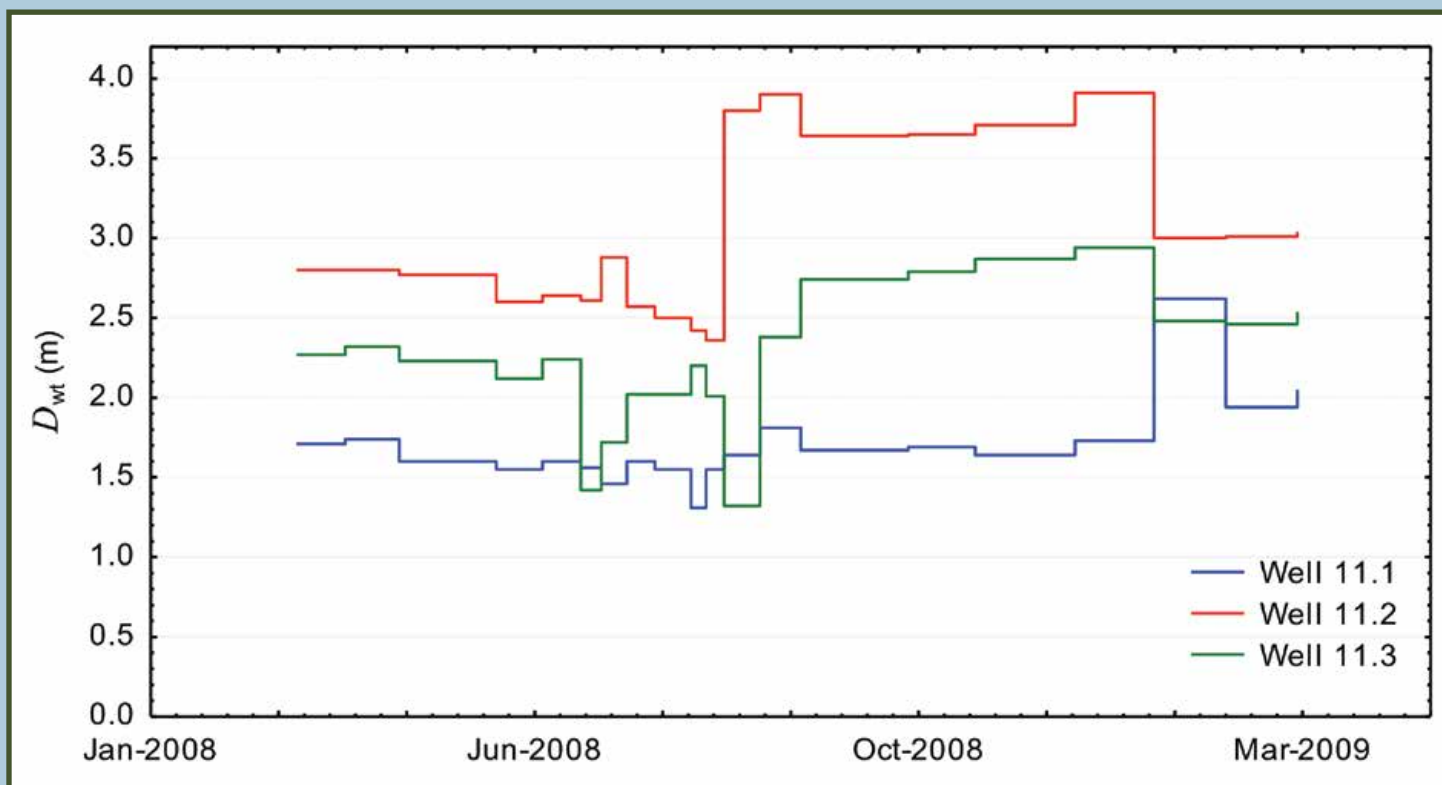
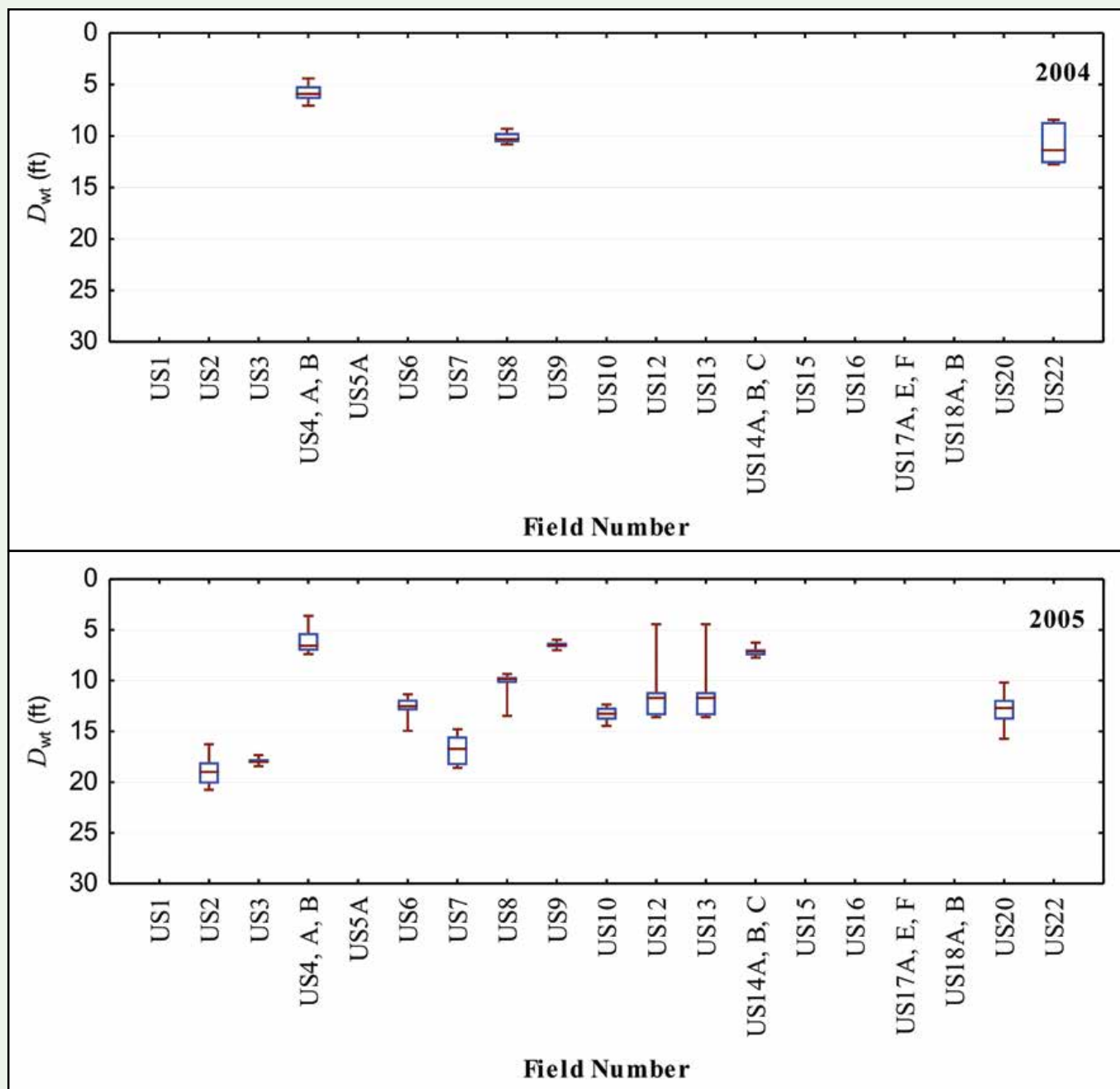
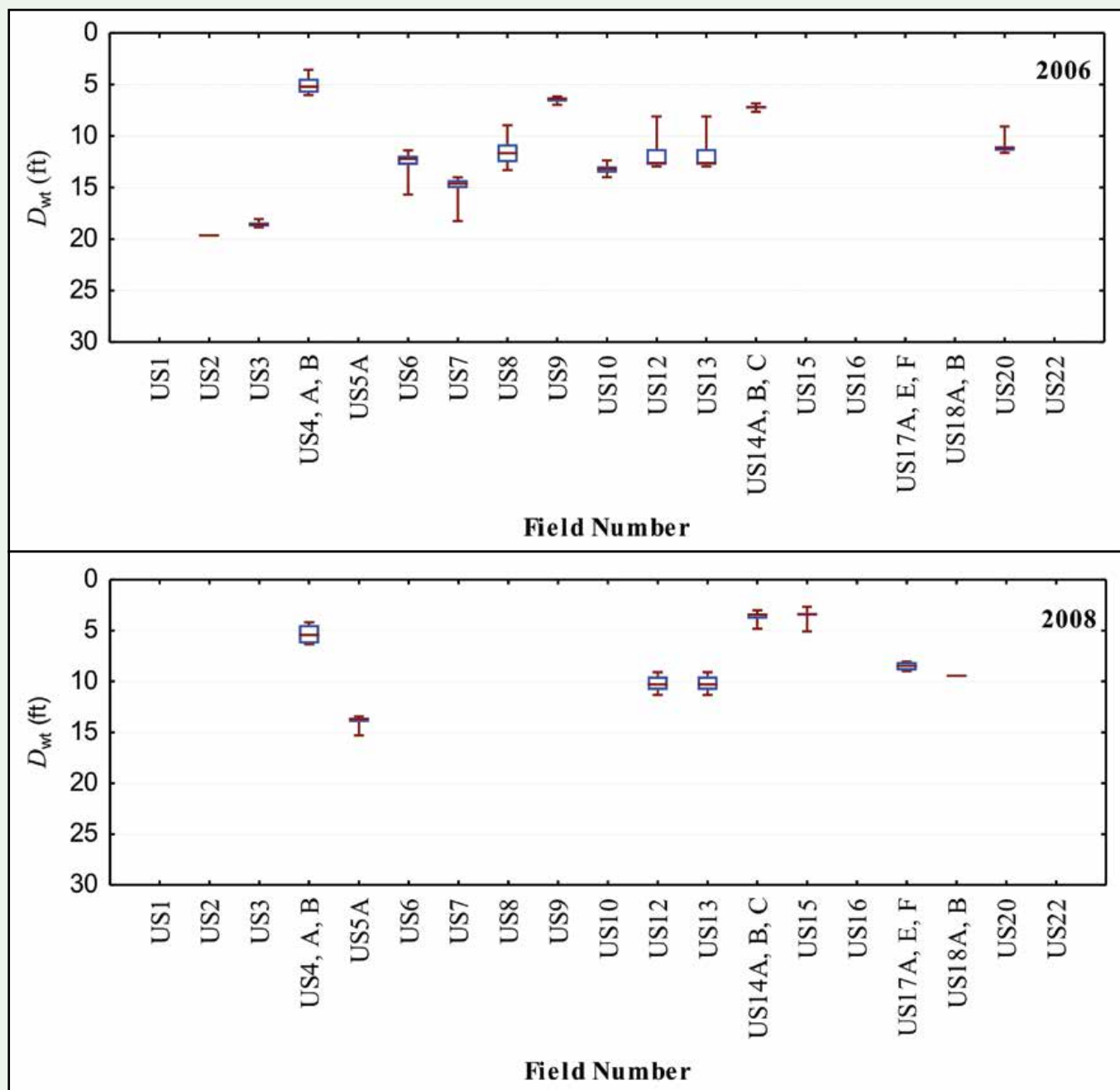


Figure 57. Seasonal variation of  $D_{wt}$  in three wells within field DS11 during 2008 and into spring 2009





**Figure 58.** Box and whisker plots of  $D_{wt}$  values measured on fields in the Upstream Study Region for years 2004 and 2005. Midline represents the median value; upper and lower edges of box represent 75 percentile and 25 percentile values, respectively; and upper and lower whiskers represented maximum and minimum values, respectively.



**Figure 59.** Box and whisker plots of  $D_{wt}$  values measured on fields in the Upstream Study Region for years 2006 and 2008. Midline represents the median value; upper and lower edges of box represent 75 percentile and 25 percentile values, respectively; and upper and lower whiskers represented maximum and minimum values, respectively.

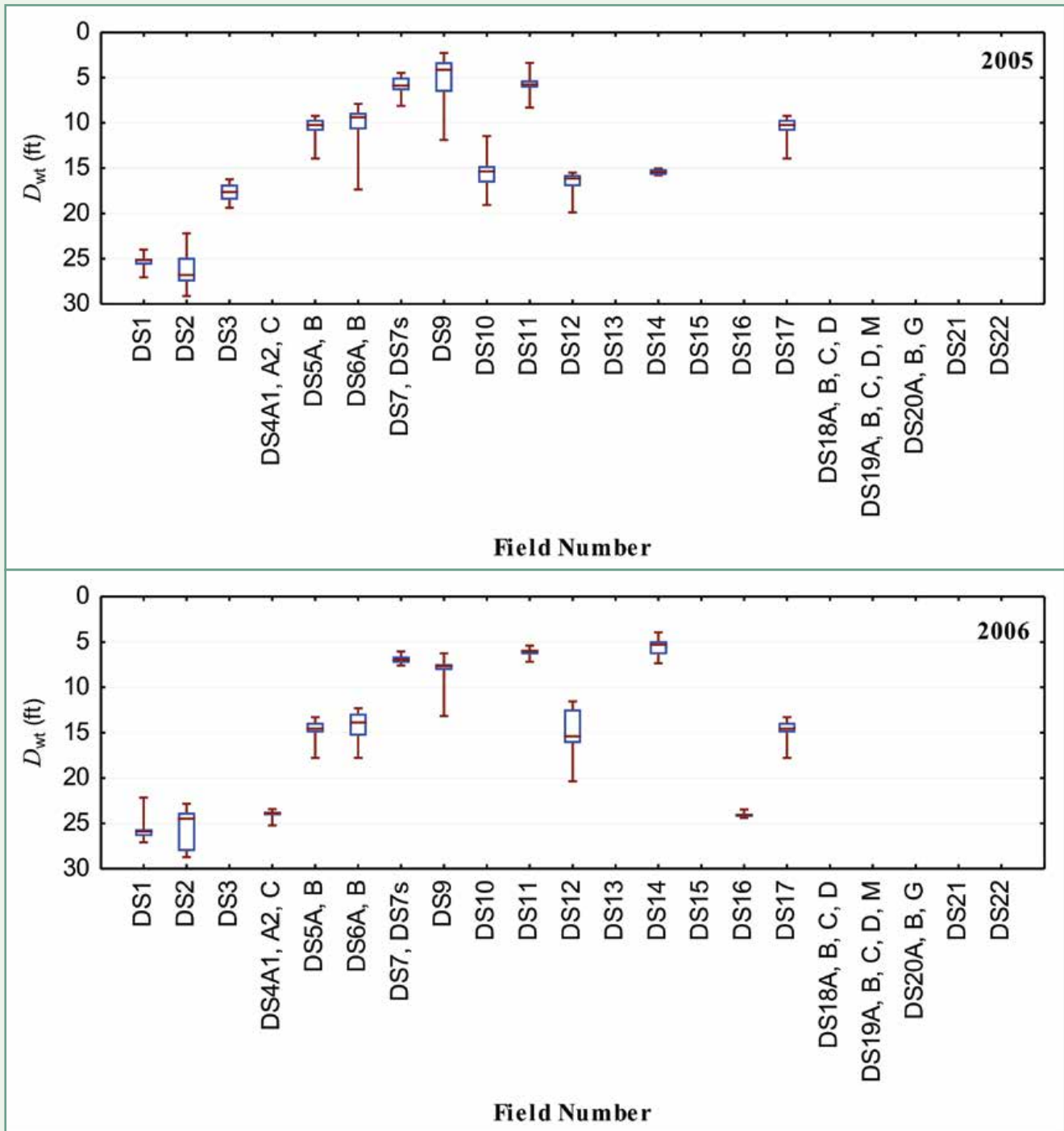


**Figure 60.** Box and whisker plots of  $D_{wt}$  values measured on fields in the Downstream Study Region for years 2005 and 2006. Midline represents the median value; upper and lower edges of box represent 75 percentile and 25 percentile values, respectively; and upper and lower whiskers represented maximum and minimum values, respectively.

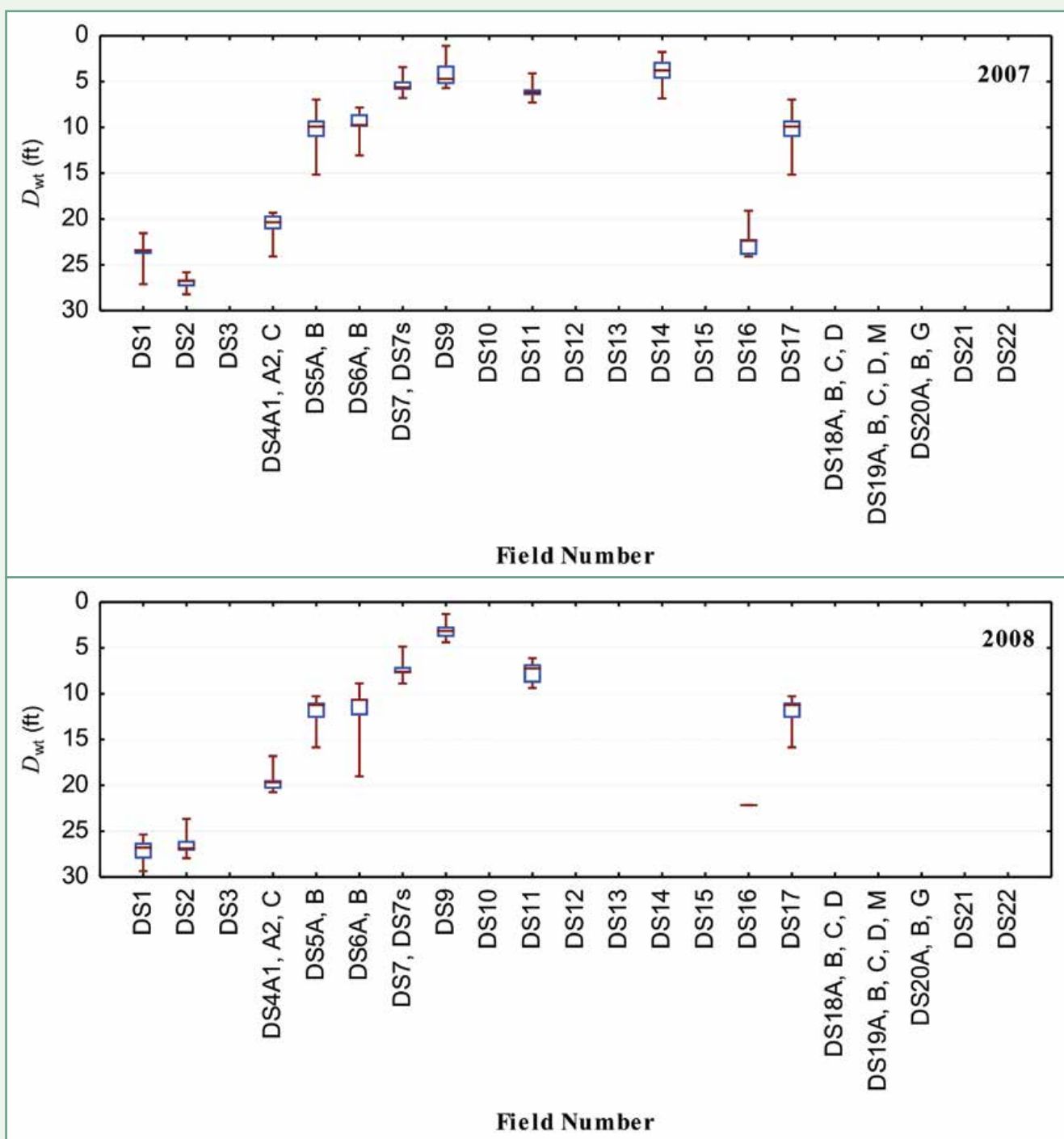


**Figure 61.** Box and whisker plots of  $D_{wt}$  values measured on fields in the Downstream Study Region for years 2005, 2006, 2007, and 2008. Midline represents the median value; upper and lower edges of box represent 75 percentile and 25 percentile values, respectively; and upper and lower whiskers represented maximum and minimum values, respectively.

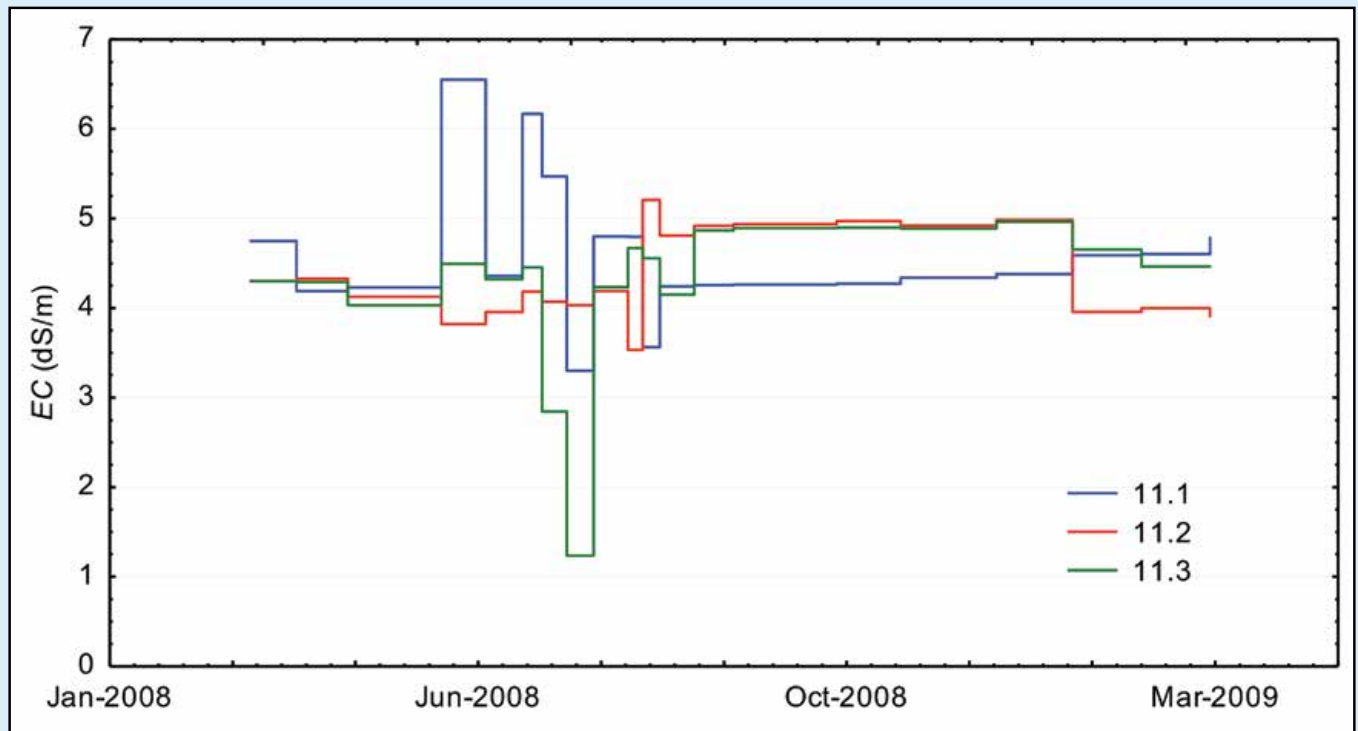


**Figure 62.** Seasonal variation of EC in three wells within field DS11 during 2008 and into spring 2009



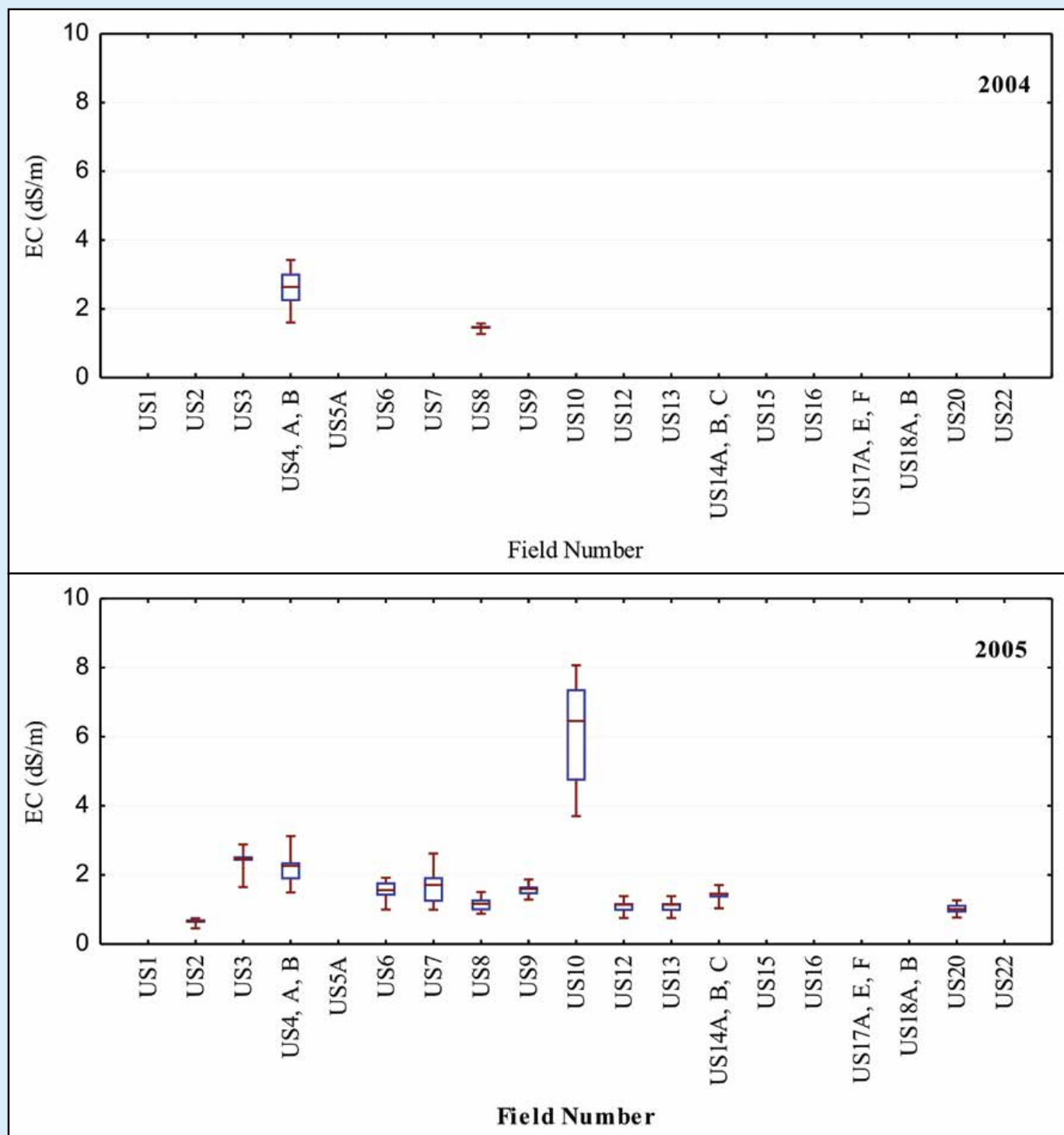


**Figure 63.** Box and whisker plots of EC values measured on fields in the Upstream Study Region for years 2004 and 2005. Midline represents the median value; upper and lower edges of box represent 75 percentile and 25 percentile values, respectively; and upper and lower whiskers represented maximum and minimum values, respectively.

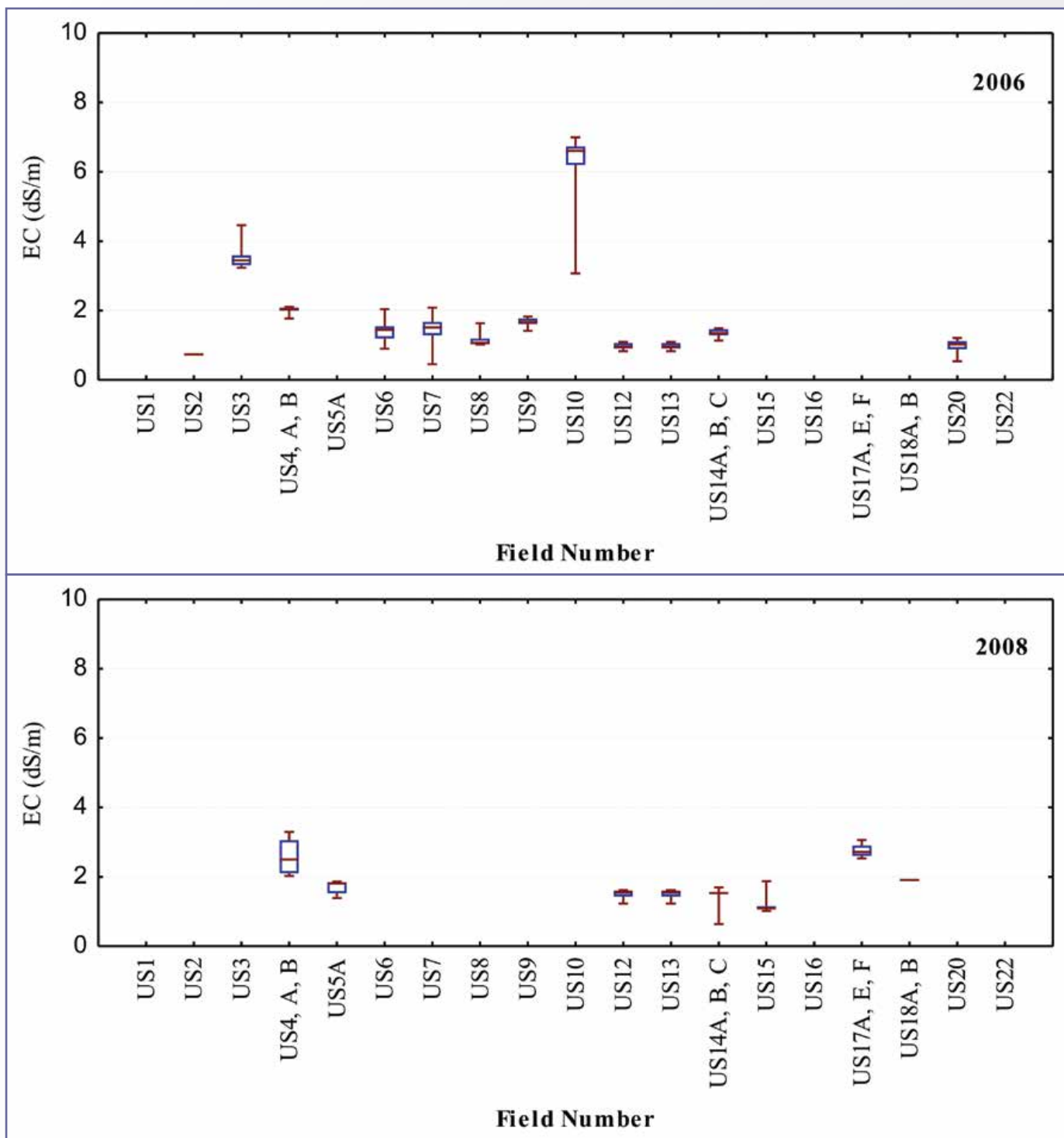


**Figure 64.** Box and whisker plots of EC values measured on fields in the Upstream Study Region for years 2006 and 2008. Midline represents the median value; upper and lower edges of box represent 75 percentile and 25 percentile values, respectively; and upper and lower whiskers represented maximum and minimum values, respectively.

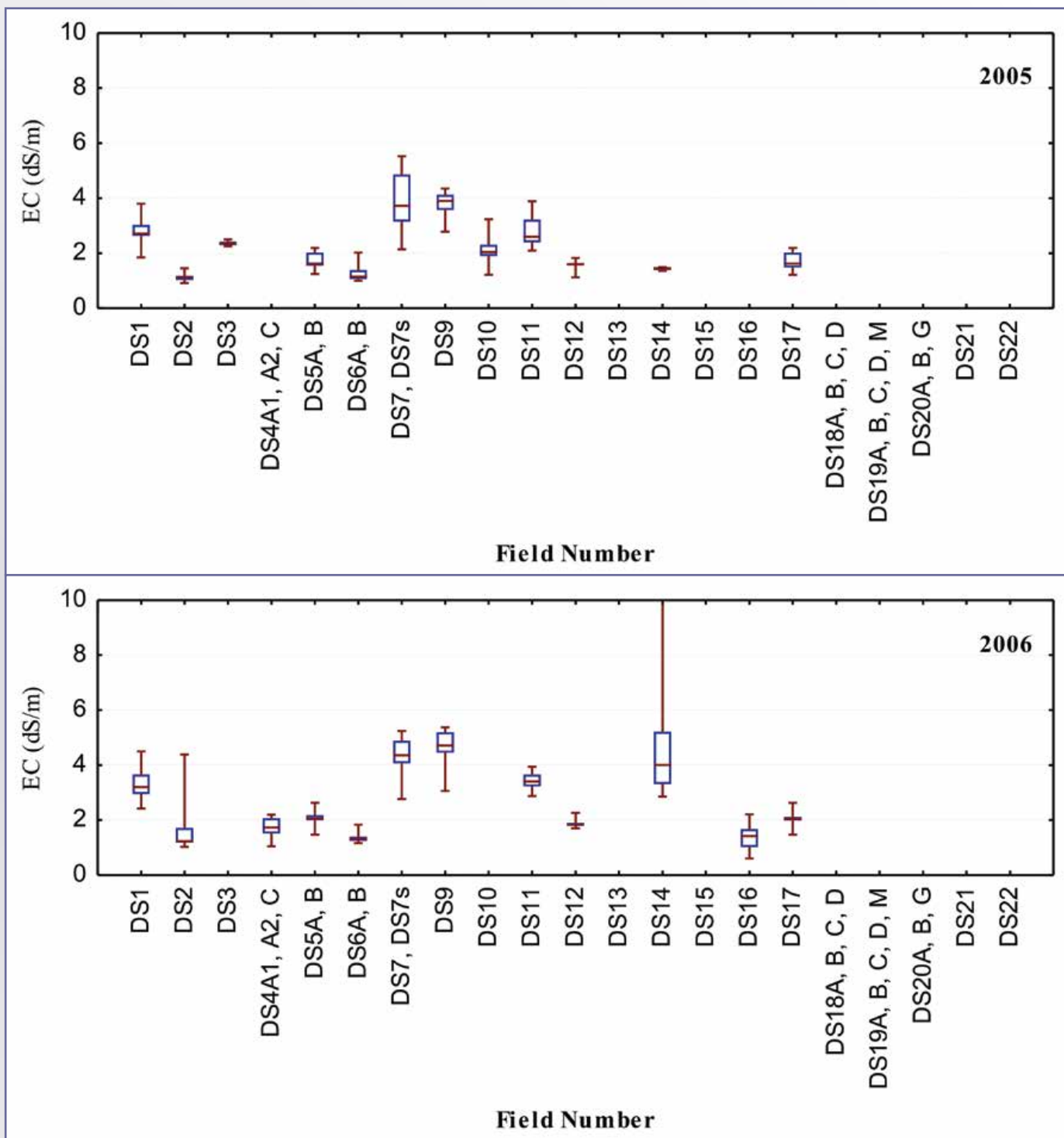


**Figure 65.** Box and whisker plots of EC values measured on fields in the Downstream Study Region for years 2005 and 2006. Midline represents the median value; upper and lower edges of box represent 75 percentile and 25 percentile values, respectively; and upper and lower whiskers represented maximum and minimum values, respectively.

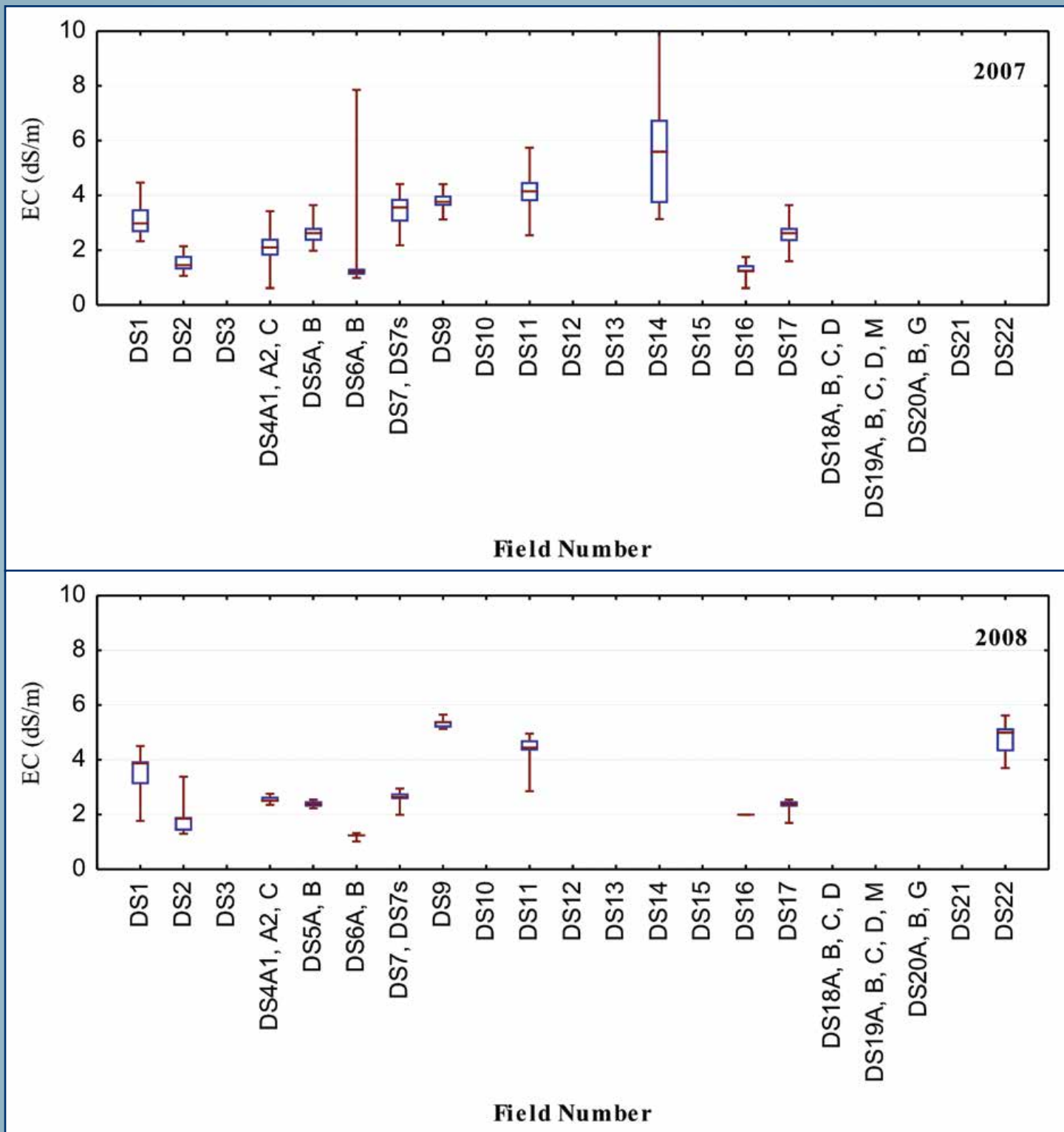


**Figure 66.** Box and whisker plots of EC values measured on fields in the Downstream Study Region for years 2007 and 2008. Midline represents the median value; upper and lower edges of box represent 75 percentile and 25 percentile values, respectively; and upper and lower whiskers represented maximum and minimum values, respectively.

## Crop Yield and ET in Relation to Soil Water Salinity and Irrigation

### *Crop Biomass in Relation to Soil Water Salinity*

Based upon controlled field experiments, the marketable yield of agricultural crops is well-known to be adversely affected by high concentrations of soil salt. This primarily is due to depressed osmotic potential that inhibits the ability of the crop roots to extract water from the soil pores, thereby reducing  $ET_a$ , but also is due to nutritional inhibition and toxic effects of certain soil salts on crop physiology (Wallender and Tanji 2012). The current study allowed the effects of soil water salinity on crop yield to be investigated for farmer-managed irrigated fields. Normalized crop biomass measured at locations within sampled fields, used as an indicator of relative crop yield, is plotted in Figure 67 against corresponding  $EC_e$  values estimated from EM38 measurements at the same locations for corn fields in the Upstream and Downstream Study Regions. Similar plots for alfalfa fields are presented in Figure 68. The relationships displayed in each plot indicate a general trend of decreasing crop yield with increasing  $EC_e$ . There is considerable scatter in the data due, especially at lower  $EC_e$  values (2-4 dS/m), to a number of other factors that influence crop yield such as crop variety, amount of fertilizer applied, type of soils, pest management, weed management, irrigation amount, etc. Crop yield appears to clearly diminish for  $EC_e > 4$  to 6 dS/m.

Average values of  $D_{wt}$ , groundwater EC,  $EC_e$ , and normalized crop biomass were computed over all measurements within an irrigation season for each monitored field. Pearson correlation,  $r$ , between these averages for each variable was computed using the Statistica® 9.0 software. The value of  $r$  can vary between -1 and 1 with  $r = -1$  indicating perfect inverse correlation and  $r = 1$  indicating perfect direct correlation between two variables. A statistically significant value of  $r$  (at  $p = 0.05$ ) between average normalized crop biomass and average  $D_{wt}$  was computed as 0.40, which is moderate. Statistically significant weak to moderate  $r$  values of -0.28 and -0.31 were computed between average normalized crop yield and average groundwater EC and between average normalized crop yield and average  $EC_e$ , respectively. These results reveal the tendency of crop yield to be adversely affected by shallow water tables, and high groundwater and soil water salinity concentrations.

### *Crop Biomass in Relation to Irrigation*

Values of  $r$  also were computed between average values of  $Q_A$ ,  $E_a$ , DPF, and TRF, and average normalized crop yield on monitored fields. Values of  $r$  between average  $E_a$ , DPF, and TRF and average normalized crop yield were not statistically significant. The  $r$  between average  $Q_A$  and average normalized crop yield was statistically significant with a weak to moderate value of 0.25. This indicated that, in general, for the fields and seasons studied, crop yield tended to increase with increased average applied irrigation depth.



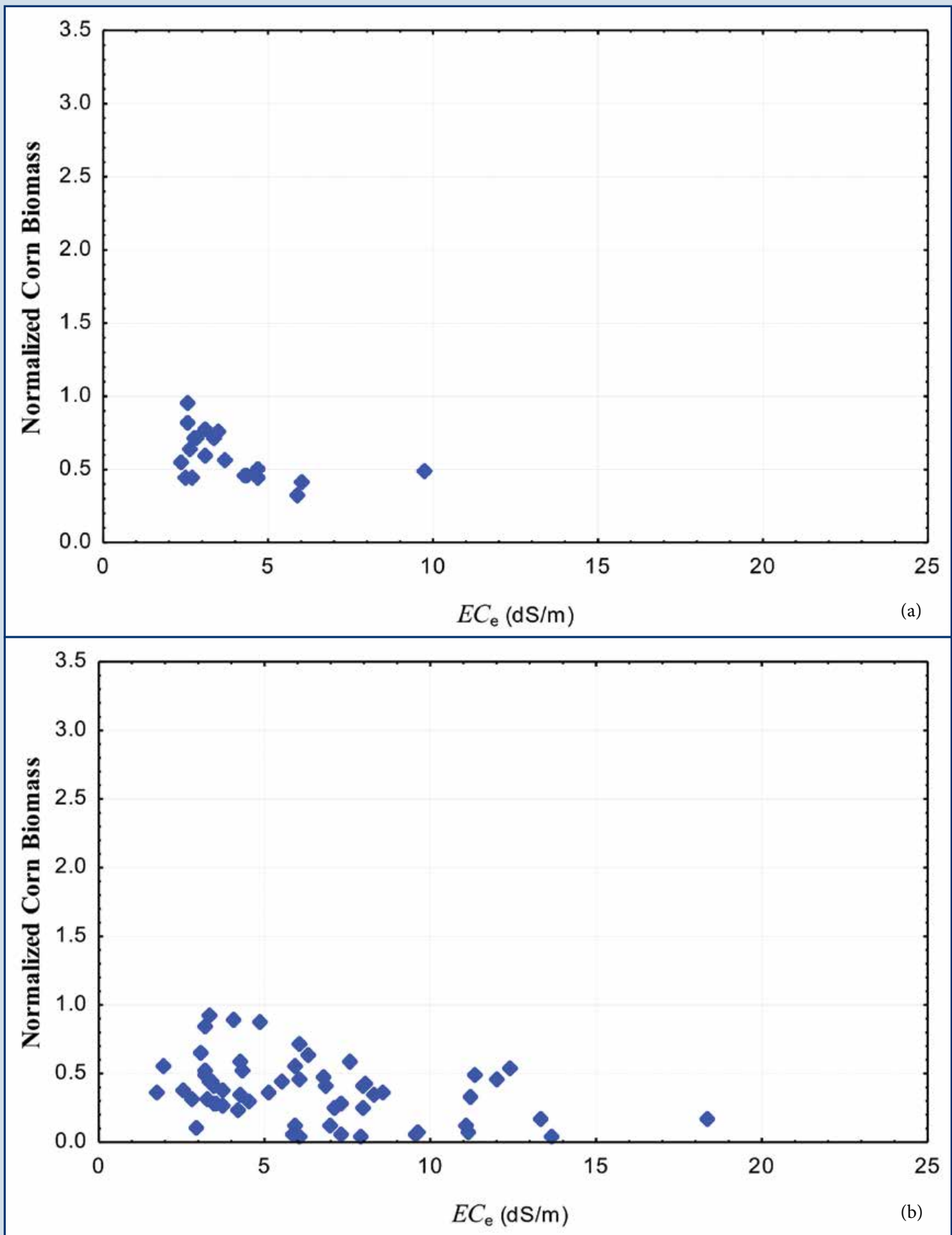


**Figure 67.** Normalized corn biomass versus  $EC_e$  measured at locations within surveyed fields in (a) Upstream Study Region, and (b) Downstream Study Region

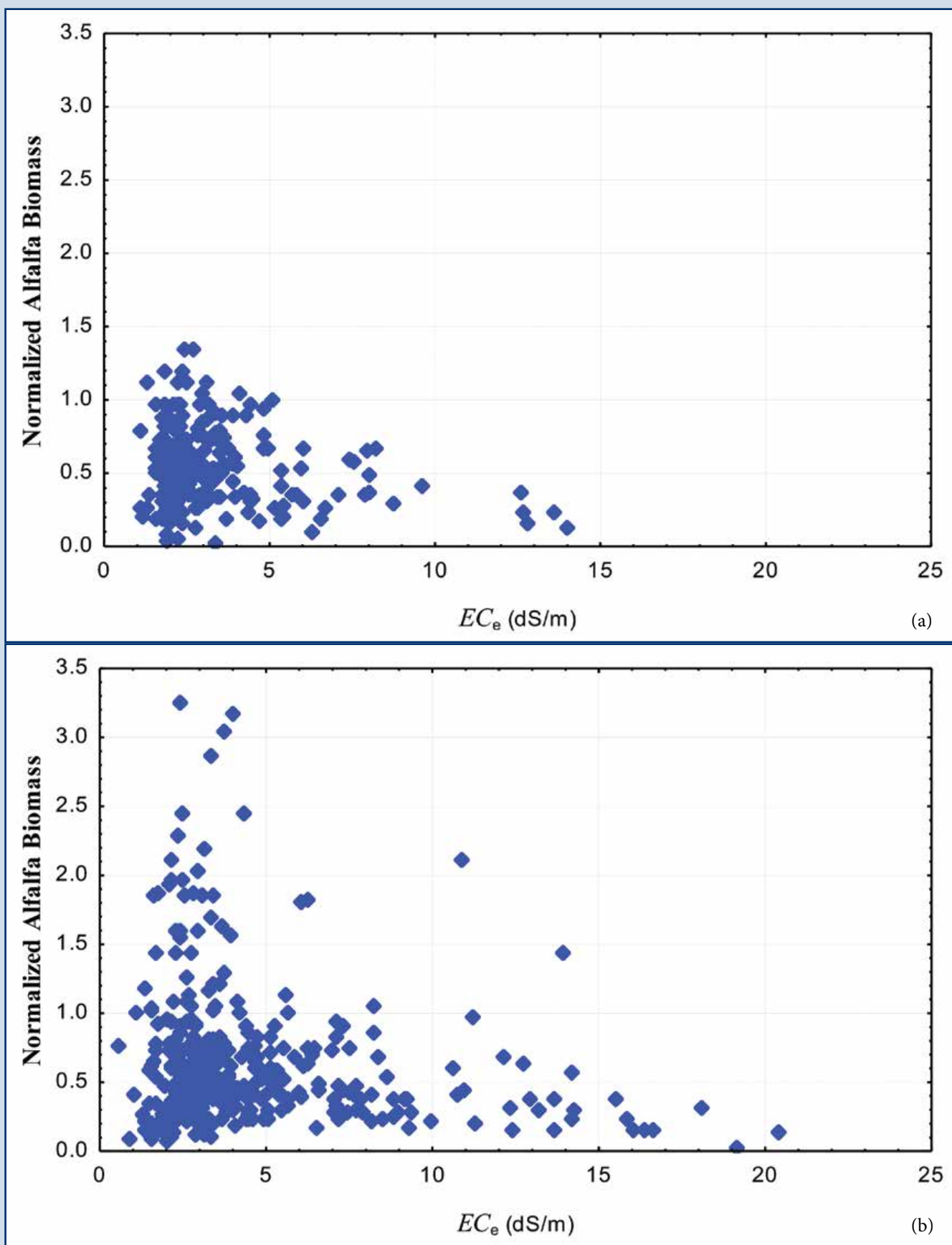


**Figure 68.** Normalized alfalfa biomass versus  $EC_e$  measured at locations within surveyed fields in (a) Upstream Study Region, and (b) Downstream Study Region

### *ET<sub>a</sub> in Relation to Soil Water Salinity*

The output of the ReSET model is a raster layer for the whole satellite image with the calculated values of  $ET_a$  for a 24 hour period in units of millimeters/day. A study of the possible effect of  $EC_e$  on  $ET_a$  in the study regions was conducted. Relationships were explored between  $ET_a$  values estimated with ReSET and values of  $EC_e$  estimated from EM38 measurements made at sample sites located with GPS. Data were used from field surveys conducted in the current study and from field surveys conducted in companion CSU projects. The ReSET  $ET_a$  raster layer first was clipped to the boundaries of the selected fields for a satellite image date closest to the date when EM38 field measurements were made. The clipped ReSET  $ET_a$  raster layer was converted to GIS polygons with each polygon retaining the model calculated  $ET_a$  value. The GIS  $ET_a$  polygons were then overlaid on the locations where EM38 measurements were made to estimate  $EC_e$ . Using a tool developed in ArcGIS, the statistical mean of the EM38 locations within each ET polygon was calculated and this information was added to the table of attributes of the GIS  $ET_a$  polygon coverage. Nonlinear regression was used with the Statistica® 9.0 software to develop a best-fit relationship with a reverse

S-curve form:

$$ET_a = \hat{a} + \frac{\hat{b}}{1 + \exp [\hat{c}(EC_e - \hat{d})]} \quad (27)$$

wherein  $\hat{a}$ ,  $\hat{b}$ ,  $\hat{c}$ , and  $\hat{d}$  are empirical coefficients determined using least-squares optimization.

Figure 69 shows Equation (27) fitted to data for six corn fields surveyed over the period 1999-2006. The relationships reveal the tendency for  $ET_a$  at locations within a field to decrease as  $EC_e$  increases. The reduction in  $ET_a$  is negligible or small at lower  $EC_e$  values with a steeper decrease in  $ET_a$  occurring over a range of  $EC_e$  values, followed by a gradual decrease or approach to a constant  $ET_a$  at higher  $EC_e$  levels. At these higher values of  $EC_e$  the crop likely is severely impacted and a significant portion of  $ET_a$  is made up of evaporation from the soil surface rather than transpiration. The steep reduction in  $ET_a$  appears to occur at  $EC_e$  values ranging between 2.5 to five dS/m. This corresponds closely to the threshold value of about 3.7 dS/m reported by Maas (1990) at which the yield of corn in gypsiferous soils, like those common to the LARV, begins to diminish. Similar studies are underway for alfalfa fields in the LARV.



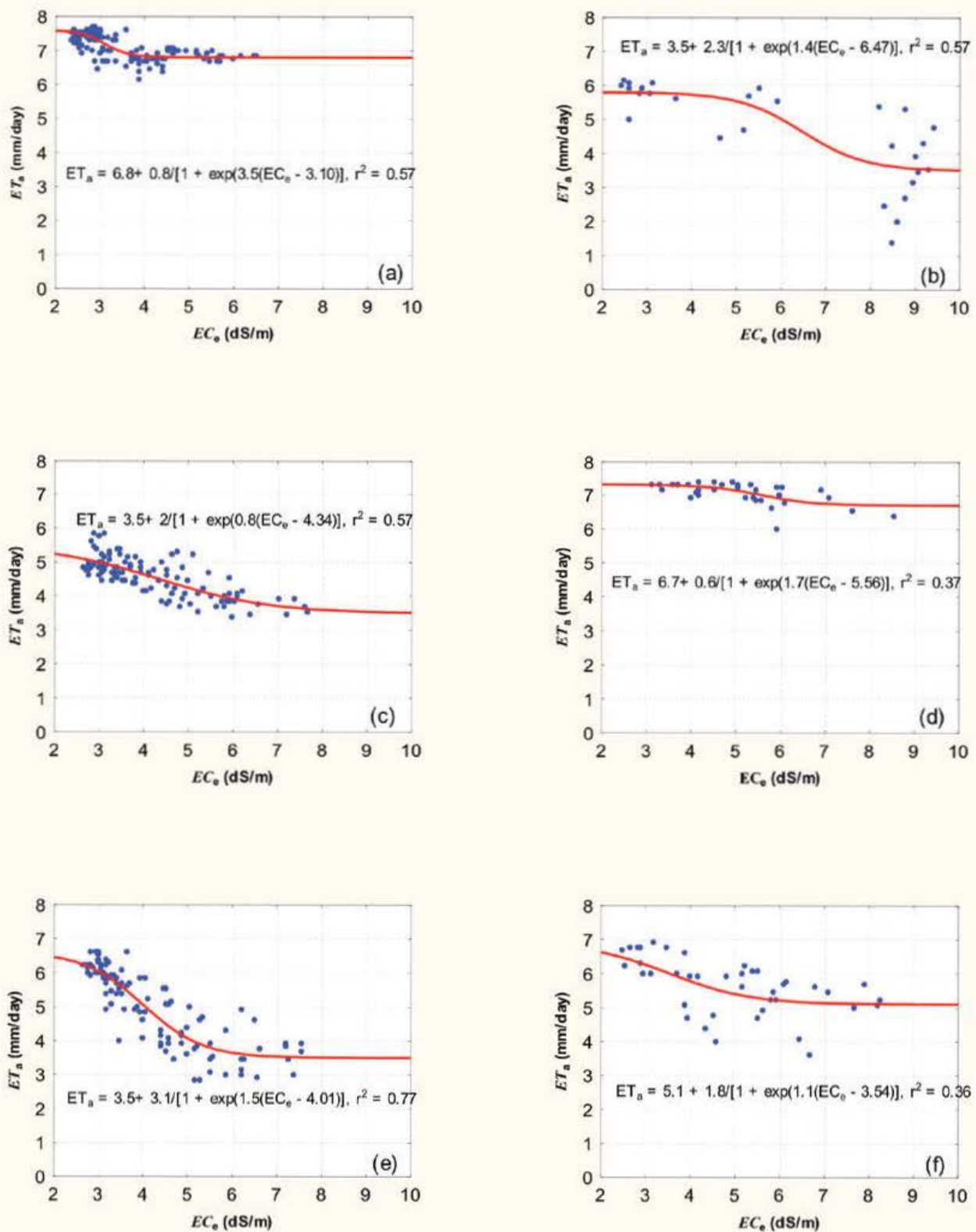


**Figure 69.**  $ET_a$  estimated with ReSET from satellite imagery versus measured  $EC_e$  for (a) field US17, July 1999; (b) field US20, July 2001; (c) field US80, June 2001; (d) field DS106, July 2005; (e) field US80, July 2001; and (f) field US38, July 2006. Fitted regression curves with  $r^2$  values are shown on each plot.

## Sensitivity Analysis

### *Sensitivity of Deep Percolation Fraction and Application Efficiency to Parameter Errors*

The sensitivity of estimated DPF for surface and sprinkler irrigation events to errors in  $ET_a$ ,  $Q_p$ , initial  $S_{SW}$ , and TAW is illustrated in Figure 70 for all monitored surface irrigation events and for all monitored sprinkler irrigation events. The plots in this figure illustrates the range of average DPF values calculated over all irrigation events for the considered range of values associated with possible errors in each input parameter to the IDSCU model. Generally, DPF values calculated by IDSCU are most sensitive to expected independent errors in the sink and source parameters,  $ET_a$  and  $Q_p$ , than to errors in the soil water storage parameters,  $S_{SW}$  and TAW. Estimated values of DPF could be expected to vary as much as about 12 percentage points due to these errors.

Similar plots illustrating the sensitivity of  $E_a$  for to errors in  $ET_a$ ,  $Q_p$ , initial  $S_{SW}$ , and TAW is illustrated in Figure 71 for all monitored surface and sprinkler irrigation events. Similar to DPF,  $ET_a$  is most sensitive to expected errors in  $ET_a$  and  $Q_p$ , indicating possible variation in estimated  $ET_a$  values as much as about 12 percentage points.

### *Sensitivity of Application Efficiency to Infiltration Distribution Pattern*

The sensitivity of estimated  $E_a$  to errors in the estimated slope of linear infiltration distribution for surface irrigation events is as much as three percentage points for Upstream fields and as much as 2.5 percentage points for Downstream fields. Hence, estimates of  $E_a$  are relatively insensitive to the estimated slope of linear infiltration distribution.

### *Recharge to and Upflux from Groundwater*

The spatial distributions of predicted average  $D_{wt}$  in the Upstream Study Region over the irrigation seasons within the period 1999-2007 and in the Downstream Study Region over the irrigation seasons within 2002-2007 are shown in Figure 72. Figure 73 presents the spatial distribution of predicted total average recharge to the groundwater table, resulting from deep percolation and from canal seepage, for corresponding seasons Upstream and Downstream. Similarly, Figure 74 illustrates corresponding spatial distributions of upflux from the groundwater table to  $ET_a$ . Comparison of Figures 73 and 74 with Figure 72 reveals the correspondence between higher recharge rates and lower  $D_{wt}$  (shallower water table) and between lower  $D_{wt}$  and higher upflux rates.



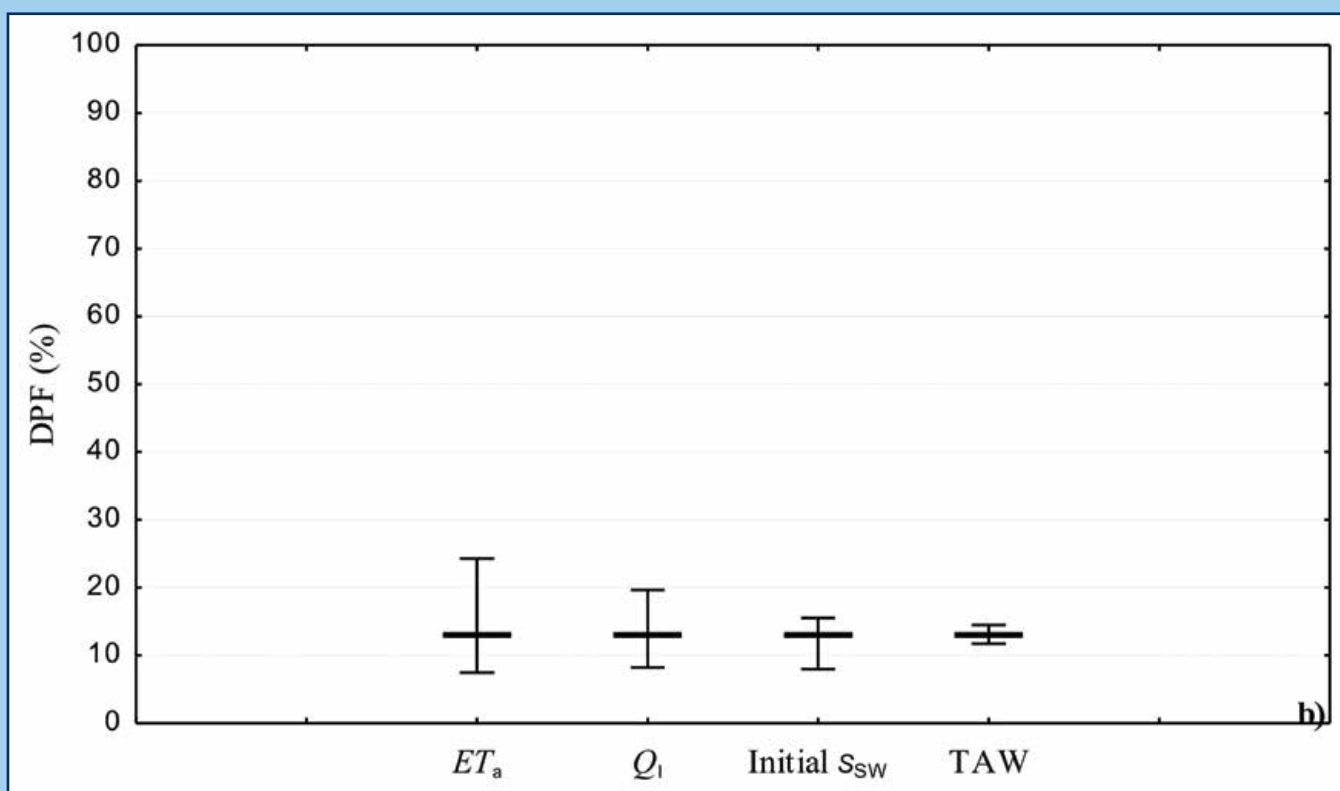
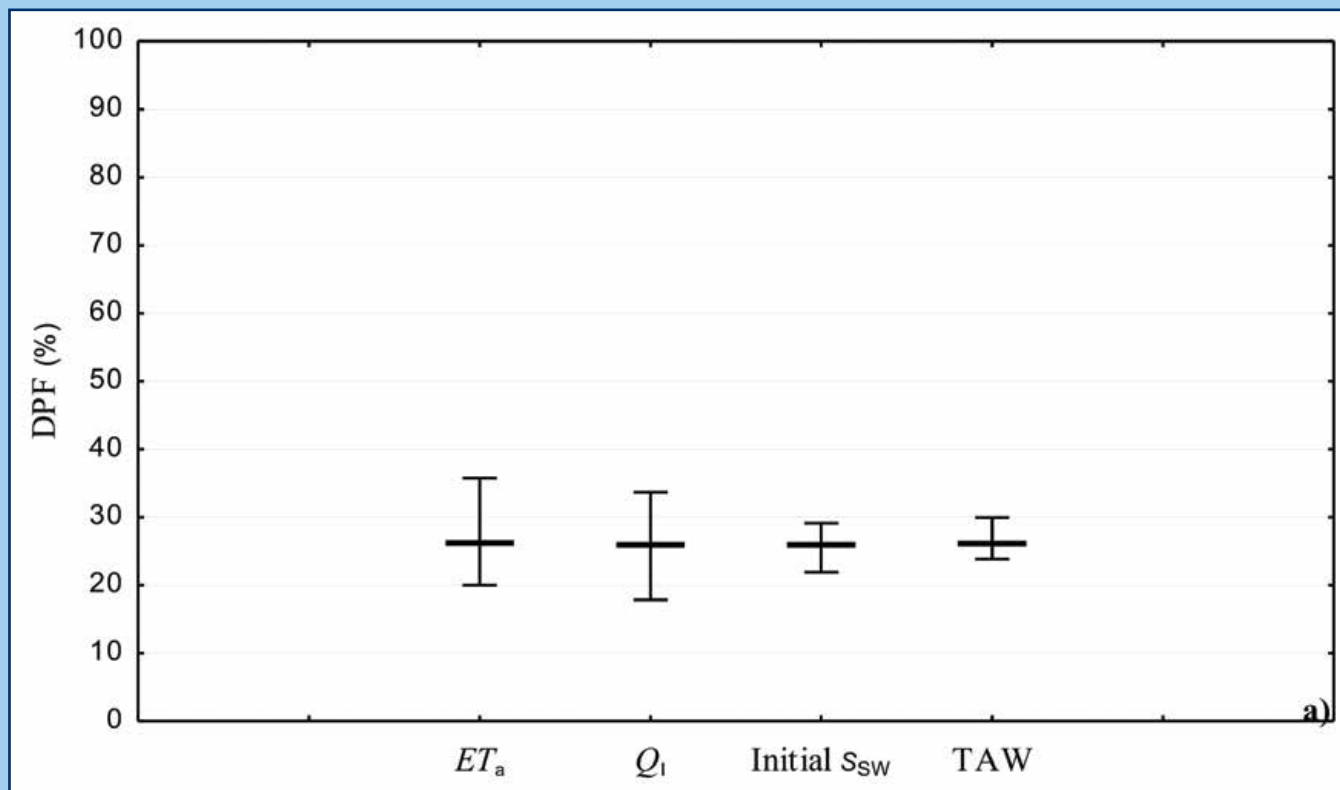


**Figure 70.** Range and baseline average values (horizontal bar) of DPF calculated over the considered range of values associated with errors in  $ET_a$ ,  $Q_l$ , initial  $S_{SW}$ , and TAW for (a) all surface irrigation events Upstream and Downstream, and (b) all sprinkler irrigation events Upstream and Downstream

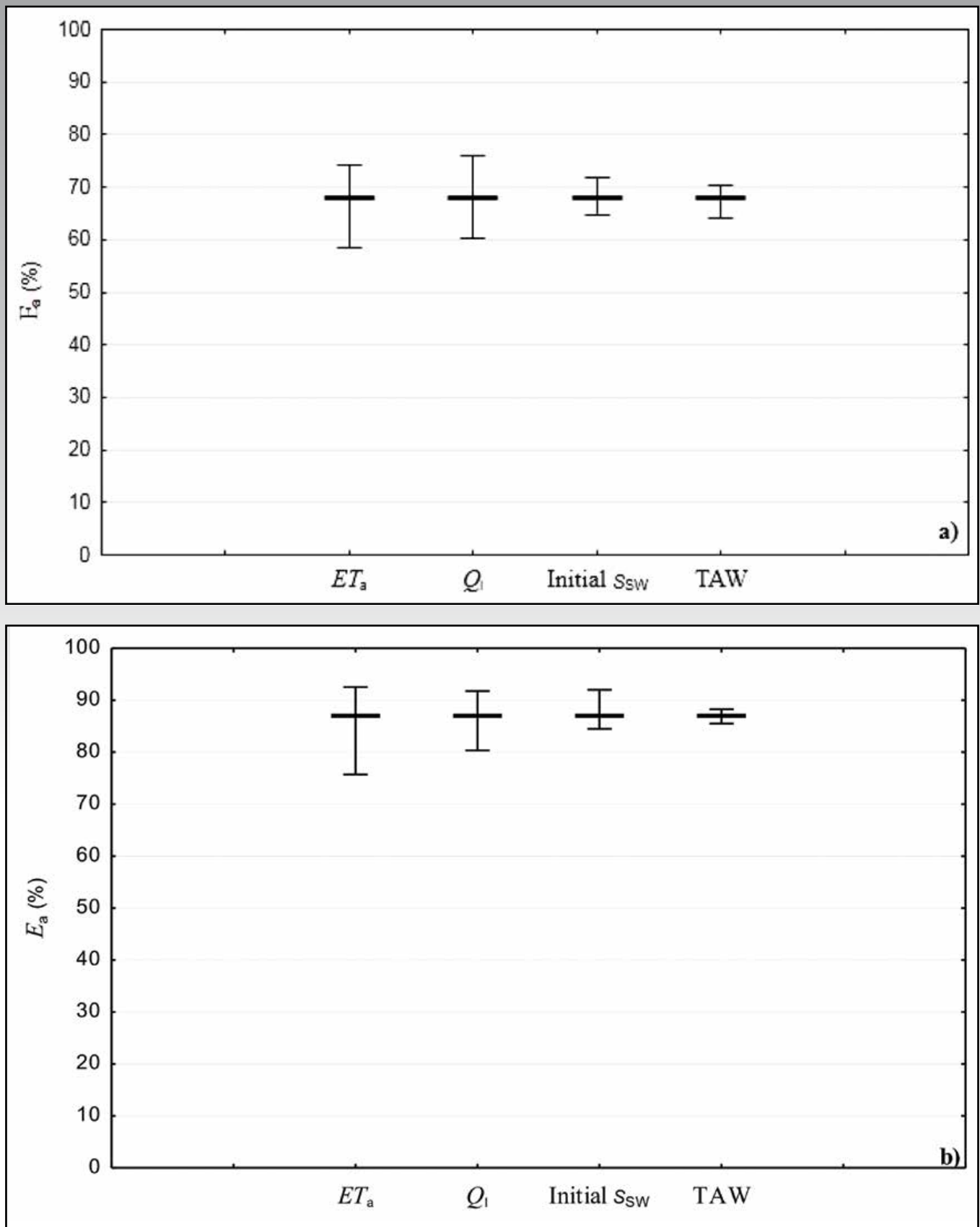


**Figure 71.** Range and baseline average values (horizontal bar) of  $E_a$  calculated over the considered range of values associated with errors in  $ET_a$ ,  $Q_i$ , initial  $S_{SW}$ , and TAW for (a) all surface irrigation events Upstream and Downstream, and (b) all sprinkler irrigation events Upstream and Downstream

Plots of spatial average infiltrated water ( $Q_I + Q_P$ ) and recharge to the groundwater table are shown in Figure 75 for the modeled periods for the Upstream and Downstream Study Regions. Predicted recharge rates to the groundwater table under irrigated fields average 0.10 in/day over irrigation seasons within 1999-2007 Upstream. Average predicted recharge rates over the seasons 2004, 2005, 2006, and 2007 are 0.08, 0.11, 0.09, and 0.16 in/day, respectively. This represents about 39 percent, 47 percent, 39 percent, and 53 percent of infiltrated water, respectively, over these irrigation seasons. In the Downstream region, predicted recharge rates averaged 0.06 in/day over the irrigation seasons within 2002-2007. Over 2004, 2005, 2006, and 2007 predicted recharge rates Downstream are 0.05, 0.07, 0.05, and 0.08 in/day, respectively, which are about 30 percent, 41 percent, 31 percent, and 41 percent of infiltrated water, respectively.

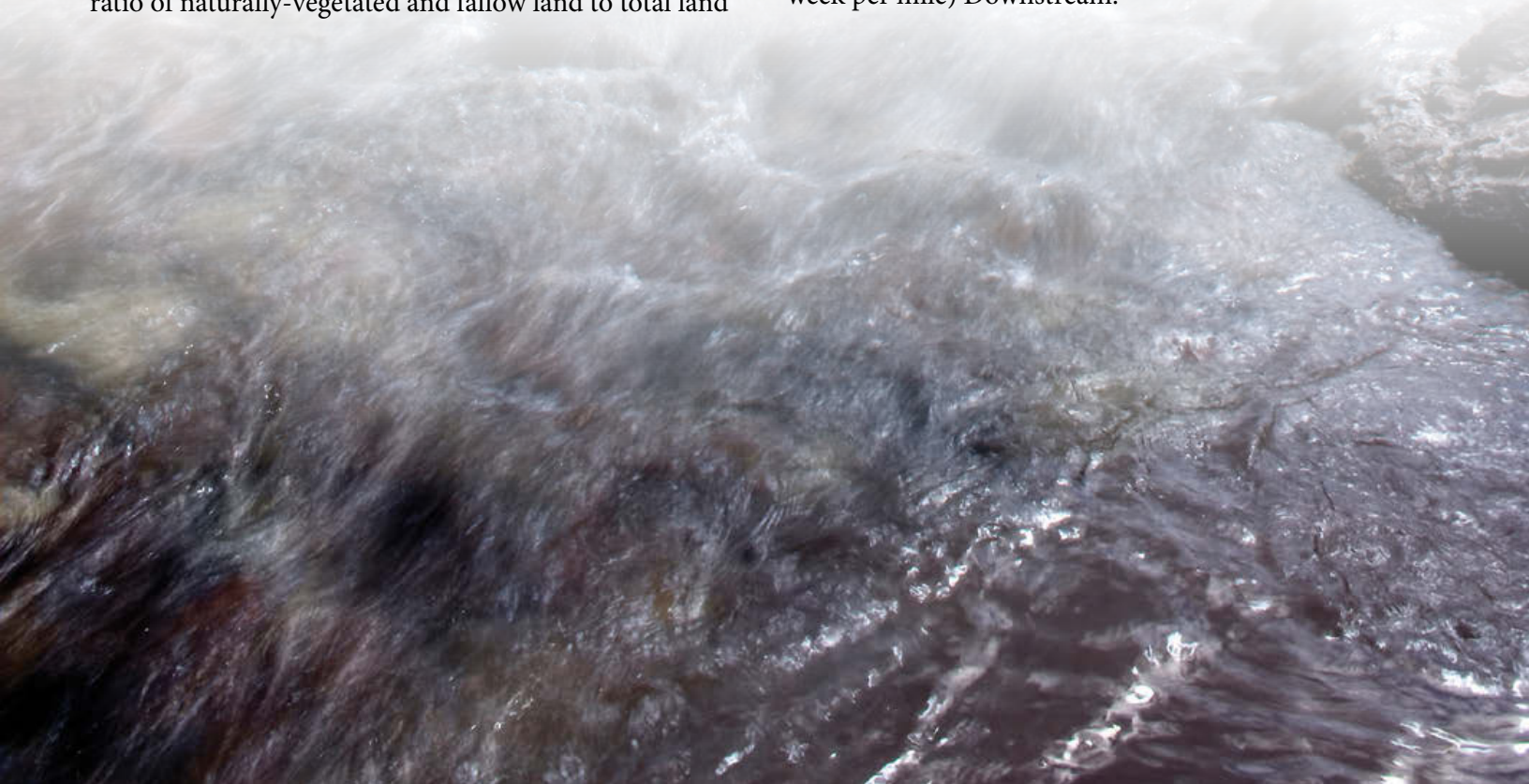
The regional scale models estimate that upflux from the groundwater table to non-beneficial  $ET_a$  under naturally-vegetated and fallow fields is substantial in relation to total crop  $ET_a$ , as seen in the plot in Figure 76. Cumulative predicted upflux to non-beneficial  $ET_a$  under naturally-vegetated and fallow fields is plotted in Figure 77 for the Upstream and Downstream Study Regions. Also, shown is the estimated cumulative upflux to non-beneficial  $ET_a$  under naturally-vegetated and fallow fields over the entire LARV. This was estimated using land survey data from 2003, assuming that the ratio of naturally-vegetated and fallow land to total land

in the Upstream and Downstream Study Regions applies to the entire LARV, and also assuming that conditions determining upflux over the entire LARV are similar to those within the study regions.

### Return Flows and Salt Loads to Streams

Figure 78 shows groundwater return flow predicted by the regional models to the Arkansas River along the Upstream and Downstream study regions. The average predicted return flow rate over the period April 1999-October 2007 is 30.9 ac-ft/week per mile along the modeled 48.6 miles of river Upstream. Downstream, the average predicted return flow rate over the period April 2002-October 2007 is 12.0 ac-ft/week per mile along the modeled 43.8 miles of river. Average predicted return flow rate over the years 2004, 2005, 2006, and 2007 is 19.4, 22.8, 22.8, and 35.3 ac-ft/week per mile, respectively, along the Upstream Study Region, and is 9.3, 8.9, 6.3, and 16.2 ac-ft/week per mile, respectively, along the Downstream Study Region.

Salt load in groundwater return flow to the river within the Upstream and Downstream Study Regions was estimated using the regional models and is plotted in Figure 79. The loads are substantial, ranging from less than 1,000 tons/week (20.6 tons/week per mile) to more than 17,500 tons/week (359.8 tons/week per mile) Upstream, and from about 1,400 tons/week (32.0 tons/week per mile) to about 11,000 tons/week (251.2 tons/week per mile) Downstream.



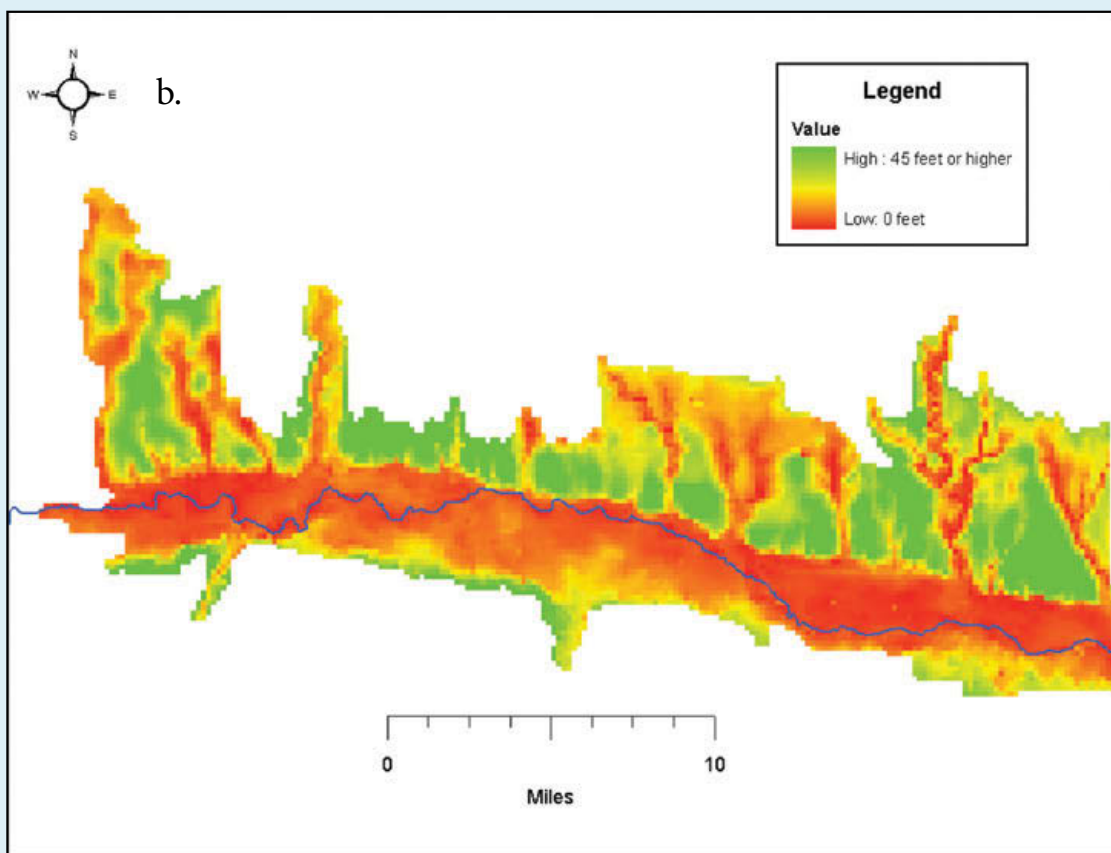
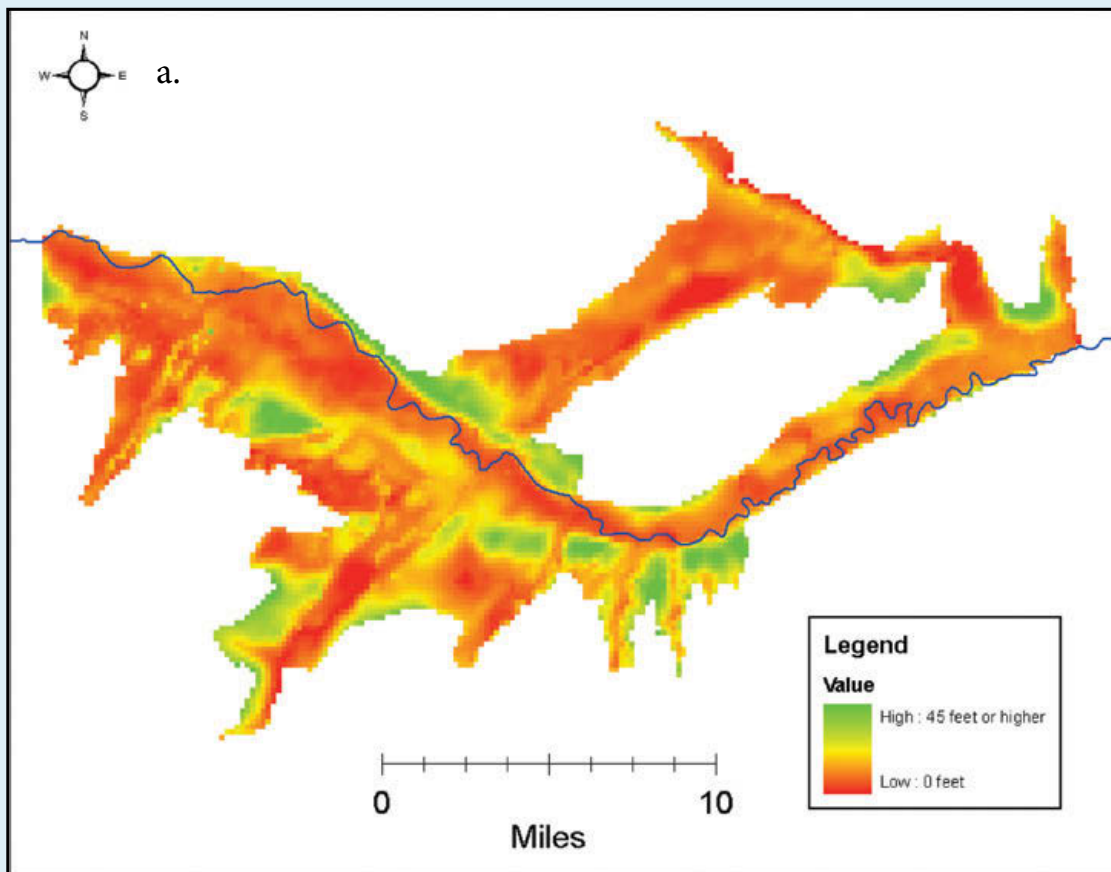


**Figure 72.** Average  $D_{wt}$  computed over irrigation seasons (a) 1999-2007 in the Upstream Study Region, and (b) 2002-2007 in the Downstream Study Region

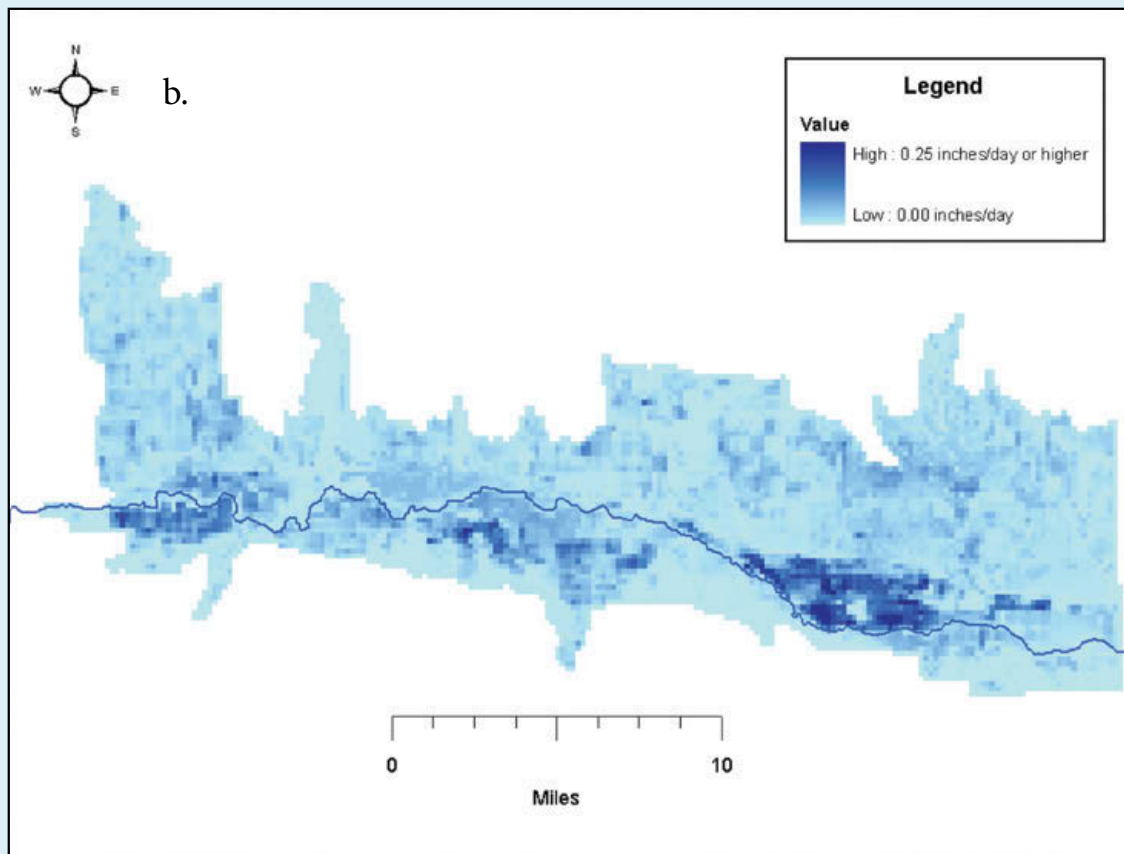
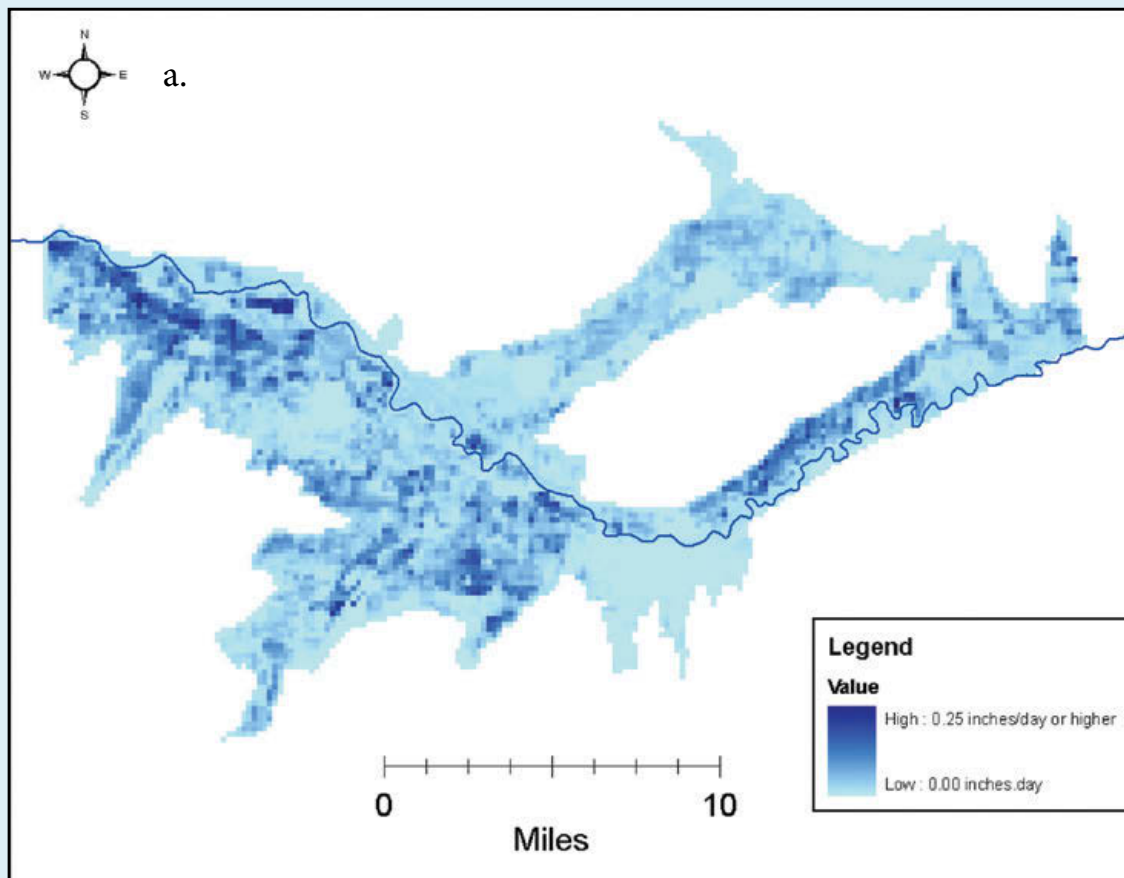


**Figure 73.** Average recharge rate to the water table computed over irrigation seasons (a) 1999-2007 in the Upstream Study Region, and (b) 2002-2007 in the Downstream Study Region

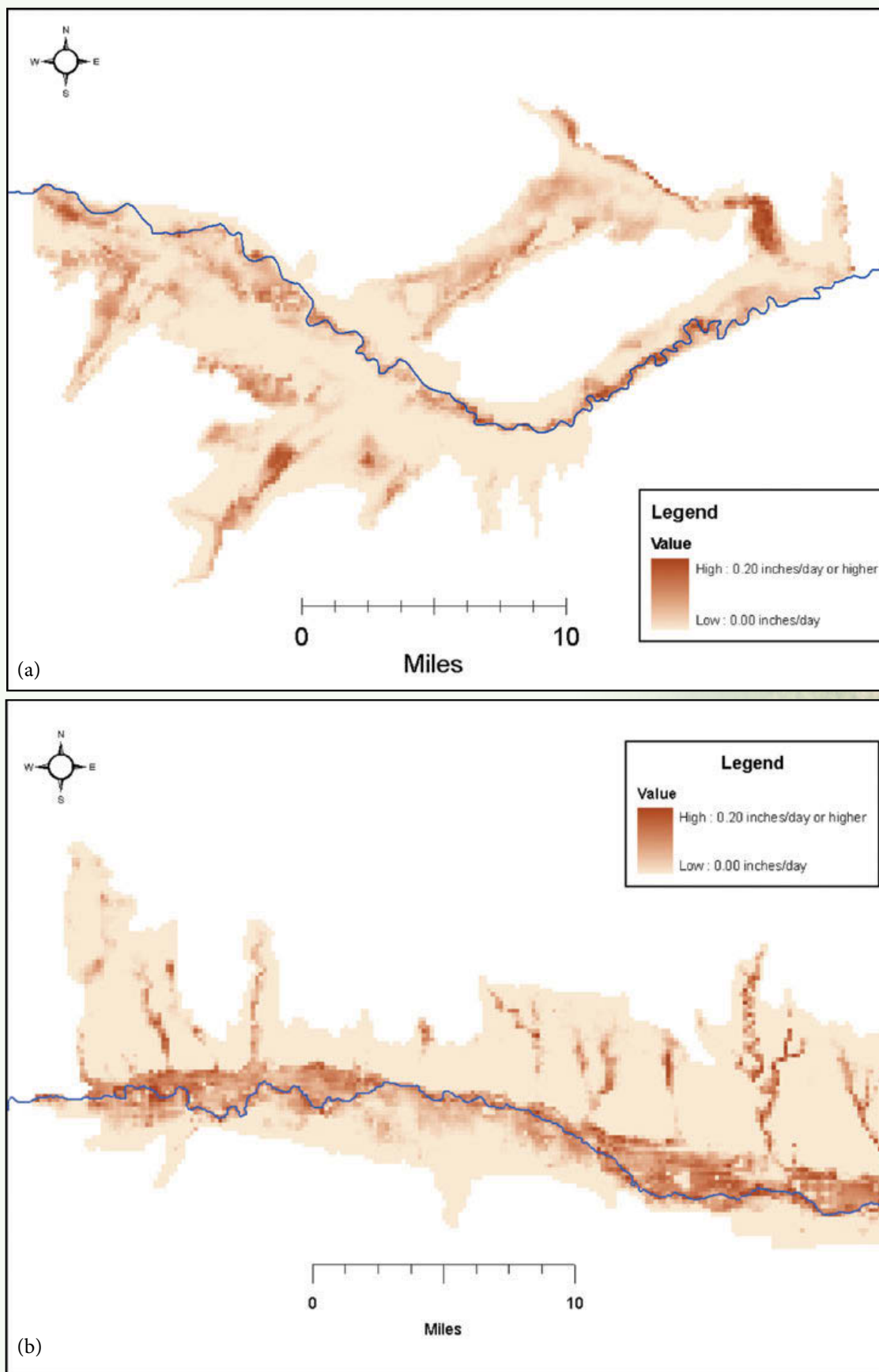


**Figure 74.** Average ground water upflux rate to  $ET_a$  computed over irrigation seasons (a) 1999-2007 in the Upstream Study Region, and (b) 2002-2007 in the Downstream Study Region

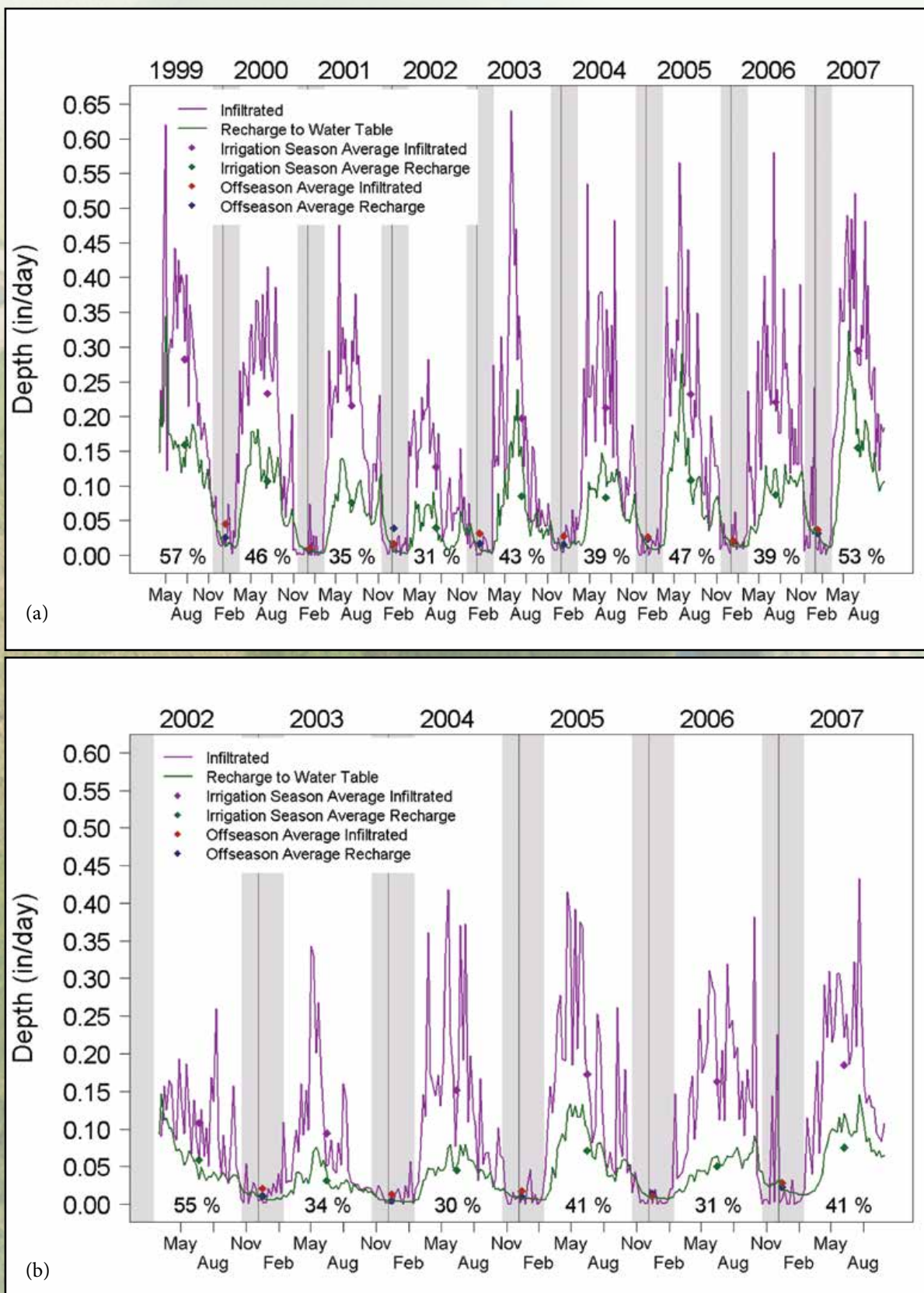


**Figure 75.** Infiltrated water ( $Q_I + Q_P$ ) and recharge to the groundwater table, showing average values during the off seasons and during the irrigation seasons as plotted points and ratios of recharge to infiltrated water over the irrigation seasons as written percentages for (a) Upstream Study Region and (b) Downstream Study Region

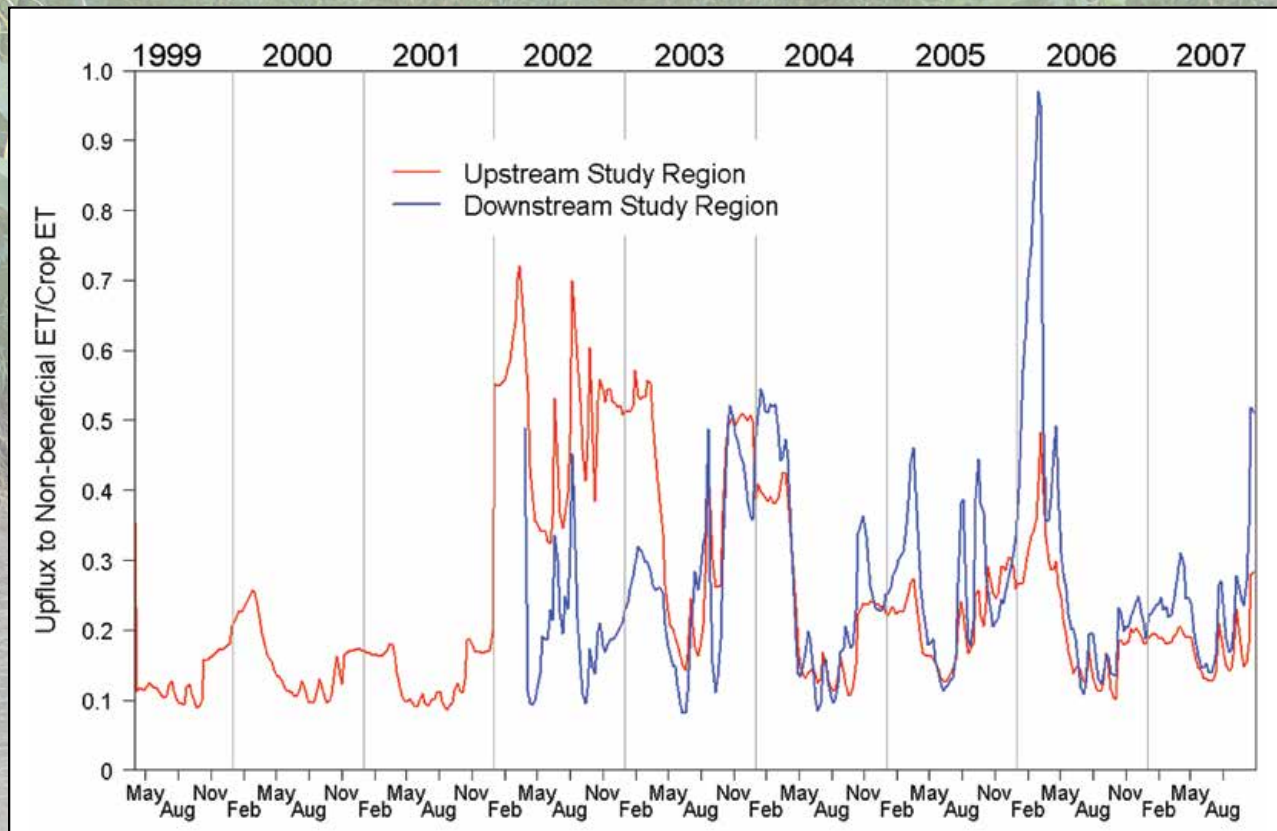


**Figure 76.** Ratio of groundwater upflux to non-beneficial  $ET_a$  to crop  $ET_a$  computed by the regional models for the Upstream and Downstream Study Regions

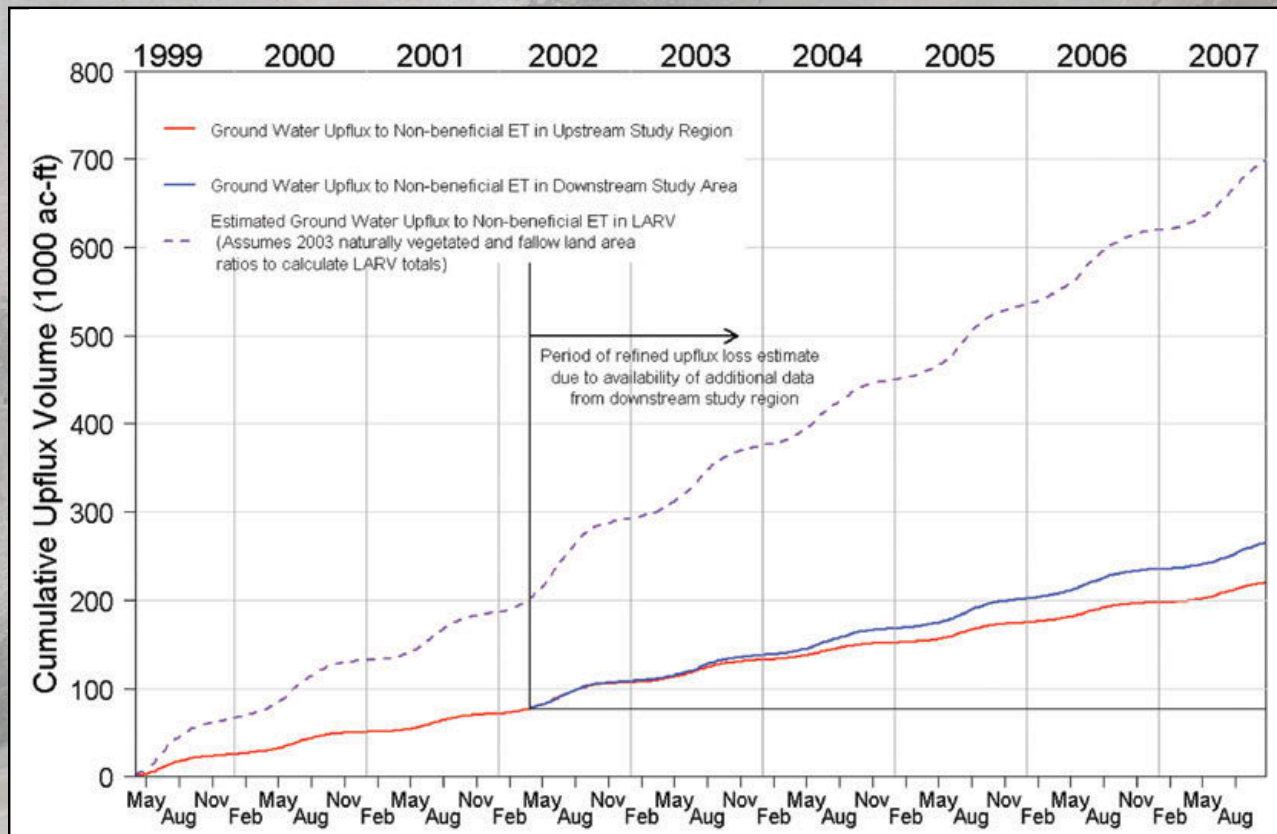


**Figure 77.** Cumulative groundwater upflux to non-beneficial  $ET_a$  computed by the regional models for the Upstream and Downstream Study Regions and estimated for the entire LARV

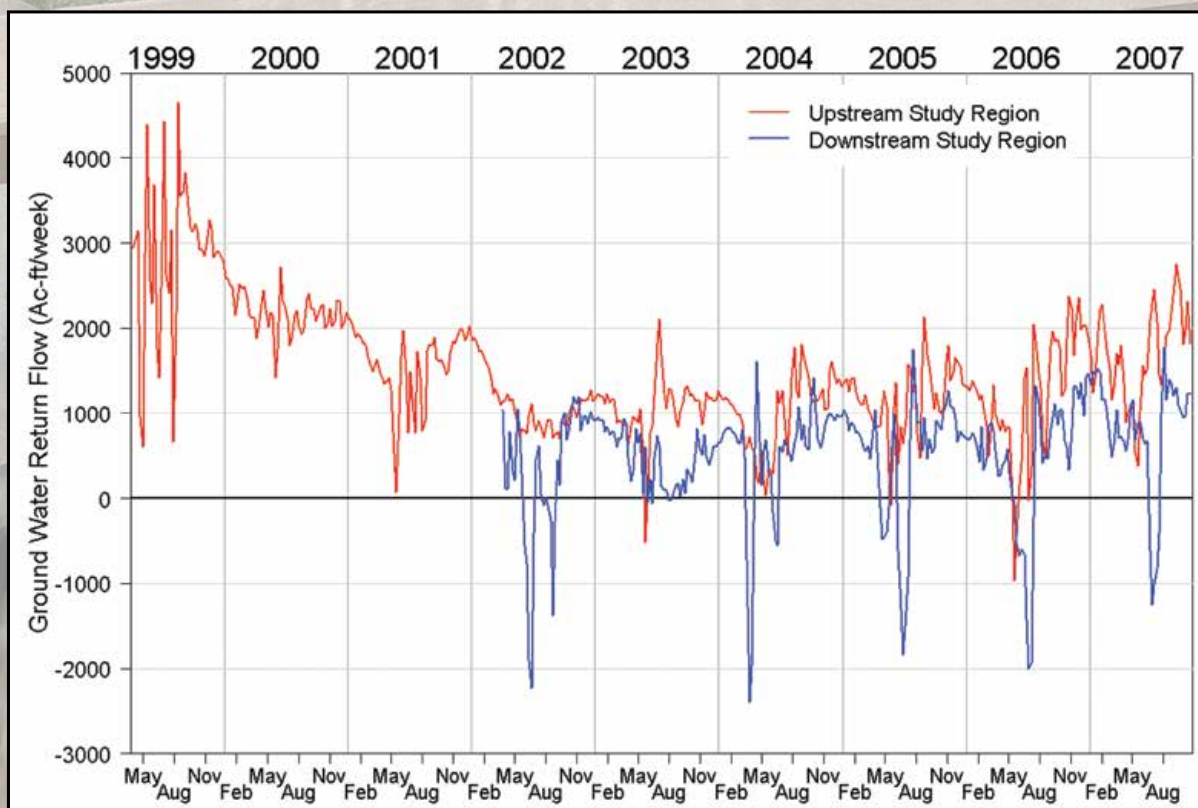


**Figure 78.** Groundwater return flow to the Arkansas River within the Upstream and Downstream Study Regions estimated with the regional models (negative values indicate net loss of water from the river to the groundwater aquifer)

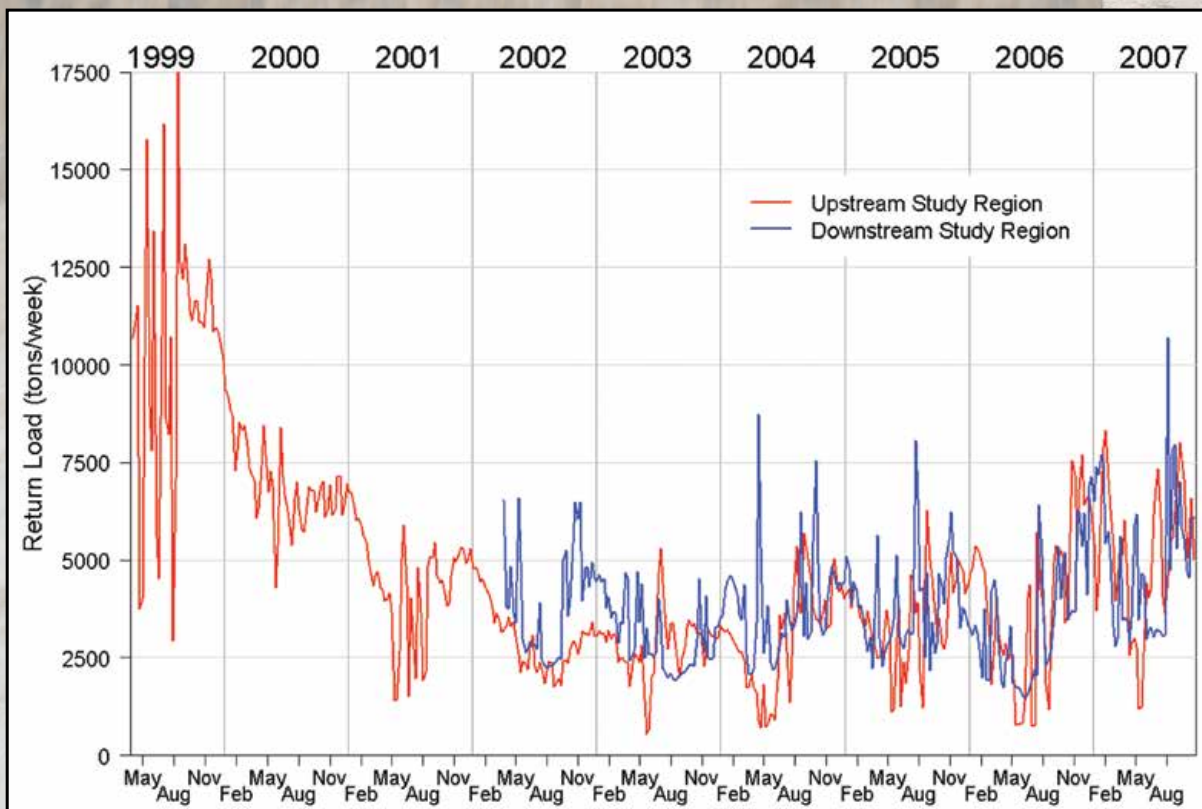


**Figure 79.** Salt load in groundwater return flow to the Arkansas River within the Upstream and Downstream Study Regions estimated with the regional models

# Summary, Conclusions, and Implications

Irrigation practices in Colorado's Lower Arkansas River Valley, and their impacts on the stream-aquifer system, have been characterized using extensive field data and calibrated regional modeling. A total of 61 irrigated fields (33 surface-irrigated, 28 sprinkler-irrigated) were monitored in two study regions of the LARV from 2004-2008. Both flow and water quality characteristics were measured or estimated. Analysis and results are presented for a total of 242 irrigation events and 279 sprinkler irrigation events. These results, as well as discoveries from companion projects, allowed groundwater flow models to be calibrated and applied in describing conditions over regional scales within both study areas.

## General Findings

The average applied irrigation depth for the monitored surface irrigation events was 8.2 in. Water losses in the form of tailwater runoff were found to be quite low on surface-irrigated fields, with an average tailwater fraction (TRF) of about eight percent. Most of the losses in surface irrigation events occurred in the form of deep percolation below the crop root zone, with an estimated deep percolation fraction (DPF) of 24 percent. Estimated values of irrigation application efficiency ( $E_a$ ) for the surface-irrigation events ranged from 10 percent to a maximum of 100 percent and averaged about 68 percent, a value that is comparable or higher than average values reported in the literature (Howell 2003, Wolters 1992).

Average applied depth for sprinkler irrigation events was 2.2 in. In this study, no significant tailwater losses were observed for any of the sprinkler irrigation events. Average DPF on monitored sprinkler-irrigated fields was about 13 percent, indicating that deep percolation on sprinkler-irrigated fields was only about 37 percent of that estimated for surface-irrigated fields. The average  $E_a$  for sprinkler irrigation events was about 82 percent. Losses from sprinkler spray to direct evaporation and wind drift were estimated to be about 5 percent for the types of sprinkler systems used in the LARV.

A limited sensitivity analysis provided insight into the range of errors in estimated average DPF and  $E_a$  values independently derived from likely errors in actual evapotranspiration ( $ET_a$ ), infiltrated irrigation volume ( $Q_p$ ) initial soil water storage volume ( $S_{SW}$ ), and total

available water (TAW). The maximum likely range of error was roughly plus or minus 10 percentage points. Sensitivity of  $E_a$  values due to errors in assumed infiltration distribution had a range of error of roughly plus or minus three percentage points.

Salt concentration in applied irrigation water on surface irrigated fields averaged about 532 mg/L in the Upstream Study Region, and about 1,154 mg/L in the Downstream Study Region. Associated applied salt loads to fields were about 997 lb/ac Upstream and about 2,480 lb/ac Downstream. On sprinkler-irrigated fields Upstream, supplied by groundwater wells, salt concentration in applied water averaged about 1,498 mg/L. In the Downstream region, where sprinklers were supplied with water from canals through stabilization ponds, measured salt concentration in applied water averaged about 849 mg/L. Loading rates of salt in applied sprinkler irrigation waters were about 1,217 lb/ac and 446 lb/ac Upstream and Downstream, respectively.

Average soil salinity as saturated paste extract electrical conductivity ( $EC_e$ ) in monitored fields Upstream ranged from 2.1 dS/m to 7.0 dS/m over all surveys conducted during the study period. Averages in Downstream fields were considerably higher, ranging from 3.7 dS/m to 12.5 dS/m. About 60 percent of the fields showed an average  $EC_e$  that exceeded the approximate salinity threshold of four dS/m.

Water table depth ( $D_{wt}$ ) varied considerably within fields over the irrigation season and from field to field. Values of  $D_{wt}$  averaged over monitored irrigated fields varied from 7.8 to 12.1 ft in the Upstream region, with an overall average value of 9.9 ft. In the Downstream region,  $D_{wt}$  averaged over monitored irrigated fields ranged from 12.6 to 15.0 ft, with an overall average of 13.8 ft. About four fields in the Upstream Study Region and 21 fields in the Downstream Study Region had values of  $D_{wt}$  exceeding the 20 to 25 ft depth to the bottom of available monitoring wells. Average electrical conductivity (EC) of groundwater varied from 1.8 to 2.3 dS/m Upstream and from 2.3-3.1 dS/m Downstream. The finding of deeper and more saline water tables in fields within the Downstream region compared to those within the Upstream region was corroborated by regional modeling results.

Data gathered on numerous fields were explored to evaluate the impact of soil water salinity on crop water use and crop yield. Crop  $ET_a$  and crop yield (biomass) were found to diminish when values of  $EC_e$  in the soil exceeded about three to five dS/m. These results closely correspond to the threshold value of about 3.7-4 dS/m, reported by Maas (1990), beyond which yields of corn and alfalfa will decline in gypsiferous soils. Since numerous fields throughout the Upstream and Downstream Study Regions show  $EC_e$  values exceeding this threshold, actual evapotranspiration ( $ET_a$ ) values over the LARV are expected to be lower than potential evapotranspiration ( $ET_p$ ) values calculated using the ASCE Standardized Equation with published crop coefficients.

Much of the deep percolation that occurs on irrigated fields in the LARV, in addition to seepage from earthen canals (Susfalk et al 2008) and effective precipitation, flows downward to recharge the underlying groundwater table. Calibrated regional groundwater models predicted an average recharge rate to shallow groundwater of 0.10 in/day and 0.06 in/day over modeled irrigation seasons within the period 1999-2007 Upstream and within the period 2002-2007 Downstream, respectively. Over these same respective periods the regional model predicted that recharge to the groundwater table during the irrigation season was equivalent to 31 percent to 57 percent of  $Q_I + Q_P$  Upstream and to 30 percent to 55 percent of  $Q_I + Q_P$  Downstream, where  $Q_P$  = effective precipitation volume.

A portion of the alluvial groundwater in the LARV returns to the unsaturated zone and contributes to  $ET_a$  via capillary rise from shallow water tables. The current study revealed that between zero and 40 percent (with an average of 5 percent) of beneficial crop  $ET_a$  on monitored irrigated fields was provided by groundwater upflux. This upflux also brings salt into the root zone, contributing to the deleterious effects of  $EC_e$ . In addition, the calibrated regional groundwater models predict that about 26,000 ac-ft/year in the Upstream region and 35,000 ac-ft/year in the Downstream region flows upward to non-beneficial  $ET_a$  demand on naturally-vegetated and fallow fields. This water loss is equivalent to about 20 to 25 percent of annual crop  $ET_a$  on the average.

Much of the remaining saline groundwater in the LARV eventually returns to tributaries and to the main stem of the Arkansas River by flow through the alluvial aquifer, dissolving additional salts and minerals along its path. Average return flow rates to the Arkansas River within the Upstream and Downstream regions were estimated by the regional models to be 30.9 ac-ft/day per mile and 12 ac-ft/day per mile along the river, respectively. Salt load in this return flow to the river over the modeled years was estimated as about 93 tons/week per mile Upstream and about 62 tons/week per mile Downstream. This is considerably more than the estimated salt loading to irrigated fields, indicating substantial dissolution of additional salts from shale and shale-derived soils, which occurs as groundwater makes its way to the streams.



## Answers to Specific Questions of Concern to Water Managers and Regulatory Agencies

When possible, answers are provided to a number of specific questions that were raised during different stages of this study:

1. *How do the characteristic irrigation water balance component (WBC) and  $E_a$  values for sampled conventional surface irrigation systems compare to those for improved technology (especially sprinkler) systems?*

There is a significant difference in the WBC and  $E_a$  values for sampled conventional surface irrigation systems compared to those for sprinkler systems.

The estimated mean value of  $Q_I$  for all monitored surface irrigation events was almost four times larger than that for sprinkler irrigation events. The

mean value of DPF for all surface irrigation events was about 1.9 times greater than for sprinkler irrigation events. Water balance calculations indicated that little to no deep percolation occurred on several monitored sprinkler-irrigated fields. Average  $E_a$  for monitored surface irrigation events was 20 percentage points lower than for sprinkler irrigation events. No tailwater runoff was observed on sprinkler-irrigated fields. On surface-irrigated fields TRF averaged about eight percent.

2. *Do the characteristic WBC and  $E_a$  values for irrigation events seem to vary significantly from canal to canal; which is to say, do the values appear to be affected by total water supply available from one canal to another, within a single year?*



While this study monitored a substantial total number of irrigation events, there were not enough observed events under the command of different canal systems to answer this question with statistical significance.

3. *Do the characteristic WBC and  $E_a$  values vary significantly from year to year within the same canal system; i.e., do WBC and  $E_a$  appear to be affected by total water supply available within a canal?*

While this study monitored a substantial total number of irrigation events, there were not enough observed events within different irrigation seasons under the command of different canal systems to answer this question with statistical significance.

4. *Do the characteristic WBC and  $E_a$  values differ between surface-water supplied sprinklers as compared to groundwater-supplied systems?*

The project focused on sprinkler-irrigated fields mainly in 2008. For that year, in the Upstream region seven monitored sprinkler-irrigated fields were supplied from groundwater pumping wells while one was supplied from surface water. On the other hand, the 19 sprinkler-irrigated fields in the Downstream region were all supplied by canal water through stabilization ponds. The average  $Q_A$ ,  $Q_P$ , TRF, DPF and  $E_a$  values for the Upstream fields were 2.0 in, 1.8 in, 0.0 percent, 12.2 percent, and 82.8 percent while for the Downstream fields the respective values were 2.3 in, 2.1 in, 0.0 percent, 7.1 percent, 87.8 percent. There was no statistically significant difference between the WBC and  $E_a$  values estimated for surface-water supplied and groundwater-supplied sprinkler systems.

5. *Is there any indication of intentional bias introduced into the study by irrigators hoping to demonstrate that the achievable WBC and  $E_a$  values using surface-supplied sprinklers is no different than that associated with flood and furrow methods?*

No intentional bias was detected. The irrigated fields that were monitored in this study were selected based on their suitability to the study objectives and their convenience (location, ability

to monitor, source of water, etc) rather than by a broad request for volunteers from among irrigators.

6. *Do the data indicate any effect of soil salinity on crop yield? If so, what conclusions can be reached with these data, and what additional information is necessary to adequately quantify the impact of soil salinity on crop yield in the LARV?*

Yes, based on the crop biomass samples collected on corn and alfalfa fields there appears to be a clear trend of decreasing crop yield as  $EC_e$  increases above a threshold value of three to five dS/m. There are many factors that affect crop yield (so such as irrigation amount, fertilizer application, pest management, crop variety, etc.). Additional data on these factors should be collected in order to remove that variability from the data. Measurements on a larger number of fields also would strengthen understanding of the crop yield –  $EC_e$  relationship for various crops.

7. *Do the data indicate any effect of irrigation timing or amount on crop yield? If so, what conclusions can be reached with these data, and what additional information is necessary to adequately quantify the impact of irrigation management practices on crop yield in the LARV?*

A statistically significant weak correlation was detected between average crop yield and average total  $Q_A$  on monitored fields. However, not enough data were collected on irrigation timing (given that all irrigation events on fields typically were not monitored) and spatial uniformity of irrigation applications to definitively answer these questions. To do so would require monitoring of a much larger number of fields and irrigation events, under more carefully controlled conditions.

8. *What are the known or assumed possibilities and limitations for correlating crop yield and soil salinity to ET for the fields included in this study?*

As stated above, clear trends of decreasing crop biomass with increasing  $EC_e$  were detected on a number of fields investigated in this study. Also, using the ReSET model with satellite imagery, estimates of the impact of  $EC_e$  on crop  $ET_a$  were

developed for a number of corn fields. There appears to be a clear trend of decreasing  $ET_a$  as  $EC_e$  increases above threshold values of roughly three to five dS/m, corresponding to the thresholds detected for impact on crop yield.

9. *Does crop type appear to affect WBC and  $E_a$  under sprinkler systems?*

An examination of differences in DPF and  $E_a$  for sprinkler-irrigated events on corn and alfalfa fields revealed no statistically significant difference.

10. *Do sprinkler operators typically apply sufficient volumes of water necessary to meet the ET requirement of crops?*

This has not yet been thoroughly examined. However, the fact that no deep percolation occurred for about 72 percent of sprinkler irrigation events indicates that fields are likely being under-irrigated.

11. *Do sprinkler irrigators apply sufficient water to meet the salt leaching requirement for the soil root zone?*

Water balance calculations indicated that no deep percolation occurred on about 72 percent of monitored sprinkler irrigation events, indicating no salt leaching occurred during these events. If this practice continues, problems associated with increased soil salinity are to be expected.

12. *What is the difference in the WBC and  $E_a$  of sprinkler systems that practice leaching to those that do not?*

Given that very little leaching (very little deep percolation) was observed on the sprinkler-irrigated fields that were monitored, this question cannot be answered with the data that were collected.

13. *Are there significant differences in deep percolation and leaching fraction for various types of sprinkler systems?*

Given that very little leaching was observed (very little deep percolation) on the sprinkler-irrigated fields that were monitored, this question cannot be answered with the data that were collected.

14. *How do alfalfa crop yields from sprinkler irrigated fields compare with those irrigated by flood and furrow irrigation methods?*

There were an inadequate number of monitored fields to provide a statistically significant evaluation of this question.

15. *How do water table depth and salinity, soil salinity, and crop yields relate to WBC and  $E_a$ ?*

No statistically significant relationships could be detected using the data from this study.

# References

- Allen, R. G., Walter, I. A., Elliott, R. L., Howell, T. A., Itenfisu, D., Jensen, M. E., and Snyder, R. L. (2005). The ASCE standardized reference evapotranspiration equation. American Society of Civil Engineers, Reston, VA.
- Allen, R.G., Tasumi, M., Trezza, R. (2007a). Satellite-based energy balance for mapping evapotranspiration with internalized calibration (METRIC) - Model. *Journal of Irrigation and Drainage Engineering*, 133(4), 380-394.
- Allen, R.G., Tasumi, M., Morse, A., Trezza, R., Wright, J.L., Bastiaanssen, W., Kramber, W., Lorite, I., Robison, C.W. (2007b). Satellite-based energy balance for mapping evapotranspiration with internalized calibration (METRIC) – Applications. *Journal of Irrigation and Drainage Engineering*, 133(4), 395-406.
- Ayars, J. E., Christen, E. W., and Soppe, R. W. (2006). “The resource potential of in-situ shallow groundwater use in irrigated agriculture.” *Irrigation Science*, 24: 147-160.
- Bastiaanssen, W. G. M., Menenti, M., Feddes, R.A., and Holtslag, A.A.M. (1998a). “A remote sensing surface energy balance algorithm for land (SEBAL). 1. Formulation.” *Journal of Hydrology*, 212-213(1-4), 198-212.
- Bastiaanssen, W.G.M., Pelgrum, H., Wang, J., Ma, Y., Moreno, J.F., Roerink, G.J., and van der Wal, T. (1998b). Remote sensing surface energy balance algorithm for land (SEBAL): 2. Validation. *Journal of Hydrology*, 212-213(1-4), 213-229.
- Bastiaanssen, W. G. M. (2000). “SEBAL based sensible and latent heat fluxes in the irrigated Gedez Basin, Turkey.” *J. Hydrology*, 229(1–2), 87-100.
- Bog, M. G. (1989). Discharge measurement structures. 3rd Ed. Pub. 20, International Institute for Land Reclamation and Improvement, Wageningen, the Netherlands.
- Burkhalter, J. P., and Gates, T. K. (2005). “Agroecological impacts from salinization and waterlogging in an irrigated river valley”. *Journal of Irrigation and Drainage Engineering*, 131(2): 197-209.
- Colorado Agricultural Experiment Station. (2008). “Arkansas Valley Research Center 2006 Report.” Tech. Rpt. TR08-16 (<http://www.colostate.edu/depts/avrc/pubs/tr08-16.pdf>).
- Duffie, J.A., and Beckman, W.A. (1991). Solar engineering of thermal processes. Wiley, New York, 762 pp.
- Eldeiry, A. A., and Garcia, L. A. (2008). “Detecting soil salinity in alfalfa fields using spatial modeling and remote sensing.” *Soil Science Society of America Journal*, 72: 201-211.
- Elhaddad, A., and Garcia, L.A. (2008). “Surface energy balance-based model for estimating evapotranspiration taking into account spatial variability in weather.” *Journal of Irrigation and Drainage Engineering*, 134(6), 681-689.
- Elliott, R.L. and Walker, W.R. (1982). “Field evaluation of furrow infiltration and advance functions.” *Trans. ASAE* 25(2):396-400.
- Garcia, L. A., and Patterson, D. (2009) “Model for Calculating Consumptive Use (CSUID),” Proceedings of the USCID Conference on Irrigation and Drainage for Food, Energy and the Environmental, November 3-6, Salt Lake City, Utah.
- Gates, T. K., Cody, B.M, Donnelly, J.P., Hertin, A.W., Bailey, R.T. and Mueller Price, J. (2009). “Assessing selenium contamination in the irrigated stream aquifer system of the Arkansas River, Colorado” *Journal Environmental Quality*, 38: 2344-2356.
- Gates, T. K., Garcia, L. A., and Labadie, J. W. (2006). “Toward optimal water management in Colorado’s Lower Arkansas River Valley: monitoring and modeling to enhance agriculture and environment.” Colorado Water Resour. Res. Inst. Completion Report No. 205, Colorado Agric. Exp. Station Tech. Report TR06-10, Colorado State University, Fort Collins, CO.

- Grismer, M. E., and Gates, T. K. (1988). "Estimating saline water table contributions to crop water use." *California Agriculture*, 42(2): 23-24.
- Harbaugh A.W. (2005). "MODFLOW-2005, The U.S. Geological Survey modular ground-water model—the Ground-Water Flow Process," In: U.S. Geological Survey Techniques and Methods, Book 6, Chapter A16.
- Hoffman, G. J., Evans, R. G., Jensen, M. E., Martin, D. L., and Elliott, R. L. (2007). *Design and operation of farm irrigation systems*. 2nd Ed. ASABE, St. Joseph, MI.
- Hoffman, G. J., and Shalhevet, J. (2007). "Controlling salinity." In: Hoffman, G. J., Evans, R. G., Jensen, M. E., Martin, D. L., and Elliott, R. L. (2007). *Design and operation of farm irrigation systems*. 2nd Ed, pp. 160-207, ASABE, St. Joseph, MI.
- Howell, T. A. (2003). "Irrigation efficiency." In: *Encyclopedia of water science*. Marcel Dekker, Inc., New York, NY, pp. 467-472.
- Howell, T.A. (2006). "Water losses associated with center pivot nozzle packages." In: *Proc. Central Plains Irrigation Conference*, February 21-22, 2006, Colby, Kansas. p. 11-24.
- Kansas State University. (1997). "Efficiencies and water Losses of irrigation systems." KSU Cooperative Extension Service, MF-2243-May 1997.
- Klute, A. (1986). *Methods of Soil Analysis: Part 1, Physical and Mineralogical Methods*. Agronomy Series, No. 9, American Society of Agronomy, Soil Science Society of America, Madison, WI.
- Liu, Y., Pereira, L. S., and Fernando, R. M. (2006). "Fluxes through the bottom boundary of the root zone in silty soils: Parametric approaches to estimate ground-water contribution and percolation." *Agricultural Water Management*, 84: 27-40.
- Maas, E. V. (1990). "Crop salt tolerance." In: Tanji, K. K., ed. *Agricultural salinity assessment and management*. ASCE Manuals and Reports on Engineering Practice No. 71, American Society of Civil Engineers, New York, NY, pp. 263-304.
- Miles, D. L. (1977). "Salinity in the Arkansas Valley of Colorado." Interagency Agreement Report EPA-IAG-DR-0544. Cooperative Extension Service, Colorado State University, and U. S. Environmental Protection Agency, Denver, CO.
- Morway, E. D., Gates, T. K., and Niswonger, R. G. (2012). "Regional-scale appraisal of options for enhancing groundwater flow conditions in an irrigated alluvial aquifer system." In preparation.
- Niemann, J. D., Lehman, B.M., Gates, T.K., Hallberg, N.O., and Elhaddad, A. (2011). "Impact of shallow groundwater on evapotranspiration losses from uncultivated land in an irrigated river valley." *Journal of Irrigation and Drainage Engineering*, 137(8): 501-512.
- Niswonger, R.G., Prudic, D.E., and Regan, R.S. (2006), "Documentation of the Unsaturated-Zone Flow (UZF1) Package for modeling unsaturated flow between the land surface and the water table with MODFLOW-2005" In: U.S. Geological Techniques and Methods Book 6, Chapter A19, 62 p.
- Pratt, P. F., and Suarez, D. L. (1990). "Irrigation water quality assessments." In: Tanji, K.K., ed. *Agricultural Salinity Assessment and Management*. ASCE Manuals and Reports on Engineering Practice No. 71, American Society of Civil Engineers, New York, NY, pp. 203-219.
- Richards, L.A. (ed.) (1954). *Diagnosis and improvement of saline and alkali soils*. U.S. Salinity Laboratory Staff. Agriculture Handbook No. 60. USDA, Washington, D.C.
- Saxton, K. E., and Rawls, W. J. (2006). "Soil water characteristic estimates by texture and organic matter for hydrologic solutions." *Soil Science Society of America Journal*, 70: 1569-1578.
- Sherow, J. E. (1990). *Watering the valley: Development along the High Plains Arkansas River, 1870-1950*. University Press of Kansas, Lawrence, KS.

Susfalk, R., Sada, D., Martin, C., Young, M., Gates, T., Rosamond, C., Mihevc, T., Arrowood, T., Shanafield, M., Epstein, B., Fitzgerald, B., Lutz, A., Woodrow, J., Miller, G., and Smith, D. (2008). "Evaluation of linear anionic polyacrylamide (LA-PAM) application to water delivery canals for seepage reduction." DHS Pub. No. 41245, Desert Research Institute, Reno, NV.

Triana, E., Labadie, J. W., and Gates, T. K. (2010a). "River GeoDSS for agro-environmental enhancement of Colorado's Lower Arkansas River Basin. I: Model development and calibration." *Journal of Water Resources Planning and Management*.

Triana, E., Gates, T. K., and Labadie, J. W. (2010b). "River GeoDSS for agro-environmental enhancement of Colorado's Lower Arkansas River Basin. II: Evaluation of strategies." *Journal of Water Resources Planning Management*, 136(2): 190-200.

United States Department of Agriculture National Agricultural Statistics Service (NASS) Colorado Field Office. (2009). "Colorado Agricultural Statistics 2009." Lakewood, CO.

United States Department of Agriculture (USDA). (1986). "Urban hydrology for small watersheds." Tech. Release 55, Natural Resources Conservation Service, Washington, DC.

United States Department of Agriculture (USDA). (2010). Natural Resources Conservation Service Soil Survey Geographic (SSURGO) Database. <http://soils.usda.gov/survey/geography/ssurgo/>

Walker, W. R. (2003). SIRM03 User's Guide and Technical Documentation. Department of Biological and Irrigation Engineering, Utah State University, Logan, UT.

Walker, W.R. (2005). "Multi-level calibration of furrow infiltration and roughness." *Journal of Irrigation And Drainage Engineering*, 131(2).

Wallender, W. W. and Tanji, K. K., ed. (2012). *Agricultural salinity assessment and management*. ASCE

Manuals and Reports on Engineering Practice No. 71, American Society of Civil Engineers, New York, NY.

Wittler, J.M., Cardon, G.E., Gates, T.K., Cooper, C.A., and Sutherland, P.L. (2006). "Calibration of electromagnetic induction for regional assessment of soil water salinity in an irrigated valley." *Journal of Irrigation and Drainage Engineering*, 132, 436-444.

Wolters, W. (1992). *Influences on the efficiency of irrigation water use*. Publication 51, International Institute for Land Reclamation and Improvement, Wageningen, the Netherlands.

